

Some pages of this thesis may have been removed for copyright restrictions.

If you have discovered material in AURA which is unlawful e.g. breaches copyright, (either yours or that of a third party) or any other law, including but not limited to those relating to patent, trademark, confidentiality, data protection, obscenity, defamation, libel, then please read our [Takedown Policy](#) and [contact the service](#) immediately

NOVEL HYDROGEL POLYMERS

JAMES JIAN-AN MA

Doctor of Philosophy

THE UNIVERSITY OF ASTON IN BIRMINGHAM

September 1995

This copy of the thesis has been supplied on condition that anyone who consults it is understood to recognise that its copyright rests with its author and that no quotation from the thesis and no information derived from it may be published without proper acknowledgement.

THE UNIVERSITY OF ASTON IN BIRMINGHAM

NOVEL HYDROGEL POLYMERS

JAMES JIAN-AN MA

Submitted for the Degree
of Doctor of Philosophy

September 1995

SUMMARY

Hydrogels are a unique class of polymers which swell, but do not dissolve in water. A range of 2-hydroxyethyl methacrylate based copolymer hydrogels have been synthesised and are described in this thesis. Initially, hydrogels were synthesised containing acryloylmorpholine, N,N-dimethyl acrylamide and N-vinyl pyrrolidone. Variations in structure and composition have been correlated with the sequence distribution, equilibrium water content (EWC), mechanical and surface properties of the hydrogels. The sequence distribution was found to be dependant on the structure and reactivity of the monomers. The EWC was found to be dependant on the water structuring groups present in the hydrogel, although the water binding abilities were modified by steric effects. The mechanical properties were also investigated and were found to be dependant on the monomer structure, sequence distribution and the amount and nature of water in the hydrogel. The macroscopic surface properties of the hydrogels were probed using surface energy determinations and were found to be a function of the water content and the hydrogel composition. At a molecular level, surface properties were investigated using an *in vitro* ocular spoilation model and single protein adhesion studies. The results indicate that the sequence distribution and the polarity of the surface affect the adhesion of biological species.

Finally, a range of 2-hydroxyethyl methacrylate based copolymer hydrogels containing both charged monomer groups and linear polyethers have been synthesised and described. Although variations in the EWC are observed with the structure of the monomers, it was observed that the EWC increased due to the polar character of the charged monomers and the chain length and hydrophilicity of the polyethers. Investigation of these hydrogel surfaces revealed subtle changes. The molecular surface properties indicate the significance of the effect of charge and molecular mobility of the groups expressed at the hydrogel surface

Keywords: acryloylmorpholine, charged monomers, equilibrium water content (EWC), polyethers, surface properties

To my family

ACKNOWLEDGEMENTS

I would like to take this opportunity to thank the following:

Firstly, I would like to thank my supervisor Prof. Brian Tighe for his advice and enthusiasm throughout the course of this work and for the opportunity to undertake this work.

Dr. Val Franklin for undertaking the *in vitro* ocular spoilation studies and for her proofreading.

Dr. R. Sariri for undertaking the single protein deposition studies.

Dr. Phil Corkhill and Dr. Helen Oxley for their help during the early months of this work.

The staff and students who have worked with me in the Biomaterials Research Group.

EPSRC and Vista Optics for financial support.

Finally, very special thanks to Nickie Bretherton for her assistance and support throughout the course of this work and especially during the period I have been writing up.

1.6	Poly(Ethylene Oxide)	42
1.6.1	Poly(Ethylene Oxide) : A General Introduction.....	42
1.6.2	Application to Protein Resistant Coatings	43
1.7	The Effect Of Ion Incorporation On The Physical And Blood- Contacting Properties Of Hydrogels	45
1.8	Sequence Distribution Of Surface Groups.....	47
1.9	Copolymer Composition.....	48
1.9.1	Historical Background.....	48
1.9.2	Terminal Model of Polymerisation	49
1.9.3	Reactivity Ratios And The Q-e Scheme.....	51
1.10	Scope And Objectives Of This Work.....	52
 CHAPTER 2 Materials and Experimental Techniques		54
2.1	Materials	55
2.2	Polymer Synthesis.....	60
2.2.1	Preparation Of Hydrogel Polymer Membranes	60
2.2.2	Solution Polymerisation	62
2.3	Determination of the Equilibrium Water Content (EWC)	64
2.4	Differential Scanning Calorimetry (DSC).....	64
2.5	Thermal Mechanical Analysis (TMA)	68
2.6	Mechanical Properties.....	70
2.7	Surface Properties	72
2.7.1	Sessile Drop Technique.....	72
2.7.2	Hamilton Method.....	72
2.7.3	Captive Air Bubble Technique.....	72
2.7.4	Dynamic Contact Angle Measurement	73
2.8	Permeability Measurements	73
2.8.1	The Ion Permeability Apparatus	76
2.8.1	Method Of Operation Of The Ion Permeability Apparatus.....	79
2.9	Copolymer Sequence Simulations.....	79
 CHAPTER 3 Acryloylmorpholine: A Novel Monomer in Hydrogel Synthesis.....		84
3.1	Introduction	85
3.2	Reactivity Of Acryloylmorpholine.....	87
3.2.1	Computer Simulations	88
3.2.2	Experimentally Prepared Copolymers	95

3.2.3	Conclusions.....	96
3.3	Effect Of Acryloylmorpholine On Equilibrium Water Content.....	96
3.3.1	Materials And Their EWC's.....	96
3.3.2	Water Binding Studies.....	98
3.4	Effect of Acryloylmorpholine On The Mechanical Properties Of The Copolymer Systems.....	104
3.4.1	Introduction.....	104
3.4.2	Materials And Results.....	105
3.5	Surface Properties Of Modified HEMA Hydrogels.....	110
3.5.1	Introduction.....	110
3.5.2	Results.....	111
3.5.2.1	Surface properties of the dehydrated copolymers.....	111
3.5.2.2	Surface properties of the hydrated copolymers.....	114
3.5.3	Conclusions.....	116
3.6	Protein Deposition Studies Of HEMA-NVP, HEMA-NNDMA And HEMA-AMO Copolymer Hydrogels.....	117
3.6.1	In Vitro Spoilation Procedures Of Membrane Materials.....	117
3.6.2	Surface Fluorescence Analysis Of Gross Spoilation Profiles.....	118
3.6.3	Results.....	121
3.6.4	Conclusions.....	130
3.7	Summary.....	131
 CHAPTER 4 High Water Content Systems.....		133
4.1	Introduction.....	134
4.2	Characterisation Of The Sequence Distributions Of The HEMA-AMO, HPMA-AMO And HPA-AMO Copolymer Systems.....	135
4.2.1	Introduction.....	135
4.2.2	Methods And Results.....	135
4.2.3	Conclusions.....	141
4.3	EWC's Of The HEMA-AMO, HPMA-AMO And HPA-AMO Copolymer Membranes.....	142
4.3.1	Materials And Methods.....	142
4.3.2	Results.....	142
4.3.3	Conclusions.....	144
4.4	Water Binding Characteristics Of The HEMA-AMO, HPMA-AMO And HPA-AMO Copolymers.....	144
4.4.1	Introduction.....	144

4.4.2	Methods	144
4.4.3	Conclusions.....	148
4.5	Mechanical Properties Of The HEMA-AMO, HPMA-AMO And HPA-AMO Copolymer Membranes.....	149
4.5.1	Methods	149
4.5.2	Results.....	149
4.5.2	Conclusions.....	153
4.6	Surface Properties Of Hydrated And Dehydrated HEMA-AMO, HPMA-AMO And HPA-AMO Copolymers.....	153
4.6.1	Methods	153
4.6.1.1	Surface properties of dehydrated HEMA-AMO, HPMA-AMO and HPA-AMO copolymers.....	153
4.6.1.2	Surface properties of hydrated HEMA-AMO, HPMA-AMO and HPA-AMO copolymers.....	156
4.6.3	Conclusions.....	162
4.7	Summary	162
 CHAPTER 5 The Effect Of Sequence Distribution.....		164
5.1	Introduction	165
5.2	Materials.....	166
5.3	Effect Of Hydrophobic Monomer On EWC And Mechanical Properties.....	167
5.3.1	Introduction	167
5.3.2	Results Of The Effect Of Hydrophobic Monomer On The EWC Of NVP Copolymer Membranes	167
5.3.3	Results Of The Effect Of The Structure Of The Hydrophobic Monomer On The Mechanical Properties Of The NVP Hydrogel Copolymers	168
5.3.4	Conclusions.....	172
5.4	The Effect Of Sequence Distribution On Hydrogel Copolymers.....	172
5.4.1	Introduction	172
5.4.2	Comparison Of The EWC's Of The AMO Copolymers And NVP Copolymers	173
5.4.3	Comparison Of The Mechanical Properties Of The AMO Copolymers And NVP Copolymers	174
5.4.4	Sequence Simulation Experiments	175
5.4.5	Glass Transition Temperatures (T _g 's) Of The AMO Copolymers And NVP Copolymers	181

5.4.6	Conclusions.....	182
5.5	Investigation Of The Minimum Quantity Of Hydrophobic Monomer Required To Produce Hydrophobic Clusters.....	182
5.5.1	Introduction	182
5.5.2	Materials.....	182
5.5.3	Results.....	183
5.5.4	Conclusions.....	188
5.6	The Reinforcement Of High Equilibrium Water Content Materials.....	188
5.6.1	Introduction	188
5.6.2	Materials And Results.....	189
5.6.3	Conclusion	191
5.7	Summary	191

CHAPTER 6 Novel Biomaterials Possessing Charged Monomer

	Units.....	192
6.1	Introduction	193
6.2	The Effect of the Incorporation of Charged Monomers on the Water- Binding Characteristics of HEMA Copolymers.....	196
6.2.1	Introduction	196
6.2.2	Materials and Methods.....	196
6.2.3	Results.....	197
6.2.4	Conclusions.....	201
6.3	Mechanical Properties of Hydrogel Polymers Containing Charge.....	202
6.3.1	Introduction	202
6.3.2	Materials and Methods.....	203
6.3.3	Results.....	203
6.3.4	Conclusions.....	205
6.4	Surface Properties of Charged Hydrogel Materials.....	205
6.4.1	Materials and Methods.....	205
6.4.2	Results.....	206
6.4.3	Conclusions.....	214
6.5	Protein Interactions with Charged Hydrogel Polymers	214
6.5.1	Introduction	214
6.5.2	Materials and Methods.....	215
6.5.3	Results.....	216
6.5.4	Conclusions.....	221
6.6	The Effect of EWC on Protein Up-take.....	222
6.6.1	Introduction	222

6.6.2	Materials.....	222
6.6.3	Results of the Effect of Crosslinker Concentration on the EWC of HEMA-MAA Copolymers.....	223
6.6.4	Results of the Spoilation of the Copolymers Containing 1 and 10% weight% EGDMA.....	223
6.6.5	Conclusions.....	224
6.7	Summary	226

**CHAPTER 7 Effect of Crosslinker Type and Concentration on the
Characteristics of Hydrogel Membranes..... 227**

7.1	Introduction	228
7.2	Reactivity Of The Crosslinking Agents.....	230
7.2.1	Introduction	230
7.2.2	Methods And Results.....	231
7.3	Effect Of Amount And Nature Of Crosslinking Monomer On The Equilibrium Water Content (EWC) Of HEMA Copolymers.....	239
7.3.1	Materials And Methods	239
7.3.2	Results.....	240
7.3.3	Conclusions.....	242
7.4	Effect Of Crosslinker Type And Concentration On The Mechanical Properties Of HEMA Copolymers.....	242
7.4.1	Materials And Methods	242
7.4.2	Results.....	242
7.4.3	Conclusions.....	246
7.5	Effect Of Crosslinking Monomer Concentration And Type On The Surface Properties Of HEMA Hydrogels.....	248
7.5.1	Introduction	248
7.5.2	Materials And Methods	248
7.5.3	Results.....	249
7.5.4	Conclusions.....	254
7.6	Ion Permeability of Poly(ethylene oxide) Crosslinked Hydrogel Copolymers	254
7.6.1	Introduction	254
7.6.2	Materials And Methods	255
7.6.3	Results.....	256
7.6.4	Conclusions.....	261
7.7	Protein And Lipid Deposition Studies.....	262
7.7.1	Introduction	262

7.7.2	Methods	263
7.7.3	Results Of Protein And Lipid Spoilation Characteristics	263
7.7.4	Conclusions.....	265
7.8	Summary	265

CHAPTER 8 Hydrogels modified with Monocapped Linear Polyethers 267

8.1	Introduction	268
8.2	The Reactivity of Long Chain Polyethers in Hydrogel Synthesis	269
8.2.1	Introduction	269
8.2.2	Sequence Simulations.....	270
8.2.3	Results.....	274
8.2.4	Conclusions.....	275
8.3	Effect of PEG Incorporation on the EWC	275
8.3.1	Materials and Methods.....	275
8.3.2	Results.....	279
8.4	Effect of Poly(ethylene oxide) Incorporation on the Mechanical Properties of HEMA Modified Hydrogels.....	280
8.4.1	Materials and Methods.....	280
8.4.2	Results.....	280
8.4.3	Conclusions.....	283
8.5	Surface Properties of Polyether Modified HEMA Membranes.....	283
8.5.1	Introduction	283
8.5.2	Materials.....	284
8.5.3	Results.....	284
8.5.4	Conclusions.....	288
8.6	Spoilation Characteristics of HEMA Membranes Modified with Poly(ethylene oxide)	290
8.6.1	Introduction	290
8.6.2	Protein Spoilations	290
8.6.3	Results.....	290
8.6.4	Conclusion	293
8.7	Examination of the Surfaces of HEMA Hydrogels Modified with Polyethers	293
8.7.1	SEM Examination of Surfaces of Hydrogels Modified with Linear Polyethers.....	293
8.7.2	Results.....	294
8.7.3	XRD Examination of Hydrogels Modified with Linear	

8.7.3 XRD Examination of Hydrogels Modified with Linear Polyethers.....	295
8.7.4 Conclusions.....	296
8.8 Summary.....	296
CHAPTER 9 Conclusions and Suggestions for Further Work.....	298
9.1 Conclusions.....	299
9.2 Suggestions for Future Work.....	308
References.....	310
Appendix I.....	328
Appendix II.....	334
Appendix III.....	336

List of Figures

Table		Page
Figure 1.1	A diagrammatic representation of the three phase model of imbibed water, redrawn from reference Hamilton.	28
Figure 1.2	Typical melting endotherm from a DSC experiment.	30
Figure 1.3	Individual components of the solid surface free energy.	33
Figure 1.4	Individual components of the surface free energy for Hamiltons technique.	34
Figure 1.5	Individual components of the surface free energy for the captive air bubble technique.	36
Figure 1.6	The interaction of blood components with hydrated poly (ethylene oxide) chains at the polymer surface (redrawn from reference 47).	44
Figure 2.1	Structures of reagents used.	56
Figure 2.2	Diagram of a membrane mould	61
Figure 2.3	Diagram of solution polymerisation apparatus	63
Figure 2.4	Schematic representation of a Differential Scanning Calorimeter (DSC).	66
Figure 2.5	Typical thermogram of a DSC experiment.	67
Figure 2.6	Diagram of a Thermal Mechanical Analyser (TMA).	68
Figure 2.7	Sample trace from a Thermal Mechanical Analysis (TMA) experiment.	69
Figure 2.8	Cross section of the cutting tool used for sample preparation.	70
Figure 2.9	Example of a stress-strain curve from a tensometer experiment.	71
Figure 2.10	Schematic diagram of the functional components of a Dynamic Contact Angle Analyser (DCA).	74
Figure 2.11	Diagram of a dynamic contact angle hysteresis curve, showing a two immersion cycle profile.	75
Figure 2.12	Schematic representation of a permeability cell.	77
Figure 2.13	Schematic representation of the permeability apparatus.	78
Figure 2.14	Sequence simulation of HEMA-AMO copolymer.	82
Figure 3.1	Chemical structure of acryloylmorpholine.	87
Figure 3.2	Sequence simulation of a HEMA-AMO copolymer.	90
Figure 3.3	Sequence simulation of a HEMA-NNDMA copolymer.	91
Figure 3.4	Sequence simulation of a HEMA-NVP copolymer.	92
Figure 3.5	Resonance structures of amide head group.	94

Figure 3.6	Effect of nitrogen-containing monomers on the equilibrium water content of their HEMA copolymers.	97
Figure 3.7	The effect of composition on the water binding characteristics of HEMA-AMO copolymers.	10
Figure 3.8	The effect of composition on the water binding characteristics of HEMA-NNDMA copolymers.	101
Figure 3.9	The effect of composition on the water binding characteristics of HEMA-NVP copolymers.	102
Figure 3.10	Effect of composition on the elastic modulus of the HEMA copolymers.	106
Figure 3.11	Effect of composition on the tensile strength of the HEMA copolymers.	106
Figure 3.12	Effect of composition on the elongation at break of the HEMA copolymers.	107
Figure 3.13	Effect of Equilibrium Water Content on the Elastic Modulus of the HEMA copolymers.	108
Figure 3.14	Effect of Equilibrium Water Content on the Tensile Strength of the HEMA copolymers.	109
Figure 3.15	Effect of Equilibrium Water Content on the Elongation at Break of the HEMA copolymers.	110
Figure 3.16	Effect of composition on the measured polar component of the surface free energy of dehydrated HEMA-AMO, HEMA-NNDMA and HEMA-NVP copolymers.	112
Figure 3.17	Effect of composition on the measured dispersive component of the surface free energy of dehydrated HEMA-AMO, HEMA-NNDMA and HEMA-NVP copolymers.	113
Figure 3.18	Effect of composition on the total surface free energy of dehydrated HEMA-AMO, HEMA-NNDMA and HEMA-NVP copolymers.	114
Figure 3.19	Variation in the polar component of the surface free energy with EWC for hydrated HEMA-AMO, HEMA-NNDMA and HEMA-NVP copolymers.	115
Figure 3.20	Variation in the dispersive component of the surface free energy of hydrated HEMA-AMO, HEMA-NNDMA and HEMA-NVP copolymers.	115
Figure 3.21	Flourescence spectrum excited at 360nm.	119
Figure 3.22	Flourescence spectrum excited at 280nm.	120
Figure 3.23	Progressive build up of lipid spoilation, excited at 360nm, of HEMA-NVP, HEMA-NNDMA, HEMA-AMO 90:10 membranes.122123	122

Figure 3.24	Progressive build up of lipid spoilation, excited at 280nm, of HEMA-NVP, HEMA-NNDMA, HEMA-AMO 90:10 membranes.	122
Figure 3.25	Progressive build up of protein spoilation of HEMA-NVP, HEMA-N125NDMA, HEMA-AMO 90:10 membranes.	123
Figure 3.26	Progressive build up of lipid spoilation, excited at 360nm, of HEMA-NVP, HEMA-NNDMA, HEMA-AMO 80:20 membranes.	124
Figure 3.27	Progressive build up of lipid spoilation, excited at 280nm, of HEMA-NVP, HEMA-N127NDMA, HEMA-AMO 80:20 membranes.	124
Figure 3.28	Progressive build up of protein spoilation of HEMA-NVP, HEMA-NNDMA, HEMA-AMO128 80:20 membranes.	125
Figure 3.29	Progressive build up of lipid spoilation, excited at 280nm, of HEMA-NVP, HEMA-NNDMA, HEMA129-AMO 70:30 membranes.	126
Figure 3.30	Progressive build up of lipid spoilation, excited at 280nm, of HEMA-NVP, HEMA-NNDMA, HEMA-AMO 70:30 membranes.	126
Figure 3.31	Progressive build up of protein spoilation of HEMA-NVP, HEMA-NNDMA, HEMA-AMO 70:30 membranes.	127
Figure 3.32	Progressive build up of lipid spoilation, excited at 280nm, of HEMA-NVP, HEMA-NNDMA, HEMA-AMO 60:40 membranes.	127
Figure 3.33	Progressive build up of lipid spoilation, excited at 280nm, of HEMA-NVP, HEMA-NNDMA, HEMA-AMO 60:40 membranes.	128
Figure 3.34	Progressive build up of protein spoilation of HEMA-NVP, HEMA-NNDMA, HEMA-AMO 60:40 membranes.	128
Figure 3.35	Progressive build up of lipid spoilation, excited at 280nm, of HEMA-NVP, HEMA-NNDMA, HEMA-AMO 50:50 membranes.	129
Figure 3.36	Progressive build up of lipid spoilation, excited at 280nm, of HEMA-NVP, HEMA-NNDMA, HEMA-AMO 50:50 membranes.	129
Figure 3.37	Progressive build up of protein spoilation of HEMA-NVP, HEMA-NNDMA, HEMA-AMO 50:50 membranes.	130
Figure 4.1	Sequence simulation of 70:30 wt/wt HEMA-AMO copolymer.	136
Figure 4.2	Sequence simulation of 70:30 wt/wt HPMA-AMO copolymer.	137
Figure 4.3	Sequence simulation of 70:30 wt/wt HPA-AMO copolymer.	138
Figure 4.4	Resonance stabilisation via α -methyl substituent.	141
Figure 4.5	Effect of increasing proportion of AMO on the EWC of HEMA-AMO, HPMA-AMO and HPA-AMO copolymer membranes.	142
Figure 4.6	Effect of composition on the water binding ability of HEMA-AMO copolymers.	145

Figure 4.7	Effect of composition on the water binding ability of HPMA-AMO copolymers.	146
Figure 4.8	Effect of composition on the water binding ability of HPA-AMO copolymers.	146
Figure 4.9	Effect of equilibrium water content on the elastic modulus of HEMA-AMO, HPMA-AMO and HPA-AMO copolymers.	152
Figure 4.10	Effect of composition on the surface free energy of dehydrated HEMA-AMO copolymers.	154
Figure 4.11	Effect of composition on the surface free energy of dehydrated HPMA-AMO copolymers.	154
Figure 4.12	Effect of composition on the surface free energy of dehydrated HPA-AMO copolymers.	155
Figure 4.13	Effect of composition on the surface free energy of hydrated HEMA-AMO copolymers.	157
Figure 4.14	Effect of composition on the surface free energy of hydrated HPMA-AMO copolymers.	157
Figure 4.15	Effect of composition on the surface free energy of hydrated HPA-AMO copolymers.	158
Figure 4.16	The variation in total surface energy versus EWC due to the contribution to the surface energy of the hydroxy monomer-AMO copolymers.	159
Figure 4.17	Variation in the polar component of the surface free energy with increasing EWC for the hydrated hydroxy monomer-AMO copolymers.	160
Figure 4.18	Variation in the dispersive component of the surface free energy with increasing EWC for the hydrated hydroxy monomer-AMO copolymers.	160
Figure 5.1	Effect of hydrophobic monomer on the EWC's of NVP-hydrophobic monomer 70:30 weight/weight hydrogel membranes.	167
Figure 5.2	A typical load/extension profile for the NVP-hydrophobic monomer 70:30 weight/weight hydrogel membranes.	169
Figure 5.3	Effect of the type of hydrophobic monomer on the elastic modulus (E_m) of NVP-hydrophobic monomer 70:30 weight/weight hydrogel membranes.	171
Figure 5.4	EWC's of equivalent NVP-hydrophobic monomer and AMO-hydrophobic monomer 70:30 weight/weight copolymer membranes.	173

Figure 5.5	Elastic modulus of equivalent NVP-hydrophobic monomer and AMO-hydrophobic monomer 70:30 weight/weight copolymer membranes.	174
Figure 5.6	Sequence simulation of an AMO-BENZMA copolymer.	176
Figure 5.7	Sequence simulation of an NVP-BENZMA copolymer.	177
Figure 5.8	Sequence simulation of an AMO-MMA copolymer.	178
Figure 5.9	Sequence simulation of an NVP-MMA copolymer.	179
Figure 5.10	Effect of composition on the EWC and tensile strength of NVP-isoBORNMA copolymers.	185
Figure 5.11	Effect of composition on the EWC and tensile strength of NVP-BENZMA copolymers.	185
Figure 5.12	Effect of composition on the EWC and tensile strength of NVP-CHEXMA copolymers.	186
Figure 5.13	Effect of composition on the EWC and tensile strength of NVP-tBUTMA copolymers.	186
Figure 6.1	Effect of increasing proportion of charged monomers on the equilibrium water contents of HEMA copolymer membranes.	197
Figure 6.2	Effect of increasing proportion of charged monomers on the total water binding capability of HEMA copolymer membranes.	199
Figure 6.3	Effect of increasing proportion of charged monomers on the freezing water content of HEMA copolymer membranes.	199
Figure 6.4	Effect of increasing proportion of charged monomers on the non-freezing water content of HEMA copolymer membranes.	200
Figure 6.5	Effect of composition on the surface free energy of dehydrated HEMA-MAA copolymers.	207
Figure 6.6	Effect of composition on the surface free energy of dehydrated HEMA-NVI copolymers.	207
Figure 6.7	Effect of composition on the surface free energy of dehydrated HEMA-SPE copolymers.	208
Figure 6.8	Effect of composition on the surface free energy of dehydrated HEMA-MAA copolymers.	208
Figure 6.9	Variation in the polar and dispersive components of the surface energy with increasing EWC for hydrated HEMA-MAA copolymers.	210
Figure 6.10	Variation in the polar and dispersive components of the surface energy with increasing EWC for hydrated HEMA-ITC copolymers.	211
Figure 6.11	Variation in the polar and dispersive components of the surface energy with increasing EWC for hydrated HEMA-NVI copolymers.	213

Figure 6.12	Variation in the polar and dispersive components of the surface energy with increasing EWC for hydrated HEMA-SPE copolymers.	213
Figure 6.13	Effect of methacrylic acid content on the absorption of positively and negatively charged proteins.	218
Figure 6.14	Effect of itaconic acid content on the absorption of positively and negatively charged proteins.	219
Figure 6.15	Effect of N-vinyl imidazole content on the absorption of positively and negatively charged proteins.	220
Figure 6.16	Effect of N-(3-sulfopropyl)-N-methacryloxyethyl-N, N-dimethylammonium betaine content on the absorption of positively and negatively charged proteins.	221
Figure 6.17	Effect of MAA content on lysozyme uptake with HEMA-MAA copolymers, at crosslinker concentrations of 1 and 10 weight %.	225
Figure 6.18	Effect of MAA content on lactoferrin uptake with HEMA-MAA copolymers, at crosslinker concentrations of 1 and 10 weight %.	225
Figure 7.1	Diagrammatic representation of the sequence simulation of the 1st vinyl group in a HEMA-EGDMA copolymer.	232
Figure 7.2	Diagrammatic representation of the sequence simulation of the 2nd vinyl group in a HEMA-EGDMA copolymer.	233
Figure 7.3	Diagrammatic representation of the sequence simulation of the 1st vinyl group in a HEMA-TAC copolymer.	234
Figure 7.4	Diagrammatic representation of the sequence simulation of the 2nd vinyl group in a HEMA-TAC copolymer.	235
Figure 7.5	Diagrammatic representation of the sequence simulation of the 1st vinyl group in a HEMA-TAR copolymer.	236
Figure 7.6	Diagrammatic representation of the sequence simulation of the 2nd vinyl group in a HEMA-TAR copolymer.	237
Figure 7.7	Effect of the nature and proportion of the crosslinking monomer on the EWC of HEMA copolymers.	240
Figure 7.8	Variation in E_m and EWC for the series of crosslinkers studied.	247
Figure 7.9	The polar and dispersive components of the surface energy due to water and the polymer structure of hydrated HEMA-EGDMA copolymers.	248
Figure 7.10	The polar and dispersive components of the surface energy due to water and the polymer structure of hydrated HEMA-PEG200DMA copolymers.	250

Figure 7.11	The polar and dispersive components of the surface energy due to water and the polymer structure of hydrated HEMA-PEG400DMA copolymers.	251
Figure 7.12	The polar and dispersive components of the surface energy due to water and the polymer structure of hydrated HEMA-PEG1000DMA copolymers.	252
Figure 7.13	The polar and dispersive components of the surface energy due to water and the polymer structure of hydrated HEMA-TAC copolymers.	253
Figure 7.14	Effect of poly (ethylene oxide) crosslink chain length on the permeation of NaCl across a HEMA membrane.	257
Figure 7.15	Effect of poly (ethylene oxide) crosslink chain length on the permeation of MgCl ₂ across a HEMA membrane.	259
Figure 7.16	Effect of poly (ethylene oxide) crosslink chain length on the permeation of CaCl ₂ across a HEMA membrane.	260
Figure 7.17	Plot of P versus H for the transport of metal chlorides across poly (ethylene oxide) crosslinked HEMA membranes.	261
Figure 7.18	Effect of crosslinker type and concentration on the protein deposition of modified poly (HEMA) membranes after 28 days.	263
Figure 7.19	Effect of crosslinker type and concentration on the lipid deposition of modified poly (HEMA) membranes after 28 days.	265
Figure 8.1	SEM micrograph of mucin on a hydrogel surface	269
Figure 8.2	Sequence simulation of a HEMA and PEG200MA copolymer.	271
Figure 8.3	Sequence simulation of a HEMA and PEG400MA copolymer.	272
Figure 8.4	Sequence simulation of a HEMA and PEG1000MA copolymer.	273
Figure 8.5	Gel permeation chromatograms for the methoxy terminated polyethylene glycol methacrylates (MPEGMA's).	276
Figure 8.6	Gel permeation chromatograms for the polyethylene glycol methacrylate 10 ethylene oxide units (PEGMA 10 EO).	277
Figure 8.7	Gel permeation chromatograms for the ethoxylated hydroxethyl methacrylate (HEMA 4,5 EO).	278
Figure 8.8	Effect of poly (ethylene oxide) incorporation and chain length on the EWC of HEMA-EGDMA (99:1) hydrogel.	280
Figure 8.9	Advancing contact angles for HEMA membranes modified with polyethers.	286
Figure 8.10	Receding contact angles obtained for HEMA membranes modified with polyethers.	287

Figure 8.11	Contact angle hysteresis for HEMA membranes modified with polyethers.	288
Figure 8.12	Diagrammatic representation of hydrated polyether chains at a polymer surface.	289
Figure 8.13	Adsorption of lysozyme to HEMA membranes modified with polyethers.	291
Figure 8.14	Adsorption of lactoferrin to HEMA membranes modified with polyethers.	292
Figure 8.15	SEM micrograph of the surface of a HEMA hydrogel modified with 20 weight% of PEG1000MA	293
Figure 8.16	SEM micrograph of the surface of a HEMA hydrogel modified with 20 weight% of PEG400MA	294
Figure 8.17	SEM micrograph of the surface of a HEMA hydrogel modified with 20 weight% of PEG200MA	295

List of Tables

Table		Page
Table 1.1	Polar and dispersive components of water and diiodomethane.	34
Table 2.1	Molecular weights and suppliers of reagents used.	55
Table 3.1	Examples of commercially available high water content contact lens materials	86
Table 3.2	The relative reactivity ratios for the HEMA-NVP, HEMA-NNDMA and HEMA-AMO copolymer systems	88
Table 3.3	Elemental analysis results for the copolymer systems studied	95
Table 4.1	Calculated reactivity ratios for the copolymer systems HEMA-AMO, HPMA-AMO and HPA-AMO	135
Table 4.2	Mechanical properties of HEMA-AMO copolymers	150
Table 4.3	Mechanical properties of HPMA-AMO copolymers	150
Table 4.4	Mechanical properties of HPA-AMO copolymers	150
Table 5.1	Hydrophobic monomers used.	166
Table 5.2	Mechanical properties of NVP-hydrophobic comonomer 70:30 weight/weight copolymer membranes.	169
Table 5.3	Glass transition temperatures (Tg's) obtained by DSC, for the series of NVP-hydrophobic monomer and AMO-hydrophobic monomer 70:30 weight/weight copolymer membranes.	181
Table 5.4	Effect of increasing the amount of isoBORNMA on the mechanical properties of NVP copolymers.	183
Table 5.5	Effect of increasing the amount of BENZMA on the mechanical properties of NVP copolymers.	184
Table 5.6	Effect of increasing the amount of CHEXMA on the mechanical properties of NVP copolymers.	184
Table 5.7	Effect of increasing the amount of tBUTMA on the mechanical properties of NVP copolymers.	184
Table 5.8	Effect of composition on the glass transition temperatures of each series of NVP:hydrophobic monomer dehydrated copolymer membranes.	187

Table 5.9	EWC's and mechanical properties of the 50 weight % HPA-AMO (50:50) and 50 weight % NVP-hydrophobic monomer (70:30) copolymers.	189
Table 5.10	Glass transition temperatures of composite materials obtained by DSC.	190
Table 6.1	Effect of the type and amount of charged monomer on the mechanical properties of HEMA copolymers.	204
Table 6.2	Quantities of protein deposited on HEMA-MAA copolymers.	216
Table 6.3	Quantities of protein deposited on HEMA-ITC copolymers.	217
Table 6.4	Quantities of protein deposited on HEMA-NVI copolymers.	217
Table 6.5	Quantities of protein deposited on HEMA-SPE copolymers.	217
Table 6.6	Effect of composition on the EWC's of HEMA-MAA copolymers containing 1 and 10 weight % EGDMA.	223
Table 6.7	Quantities of protein deposited on HEMA-MAA copolymers with 10% crosslinking agent.	224
Table 7.1	Reactivity ratios of 1st and 2nd vinyl groups for HEMA:crosslinking agent copolymer system	230
Table 7.2	Effect of crosslinker type and concentration on the EWC of HEMA copolymers	240
Table 7.3	Effect of proportion of EGDMA upon the mechanical properties of HEMA copolymers	243
Table 7.4	Effect of proportion of PEG200DMA upon the mechanical properties of HEMA copolymers	243
Table 7.5	Effect of proportion of PEG400DMA upon the mechanical properties of HEMA copolymers	244
Table 7.6	Effect of proportion of PEG1000DMA upon the mechanical properties of HEMA copolymers	245
Table 7.7	Effect of proportion of TAC upon the mechanical properties of HEMA copolymers	245
Table 7.8	Effect of TAR upon the mechanical properties of HEMA copolymers	245
Table 7.9	Effect of polyether crosslink chain length on the permeability coefficients (P) for the permeation of 0.25M solutions of NaCl, MgCl ₂ and CaCl ₂ across crosslinked HEMA membranes	258
Table 8.1	Reactivity ratios of polyethers with HEMA	270
Table 8.2	Effect of poly(ethylene oxide) incorporation on the EWC of polyether modified HEMA membranes	279

Table 8.3	Mechanical properties of HEMA membranes modified with poly(ethylene oxide)s	281
Table 8.4	Advancing and receding contact angles for HEMA copolymers modified with linear polyethers	285

List of Abbreviations

AMO	Acryloylmorpholine	BENZMA	Benzyl methacrylate
CHEXMA	Cyclohexyl methacrylate	DSC	Differential Scanning Calorimetry
Eb	Elongation at break	EGDMA	Ethylene glycol dimethacrylate
Em	Elastic modulus	EWC	Equilibrium Water Content
γ^d	Dispersive component of the surface free energy	γ^p	Polar component of the surface free energy
γ^t	Total surface free energy	HEMA	2-Hydroxyethyl methacrylate
HEMA EO	Hydroxyethyl methacrylate ethylene oxide	HPA	2-Hydroxypropyl acrylate
HPMA	2-Hydroxypropyl methacrylate	ITC	Itaconic acid
isoBORNMA	iso-bornyl methacrylate	MAA	Methacrylic acid
MMA	Methyl methacrylate	MPEGMA	Methoxy polyethylene glycol monomethacrylate
NMR	Nuclear magnetic resonance spectroscopy	NNDMA	N,N-dimethyl acrylamide
NVI	N-vinyl imidazole	NVP	N-vinyl pyrrolidone
PEG	Polyethylene glycol	PEGMA	Polyethylene glycol methacrylate
PEO	Polyethylene oxide	SEM	Scanning electron micrograph
SPE	N-(3-sulfopropyl)-N- methacryloxyethyl-N,N- dimethyl ammonium betaine	TAC	2,4,6-triallyl-s-triazine
TAR	N,N-diallyl-tartardiamide	TBUTMA	tertiary-butyl methacrylate
Tg	Glass transition temperature	Ts	Tensile strength
XRD	X-ray diffraction		

CHAPTER 1

Introduction

1.1 General Introduction

Hydrogels are crosslinked macromolecular networks swollen in water or biological fluids. Their unique biomedical properties were first reported by Wichterle and Lim¹ who observed the remarkable properties of poly(2-hydroxyethyl methacrylate) as a potential candidate for soft contact lens applications. To date, this has been the most successful commercial application of these materials, although this is only one area in a diverse field of both medical and pharmaceutical applications². Other medical applications include synthetic articular cartilage³, drug delivery systems⁴, artificial tendons⁵ and wound dressings⁶.

Hydrogels are unique in the biomaterials field because of their ability to simulate the hydrated properties of natural tissue. This is due to the large amount of water which is absorbed by the gel and it is this imbibed water which gives hydrogels their unique mechanical, permeability and surface properties. The applications of hydrogels are diverse, since the amount of water absorbed by the gel may be controlled by copolymerisation of the main hydrophilic component with other monomers which are more or less hydrophilic, thus providing a range of water contents, mechanical and surface properties. However, the major disadvantage of these materials is their relatively low mechanical strength, although this may be overcome for certain applications either by crosslinking, the production of interpenetrating networks⁷, composites⁸, or by reinforcement via crystallite formation. In recent years there has been a great amount of interest in hydrogels for biomedical use and a wide range of literature has been published relating to this area⁹⁻¹³.

1.2 Equilibrium Water Content (EWC) of Hydrogels

The amount of water absorbed by a hydrogel may be expressed as the equilibrium water content, EWC, (Equation 1.1), which is defined as the ratio of the weight of water in the gel to the total weight of the hydrated gel, expressed as a percentage.

$$\text{EWC} = \frac{\text{Weight of water in the gel}}{\text{Total weight of hydrated gel}} \times 100\% \quad \text{Equation 1.1}$$

The EWC is an important property in that it imparts hydrogels with their unique mechanical, surface and transport properties. It has been found that the water within a hydrogel can exist in more than one state¹⁴.

1.2.1 Water In Hydrogels

The large amount of published literature on the characterisation of water indicates that the water in hydrogel membranes exists in more than one state¹⁵⁻³⁹.

It has been observed with calorimetric techniques that not all of the water within the hydrogel freezes. The proportion of water that does not freeze is referred to as non-freezing water or 'bound' water which is thought to interact strongly with the polymer network. The proportion of water that does freeze is referred to as freezing water or 'non-bound' water because it only has weak interactions with the polymer network.

In the use of nuclear magnetic resonance spectroscopy (NMR) to study water in polymers, the structure of water within the polymer is investigated by changes in line widths or relaxation times of the hydroxyl protons. The values obtained are compared with the NMR signals for liquid water which has a tall, narrow peak signal and ice which has a low, broad signal. The signals obtained for the polymers are interpreted as being weakly associated with the polymer network when the signal is equivalent to that of pure water.

It is unlikely that the water in hydrogels exists in only one of the two states mentioned, but it is more realistic that the water exists in a continuum of states between the two extremes. Andrade and coworkers^{15, 16, 28} have studied the states of water in hydrogels. The results obtained supported a model which proposes three phases of water as shown in Figure 1.1.

The three phases of water are classified as X, Y and Z, where X represents the bound water, Y is the interfacial water and Z represents the bulk water.

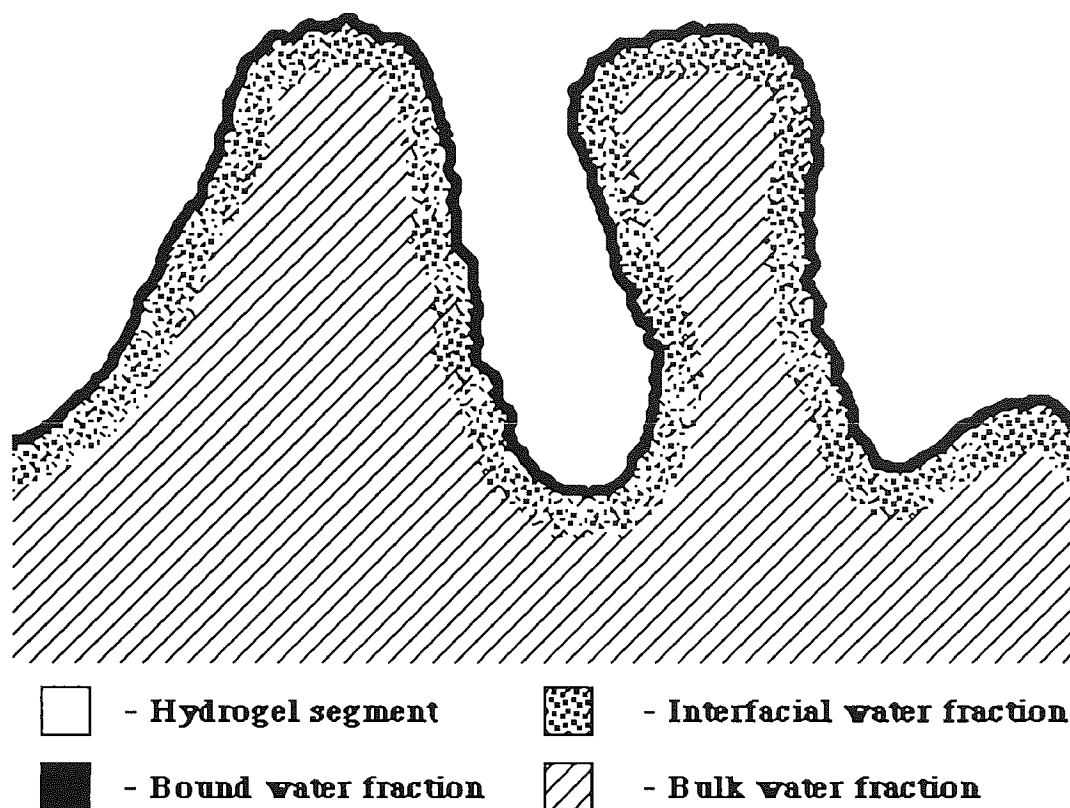


Figure 1.1 A diagrammatic representation of the three phase model of imbibed water, redrawn from reference 40

A detailed overview of the terms used in the classification of the different states of water characterised in hydrogels is provided by Corkhill⁴¹.

1.2.2 Techniques Used To Study The Water In Polymers

A wide variety of techniques have been used to characterise the water in hydrogels. These include differential scanning calorimetry (DSC), nuclear magnetic resonance spectroscopy (NMR), specific conductivity, dilatometry and dielectric measurements^{42, 43}.

1.2.2.1 Differential scanning calorimetry (DSC)

It has been observed that when polymer networks containing water are cooled to very low temperatures using calorimetric techniques, only a fraction of the water within the network

freezes. Differential scanning calorimetry was developed in 1964 by Perkin-Elmer. The technique works by measuring the energy required to keep both the sample and the reference materials at the same temperature. In the case of endothermic transitions the energy to the sample is increased and to maintain equal sample and reference temperatures and for exothermic transitions the energy to the reference holder is increased. When a transition occurs the energy input is recorded and this corresponds to the energy of the transition. A typical transition is illustrated in Figure 1.2.

Early work using calorimetric techniques has shown that the heat of fusion for water associated with polymers is the same as the value for pure water. This therefore enables the amount of water in a polymer that freezes to be determined from the area under the melting endotherm.

1.2.2.2 Nuclear magnetic resonance spectroscopy (NMR)

The line widths and changes in relaxation times of hydroxyl protons in both liquid water and solid ice have been determined using NMR. It has been found that the ^1H NMR signal for pure liquid water is a tall, narrow peak and the equivalent signal for ice is low and broad. The signal obtained for polymers containing water is between these two extremes and is generally interpreted by matching the signal that has the same peak height and line width as pure water to determine the amount of free water in the polymer. The remaining peak area is attributed to water closely associated with the polymer network.

1.2.2.3 Specific conductivity

Water in polymers has been studied by specific conductivity, K , measurements⁴⁴. This is done by measuring the specific conductivity of the hydrogel over the temperature range 258-293K. A plot of $\log K$ versus $1/T$ reveals a sharp discontinuity at the melting point of water. The types of water in the gel are related by the size and shape of the change at the transition point compared to the transition point for pure water.

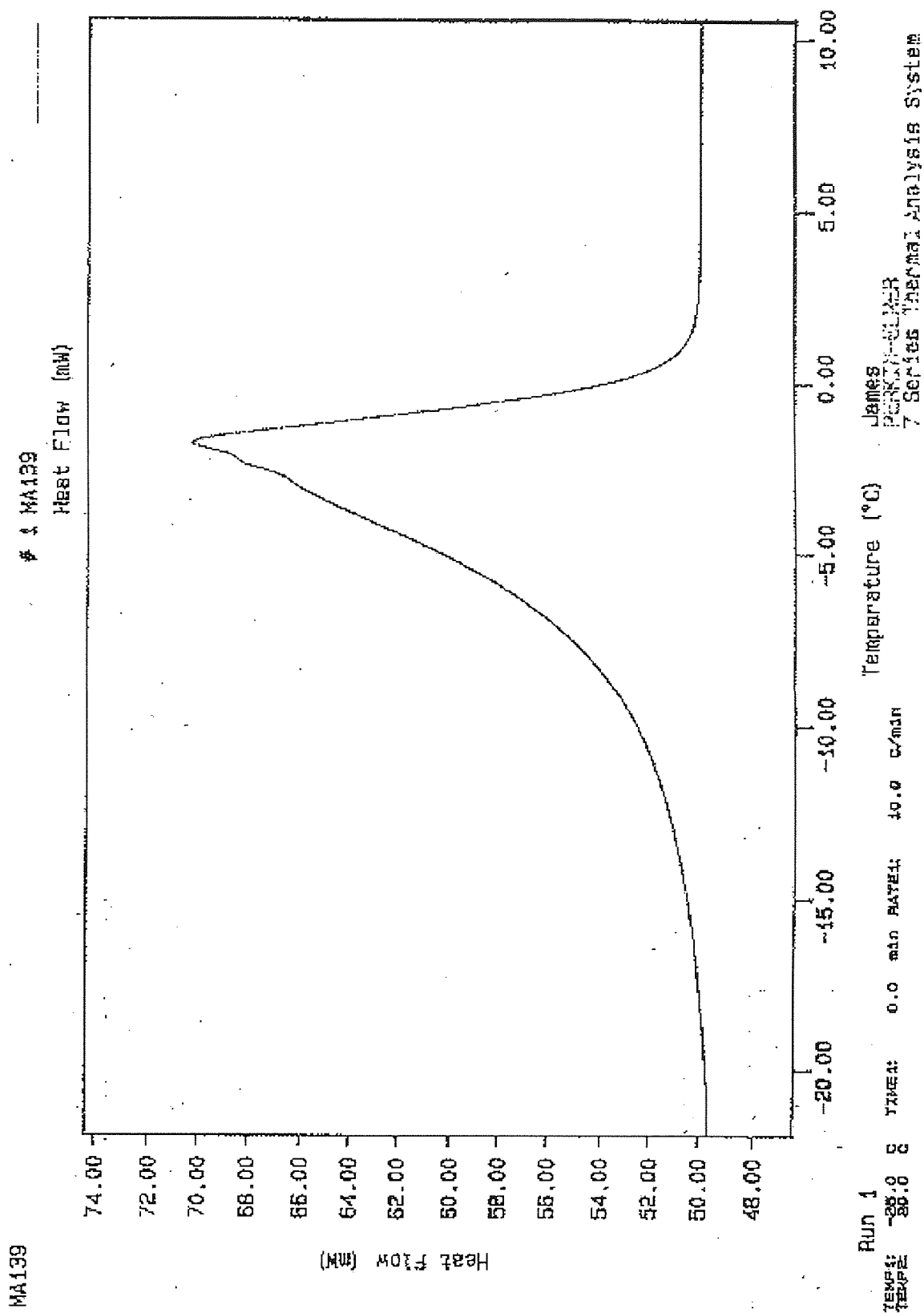


Figure 1.2 Typical melting endotherm from a DSC experiment

1.2.2.4 Dilatometry

Dilatometry has been used to determine the characteristics of water in hydrogels⁴⁵. Heating and cooling curves over the temperature range 240-300K are used to determine the specific volume change with temperature of the hydrogel sample. Comparison with the specific volume change for pure water and the shapes of the cooling and heating curves are used to determine the classification of the states of water in the polymer.

1.2.2.5 Dielectric measurements

Dielectric permittivity and loss data are generally measured by supercooling followed by heating over the temperature range of 77-273K. The permittivity and loss data are acquired for supercooled water in the hydrogel sample and the size and strength of relaxations taking place at phase changes, are compared to the strength of the relaxation transitions of supercooled water. Differences in the shapes and sizes of relaxation transitions of water in the hydrogel and pure water have enabled the water in the hydrogel to be classified into three phases, interfacial, bound and bulk water. Bulk water readily crystallises and the former two states readily supercool without crystallisation. The greater the size of the relaxation of crystallised water the greater the amount of bulk water within the hydrogel.

1.2.3 The Hydrogel-Water Interface

Hydrogels have been extensively investigated for use in biomedical applications⁴⁶. Their success to date has been attributed to their ability to simulate biological tissue due to their water content and unique surface properties. The degree of tolerance of hydrogels in the biological environment has been attributed to the surface properties and it is clear that for a material in intimate contact with a biological system (or fluid) that the surface properties will affect the nature and type of interactions that occur at that interface. It is therefore necessary to characterise the surface of the hydrogel. Techniques which are used to characterise the surface of the hydrogel will be subsequently discussed.

1.2.3.1 Contact angle measurements

Contact angle measurements are a simple experimental technique to examine the characteristics of a hydrogel surface. The results of contact angle measurements can be used to calculate the surface free energy. The detailed theory of contact angle measurements and the subsequent determinations of surface energy values has been described by Corkhill⁴¹ and a brief overview is presented here. It is necessary to study the polar and dispersive components of hydrogel surfaces because the components have been shown to have a significant influence on the biotolerance and blood compatibility of the hydrogel and this will be discussed later.

The theory for each of the techniques is dependant on the resolution of three forces at a three phase interface. The three phase interface is normally formed by a drop of liquid on a solid surface in air or by a drop of liquid (or vapour) on a solid surface immersed in a liquid. Several techniques are available for the determination of contact angles. The theory of each technique is outlined below.

1.2.3.1.1 Surface Energy Measurements Of Dehydrated Surfaces

In 1805 Young derived an equation to resolve the forces at the point of contact of a sessile drop of liquid on a solid surface⁴⁷, the equation he proposed is shown below. The forces are indicated in Figure 1.3.

$$\gamma_{sv} = \gamma_{sl} + \gamma_{lv} \cos\theta \quad \text{Equation 1.2}$$

It was not until sixty years later that Dupre⁴⁸ showed that the reversible work of adhesion of a liquid and a solid, W_a could be expressed as :-

$$W_a = \gamma_s + \gamma_{lv} - \gamma_{sl} \quad \text{Equation 1.3}$$

Equations 1.2 and 1.3 are combined to give the well known Young-Dupre equation :-

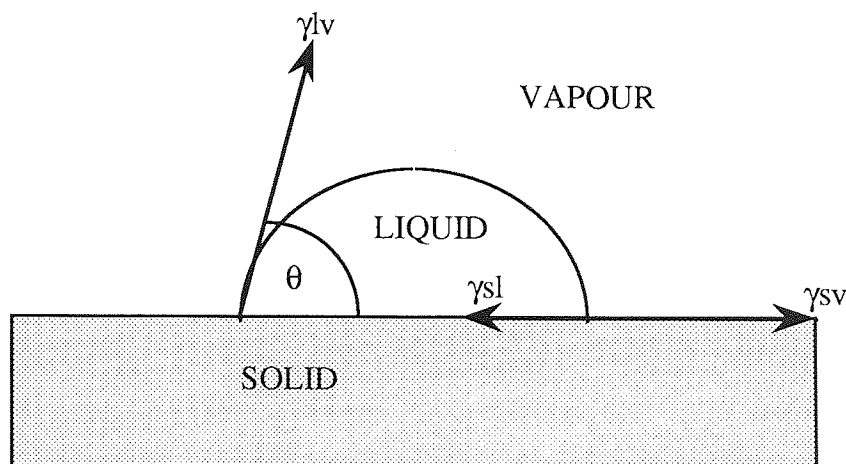
$$W_a = (\gamma_s - \gamma_{sv}) + \gamma_{lv} (1 + \cos\theta) \quad \text{Equation 1.4}$$

For many years the reversible work of adhesion was expressed by the Dupre equation, but the equation was found to be inadequate when polar forces acted across the interface.

Owens and Wendt⁴⁹ resolved the polar and dispersive components to give the expression

$$1 + \cos\theta = (2/\gamma_{lv}) [(\gamma_{lv}^d \gamma_s^d)^{0.5} + (\gamma_{lv}^p \gamma_s^p)^{0.5}] \quad \text{Equation 1.5}$$

This equation is used to determine the surface energies of dehydrated polymer surfaces.



where γ_{lv} = liquid-vapour interfacial free energy

γ_{sl} = solid-liquid interfacial free energy

γ_{sv} = solid-vapour interfacial free energy

Figure 1.3 Individual components of the solid surface free energy

As the Owens and Wendt equation relates the contact angle θ , to the polar γ_s^p and dispersive γ_s^d forces of the solid, it is possible to determine these components for the solid by solving simultaneous equations for two wetting solutions for which the polar and dispersive components are already known. Once the individual polar and dispersive components for the solid are known then the total surface free energy γ_s^t , can be obtained using Equation 1.6 :-

$$\gamma_s^t = \gamma_s^d + \gamma_s^p \quad \text{Equation 1.6}$$

Several wetting liquids have been considered for their use in surface free energy determinations⁵⁰. The two most widely used wetting liquids and the ones used in this work are water and diiodomethane. This is because of their high total surface free energies and their balance of polar and dispersive forces. The values of γ_s^t , γ_s^d and γ_s^p are shown in Table 1.1.

Table 1.1 Polar and dispersive components of water and diiodomethane⁵⁰

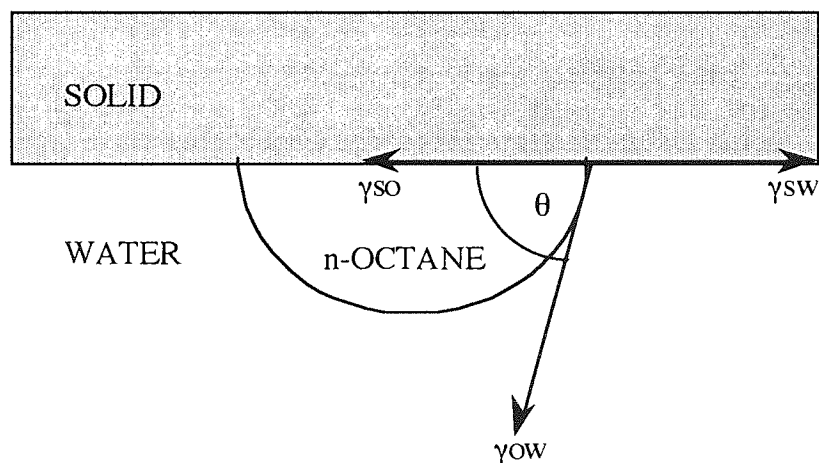
Liquid	γ_s^d (mN/m)	γ_s^p (mN/m)	γ_s^t (mN/m)
Water	21.8	51.0	72.8
Diiodomethane	48.1	2.3	50.8

1.2.3.1.2 Surface Energy Measurements Of Hydrated Surfaces

The major problems associated with the surface energy determination of hydrated polymers in air are the dehydration of the polymer surface and the reproducibility of removing excess water from the polymer surface. Two techniques have been developed which attempt to overcome these problems. Both methods enable the surface energy of the polymer sample to be measured in the fully hydrated state.

1.2.3.1.2.1 Hamiltons method ^{51, 52}

Hamilton resolved the forces at three phase interface for the three phase system of polymer solid, water and n-octane. These components are illustrated in Figure 1.4.



where γ_{sw} = solid-water interfacial free energy
 γ_{so} = solid-octane interfacial free energy
 γ_{ow} = octane-water interfacial free energy

Figure 1.4 Individual components of the surface free energy for Hamiltons technique

The original equation for the work of adhesion (Equation 1.7) at a solid-liquid interface was developed by Fowkes⁵³, but it did not account for polar forces acting across the interface.

$$\gamma_{sl} = \gamma_s + \gamma_{lv} - 2(\gamma_{lv}^d \gamma_s^d)^{0.5} \quad \text{Equation 1.7}$$

It was not until Tamai *et al*⁵⁴ modified the Fowkes equation that the contribution to the stabilisation of a solid surface could be accounted for.

$$\gamma_{sl} = \gamma_s + \gamma_{lv} - 2(\gamma_{lv}^d \gamma_s^d)^{0.5} - I_{sl} \quad \text{Equation 1.8}$$

where

$$I_{sl} = 2(\gamma_{lv}^p \gamma_s^p)^{0.5} \quad \text{Equation 1.9}$$

The dispersive components of n-octane and water γ_{lv}^d are identical and n-octane has no polar component. Therefore it is possible to combine Equations 1.2 and 1.8 to produce Equation 1.10 which corresponds to the polar stabilisation energy between water and the solid.

$$I_{sw} = \gamma_{w'v} - \gamma_{ov} - \gamma_{ow} \cdot \cos\theta \quad \text{Equation 1.10}$$

where

I_{sw} is the polar stabilisation energy between water and the solid

$\gamma_{w'v}$ is the surface tension of n-octane saturated water

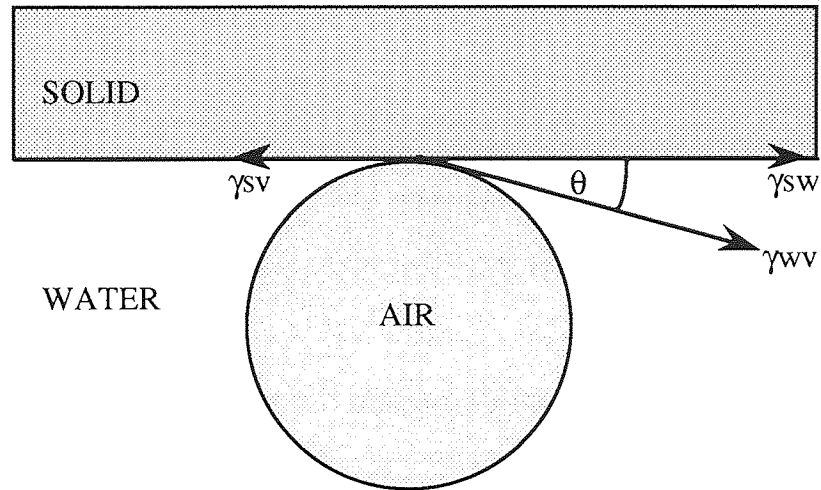
γ_{ov} is the surface tension between n-octane and its vapour

γ_{ow} is the surface tension between n-octane and water

The components γ_{ov} and γ_{ow} have been determined experimentally, which enables I_{sw} to be calculated. Substitution of the subsequent value of I_{sw} into Equation 1.9 enables the polar component of the surface free energy, γ_s , to be determined.

1.2.3.1.2.2 Captive air bubble technique⁵⁵

This technique uses the same experimental set-up as the Hamilton method, but instead of putting a drop of n-octane on the solid surface, an air bubble is placed in contact with the surface as shown in Figure 1.5. This enables the resultant forces at each interface for a three phase system to be determined.



where γ_{sw} = solid-water interfacial free energy
 γ_{wv} = water-vapour interfacial free energy = surface tension of water
 γ_{sv} = solid-vapour interfacial free energy $\approx \gamma_s$ = solid surface free energy

Figure 1.5 Individual components of the surface free energy for the captive air bubble technique

Using contact angles obtained from both the Hamilton method and captive air bubble techniques it is possible to determine values for γ_{sv} , γ_{sv}^p , γ_{sv}^d and γ_{sw} . This was first shown by Andrade *et al* 56.

Application of Youngs equation to the captive air bubble technique, with water as the liquid phase gives :-

$$\gamma_{sv} - \gamma_{sw} = \gamma_{wv} \cos\theta \quad \text{Equation 1.11}$$

As γ_{wv} is equal to the surface tension of water which is 72.8 mN/m and θ is obtained by direct measurement of the air bubble contact angle it is possible to determine $\gamma_{sv} - \gamma_{sw}$ in Equation 1.11.

From Equation 1.10 the polar stabilisation parameter is given by :-

$$I_{sw} = \gamma_{w'v} - \gamma_{ov} - \gamma_{ow} \cdot \cos\theta \quad \text{Equation 1.10}$$

For the captive air bubble technique $\gamma_{wv} = 72.8$ mN/m, $\gamma_{ov} = 21.8$ mN/m and $\gamma_{ow} = 51.0$ mN/m then :-

$$I_{sw} = 51.0 (1 - \cos\theta) \quad \text{Equation 1.12}$$

By combining Equations 1.8 and 1.11 and with appropriate rearrangement, it is possible to determine the dispersive component of the hydrogel, γ_{sv}^d .

$$\gamma_{sv}^d = \{ (\gamma_{sv} - \gamma_{sw}) - I_{sw} + \gamma_{wv} \} / 2(\gamma_{wv}^d)^{0.5} \quad \text{Equation 1.13}$$

The polar component of the hydrogel is obtained by rearranging Equation 1.9 to give :-

$$\gamma_{sv}^p = I_{sw}^2 / (4 \gamma_{wv}^p) \quad \text{Equation 1.14}$$

The equations shown were put into Macintosh WorksTM, (a spreadsheet and calculations computer program), which then enabled $(\gamma_{sv} - \gamma_{sw})$, I_{sw} , γ_{sv}^d , γ_{sv}^p , γ_{sv} and γ_{sw} to be calculated from contact angle measurements for the hydrogels.

It is also possible to determine the dispersive component of the surface free energy of hydrated hydrogels by using the Owens and Wendt equation, (Equation 1.5). This is achieved by determining the polar component of the surface free energy using Hamiltons method. The value of the polar component together with the experimentally determined water / air contact angles are substituted into the Owens and Wendt equation and the dispersive component calculated. Corkhill⁴¹ has shown that dispersive components obtained by this method and from Equation 1.13 are in good agreement (to within 0.2 mN/m), showing identical trends.

1.3 Mechanical Properties Of Hydrogels

Hydrogel polymers have been widely investigated for their use in biomedical applications, particularly in the area of soft contact lenses, which is the most successful commercial application for these materials. The tolerance of hydrogels in biological environments has been attributed to the imbibed water which gives the polymers the ability to simulate the hydrated characteristics of natural tissues. However, although water in these polymers enhances their general biotolerance with body tissues, it also makes the polymers mechanically weak, because the imbibed water acts as an internal plasticiser. This has

been overcome for some applications by crosslinking⁵⁷⁻⁶⁰, reinforcement with areas of crystallinity⁶¹, the formation of interpenetrating networks⁶² and the production of hydrogel composites^{63, 64}. Some of the techniques which have been used to investigate the mechanical properties of hydrogels are described below.

1.3.1 Tensile Testing

Perhaps the most widely used technique for the mechanical property determination of hydrogels is static tensile testing. It has been found that the tensile method of testing of hydrogels is sensitive to small changes in composition and/or sample preparation. For example Lee *et al*⁶⁵ used tensile testing to investigate the influence of tacticity on poly(HEMA) and Barnes *et al*⁶⁶ investigated the structure-property relationships of a series of hydroxyalkyl acrylate and methacrylate copolymers using tensile testing. It is because of the sensitivity of this technique that static tensile testing has been widely used to investigate the relationship between polymer structure and mechanical properties⁵⁷⁻⁶⁵. To determine the mechanical properties of hydrogels for use as biomaterials, the use of mechanical tensile tests is an extremely useful technique. The technique is simple to perform and data acquisition is rapid and the method has been applied to the samples prepared during this work. A description of the tensile testing methodology used during this work can be found in Chapter 2.

1.3.2 Compression Measurements

Another technique that has been used to investigate the mechanical characteristics of hydrogels is compression testing. Huglin *et al*⁶⁷⁻⁷⁰ used compression testing to investigate the compressive properties of hydrogels due to changes in the crosslink density and swelling behaviour.

1.3.3 Viscoelastic Measurements

Further investigations of structure-property relationships have been studied by viscoelastic measurements. Measurements of this type provide information to their mechanical

response with respect to time, temperature and previous loading history. Janacek⁷¹ and Migliaresi⁷² studied the viscoelastic behaviour of hydrogels.

Raab and Janacek⁷³ attempted to characterise the properties of poly(HEMA) in more detail by using tensile tests at different strain rates and temperatures for a series of hydrogels with different crosslink densities and developed a universal failure envelope for poly(HEMA).

Another mechanical characteristic of some importance which is often overlooked is the tear resistance or the fracture toughness of the polymer. Peppas⁷⁴ was perhaps the first to recognise this in hydrogel design, in his attempts to develop a synthetic articular cartilage. A fracture toughness approach has been used to compare the characteristics of commercially available hydrogel contact lenses by Jackson⁷⁵.

1.4 Protein Adsorption on Hydrogel Surfaces

For many biomedical applications of hydrogels the gel or material is in intimate contact with a biological fluid. An example being tear fluid on a contact lens. Within biological fluids are proteins, which are complex macromolecules possessing molecular weights which range from thousands to millions. Most proteins exist in aqueous solution and when placed in contact with another phase, proteins tend to accumulate at the interface. The accumulation of proteins at an interface produces proteinaceous deposits. Protein adsorption onto both hydrogel and non-hydrogel surfaces has been studied and Baker & Tighe⁷⁶ and Horbett^{77, 78} have compiled reviews on the adsorption of proteins to surfaces.

The mechanism of protein adsorption is a result of interactions between the different components acting across the interface, such as the polar and dispersive forces due to the polymer and / or protein. An important factor which influences protein adsorption is the surface energy of the material and the resulting interfacial tension between the material and

the biological fluid. Several workers have proposed theories which relate the surface energy of the hydrogel to lower levels of protein adsorption^{79, 80, 81}.

The hydrophilicity of the material has also been suggested as an important factor which affects the level of protein adsorption to surfaces⁸². Castillo *et al*⁸³ studied HEMA and HEMA-MAA hydrogels and observed that albumin denatured more slowly on the high water content HEMA-MAA copolymers. However, other work by Hosaka *et al*⁸⁴ on high water content materials made from HEMA-NVP copolymers has shown that the deposits were identical in type and amount to the deposits found on HEMA polymers.

The effect of surface charge was considered in an initial study of the strong effect of methacrylic acid, present as a contaminant in most HEMA preparations, on protein adsorption⁸⁵. The workers observed that the protein with the most positive charge at pH = 7.4 was adsorbed most strongly by the negatively charged methacrylic acid groups. More recently work has suggested that proteins with a net charge similar to the charge on the material surface will adsorb to localised patches of opposite charge on that surface⁸⁶ and that the driving force was an increase in entropy due to conformational changes of the protein although this explanation was insufficient for proteins which did not undergo significant structural rearrangement.

It is evident that protein adsorption to surfaces is a fundamental process in biomedical device and biological solution interactions and that the surface and environmental chemistry are significant in governing the processes that occur. It is clearly necessary to study and characterise the interactions of single protein and mixed protein solutions with synthetic biological materials to fully characterise the underlying mechanisms which determine protein adsorption.

1.5 Biocompatibility

Since the first discovery of poly(HEMA) as a material for biomedical applications¹, there has been a great deal of research into the factors that affect and govern the interactions of a synthetic material with natural tissue. The reason for this is to be able to design a material which is accepted by the environment and does not undergo any adverse reactions which result in rejection or failure of the material for its application. Materials that are currently in use are prone to deposition of proteins and other biological species which ultimately lead to the rejection of the material from its host application. Examples of these interactions which result in the rejection of a synthetic material include the formation of deposits on contact lenses which reduce visual clarity, decrease comfort and can be the cause of infections within the eye or deposits on materials for blood contacting applications, such as thrombus formation on artificial arteries which can clearly lead to more dramatic consequences. One stage is common to all processes of this type and that is protein deposition onto the synthetic substrates.

The surface energy of the synthetic material has been suggested as being an important parameter in predicting the biotolerance. In 1970 Baier *et al*⁸⁷ suggested that the blood compatibility was dependant upon the surface energy of the material. The workers proposed that a material with a moderate surface energy was required for compatibility. However, this theory was based on the measurements of the surface properties of polymers which had critical surface tensions in the range 20 - 30 mN/m which had been found to exhibit non-thrombogenicity, (compatibility with blood). However, after this initial work it has been found that there are exceptions to this theory.

Ratner *et al*⁷⁹ studied the interaction of blood components with a series of HEMA-ethyl methacrylate (EMA) copolymers and found that non-thrombogenic interactions were lower than for either of the homopolymers. It was therefore proposed that non-thrombogenicity was enhanced by a balance of polar and non-polar groups.

Andrade⁸⁰ produced an alternative theory referred to as the minimum interfacial energy hypothesis. It was suggested that for a material to exhibit compatibility with its biological environment that a low interfacial tension was required. More recently than this proposed work Andrade *et al* ⁸¹ studied a range of HEMA-methyl methacrylate (MMA) copolymers and concluded that the results obtained could not be explained in terms of a minimum interfacial energy hypothesis. It was therefore proposed that it was necessary to also consider the balance of polar and non-polar groups expressed at the surface as well as the interfacial energy.

More recently the incorporation of poly(ethylene oxide) has been investigated extensively for its use in biomedical devices and its effectiveness in reducing the adsorption of biological species is now widely recognised⁸⁸. A brief overview of poly(ethylene oxide) and its effectiveness is included here.

1.6 Poly(Ethylene Oxide)

As mentioned in section 1.3. compatibility and thrombogenesis are a major problem in biomaterials design and it is known that the incorporation of long poly(ethylene oxide) chains, with a degree of polymerisation of approximately 100, existing on the surface of hydrogels exhibit a superior, long-lasting antithrombogenicity⁸⁹⁻⁹². Work has shown that the percentage of poly(ethylene oxide) groups at the surface was independent of the poly(ethylene oxide) chain length, but protein and platelet adsorption are decreased with increasing chain length and that chain separation or surface coverage is also important. More recent work however, has shown degrees of polymerisation of 400 and above may be required in providing more effective protein resistance⁹³ and that a threshold concentration of poly(ethylene oxide) is required.

1.6.1 Poly(Ethylene Oxide) : A General Introduction

Poly(ethylene oxides), PEO or poly(ethylene glycols), PEG's as they are known, are materials which contain multiple -CH₂CH₂O- units. They are non-ionic materials which

exhibit complex solubility behaviour and interaction with solvents and polymer molecules. They clearly have a regular backbone structure which has few side chains. The polymer is therefore normally crystalline with melting points up to 70°C, but in the absence of crystallinity, the amorphous material exhibits a maximum glass transition temperature (T_g) of -60°C. Their solution properties have been reviewed^{94, 95} and their behaviour with water is quite different from the interaction with other solvents.

1.6.2 Application to Protein Resistant Coatings

PEO can be used to produce hydrogels or be incorporated with other monomers by a variety of techniques⁹⁶. There are two primary methods which have been used to synthesise polymers containing poly(ethylene oxides). These methods are copolymerisation with isocyanates to form a polyether polyurethane network and grafting of the poly(ethylene oxide) on to the polymer surface. In this study, however, methacrylate derivatives of poly(ethylene oxides) have been copolymerised with other vinylic monomers.

The importance of PEO in hydrogel chemistry has been recognised for its effectiveness for low protein adsorption and low cell adhesion⁹⁷. This is in part due to the hydrophilicity of PEO and its unique solubility properties, which produce surfaces in a liquid-like state because the polymer chains exhibit a large degree of flexibility and mobility^{94, 98, 99} and due to their lack of ionic charge¹⁰⁰. This has been observed using spectrophotometric techniques such as ESCA, or NMR under hydrated conditions and has shown that the thermal mobility of poly(ethylene oxide) chains is greater than that of other hydrophilic polymers such as poly(2-hydroxyethyl methacrylate) or poly(N-vinyl pyrrolidone). It is believed that this mobility of the poly(ethylene oxide) chains prevents the adhesion of proteins⁹⁹, since the rapid movement of the chains may prevent stagnation of the blood components on the surface of the hydrogel, thereby reducing the contact time of the components with the surface of the hydrogel. Since one of the requirements for irreversible adhesion is a certain amount of contact time, protein adsorption is decreased. There is also believed to be a thermodynamical volume restriction effect¹⁰¹, which results

in a repulsive force when a protein or other particle approaches the poly(ethylene oxide) surface. These effects are illustrated in Figure 1.6.

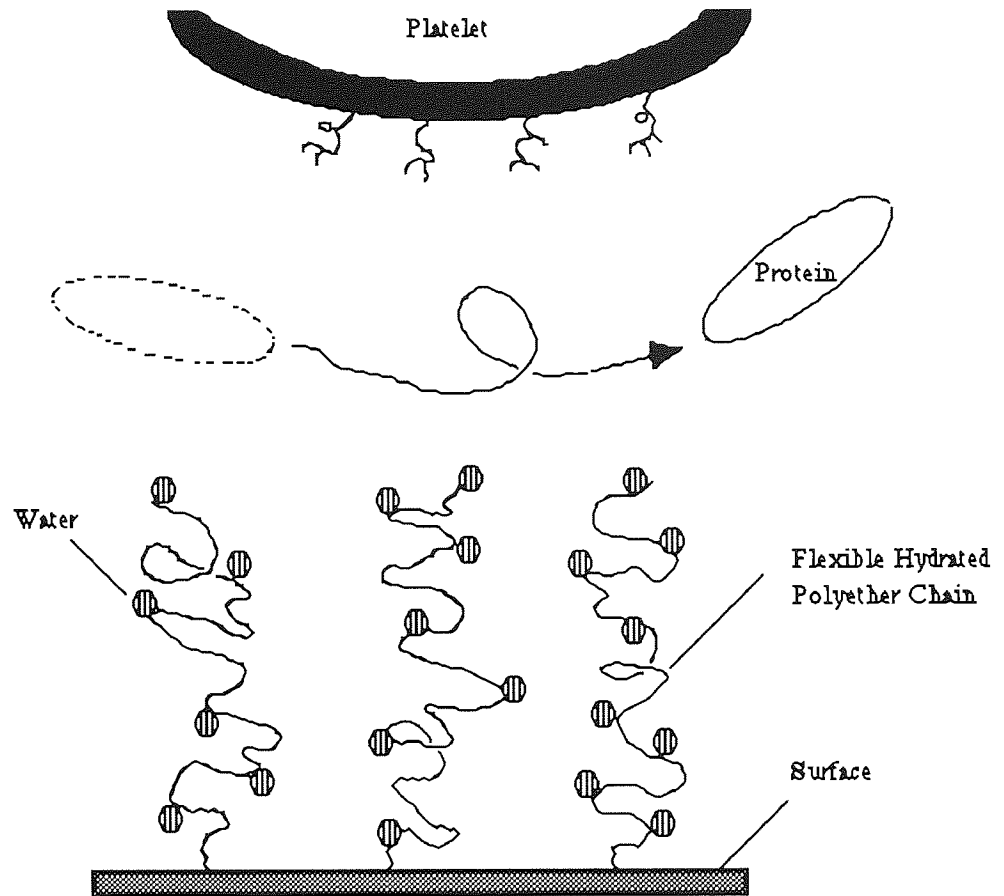


Figure 1.6 The interaction of blood components with hydrated poly (ethylene oxide) chains at the polymer surface (redrawn from reference 101)

The effect of the poly(ethylene oxide) chains has been used to study the influence of hydrophilic and hydrophobic balance on interfacial interactions of copolymers and blood components¹⁰², but a direct correlation between protein resistance and bulk hydrophilic and hydrophobic contents could not be made. Although it was concluded that the incorporation of poly(ethylene oxides) was effective in trying to produce a synthetic material which matches the thromboresistance of living endothelium (which is a biologically active hydrogel) and is highly wettable.

However, it has been found that there are limitations in producing stable poly(ethylene oxide) surfaces¹⁰³. Previous methods have involved using commercially available surfactants, but problems arose in the mixing of phases. In attempting to produce a stable, protein resistant poly(ethylene oxide) surface, studies investigated the effect of the weight percentage of poly(ethylene oxide) and the polarity of the mixed soft segment phase of copolymers¹⁰⁴ and found that the degree of mixing in the polymers increased with increasing poly(ethylene oxide) fraction, which in turn produced a lower concentration of soft segment at the polymer surface and therefore a less effective protein resistance. It was concluded that a threshold poly(ethylene oxide) concentration existed where a minimum poly(ethylene oxide) surface coverage is required. It has also been found that copolymers of alkyl methacrylates with methoxy (polyethylene oxide) methacrylates give effective protein resistance¹⁰⁵, although preparation of these surfaces is also questionable because of the differences in the copolymerisation parameters of the monomers used. Therefore, for effective surface production it was suggested that the copolymerisation parameters used be as similar as possible for all combinations of monomers¹⁰⁵ and that an optimum concentration of the (ethylene oxide) monomer be used.

1.7 The Effect Of Ion Incorporation On The Physical And Blood-Contacting Properties Of Hydrogels

As mentioned earlier there are several hypotheses for enhancing the blood contacting properties of polymers¹⁰⁶. One more recent method was developed by Sawyer who emphasised the role of the electrical properties of the surface¹⁰⁷. Sawyer studied the interactions of blood components on natural blood vessels and suggested that the vessel was thromboresistant due to the repulsion between negative charges on the vessel and within the blood component. Further to Sawyers work, Lelah *et al*¹⁰⁸ studied the blood compatibility of negatively charged polymers and found them to be relatively blood compatible. Heparin, a naturally occurring mucopolysaccharide displays unique anticoagulant activity and it is thought that this characteristic is due to the sulphate and

aminosulphate groups within the heparin molecule which give the molecule optimum surface electrical properties¹⁰⁹.

The incorporation of ion-containing groups onto a polymer backbone has been one method of improving the blood-contacting properties of a variety of polymers¹¹⁰. One method of introducing ions onto a polymer backbone is the incorporation of sulphobetaine monomers or polymers. Sulphobetaine polymers are macromolecules which contain a zwitterion or 'inner salt' in the polymer side chain. The potential of sulphobetaine based polymers as hydrogels was suggested by Salamone *et al*¹¹¹ who prepared polymers from vinylimidazolium sulphobetaines by free radical polymerisations. It has been found that the incorporation of such ion-containing groups onto a polymer backbone improves the blood contacting properties of a range of polymers and increases their wettability¹¹⁰. Previous studies investigating blood contacting properties have shown that carboxylate or sulphonate ionic groups improve antithrombotic activity, reduce complement activation and give lower platelet deposition and activation^{110, 112}, although too great a concentration when combined with other polar molecules at the hydrogel surface, such as poly(ethylene oxide), enhances the thrombogenicity of the polymer. The incorporation of ions also gives rise to coagulant behaviour. Jozefonwicz¹¹³ evaluated the anticoagulant behaviour of carboxylate and sulphonate derivatised polymers and concluded that the carboxylate polymers had a lower anticoagulant behaviour than the sulphonate containing analogues. These studies illustrated the dependence of the ionomer's biological activity on the polymer backbone structure, the ion type and the ion content.

Ion incorporation also effects the physical properties of the polymer. In general, the modified materials have greater tensile strength and modulus in the dehydrated state than the underivatised polymer and this is believed to be due to the clustering of the ionic groups which serve to act as physical crosslinks. However, upon swelling, ion incorporation increases the equilibrium water content and the water acts as a plasticiser thereby reducing the mechanical properties of the hydrated polymer. This can be a major

problem since hydrogels in general have poor mechanical properties to begin with, therefore, ion content must be selected to optimise the two effects.

1.8 Sequence Distribution Of Surface Groups

From the previous sections it can be seen that the presence of charged chemical groups, the balance of polar and dispersive forces and the presence of strongly water structuring, highly mobile groups are factors which affect the adsorption of proteins. Work within the Speciality Materials Research Group at Aston has found that polymers containing long repeat units or long sequences of individual monomer units have a greater tendency to produce non-specific protein adsorption than polymers which mimic the molecular architecture of naturally occurring polymers by possessing regular, short sequences of monomer units¹¹⁴.

It has been shown that protein adhesion requires areas of surface chemistry which are large enough to achieve stable physicochemical interactions between the protein and the material surface¹¹⁵⁻¹¹⁷. The work suggests that biological cells of a particular type are able to form adhesive focal or contact points on a surface, but require a specific chemistry and area to adhere permanently. If a zone of contact is too small and too far apart from another equivalent zone then the cells are unable to spread and unable to attain adhesion.

Lai¹¹⁸ has also investigated the adsorption of adhesion proteins and platelets onto copolymer surfaces using immuno-technology methods. It was shown that preferential adsorption was affected by the surface distribution of chemical groups and that surface domains as small as nanometre scale were critical in determining adsorption.

It is therefore necessary to consider the sequence distribution and the length of the monomer sequences formed in a copolymerisation, together with the criteria mentioned earlier if protein adsorption to biomaterials is to be fully understood.

1.9 Copolymer Composition

It is evident from the extensive research conducted into the reasons for and the theories to prevent protein adsorption to hydrogel surfaces that a balance of chemical structure, charge and chemistry is required. Work in these laboratories has shown that polymers containing chemical domains of one molecular type display increased levels of protein deposition. It is therefore useful to be able to predict the order of chemical constituents at different compositions within the polymer to provide an indication that the formation of blocks of one component are avoided. A computer program simulating free radical copolymerisation has been developed at this university which is able to simulate copolymer or terpolymer reactions. The background to its development is given below.

1.9.1 Historical Background

Attempts for producing computer simulations of copolymers generally rely on the two primary structural variables which can be used to describe the polymer chains. Firstly, the copolymer composition which gives the relative proportions of each comonomer and secondly, the comonomer sequence distribution which gives the order of the comonomer units. The difficulty in producing accurate figures for the composition and the distribution of the comonomers is in the understanding of the kinetics of the polymerisation reaction. The historical background to the current theories of reaction kinetics suggests that complex reactions are derived from simple basic processes involving two molecules. This concept for the formation of macromolecules via a succession of reactions was first considered in 1915 by Ostromysslensky¹¹⁹ who studied the 'stepwise' synthesis of hydrocarbon polymers and was opposed by the view of Staudinger¹²⁰ who proposed the theory of a chain reaction. Several kinetic models have been postulated and are described in the literature¹²²⁻¹²⁴.

The stepwise polymerisation considers the intermediate species to possess approximately the same reactivity as the unreacted monomer, therefore each step of the process occurs with an equal degree of reactivity. Alternatively, the 'chain' polymerisation begins with an

initial slow step to form the reactive intermediate and is succeeded by rapid growth reactions. In this situation the reaction intermediates are chemically similar but of differing molecular sizes. This theory essentially became the basis of vinyl polymerisations and is still used today. The mechanism was further developed upon the realisation that such a mechanism need not necessarily involve free radicals, but under different conditions the intermediates formed involved the formation of ions. This was first proposed by Whitmore¹²⁵ who attempted to account for the acid initiated polymerisation of isobutylene.

1.9.2 Terminal Model of Polymerisation

The standard kinetic treatment of free radical polymerisation was further developed by Alfrey and Goldfinger in 1943. They proposed that the rate constant for the addition of each monomer unit was dependant on the chemical nature of the terminal unit of the growing polymer chain. The model consists of four propagation steps,



where : M = monomer
 M[•] = monomer radical
 k = rate constant
 [] = concentration

Alfrey and Goldfinger used these elementary steps to derive an overall expression for the conversion of monomer to polymer, shown in Equation 1.19 :-

$$\frac{\delta[M_1]}{\delta[M_2]} = \frac{[M_1] \cdot r_1[M_1] + [M_2]}{[M_2] [M_1] + r_2[M_2]} \quad \text{Equation 1.19}$$

The influence of the reactivity ratios on the polymer composition is evident in this equation and four limiting situations on the mechanism of the polymerisation can be considered.

The first two cases are when the two monomers have the same values of the reactivity ratios. Firstly, if $r_1 \approx r_2 \approx 1$ then Equation 1.19 simplifies to :-

$$\frac{\delta[M_1]}{\delta[M_2]} = \frac{[M_1]}{[M_2]} \quad \text{Equation 1.20}$$

This equation indicates that each of the terminal radical units show no preference for either of the unreacted monomers and the relative rates of the monomer consumption are determined by the feed composition. If $r_1 \approx r_2 \approx 0$ then Equation 1.19 becomes :-

$$\frac{\delta[M_1]}{\delta[M_2]} = \frac{[M_1] \cdot [M_2]}{[M_2] \cdot [M_1]} \quad \text{Equation 1.21}$$

In this case each of the radical centres exhibit a preference for cross propagation and therefore produce an alternating composition.

The remaining two situations arise from r_1 and r_2 having different degrees of reactivity. For example, if $r_1 > 1$ and $r_2 < 1$ then the radical centre prefers to add to unreacted monomer M_1 and the copolymer becomes enriched in monomer 1, irrespective of the feed composition. However, a unique case arises when the product of r_1 and r_2 is one, because both radical centres have an equal preference of addition to each of the monomers. This situation has been referred to as 'Ideal Copolymerisation' as it is a completely random process.

The final situation is that when $r_1 < 1$ and $r_2 < 1$. These reactivities give rise to cross propagation, but the preference is not absolute. The result is a tendency towards an alternating copolymer structure which increases as r_1 and r_2 tend to zero.

The terminal model is extremely useful in describing the compositions of copolymers prepared from vinyl monomers with varying structure and reactivities and Ashraf¹¹⁴ has provided experimental evidence for the accuracy of the computer simulations of copolymers based on this method.

1.9.3 Reactivity Ratios And The Q-e Scheme

To be able to use the computer simulation program in this work the reactivity ratios r_1 and r_2 for the monomers used must be known. In most cases the values are obtained for experimentally determined values which are quoted in the literature, but on some occasions the values may not be known. A method which is used to overcome this difficulty and the lengthy experimental procedure required to determine the reactivity ratios is an approximation technique known as the Q-e scheme^{126, 127}. The scheme was developed to quantify the polar and resonance stabilisation effects which influence copolymerisation reactions.

The reactants in a copolymerisation are assigned values e_1 and e_2 respectively to represent their charges. Identical charges are assumed for a monomer and the radical it produces. The general reactivities of the radicals and monomers are denoted by P and Q respectively and the rate of reaction was determined by the quantities P_1 , Q_1 , e_1 and e_2 as indicated in equation 1.22 :-

$$k_{12} = P_1 \cdot Q_1 \exp(-e_1 \cdot e_2) \quad \text{Equation 1.22}$$

Four such equations are obtained for the propagation steps outlined in equations 1.15 - 1.18 which can be combined and rearranged to give :-

$$r_1 = (Q_1/Q_2) \exp[-e_1(-e_1-e_2)] \quad \text{Equation 1.23}$$

and

$$r_2 = (Q_2/Q_1) \exp[-e_2(-e_1-e_2)] \quad \text{Equation 1.24}$$

Combination of equations 1.23 and 1.24 gives :-

$$r_1 \cdot r_2 = \exp[-(e_1-e_2)^2] \quad \text{Equation 1.25}$$

The use of the Q-e scheme enables theoretical predictions to be made for the reactivity ratios for a pair of vinyl monomers which have not been studied experimentally.

1.10 Scope And Objectives Of This Work

The initial aim of this project was to synthesise a range of vinyl based hydrogels containing monomers whose characteristics had been shown or would be expected to affect the interaction of hydrogel surfaces with biological species such as proteins and lipids.

The first step was to synthesise and characterise hydrogels based on acryloylmorpholine. There were a number of reasons for this. Acryloylmorpholine has been described as a hydrophilic monomer¹²⁸, but has no definite usage examples. Acryloylmorpholine bears structural similarities to N-vinyl pyrrolidone and N,N-dimethylacrylamide, two monomers which have been widely investigated in the production of high water content (equilibrium water content >55%) hydrogels. N-vinyl pyrrolidone is used widely in the production of hydrogels for commercial contact lens applications, but its hydrogels have been shown to be prone to deposition of biological debris¹¹⁴ due to the formation of domains of one chemical type within its copolymers. Acryloylmorpholine has a greater reactivity ratio than N-vinyl pyrrolidone towards vinyl polymerisations and therefore acryloylmorpholine was investigated as a potential hydrophilic monomer for the production of high equilibrium water content hydrogels which might be expected to exhibit lower levels of protein adsorption than copolymers made with N-vinyl pyrrolidone.

N,N-dimethyl acrylamide was also used as a monomer for comparison with acryloylmorpholine, to investigate the mechanical integrity of hydrogels containing acryloylmorpholine. The reason for this is N,N-dimethyl acrylamide is well known for undergoing chain transfer reactions, via pendant methyl groups, during vinyl polymerisations. As a result mechanically imperfect networks are produced which give poor values for the mechanical properties of N,N-dimethyl acrylamide containing copolymers. By virtue of the ring structure within acryloylmorpholine it is sterically unlikely that chain transfer reactions via the pendant group would occur and therefore mechanical integrity of the copolymer network would be maintained.

The second part of this work was to synthesise a range of hydrogels containing chemical groups possessing charged monomer units. The reason for this was the literature survey illustrated that the incorporation of ionic charge has been shown to enhance the thrombogenicity of hydrogels. It was hoped that the incorporation of charged monomer groups within vinyl polymer hydrogels would produce novel hydrogel polymers with interesting surface properties. The surface properties would in turn govern the interactions between the hydrogel surface and biological moieties.

In addition a range of polymers incorporating polyethers were investigated. The literature survey demonstrated the use of polyethers in biomedical materials for reducing the amount of proteins deposited on surfaces incorporating these structures. Therefore hydrogels containing polyethers were synthesised and characterised for their potential as biomedical materials.

By characterising the hydrogel materials mentioned previously, it was hoped that the information derived from this study would enable biomaterials to be designed which exhibited improved compatibility, by virtue of lower amounts of protein adhesion, within a biological environment.

CHAPTER 2

Materials and Experimental Techniques

2.1 Materials

The materials used for this work are listed in Table 2.1 and their structures are shown in Figure 2.1. Before use, all liquid monomers were purified to remove the inhibitor using reduced pressure distillation as described in the literature¹²⁹. The inhibitor in methyl methacrylate was removed with two caustic washes followed by drying overnight over magnesium sulphate.

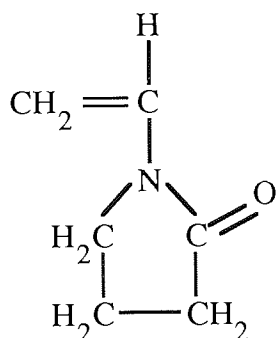
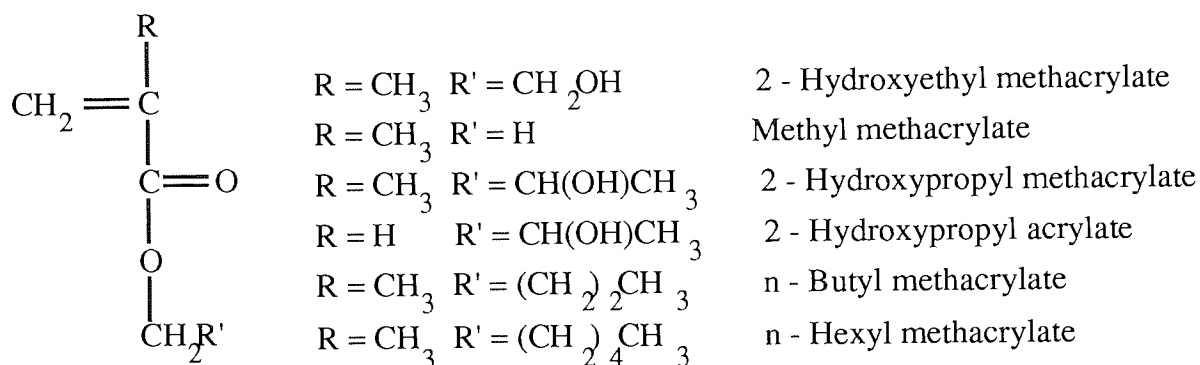
Table 2.1 Molecular weights and suppliers of reagents used

Monomer	M.Wt	Abbreviation	Supplier
2-hydroxyethyl methacrylate	130	HEMA	International Speciality Chemicals
Methyl methacrylate	100	MMA	Vickers Laboratories
N-vinyl pyrrolidone	111	NVP	Vickers Laboratories
N,N-dimethyl acrylamide	99	NNDMA	BDH
Acryloylmorpholine	141	AMO	Kohjin Co. Ltd.
Methoxy polyethylene glycol x methacrylate, where x = 200, 400 or 1000 M.Wt	300 500 1100	MPEG x MA	Polysciences
Hydroxyethyl methacrylate x ethylene oxide, where x= 4, 5 or 10 repeat units	354 594	HEMA x EO	Polysciences
Polyethylene glycol x dimethacrylate, where x = 200, 400 or 1000 M.Wt	398 498 1098	PEG x DMA	Polysciences
Ethyleneglycol dimethacrylate	198	EGDMA	BDH
N-(3-sulfopropyl)-N- methacryloxyethyl-N, N- dimethyl ammonium betaine	250	SPE	Scientific Polymer Products
Itaconic acid	130	ITC	Aldrich
Methacrylic acid	86	MAA	Aldrich

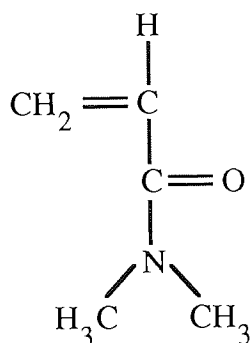
Table 2.1 (continued) Molecular weights and suppliers of reagents used

1-vinyl imidazole	94	NVI	Aldrich
Iso-bornyl methacrylate	209	isoBORMA	Scientific Polymer Products
Tertiary-butyl methacrylate	142	tBUTMA	Scientific Polymer Products
Cyclo-hexyl methacrylate	167	CHEXMA	Scientific Polymer Products
Benzyl methacrylate	162	BENZMA	Scientific Polymer Products
2,4,6-triallyloxy-s-triazine	249	TAC	Aldrich
N,N-diallyl-tartardiamide	228	TAR	Aldrich

Figure 2.1 Structures of reagents used

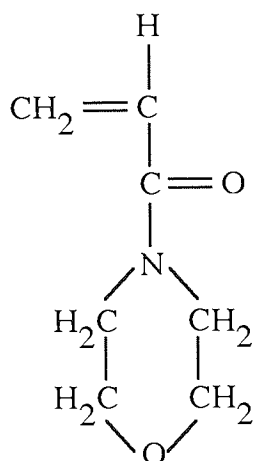


N - vinyl pyrrolidone

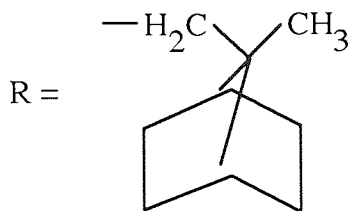
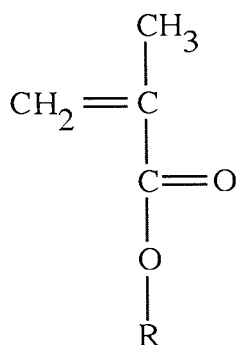


N,N' dimethyl acrylamide

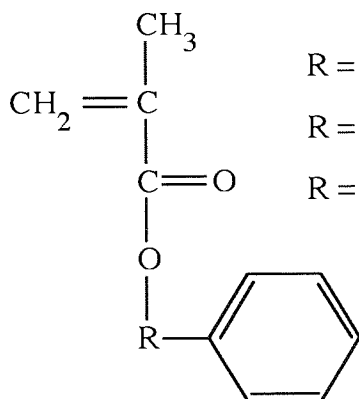
Figure 2.1 (continued) Structures of reagents used



Acryloylmorpholine



iso-Bornyl methacrylate



R = CH₂

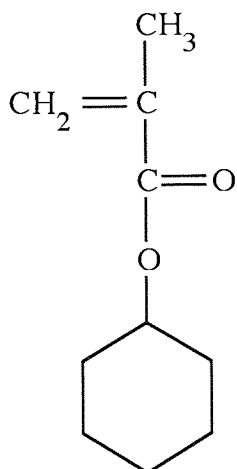
R = (CH₂)₃

R = (CH₂)₃O

Benzyl methacrylate

2-Phenyl ethyl methacrylate

Phenoxyethyl methacrylate



Cyclohexyl methacrylate

Figure 2.1 (continued) Structures of reagents used

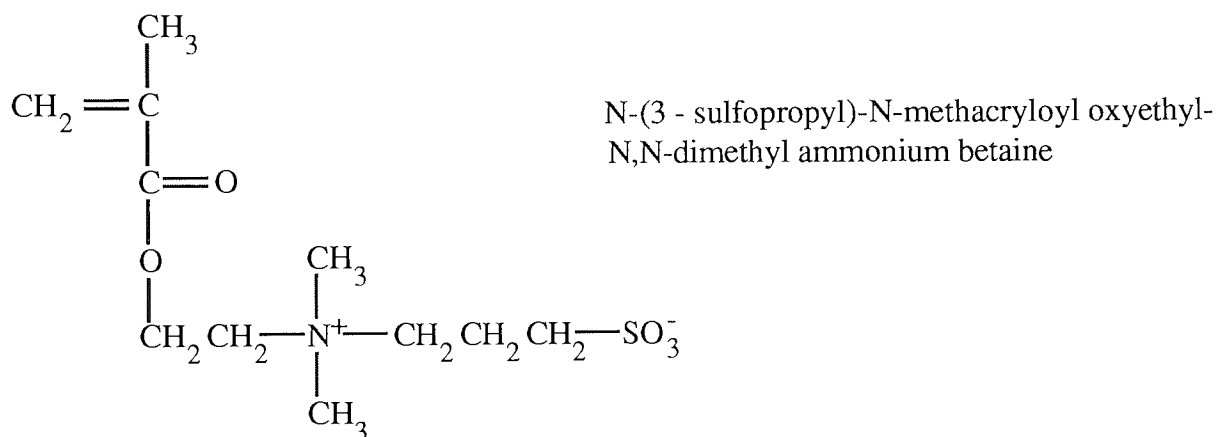
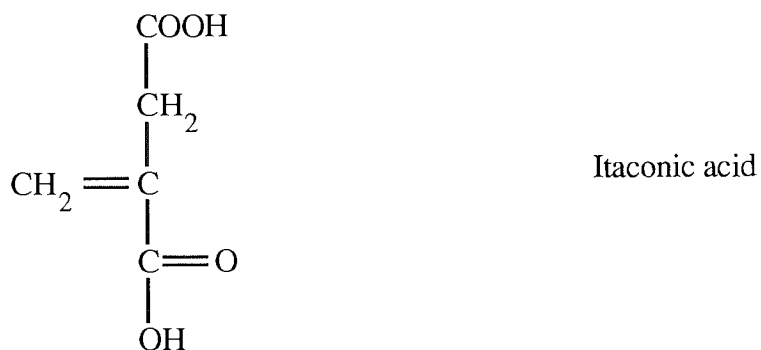
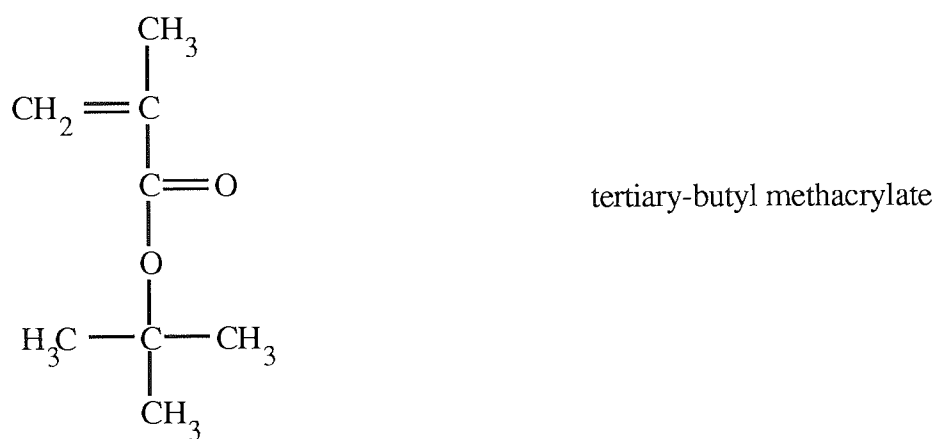
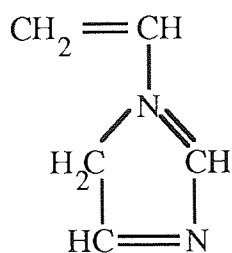
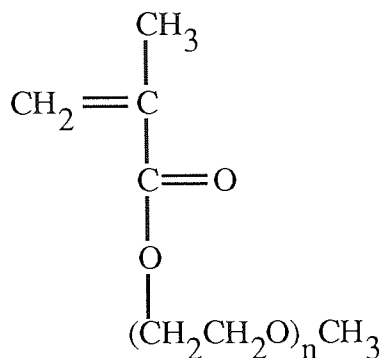


Figure 2.1 (continued) Structures of reagents used



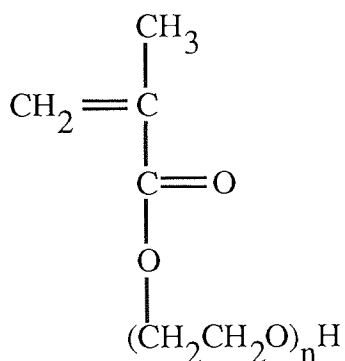
N - vinyl imidazole



n = 4 to 5 MPEG 200 MA

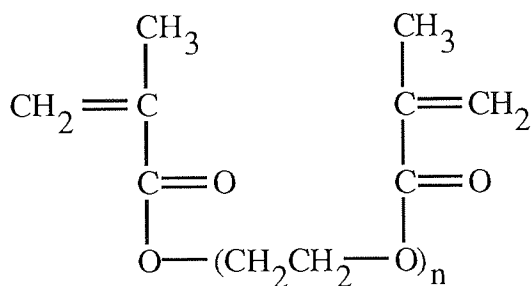
n = 9 to 10 MPEG 400 MA

n = 22 to 23 MPEG 1000 MA



n = 5 to 6 HEMA 4,5 EO

n = 10 PEGMA 10 EO

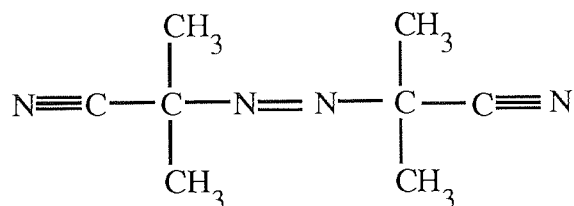


n = 1 Ethylene glycol dimethacrylate

n = 4 to 5 Polyethylene glycol 200 dimethacrylate

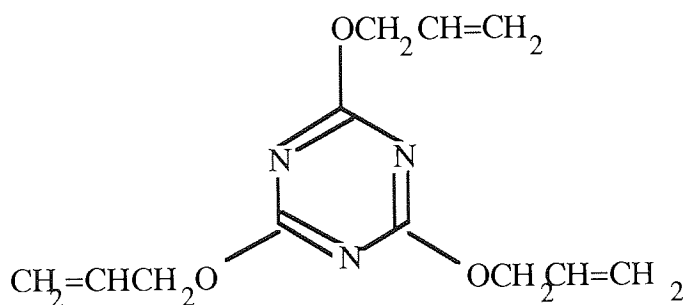
n = 9 to 10 Polyethylene glycol 400 dimethacrylate

n = 22 to 23 Polyethylene glycol 1000 dimethacrylate

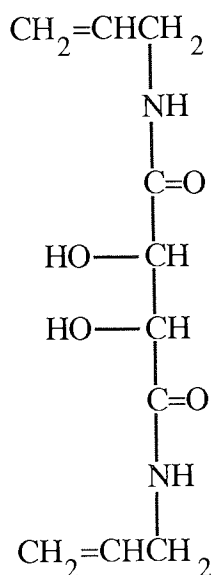


Azo -bis - isobutyronitrile

Figure 2.1 (continued) Structures of reagents used



2,4,6-Triallyloxy-s-triazine



N,N-Diallyltartardiamide

2.2 Polymer Synthesis

2.2.1 Preparation Of Hydrogel Polymer Membranes

Hydrogel polymer membranes were prepared using the cell shown in Figure 2.2. The cell consisted of two glass plates (15 x 10cm) which were each covered with a sheet of 'Melinex', (poly (ethylene terephthalate)) to prevent adhesion of the polymer membrane to the glass plates. The covered glass plates were placed face to face and separated by two polyethylene gaskets (0.2mm thick). To obtain membranes of different thicknesses the number of polyethylene gaskets was altered accordingly. The cell was then clamped together using spring clips.

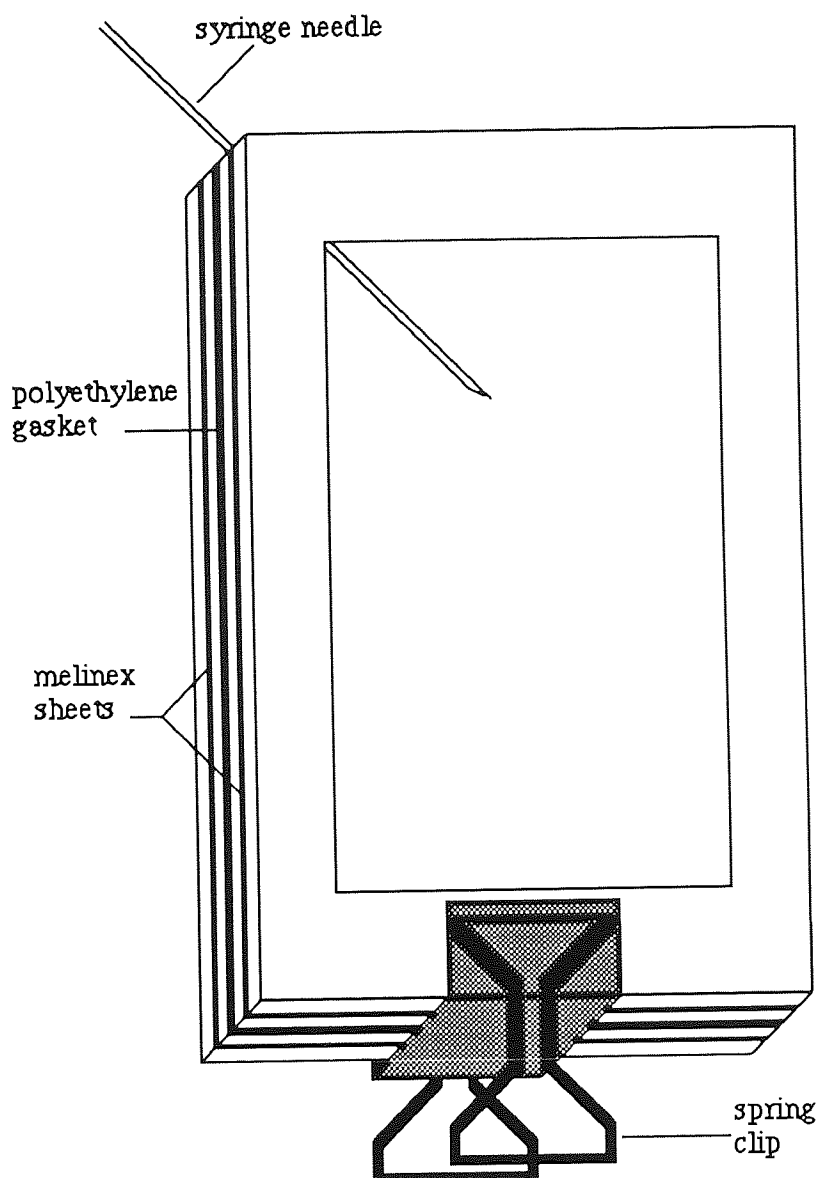


Figure 2.2 Diagram of a membrane mould

Purified liquid monomers were mixed together to obtain a homogeneous solution; in the case of solid monomers it was necessary to use a diluent to ensure homogeneity. The appropriate quantity of cross linking monomer was added and the resulting solution was outgassed with a nitrogen bleed for 5 minutes. After degassing, approximately 0.5w/w % of initiator was dissolved in the monomer solution. The resulting mixture of monomers, cross linkers and initiators was injected into the cell using a G22 syringe and needle. The cell was then placed into a 60°C oven for 3 days to allow polymerisation. Following this the cell was removed and placed into a 90°C oven for a post-cure period of 2-3 hours.

Upon completion of the required curing time the spring clips were removed and the glass plates and the 'Melinex' sheets were carefully removed from the polymer film. The film was then hydrated for two weeks by soaking it in a tray of distilled water. In some cases the 'Melinex' sheets could not be removed without fracturing the polymer film. To overcome this the hydration procedure was employed on the polymer film with the 'Melinex' sheets still in place; this allowed for easier removal of the sheets. The distilled water was changed daily to ensure the complete removal of any unreacted monomer residues or any diluents used in the polymerisation process. After the required soaking period the equilibrium water content of the hydrogel polymer membranes was determined.

2.2.2 Solution Polymerisation

Solution polymerisations were used to carry out free radical polymerisations of linear polymers. The polymerisation was performed using the apparatus shown in Figure 2.3. A 500ml reaction flask which was equipped with an overhead stirrer, water condenser, thermometer, dropping funnel and nitrogen bleed and was suspended in a temperature-controlled water bath at 60°C for a period of eight hours. In a typical reaction 200ml of methanol was added to the reaction flask. Nitrogen was bubbled through the solution in the reaction flask throughout the reaction. A homogeneous mixture consisting of 25grams of the liquid monomers and 0.5% weight / weight initiator dissolved in 50ml of methanol, (which had previously been outgassed with nitrogen) was added dropwise to the reaction flask. The mixture was refluxed at 60°C with continuous stirring for eight hours. Following this, the contents of the reaction flask were allowed to cool and then added dropwise with continuous stirring to 1 litre of ether which had been previously cooled using solid carbon dioxide. A fine white precipitate was formed. The precipitate was filtered, washed with ether and finally dried in a vacuum oven at 60°C.

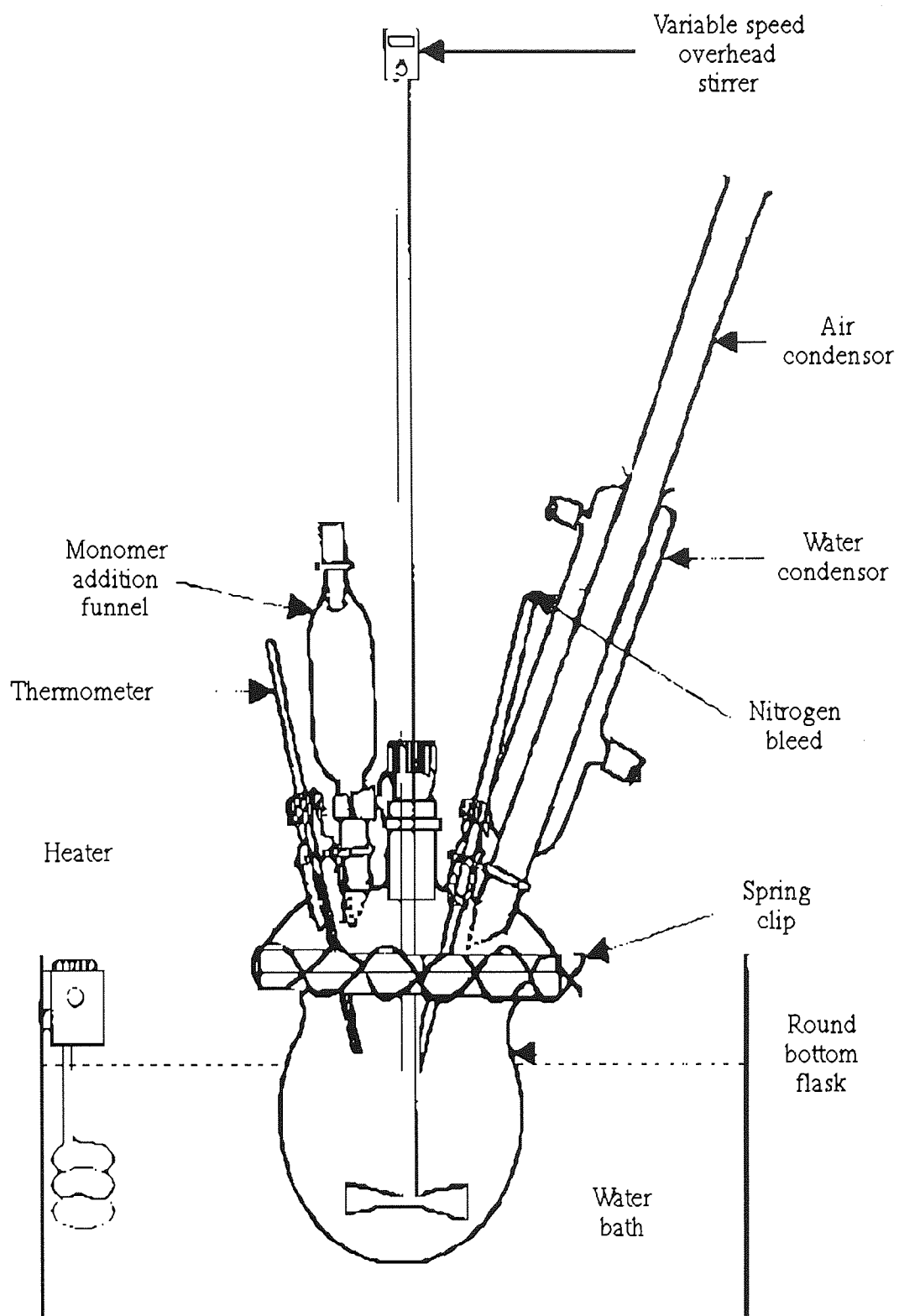


Figure 2.3 Diagram of solution polymerisation apparatus

2.3 Determination of the Equilibrium Water Content (EWC)

The EWC was determined using a weight difference method. Disks were cut from a hydrated sheet of hydrogel using a size seven cork borer. Any surface water on the sample was carefully removed by blotting with a piece of filter paper. The sample was weighed on an electronic balance. A minimum of 5 disks were used from each sheet in order to gain an average value for the sheet.

After weighing, the hydrated samples were dehydrated in a microwave oven for 10 minutes. The samples were then immediately reweighed to obtain their dehydrated sample weight. The EWC was calculated using Equation 2.1 below and the final quoted EWC was the average value taken from the number of samples used.

$$\text{EWC} = \frac{\text{Weight of water in gel}}{\text{Total weight of hydrated gel}} \times 100\% \quad \text{Equation 2.1}$$

The accuracy of this technique depends on the assumption that upon dehydration no water remains within the sample. A more sensitive method of determining traces of water in hydrogels is the Karl Fischer titration¹³⁰. This has been used as a rapid method of EWC determination and was used previously in confirming the validity of the dehydration and gravimetric technique described here⁴¹.

2.4 Differential Scanning Calorimetry (DSC)

DSC thermograms were obtained using a Perkin-Elmer differential scanning calorimeter, DSC7, which was fitted with a liquid nitrogen sub ambient accessory. DSC was developed in 1964 by Perkin-Elmer. In conventional differential thermal analysis (DTA) the difference in temperature between the sample and reference materials is measured, whereas in DSC the energy required to maintain both the sample and reference materials at the same temperature is measured. This means that for an endothermic transition such as the glass transition temperature, the energy input to the sample is increased to equalise the temperature difference and for exothermic transitions the energy input to the reference is increased. The glass transition temperature is therefore obtained from a change in the heat

flow to the sample. A schematic representation of a DSC calorimeter is shown in Figure 2.4 and a typical thermogram from a DSC experiment is shown in Figure 2.5.

DSC was used to determine the glass transition temperature of dehydrated hydrogel membranes. The dehydrated samples were cut to size using a size 1 cork borer and placed into an aluminium pan which was then sealed. The pan was placed into the sample holder of the thermal analyser unit. The sample was heated rapidly to a temperature above its glass transition temperature to quench the material. This was followed by a cooling cycle to -10°C and a final controlled heating of the sample was applied at a rate of $10^{\circ}\text{C}\cdot\text{min}^{-1}$. The glass transition was observed as a positive change in the resulting endotherm. The method was repeated at least five times for each particular sample.

DSC was also used to determine the freezing water contents of the hydrogel polymer membranes. 1-4mg samples of the polymers were cut from membranes using a size 1 cork borer. Surface water was carefully removed from the sample by blotting with filter paper and the sample was weighed. The sample was then placed into an aluminium pan which was sealed. The pan was then placed into the sample holder of the thermal analyser unit. The sample was cooled to -50°C and allowed to reach equilibrium. The sample was then heated to -20°C at a rate of $20^{\circ}\text{C}\cdot\text{min}^{-1}$ and subsequently heated to room temperature at a rate of $10^{\circ}\text{C}\cdot\text{min}^{-1}$. The $10^{\circ}\text{C}\cdot\text{min}^{-1}$ heating rate was used over the temperature range to be studied because this condition offered the maximum resolution and sensitivity available. The resulting thermogram was used to determine the proportion of freezing water. The area obtained under the melting peak corresponds to the quantity of energy required to melt the water which was frozen in the sample. The value of this endotherm was measured and the amount of freezing water in the sample, expressed as a percentage, was calculated using the following equation;

$$\% \text{ freezing water} = \frac{\text{energy required to melt the water in 1g of sample}}{\text{energy required to melt 1g of pure water}} \times 100\%$$

Equation 2.2

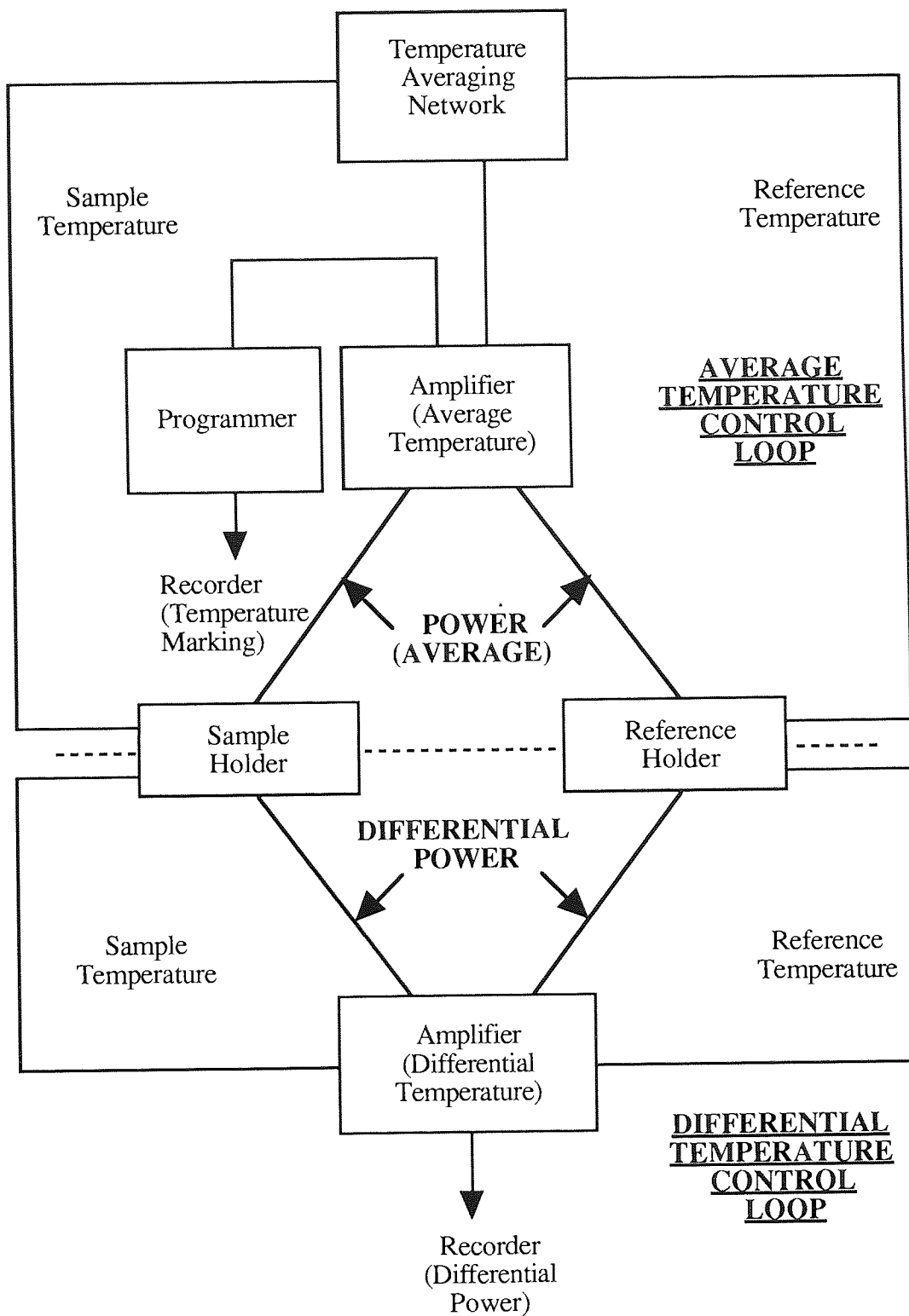


Figure 2.4 Schematic representation of a Differential Scanning Calorimeter (DSC)

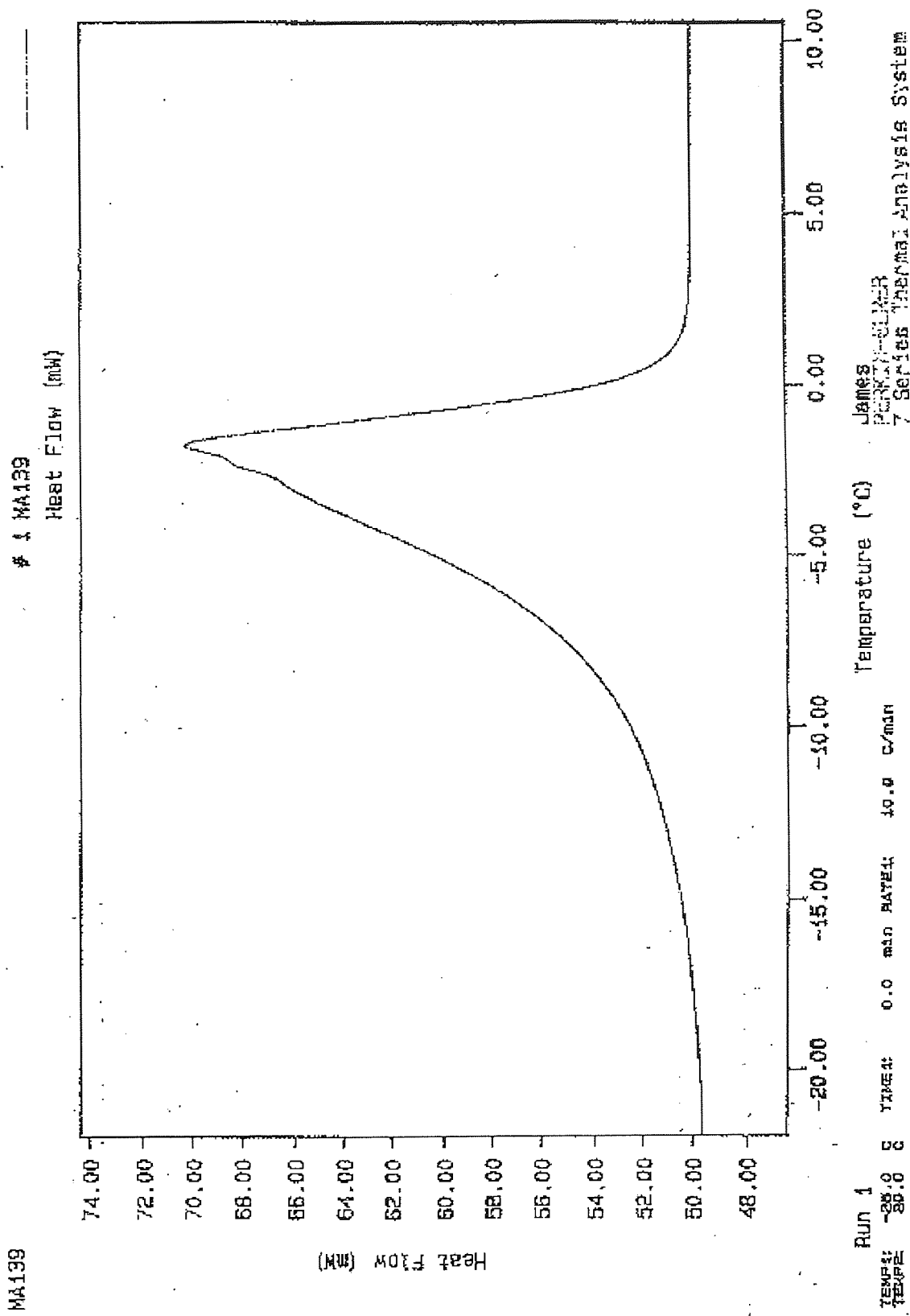


Figure 2.5 Typical thermogram of a DSC experiment

2.5 Thermal Mechanical Analysis (TMA)

TMA was used to determine the glass transition temperatures of dehydrated polymer membranes. A schematic diagram of a TMA is shown in Figure 2.6. The hydrated membranes were cut in to disks using a size 3 cork borer and dehydrated in a microwave oven for 10 minutes. The samples were then stored overnight in a vacuum oven before use. The sample was placed horizontally on to the sample platform and the furnace was brought in to a raised position around the sample. The sample probe was lowered onto the sample under a constant force and the probe was allowed to reach an equilibrium position. The samples were then heated to a temperature above the glass transition temperature of the sample at a rate of $10^{\circ}\text{C}\cdot\text{min}^{-1}$. The glass transition temperature was observed at the point when the sample probe showed a large penetration depth into the sample. A typical trace is shown in Figure 2.7.

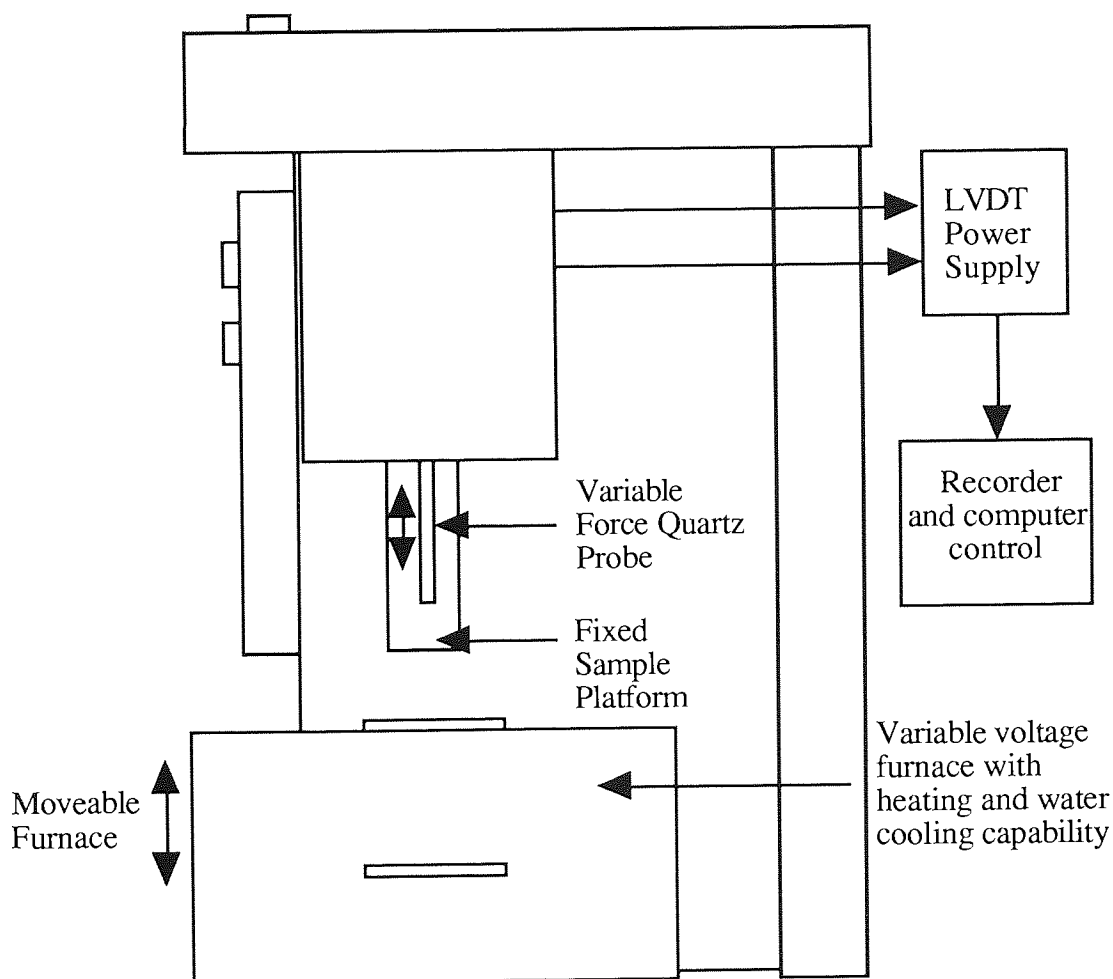


Figure 2.6 Diagram of a Thermal Mechanical Analyser (TMA)

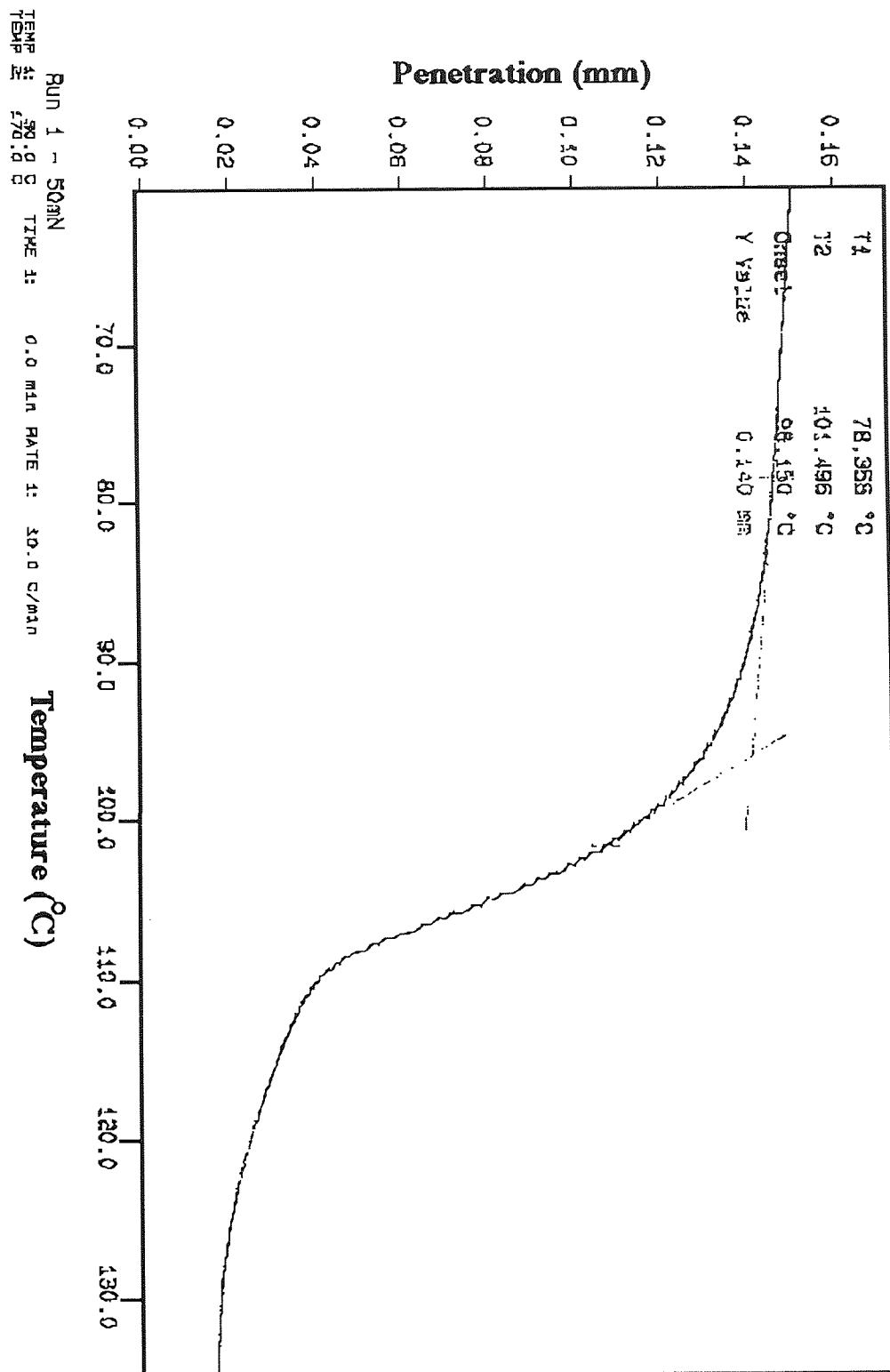


Figure 2.7 Sample trace from a Thermal Mechanical Analysis (TMA) experiment

2.6 Mechanical Properties

The mechanical properties of the hydrogel samples were investigated using a Hounsfield HTi tensometer which was interfaced to an IBM 55SX computer. The tensometer was fitted with a 10N load cell attached to the instrument crosshead which moved in a vertical plane. A clamp was suspended from the load cell by a chain and was directly above the lower clamp which was permanently attached to the tensometer. The relative positions of the clamps enabled the sample to be held in a vertical position. The gap between the sample clamps was adjusted to the required sample size by raising or lowering the crosshead. The crosshead speed and the maximum tensile force exerted on the sample were controlled by conditions entered into the computer. Samples to be examined were placed into the sample clamps in the vertical position. The crosshead was raised at a predetermined speed until the sample broke completely. The validity of this technique and its protocol has been discussed in greater detail¹³¹ by Trevett who studied the application of tensile testing to the determination of the mechanical properties of hydrogel samples.

Samples to be examined were cut from a hydrated membrane sheet into dumbbell shaped test pieces of gauge length 8mm and width 3.3mm using a purposely designed cutting tool. The cross section of this tool is shown in Figure 2.8.

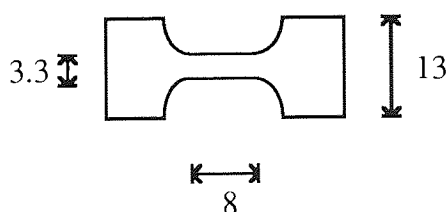


Figure 2.8 Cross section of the cutting tool used for sample preparation

The test pieces were equilibrated in distilled water to ensure complete hydration for testing. The sample thickness was measured using a micrometer and test pieces of known thickness were clamped into the sample jaws of the tensometer. A test speed of $10\text{mm}\cdot\text{min}^{-1}$ and maximum tensile force of 10N was used under conditions of room temperature and pressure. To maintain the test pieces in a hydrated state (measured

humidity of 100%) samples were sprayed with distilled water before and during the test. A computer program calculated the Young's modulus (E_m), tensile strength at break (T_s) and elongation at break (E_b). The values were calculated using the following equations:-

$$\text{Elastic modulus (E)} = \frac{\text{stress}}{\text{strain}} \quad \text{Equation 2.3}$$

where

$$\text{stress } (\epsilon) = \frac{\text{load}}{\text{cross-sectional area}} \quad \text{Equation 2.4}$$

and

$$\text{strain } (e) = \frac{\text{extension of gauge length}}{\text{original gauge length}} \quad \text{Equation 2.5}$$

$$\text{Tensile strength } (\sigma_b) = \frac{\text{load at break}}{\text{cross sectional area}} \quad \text{Equation 2.6}$$

$$\text{Elongation at break} = \frac{\text{extension of gauge length}}{\text{original gauge length}} \times 100 \% \quad \text{Equation 2.7}$$

An example of a stress-strain curve obtained from tensometer experiments is shown below

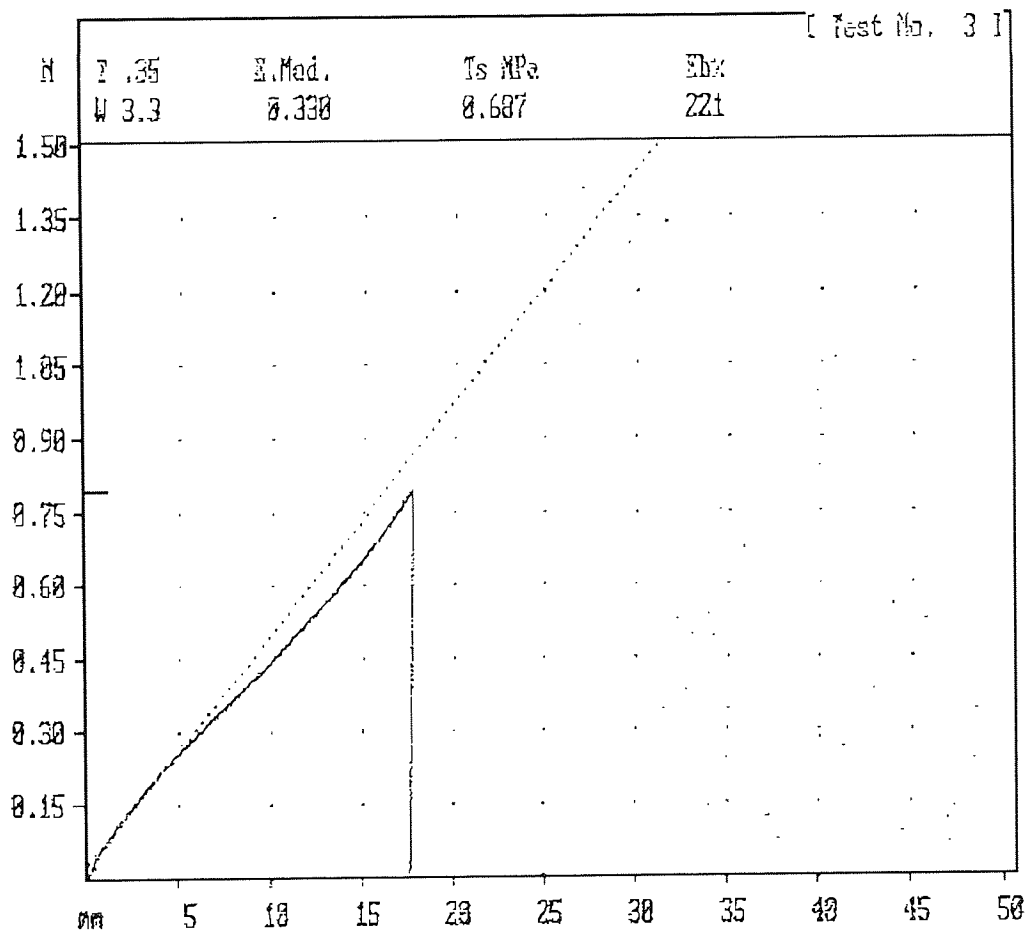


Figure 2.9 Example of a stress-strain curve from a tensometer experiment

2.7 Surface Properties

The surface energies of the hydrogels studied were obtained in the dehydrated state using the conventional sessile drop technique and in the hydrated state using the Hamilton and captive air bubble methods. These methods are described below. The theory used to determine the surface energy from contact angle measurements has been previously discussed in Chapter 1.

2.7.1 Sessile Drop Technique

Disks of hydrated hydrogel were cut from the polymer membrane using a size 7 cork borer. Before any contact angle measurements were made the polymer surface was cleaned with a Teepol detergent solution. The polymer was rinsed thoroughly and allowed to soak in distilled water overnight. After soaking, the polymer samples were dehydrated in a microwave oven for ten minutes and stored in a dessicator prior to use. The samples were mounted horizontally onto a microscope slide and a drop of distilled water was placed on to the hydrogel surface using a G25 syringe needle.

The contact angle was measured directly using the Rame-Hart contact angle Goniometer model 100-00 eyepiece. A minimum of 5 disks of each hydrogel were used. A second set of contact angles were determined using methylene iodide and the hydrogel. This was achieved by repeating the process described for determining contact angles between sample and distilled water, but replacing the distilled water with methylene iodide.

The two sets of contact angles were then used to determine the total surface free energy, the polar and dispersive components of the surface free energy using Macintosh Works™ which was programmed with the appropriate equations outlined in Chapter 1.

2.7.2 Hamilton Method

Hydrated hydrogel samples were cut into disks using a size 7 cork borer. Surface water was removed from one side of the hydrogel sample by blotting with a piece of filter paper.

The sample was mounted onto a glass microscope slide and suspended in an inverted position in a glass cell with optically perfect sides. The cell was filled with distilled water which was saturated with n-octane and a drop of n-octane was placed onto the surface of the hydrogel sample using a G25 syringe needle and syringe. The point of the needle had been removed to ensure that the drop formed on the sample surface was symmetrical. The contact angle between the hydrogel sample and the octane bubble were measured directly using a Rame-Hart contact angle Goniometer model 100-00.

2.7.3 Captive Air Bubble Technique

This technique was performed in almost the same way as the Hamilton method; instead of droplets of n-octane being placed onto the sample surface, bubbles of air were used. An air bubble was placed onto the surface of the hydrogel using a G25 syringe needle and syringe. The contact angle was measured directly.

The contact angles obtained by the Hamilton and Captive Air Bubble techniques were used to determine the surface energies of the hydrated polymer membranes. The contact angles were converted to surface energies using Macintosh Works™ which was programmed with the appropriate equations outlined in Chapter 1.

2.7.4 Dynamic Contact Angle Measurement

Dynamic contact angles for hydrogel membranes were obtained using a DCA 300 series analyser from Cahn instruments which was interfaced to an IBM computer. A schematic representation of the instrument is shown in Figure 2.10.

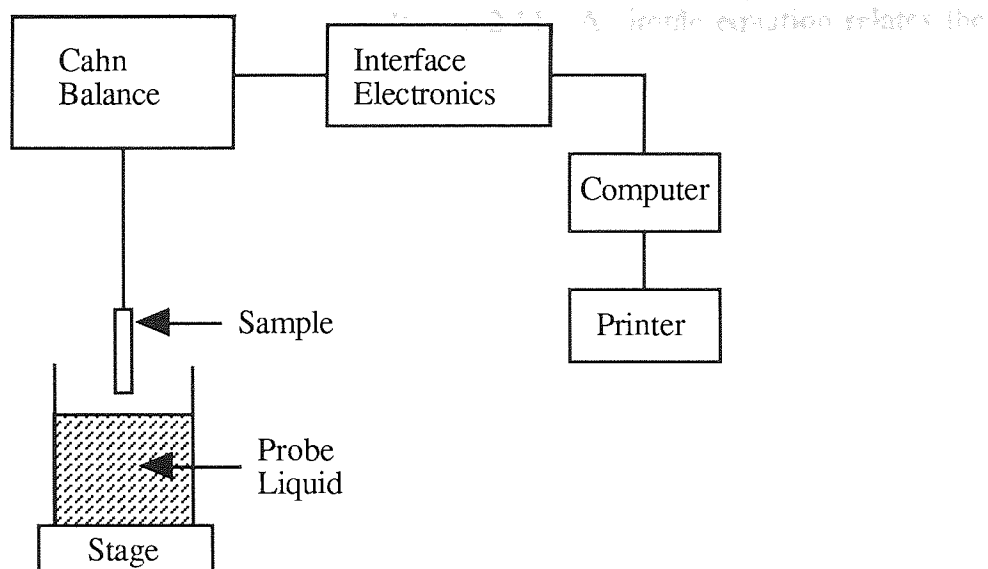


Figure 2.10 Schematic diagram of the functional components of a dynamic contact angle analyser (DCA)

The instrument was used to determine the values of the advancing and receding contact angles of hydrated hydrogel samples. Hydrogel membranes were polymerised by the method described earlier. After the required period of hydration the samples were cut into strips of length 10mm and width 3.3mm using a cutter. The thickness of the strips of sample were measured with a digital micrometer and the values recorded.

The hydrated sample was suspended from the Cahn balance by a connecting wire and a small crocodile clip and held in a vertical position with the lowest edge 3mm above the level of the probe liquid. Prior to sample preparation the instrument had the depth of immersion and number of immersion cycles programmed into the computer. Once the sample was in place and the required information installed, the sample was lowered into the probe liquid at a rate of $0.1\text{mm}\cdot\text{s}^{-1}$ to a depth of 7mm. The sample was immediately raised at the same rate until it returned to the starting height. At this point, it was ensured that the sample made no contact with the meniscus of the probe liquid (nominally 2-3 mm above the probe liquid.) This dipping procedure was repeated for the required number of immersion cycles; a minimum number of three cycles were performed for each sample . The computer plotted the results obtained as force versus immersion depth, a typical

dynamic hysteresis profile is illustrated in Figure 2.11. A simple equation relates the wetting force to the cosine of the contact angle,

$$\cos \theta = F / pq \quad \text{Equation 2.8}$$

where

F = force of the meniscus at the solid / liquid / vapour interface, measured directly by the Cahn balance

p = perimeter of the sample in contact with the probe liquid

q = surface tension of the probe liquid

The values of the advancing and receding contact angles are calculated automatically via the computer using this equation.

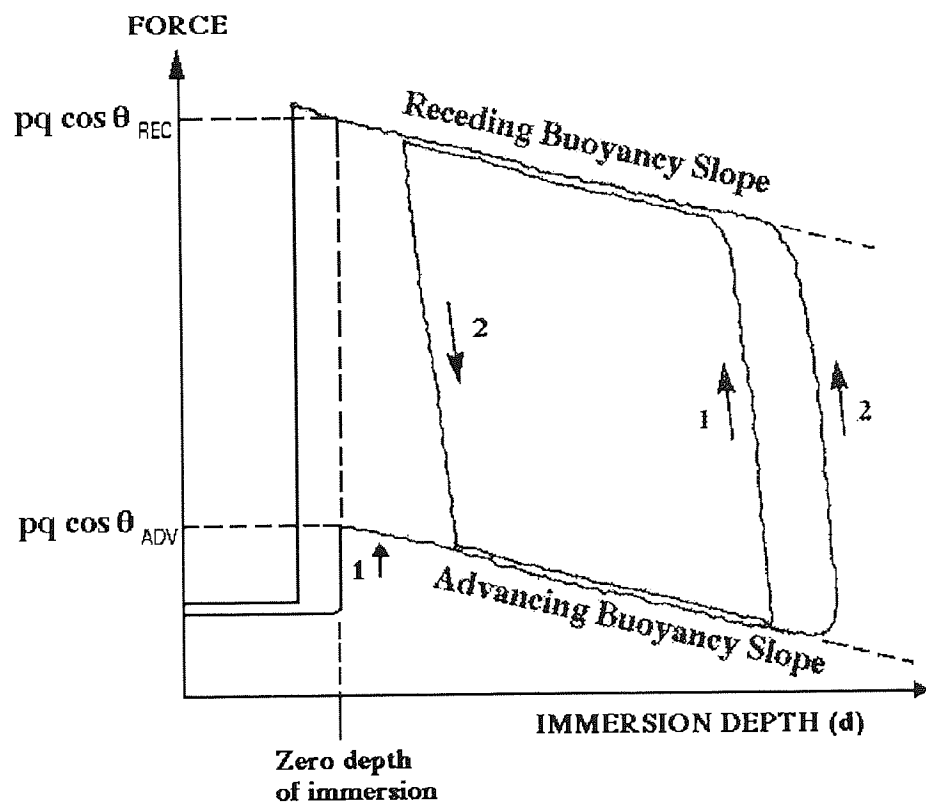


Figure 2.11 Diagram of a dynamic contact angle hysteresis curve, showing a two immersion cycle profile

2.8 Permeability Measurements

2.8.1 The Ion Permeability Apparatus

The permeability cell used was based on a design from D.C. Sammon of AERE Harwell. The cell is illustrated in Figure 2.12 and a schematic representation of the system is shown in Figure 2.13.

The cell was essentially a Perspex cylinder (9 cm diameter x 14 cm long) which was divided into two chambers (each approximately 4 cm diameter x 6 cm long). These were separated by the test membrane, which was held in place by two silicone rubber gaskets (9 cm outer diameter and 4 cm inner diameter). The cell was held in a horizontal position to hold the test membrane vertically. This orientation reduced both the hydrostatic head pressure and bubble formation at the membrane surface. The two chambers were held together by six bolts, the pressure of these bolts being critical in obtaining reproducible results; if the bolts were too tight the membrane may have ruptured and if they were too loose a poor seal leading to leakage between the chambers may have occurred.

In each of the chambers, adjacent to the membrane, a paddle was constantly rotated by a magnetic couple linked to an external stirrer motor. Stirring the fluid was important to prevent the formation of a stagnant layer at the membrane surface. Each chamber had an inlet and outlet port which enabled the continuous circulation of the permeating fluid. The ports were diametrically opposed to allow easy removal of air bubbles.

Each chamber was connected via a continuous loop to a separating funnel which acted as a reservoir. It was through these reservoirs that the system could be filled with distilled water or salt solutions. Once the system was full the reservoirs were sealed off and the fluid in the system was circulated by a peristaltic pump. To obtain data on the permeation of ions, the conductivity of the circulating solution on the low side was determined using a conductivity flow through cell. This was connected directly in to the continuous circulation loop of the low side just above the top port of the sample chamber. Once

assembled the cell was immersed in a purposely designed thermostated water bath at a temperature of 37°C.

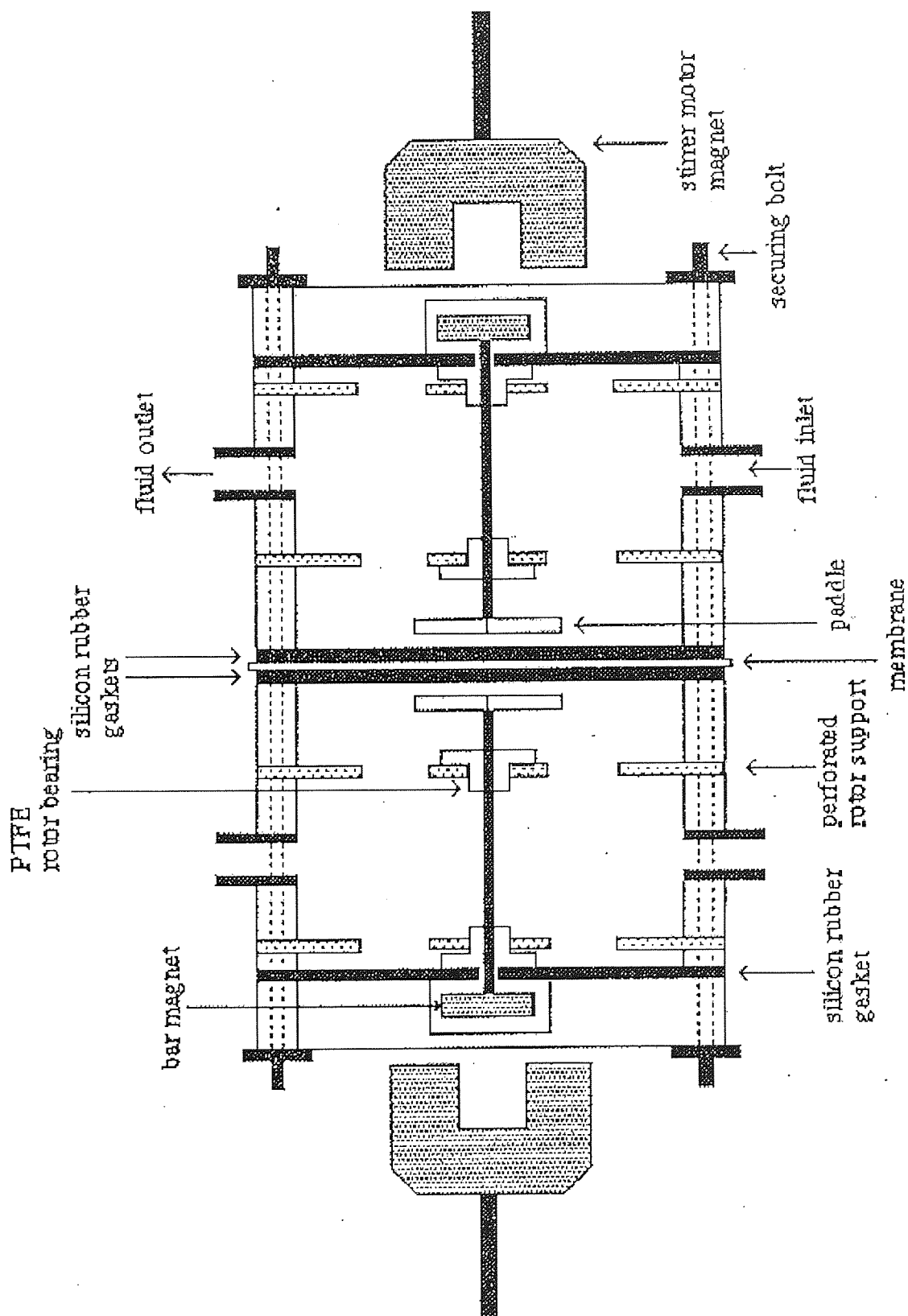


Figure 2.12 Schematic representation of a permeability cell

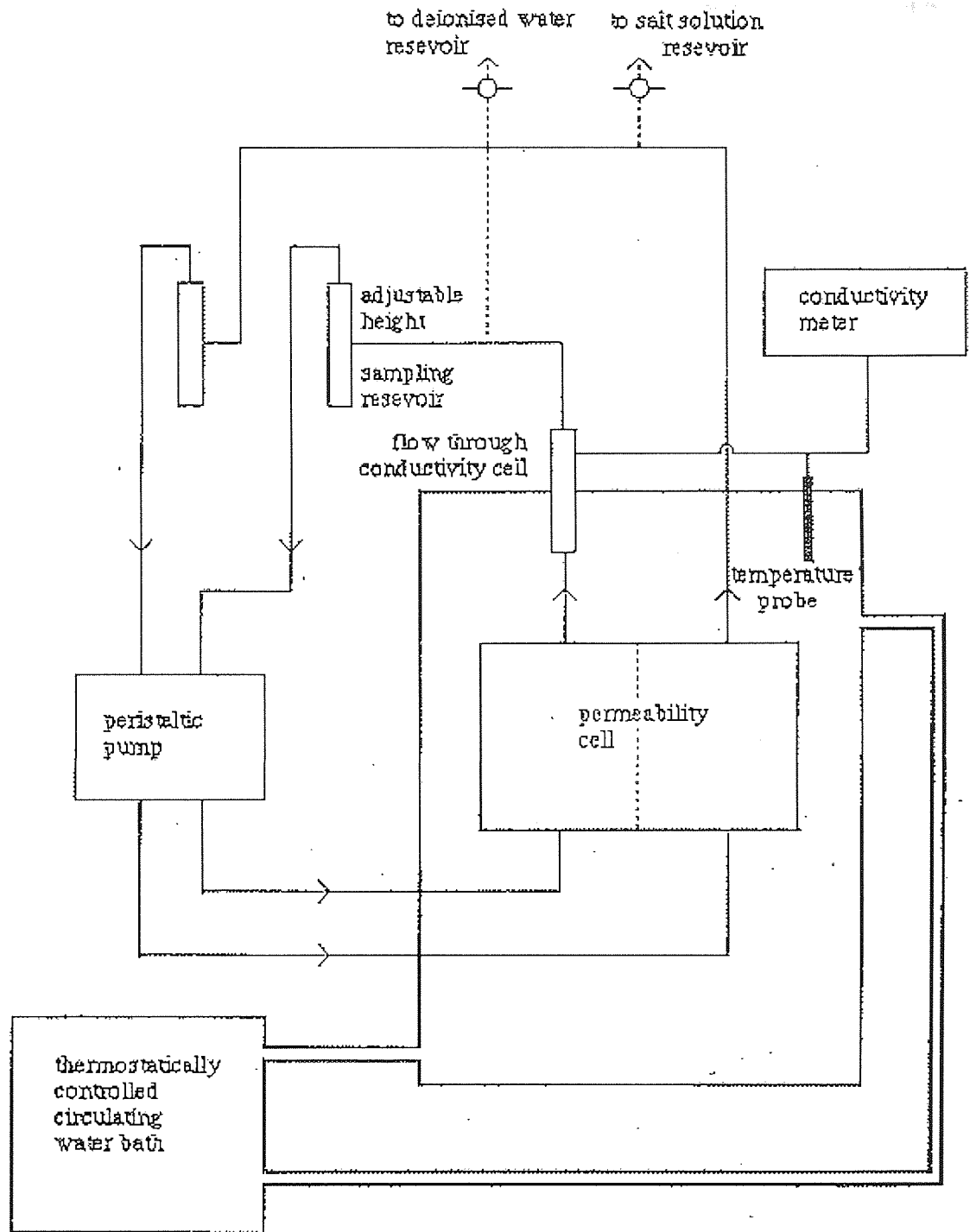


Figure 2.13 Schematic representation of the permeability apparatus

2.8.2 Method Of Operation Of The Ion Permeability Apparatus

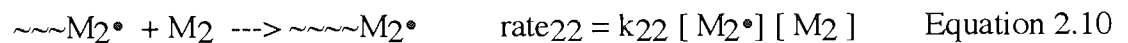
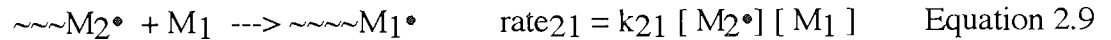
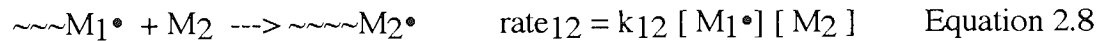
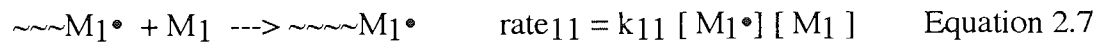
The test membrane was cut to a 5cm diameter disc and placed between the silicone rubber gaskets. The permeability cell was sealed whilst carefully controlling the pressure of the retaining bolts and the cell was placed in to the thermostated water bath overnight at a temperature of 37°C. Each chamber was filled via the reservoirs using solutions which had been allowed to equilibrate overnight. The right hand side was filled with the standard ion solution and the left hand side was filled with distilled water. The peristaltic pump was switched on and the timer was started once the chambers were half full. When the chambers were completely full of water and salt solution, any air bubbles were eliminated from the chambers by careful tilting of the cell. The stirrer paddles were switched on. Conductivity readings were taken every 15 minutes for the first hour and then every 30 minutes for a period of 6-10 hours. To convert the conductivity readings to concentrations calibration graph of conductivity versus concentration was plotted for a series of concentrations of the metal chlorides from 1 μ M to 0.25M. This enabled the concentration of metal chloride to be determined from the conductivity reading obtained during the experiment.

2.9 Copolymer Sequence Simulations

The sequence distributions and the effect of monomer reactivity ratios were studied using a computer simulation model. A listing of the computer program used is given in Appendix 1. The program is based on the Monte Carlo method (method of statistical trials), which solves problems of computational mathematics by constructing some random process for the problem. The parameters of the process are equal to the required quantities of the problem and these quantities are determined by means of observations of the random process and the computation of its statistical characteristics, which are approximately equal to the parameters required.

The development of the model, upon which the computer simulation is based, was constructed using the basic free radical polymerisation model. The standard hypothesis for

the reaction kinetics of this model is that the reactivity of the radical centre is governed by the monomer unit upon which the active radical centre is located. Four propagation steps for the polymerisation may be considered¹³²:



where :

M = monomer

M[•] = monomer radical

k = rate constant

[] = concentration

Considering the reactions which involve polymer chains ending with a M₁ radical, gives an overall rate for these reactions of :-

$$R_1 = \text{rate}_{11} + \text{rate}_{12} \quad \text{Equation 2.11}$$

and the fraction of these polymer chains that will add a further unit of M₁ at the radical end will be given by :-

$$f_{11} = \text{rate}_{11} / R_1 \quad \text{Equation 2.12}$$

where f_{11} is the fraction of polymer chains ending in an M₁ radical adding to another unit of M₁. Substitution of the above equations in to equation 2.12 gives :-

$$f_{11} = k_{11}[A] / k_{11}[A] + k_{12}[B] \quad \text{Equation 2.13}$$

where A is monomer 1 and B is monomer 2. This equation further simplifies to :-

$$f_{11} = 1 / \{1 + k_{12}[B] / k_{11}[A]\} \quad \text{Equation 2.14}$$

The individual reactivity ratios of M₁ and M₂ are defined as the ratio of the rates of reaction of a polymer chain ending in a radical of one type adding to itself to the rate of its reaction with the second monomer in the copolymer system. Therefore :-

$$r_1 = k_{11} / k_{12} \quad \text{Equation 2.15}$$

and

$$r_2 = k_{22} / k_{21} \quad \text{Equation 2.16}$$

where r_1 and r_2 are the reactivity ratios of the monomers M_1 and M_2 respectively.

Substitution of equation 2.15 in to equation 2.14 gives :-

$$f_{11} = 1 / \{ 1 + 1/r_1 \cdot [B] / [A] \} \quad \text{Equation 2.17}$$

Similarly it follows that :-

$$f_{22} = 1 / \{ 1 + 1/r_2 \cdot [A] / [B] \} \quad \text{Equation 2.18}$$

Therefore if the initial concentrations of the monomers and their reactivity ratios are known then the fraction of polymer chains ending in the radical M_1 that will add to unreacted monomer M_1 will be given by f_{11} . The fraction of polymer chains ending in M_1 that will therefore add to unreacted monomer M_2 may then be calculated and is represented as f_{12} . These fractions may be illustrated as a range of values along a number line as follows :



This line would represent a situation where f_{11} is greater than f_{12} . The computer simulation at each step of monomer addition generates a random number, (RN), in the range between 0 and 1.0 and compares it to the value of f_{11} generated from the initial concentrations and reactivity ratios. If $f_{11} \geq RN$ then the program adds another M_1 monomer unit to the growing free radical polymer chain. If $f_{11} < RN$ then the program adds an unreacted M_2 monomer unit to the growing polymer chain. Upon the addition of an M_2 monomer unit the program considers the equations involving the fractions of M_1 and M_2 adding to polymer chains ending with the M_2 radical. The random number is generated and compared to the value of f_{22} and f_{21} to determine the addition of the next monomer unit. This total procedure continues until 100% conversion of monomer to polymer. A sample of the display generated using the copolymer sequence simulation program is illustrated in Figure 2.14.

Ashraf¹¹⁴ studied the viability of the computer simulation program. Computer simulations were prepared using a number of methacrylate based comonomer systems together with the experimental preparation of the same copolymers. The experimental copolymers were analysed using standard analytical techniques. The most widely used methods are elemental analysis and nuclear magnetic resonance (NMR)-based analyses. Elemental analysis of the copolymers can prove difficult due to the problems of obtaining solvent and unreacted monomer free systems. NMR can also prove to be problematic because the technique relies upon significant differences existing between the comonomer structures in order to provide clear individual resonance signals for each monomer. Ashraf used ¹³C NMR to analyse the copolymers and was able to summate the individual cotactic sequences for a particular triad sequence within the copolymer. The triad sequences were then used to calculate the number of average sequence lengths for the individual monomer units within the copolymer. It was found that the sequence lengths determined using the methods of ¹³C NMR and elemental analysis were within 3% of the sequence lengths produced by the computer simulation. Therefore it is reasonable to assume that the computer simulation is accurate enough to simulate the reactivity of comonomers in a free radical polymerisation and hence warrant its use in comparing the sequence distributions of the copolymers studied in this work.

CHAPTER 3

Acryloylmorpholine: A Novel Monomer in Hydrogel Synthesis

3.1 Introduction

To date one of the most successful biomedical applications of hydrogel materials has been the synthesis and design of soft contact lenses. Since the introduction of such lenses in 1960 many novel monomer structures of the hydrogel materials have been investigated. This is attributed to two reasons; principally because of the ease of fabrication of the lenses but also because of the comparative ease with which clinical investigations can be performed with new contact lens materials when compared to the difficulties which occurred when investigating new biomedical materials associated with blood contacting applications.

Contact lenses are essentially a prosthetic extension of the cornea and it is the cornea and the eye environment which govern the mechanical, surface and permeability properties required of a contact lens material. The characteristics of the cornea and its role in materials design, which are beyond the scope of this thesis have been considered in more detail by Tighe *et al.*¹³³.

Although the availability of hydrogel materials for contact lens applications has diversified, it may be observed from Table 3.1 that the production of high water content materials (EWC > 55%) is dependant on a limited number of monomer components. This is in part due to the lack of highly hydrophilic monomers which produce a material that satisfies the water content, mechanical, surface and permeability requirements for the application.

It is evident in Table 3.1 that the hydrophilic monomer N-vinyl pyrrolidone (NVP), was widely used to produce material compositions which had a high equilibrium water content. Although NVP enjoys commercial success, its limitations are not immediately apparent.

NVP is relatively unreactive towards vinyl polymerisations and therefore tends to produce polymers which have a block type structure. Work carried out at Aston and by other workers¹³⁴ suggested that the production of polymers containing molecular domains of the same chemical type are important factors in controlling the deposition of biological debris,

since the formation of biological deposits on a synthetic material surface may render the material incompatible with the biological environment it is in contact with.

Table 3.1 Examples of commercially available high water content contact lens materials

Name	Manufacturer	Principal Components	EWC /%	USAN* Nomenclature
Calendar	Pilkington Barnes-Hind	VP, MMA	74	Surfilcon-A
Cristelle	Lunelle	VP, MMA	78	-
Focus	Ciba	HEMA, PVP, MA	55	Vifilcon-A
Frequency 73	Aspect	HEMA, VP	73	-
Igel-68	Igel Optics	MMA, VP, CMA	68	Xylofilcon-A
Lunelle	Essilor	AMA, VP	70	-
Omniflex	Hydron	MMA, VP	70	Lidofilcon-A
Permalens	Pilkington Barnes-Hind	HEMA, VP, MMA	71	Perfilcon-A
Precision UV	Pilkington Barnes-Hind	VP, MMA	74	Vasurfilcon-A
Permaflex	Pilkington Barnes-Hind	MMA, VP	74	Surfilcon-A
Rythmic	Lunelle	VP, MMA	73	Lidofilcon
Sauflon-70	Contact Lens Mfg	VP, MMA	70	Lidofilcon-A

AMA = alkyl methacrylate; CMA = cyclohexyl methacrylate; HEMA = 2-hydroxyethyl methacrylate; MA = methacrylic acid; MMA = methyl methacrylate; PVP = Poly vinyl pyrrolidone; VP = vinyl pyrrolidone.

*USAN = United States Adopted Name Council

A potential new monomer for producing high water content systems is acryloylmorpholine, which has the structure shown in Figure 3.1.

The synthesis of acryloylmorpholine was first described in the literature by Parrod and Elles in 1957. It has since been used to synthesise hydrophilic and lipophilic gels¹²⁸. Both the monomer and polymer of acryloylmorpholine are water soluble, but do not yet have definite usage examples.

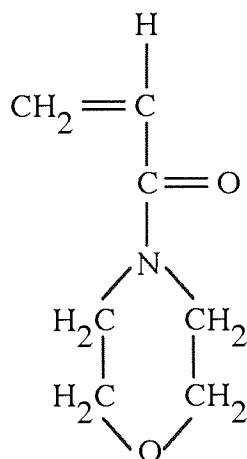


Figure 3.1 Chemical structure of acryloylmorpholine

The work presented in this Chapter was designed to investigate the properties of copolymer hydrogels made from 2-hydroxyethyl methacrylate (HEMA) copolymerised with increasing amounts of acryloylmorpholine (AMO). In doing this, the major properties considered were the reactivity of AMO in free radical polymerisations, the water binding capability, the mechanical properties and surface properties of the series of copolymers.

To obtain a measure of the potential usefulness of AMO in hydrogel synthesis, a comparison of the properties of its copolymers with HEMA were made with a series of two sets of copolymers. The first set was made from HEMA copolymerised with N-vinyl pyrrolidone (NVP) which is used in the production of commercially available hydrogel contact lenses and the second set of materials was made from HEMA copolymerised with the N,N-dimethyl acrylamide (NNDMA) which is structurally similar to AMO.

This Chapter presents the results obtained from this comparative study of the characteristics of hydrogel membranes prepared from acryloylmorpholine, N-vinyl pyrrolidone and N,N-dimethyl acrylamide.

3.2 Reactivity of Acryloylmorpholine

As mentioned previously, there is evidence in the literature to support the theory that copolymers containing molecular domains of the same monomer type lead to the increased

deposition of biological debris¹³⁵⁻¹³⁸. This observation has been made with hydrogels containing NVP which tend to have a block copolymer structure. This is because of the low reactivity of NVP with other monomers which are commonly used in contact lens synthesis, for example HEMA.

It was therefore necessary to consider the reactivity of AMO in free radical polymerisations. This was investigated by producing computer simulations (mentioned in Chapter 2), for HEMA-AMO copolymers. A comparison of the computer-simulated reactivity of HEMA-AMO copolymers was made with HEMA-NVP and HEMA-NNDMA copolymers.

3.2.1 Computer Simulations

The three sets of copolymers simulated were based on 70 mole% of 2-hydroxyethyl methacrylate (HEMA) copolymerised with 30 mole% of firstly, acryloylmorpholine (AMO), then N,N-dimethyl acrylamide (NNDMA) and finally, N-vinyl pyrrolidone (NVP). The values for the monomer reactivity ratios of these nitrogen-containing monomers in a free radical copolymerisation with HEMA were obtained from the literature¹³⁹⁻¹⁴¹. Where literature values were not available the relative reactivity ratios r_1 and r_2 were calculated using the Alfrey-Price Q-e scheme¹⁴². The reported values for the copolymerisation parameters are shown in Table 3.2.

Table 3.2 The relative reactivity ratios for the HEMA-NVP, HEMA-NNDMA and HEMA-AMO copolymer systems

Monomer 1	Monomer 2	r_1	r_2
HEMA	NVP	3.12±0.38	0.05±0.09
HEMA	NVP	4.43±0.24	0.04±0.14
HEMA	NNDMA	1.56*	0.34*
HEMA	AMO	3.79*	0.21*

*values calculated using the Q-e scheme

Computer simulations for the copolymer sequence distributions at a composition of 70:30 weight % of HEMA:nitrogen-containing monomer were obtained for AMO, NNDMA and NVP using the computer program described in Chapter 2. They are illustrated in Figures 3.2 - 3.4.

The simulation below represents 70 mole% of HEMA copolymerised with 30 mole% NNDMA and has been continued to 100% conversion. In the simulated copolymer HEMA is represented by O and NNDMA is represented by X.

```

OOOXOOOOOOOOOOOXOXOOOOOOXOXOOOOOOOOOOOOOOOXOOOOOOOXOOOOOOOXOOOO
XOXOOOOOOOXOOXOXOXOOOOXOOOOXXOOOOOOOXOOOOOOOOOOOXOOOOOOOOOOOOOOO
OXXOOOXOOXOOXOOOOXXOOOOOOOOOOOOOOOXOOOOOOOOOXOOOOOXOOXOOOOOOXOO
OOOXOOXXOOOOOOOXOXOOOOXOOXXOOOOOOOXOXOOOXOOXOOOXOOOOXOXOOOOOXOO
OXXXOOOOOOXXOXOOOOOXOOOOOOOOOOOOOOOXOOOOOOXOOOOOOOOOOOOOXOXOOO
OOOOOOOXOOOXOOOOOOXOOOOOOOOOOOOOOOXOOOOOOOOOOOOOXOOXOOOOOOOOXXO
OOOXOOXXOXOXOXOOOOOOOOOOOXOOOXOOOXOOOXOOOOOXOOOXOOOXOOOXOOOXOO
OXOXXOOOOOXOOOXOXOXOOOXOOOXOXOOOXOOOXOOOXOOOXOOOXOOOXOOOXOOOXOO
OOOOOOOXOOXOOOOOXOOOOOXOOOXOOOOOOOOOXOOOOOOOOOOOOOXOOXXOOXXOOXOO
OOOOOOOXOXOXOOOXOOOXOOOOOXOOOOOXOOOOOOOOOOOOOXOXOOOOOXOOOOOOOOOX
OOOOOXOXOXOOOXOOOXOOOOOXOOOOOXOOOOOOOOOOOOOXOOXOXOOOXOOOOOXOXOXO
OXXXOOXOOOXOOOOOOOOOOOXOOOXOOXOOXXOOOOOOOXOOOXOOOOOXOOOOOXOXOXO
OXOXXOOOOOOOOOOOXOOXOOXOOOXOOOOOXOOOXOOOXOXOXOOOXOOOXOOOXOOXX
OOOOOOOOOXOXOXOOOOOOXXOXOOOOOOOOOOOXOOOXOOOXOXOXOOXOOXOOOXOOXO
OXOOXOOXOOOXOOOXOOXOOOOOOOXOOXOOOXOOOOOOOXOOOXOOOOOXOOOOOOXX
OXOOOOOOOXOOXXOOXXOOOOOXOXOXXXXXXOXOOXOOXOOXOOOXOOOXOOOXOOOXOO
OOOXOXOOOOOXOOXOXOOOOOXOOOOOOOOOXOXOXOXOOOOOOOXOOOOOOOOOOOO
OOOOOXOOOXOOXOOOXOOOXOOOOOOOOOOOOOOOOOOOOOXOOOOOXOOOXOOOXOOOX
XXOOOXOOOOOXOOXOOXOOXOOOXOOOXOOOOOOOXOOOXOOOXOXOXOOXOOOXOOOXOO
OXOOOXOOOXOXOOXOOOXOOOXXXOOOOOXOOXOOOXOOOXOOOXOOOXOOOXOOOXOOOX
XOOOXOXOXOXOOOXOOOOOOOOOOOOOOOXOOOOOOOOOXOOOOOOOOOOOOOXOOOOOOO
OOOXOXOXOOXOXOXOXXOOOOOXOOOXOOOXOXOXOOOXOOOXOOOXOOOXOOOXOOOXOO
OOXOXOOOOOXOOXOOOOOXOOOOOXOOXOOOXOOOXOOOXOOOXOOOXOOOXOOOXOOOXOO
OXOOXOXOOXOOXXOXOXOXOOXOOOXOOOXOOOXOOOXOOOXOOOXOOOXOOOXOOOXOOOX
XXOOXOOOOOXOOXOOOXOOXOOXOOXOOOOOOOXOXOOOXOOOXOOXOOXOOXOOXOOOXOO
XOXOXXOOXOXOOXOXOOXOXOOXOOOXOOOXOOOXOOXOOXOOXOOXOOXOOXOOXOOXOO
XXOOXOOXOOXXOXXOXOXOXOOXOOXOOOXOOOXOOOXOOXOOXOOXOOOXOOOXOOOXOO
OXXOXOOXOOXOOOXOOOXOOOXOOOXOOOXOOOXOOOXOOOXOOOXOOOXOOOXOOOXOO
OOOOOXOXOXOOOXOOOXOOOXOOOXOOOXOOOXOOOXOOOXOOOXOOOXOOOXOOOXOOOX
OXOXOXOXOXOXOXXOOOXOXOOXOOXOOXOOXOOXOOXOOXOOXOOXOOXOOXOOXOOOX
OXXXOXXOXXXOXXOXXXXXXXXXXXXXXXXXXXXXXXXXXXXXXXXXXXXXXXXXXXXXXXXXX
XXXXXXXXXXXXXXXXXXXX

```

The simulated copolymer contains 1400 HEMA units and 600 NNDMA units

Sequence Length	Number of Sequences	
	HEMA	NNDMA
1	149	369
2	95	53
3	67	16
4	50	6
5	24	0
6	19	0
7	10	0
8	10	0
9	6	1
10	1	0
11	2	0
12	3	0
13	4	0
14	3	0
15	4	0
44	0	1

Figure 3.3 Sequence simulation of HEMA-NNDMA copolymer

The reactivity of the nitrogen-containing monomers, AMO, NNDMA and NVP are a function of three aspects of their individual chemical structures. The three aspects of their structures which affect their reactivity that must be considered are steric effects, polar effects and resonance stabilisations.

Steric and polar effects are important in the reacting radical and monomer and both species must be considered simultaneously. Whereas the resonance energy which accompanies the conversion of monomer to radical is more important than the general reactivity of the radical.

For the monomers AMO, NNDMA and NVP consideration of the vinyl side chains for each of these monomers would suggest that they differ little in their steric characteristics because of the similarities of their structures and the size of the constituents within their structures.

With respect to the resonance stabilisation characteristics of the monomers AMO, NNDMA and NVP, Evans *et al*¹⁴³ have considered the relationship between the resonance stabilisation of the radical and the reactivity of the monomer. These workers postulated that the net loss in resonance energy for the reaction:-



was equal to Δq and Δq was given by:-

$$\Delta q = R_{a\bullet} + R_b - R_{b\bullet} \quad \text{Equation 3.2}$$

where R = resonance energy of the species indicated by the subscript

The increase in activation energy for the reaction given in Equation 3.1 corresponds to the decrease in resonance energy which is given by:-

$$\Delta E = \alpha \cdot \Delta q \quad \text{Equation 3.3}$$

where ΔE = activation energy

$$\alpha = \text{constant}$$

It follows from Equations 3.1 and 3.3 that a high resonance stabilisation of radical B corresponds to a large lowering of the activation energy and therefore a high rate of reaction for the addition of monomer B to radical A.

The monomers AMO and NNDMA have a higher resonance stabilisation energy, of their respective radicals, than the radical formed from NVP, because of the formation of resonance structures of the type in Figure 3.5

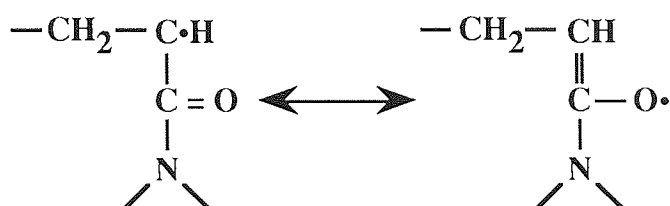


Figure 3.5 Resonance structures of amide head group

This resonance stabilisation does not occur with NVP. Therefore for the reaction with HEMA monomer it would be expected that AMO and NNDMA would add to HEMA at a greater rate than NVP, because of the lower activation energy of the reaction for their addition. Hence, AMO and NNDMA have a higher reactivity than NVP towards HEMA. The higher reactivity is reflected in the sequence simulations shown in Figures 3.2 - 3.4. AMO and NNDMA are consumed faster than NVP in their respective copolymerisations with HEMA. NVP because of its low rate of reaction is only consumed in the latter stages of the polymerisation once the HEMA monomer has been consumed and therefore forms a terminal block of NVP.

The computer simulations were obtained for 100% conversion. The simulations indicate that the reactivity of the monomers decreases in the order NNDMA > AMO > NVP. The reactivities suggest that a greater amount of NNDMA will be incorporated into the copolymer as single sequences and that NVP is the most likely to produce domains of one chemical type. AMO is more similar to NNDMA in its reactivity and therefore shows potential as a replacement for NVP in copolymers containing shorter sequence lengths for biomedical applications.

3.2.2 Experimentally Prepared Copolymers

Further support of the order of the reactivities of the nitrogen-containing monomers was provided by preparing linear copolymers for sets of HEMA-NVP, HEMA-NNDMA and HEMA-AMO copolymers.

A series of each of these copolymers were prepared by solution polymerisation as described in Chapter 2, at feed ratios of 90:10, 70:30 and 50:50 weight% of HEMA and the nitrogen-containing monomer respectively.

Elemental analysis for carbon, hydrogen and nitrogen showed there was a marked difference between the composition of the feed ratio and the resulting copolymer. The results are shown in Table 3.3. The results show that the initial feed composition and true weight ratio are near identical for the more reactive NNDMA and AMO monomers. In the case of NVP there is a significant difference between the feed ratio and the true composition. The larger disparity is due to the lower reactivity of NVP towards HEMA in the free radical polymerisation.

Table 3.3 Elemental analysis results for the copolymer systems studied

Copolymer Composition	Initial Feed Ratio (weight%)	True Weight Ratio from C, H, N analysis
HEMA-NVP	90:10	95:5
	70:30	83:17
	50:50	61:39
HEMA-NNDMA	90:10	91:9
	70:30	71:29
	50:50	50:50
HEMA-AMO	90:10	92:8
	70:30	73:27
	50:50	52:48

3.2.3 Conclusions

From the results presented in Section 3.2 AMO has a greater reactivity than NVP in free radical polymerisations. AMO therefore has the potential for designing copolymers with shorter sequence lengths than the equivalent NVP copolymers. These shorter sequence length polymers obtained using AMO may be of use in producing hydrogel copolymers which are less prone to deposition by biological debris. It is therefore necessary to study the physical characteristics of copolymers containing AMO.

3.3 Effect Of Acryloylmorpholine On Equilibrium Water Content

Acryloylmorpholine (AMO) is a hydrophilic monomer. This section of work was designed to investigate the water binding capability of this monomer. The characteristics of the AMO copolymers were compared to an equivalent series of N,N-dimethylacrylamide (NNDMA) copolymers and a series of N-vinyl pyrrolidone copolymers.

3.3.1 Materials And Their EWC's

Three sets of HEMA copolymer membranes were prepared which contained increasing amounts of one of acryloylmorpholine, N,N-dimethyl acrylamide and N-vinyl pyrrolidone nitrogen-containing monomers. The membranes were prepared using the polymerisation technique described in Chapter 2. All the copolymer systems were brittle in the dehydrated state and became flexible when hydrated in distilled water. The equilibrium water contents (EWC's) were determined after the required hydration period. The effect of the nitrogen-containing hydrophilic component on the equilibrium water content for each set of copolymer membranes is illustrated in Figure 3.5.

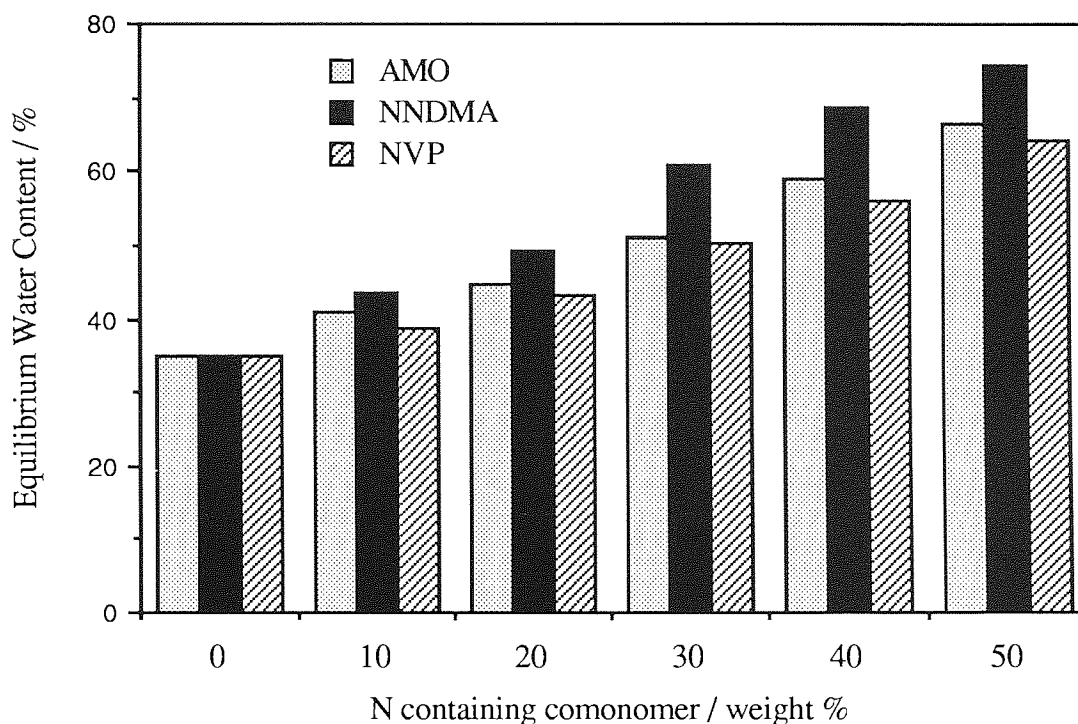


Figure 3.6 Effect of the proportion of nitrogen-containing monomer on the EWC of HEMA copolymers

In each series of the copolymer membranes the EWC increased with increasing proportion of the nitrogen-containing monomer. The precise value of the EWC depends on the contributing steric and polar effects of each of the hydrophilic monomers. For poly(HEMA) the polar component is due to the hydroxyl and ester groups, whereas the steric component is due to the α -methyl group and the alkyl side chain. These elements are constant for each series of copolymers and therefore the differences in total EWC between the three sets will be due to the nitrogen-containing monomers.

From Figure 3.6 it was at first evident that the hydrophilicities decreased in the order NNDMA > AMO > NVP. This would be expected as both acryloylmorpholine and N-vinyl pyrrolidone possess an alkyl ring structure which will exclude a proportion of water from

the copolymer by virtue of steric hindrance and because of the hydrophobicity of the extra methylene units in their structure compared to N,N-dimethyl acrylamide.

However, it might be expected that the acryloylmorpholine would be slightly less hydrophilic than the N-vinyl pyrrolidone. Comparison of the solubility parameters of morpholine and pyrrolidone indicate that the free energy of mixing, ΔG , for water and pyrrolidone would be more negative than for water and morpholine. Solubility occurs when ΔG is negative. However, the one important difference between the copolymers previously mentioned is the relative reactivity ratios of the two monomer pairs. As can be seen from Table 3.3 there is a significant difference between the feed ratio and the actual copolymer composition. The acryloylmorpholine copolymer has a greater percentage conversion than the N-vinyl pyrrolidone system at the same feed ratios and this would account for the fact that the EWC's of its copolymers are higher than those prepared with the equivalent feed amount of NVP.

3.3.2 Water Binding Studies

Closer inspection of the water binding in the series of HEMA and nitrogen-containing copolymers was achieved using Differential Scanning Calorimetry (DSC). This is perhaps a more convenient technique than nuclear magnetic resonance or dilatometry methods as it enables data to be obtained more rapidly. It is also possible to carry out successive freeze / melt cycles which provide greater detail of the water structuring information¹⁴⁴.

Ranges of values for the water binding characteristics of poly(HEMA) hydrogels have been obtained¹⁴⁵⁻¹⁴⁷ and it must be noted that the values were influenced by the analytical technique used. Therefore one technique has been used for comparison of each series of copolymer membranes used in this work.

In determining the water binding characteristics using DSC, Corkhill⁴¹ suggests that although percentages illustrate the general changes observed in the EWC and freezing and

non-freezing water contents, that more precise information is obtained by expressing the water content in grams of water / gram of polymer or moles of water / mole of repeat unit. This method gives an indication of the water binding potential of a single monomer unit and is clearly advantageous when systems such as the HEMA-NVP copolymers show a clear disparity between the feed ratios and actual copolymer composition.

Figures 3.7 - 3.9 show the effect of increasing the proportion of nitrogen-containing monomer on the water binding characteristics of the hydrogel copolymers. The values have been expressed both as a percentage and as grams of water / gram of polymer to provide a clearer indication of the nature of the water binding in these systems.

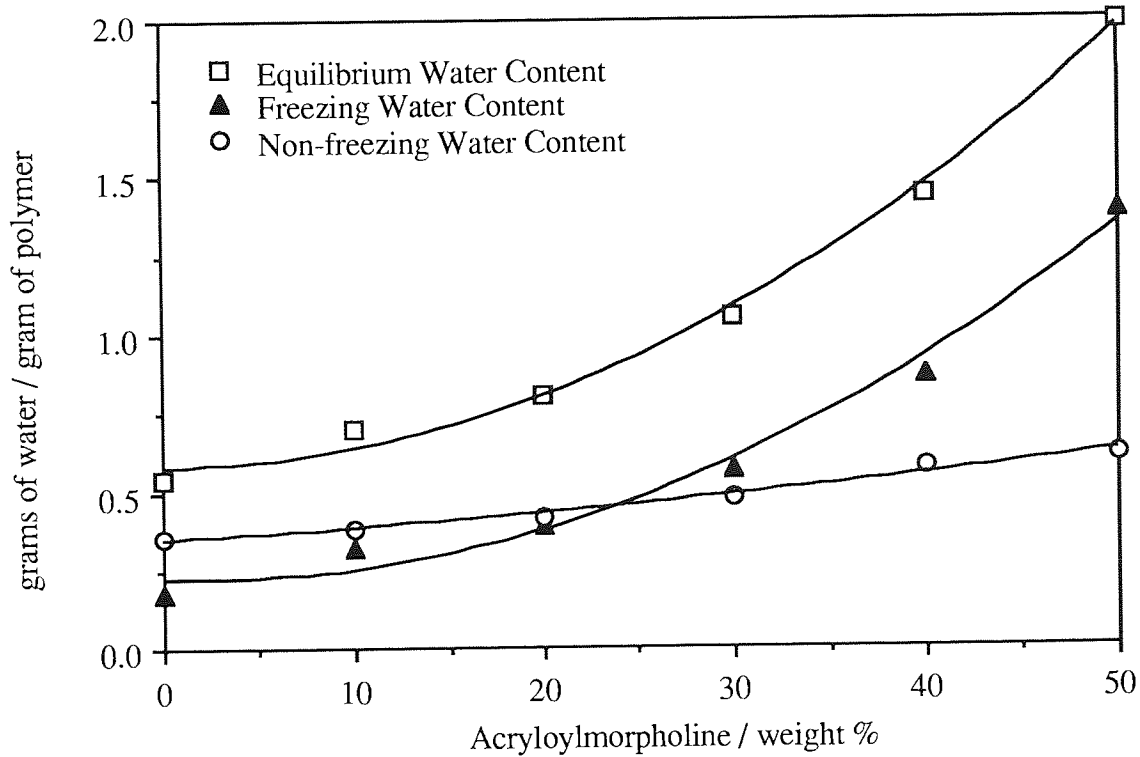
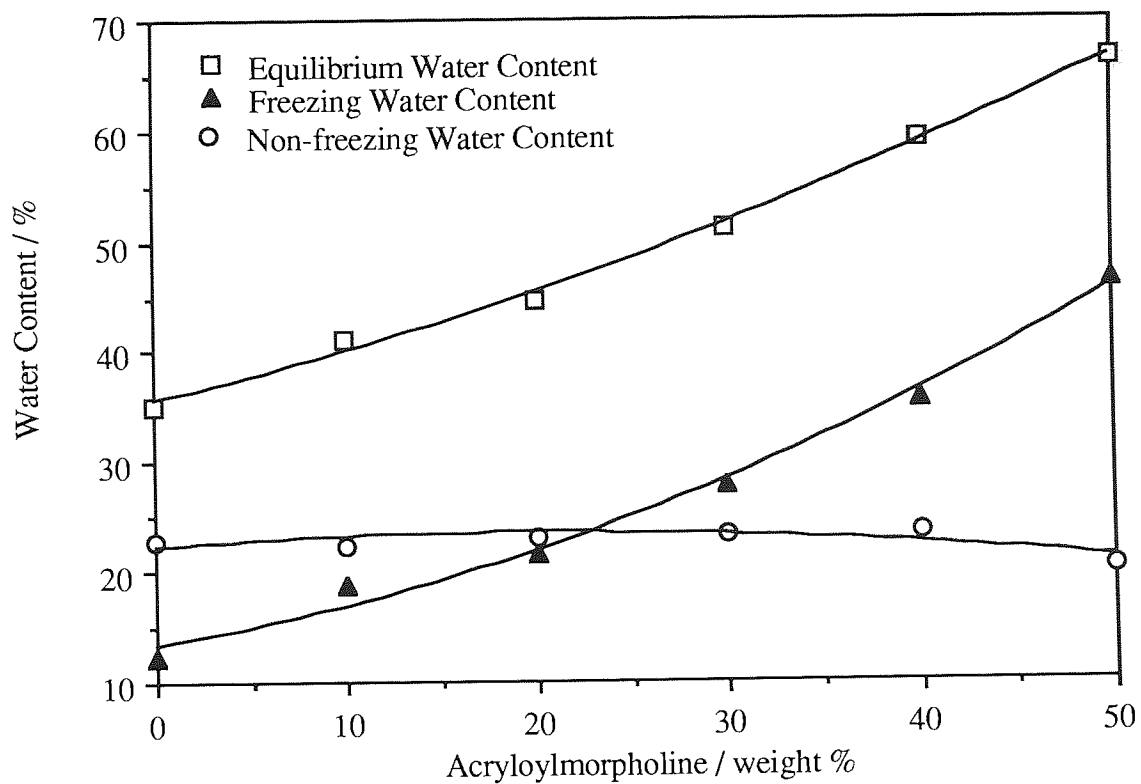


Figure 3.7 The effect of composition on the water binding characteristics of HEMA-AMO copolymers

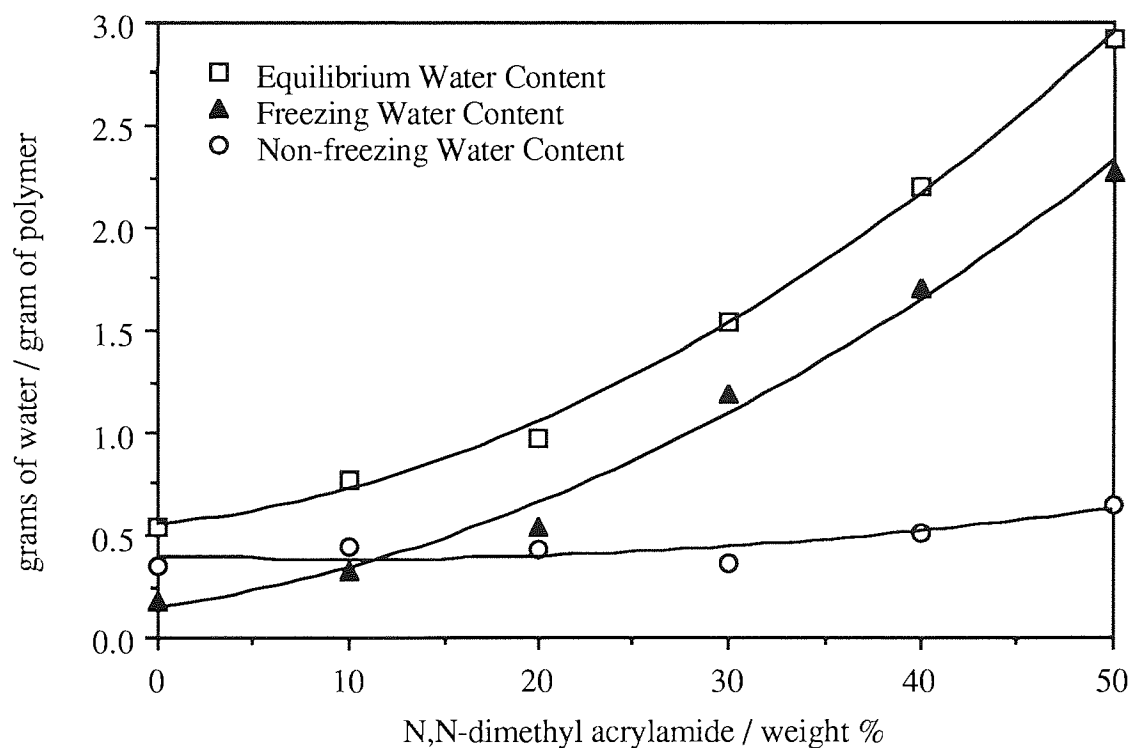
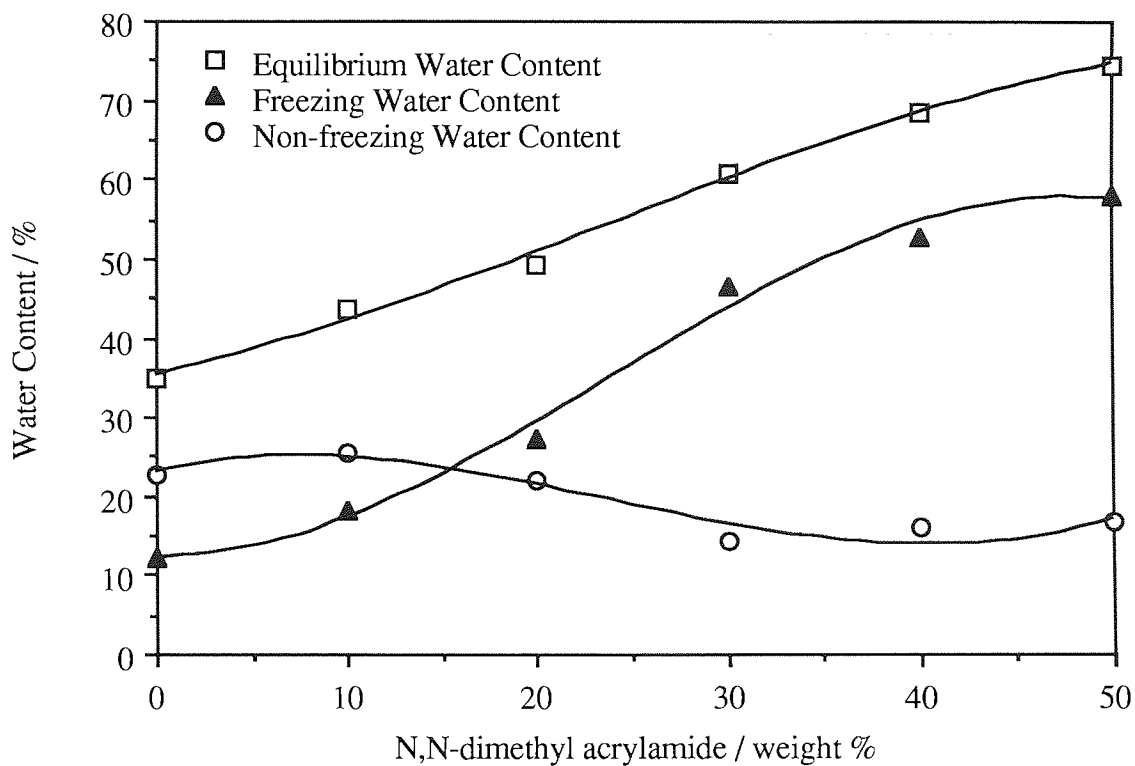


Figure 3.8 The effect of composition on the water binding characteristics of HEMA-NNDMA copolymer

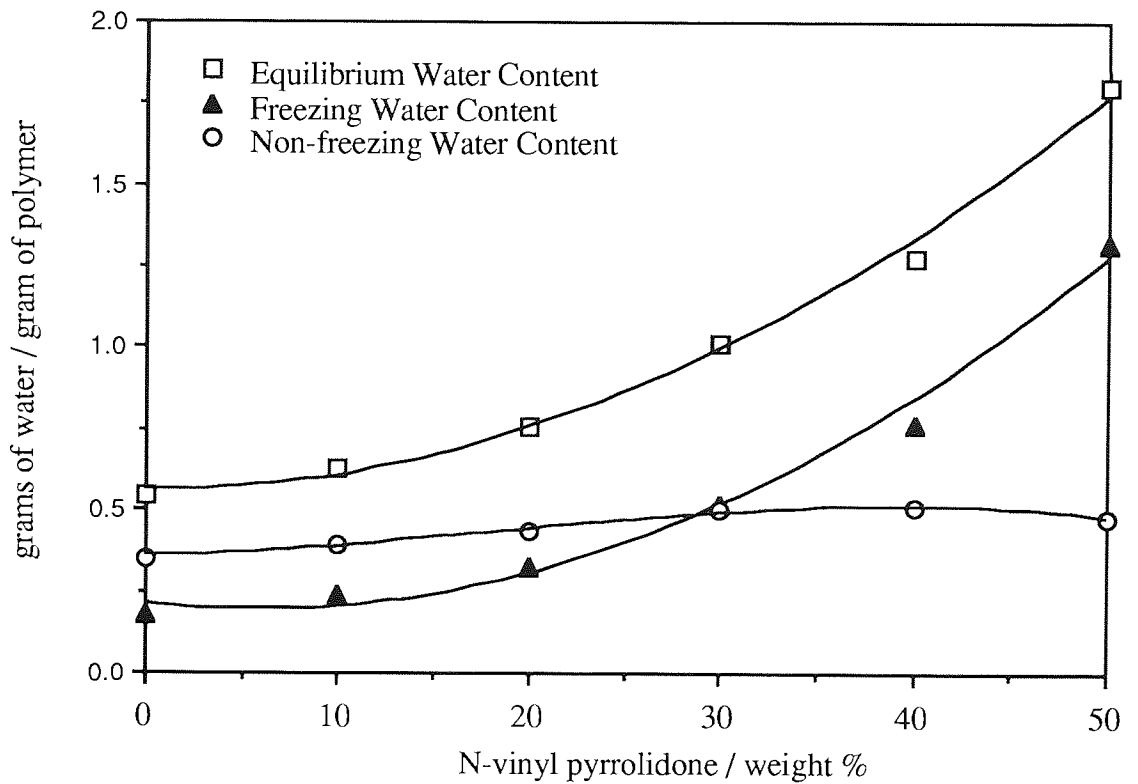
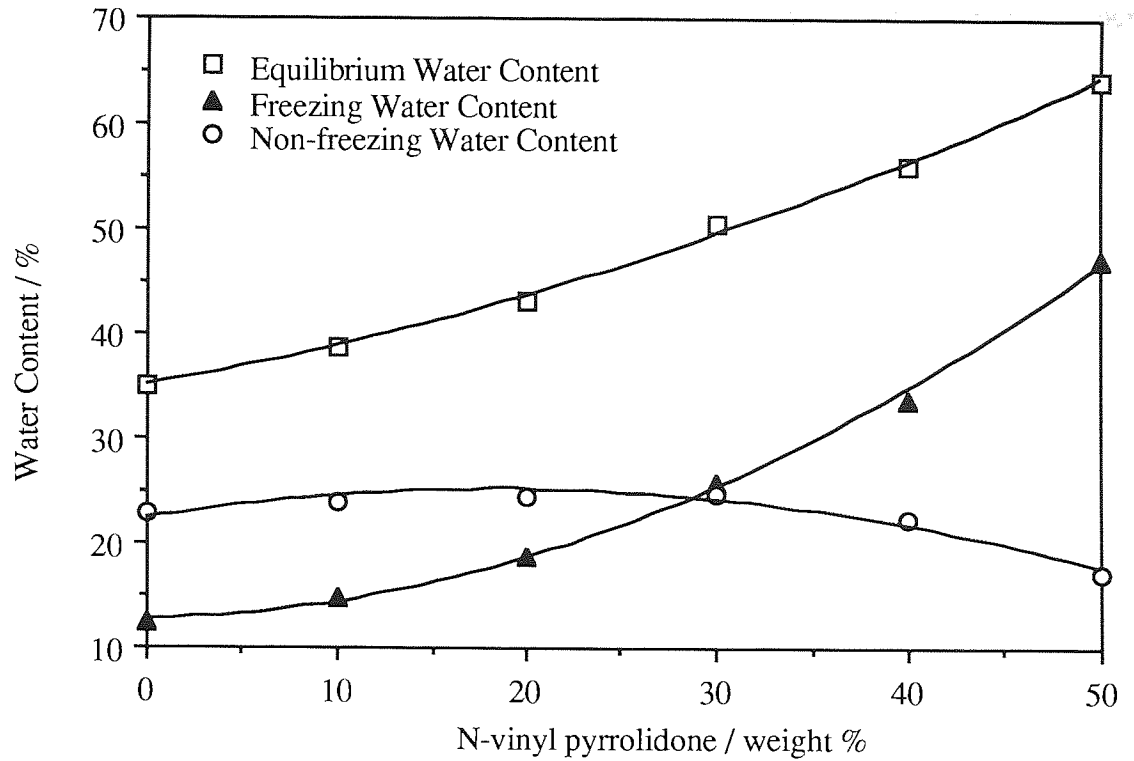


Figure 3.9 The effect of composition on the water binding characteristics of HEMA-NVP copolymers

The water binding information of each of the systems may not be compared directly due to the lower reactivity of NVP. However, combination of the information with the elemental analysis results gives an interesting result in terms of the water binding potential of the individual nitrogen-containing monomers.

For the poly(HEMA) system a value of 2.54 moles of water per mole of polymer is obtained. Ranges of values have been reported, discrepancies of which may arise due to the technique used to determine the water binding information and to the extent of impurities such as ethylene glycol dimethacrylate and methacrylic acid. Larger quantities of the crosslinking agent ethylene glycol dimethacrylate reduce the molecular weight between crosslinks and sterically exclude water from the copolymer, whereas the presence of methacrylic acid provides a greater number of carboxyl groups in the polymer available for water binding. Using the data illustrated in Figures 3.7 - 3.9 the water binding capabilities rise to 3.26 moles of water per mole of polymer for the 50:50 HEMA-NVP copolymer, to 4.57 moles of water per mole of polymer for the 50:50 HEMA-NNDMA copolymer and to 4.14 moles of water per mole of polymer for the 50:50 HEMA-AMO copolymer.

Of further significance from the water binding data in Figures 3.7 - 3.9 are the relative proportions of freezing and non-freezing water in the series of copolymers. The difference between the EWC and the freezing water content is greatest for the HEMA-AMO copolymers indicating that copolymers of this type will contain a greater proportion of non-freezing water than the HEMA-NNDMA or HEMA-NVP copolymers.

The significance of the water binding characteristics of the monomer on the physicochemical interactions between hydrogel surfaces and proteins has been studied¹⁴⁸. It was apparent that it was not only the chemical groups at a surface which affected the amount and conformation of adsorbed adhesion proteins, but the reorganisation of the structural arrangement of water molecules at the interface. It was observed that the introduction of monomers with high proportions of non-freezing water, such as charged monomers, into

HEMA hydrogels increased the water structuring effects and produced a surface that was less adhesive than the unmodified polymer. In the case of non-polar groups, which have lower proportions of non-freezing water than charged groups for example, the surfaces were found to be more adhesive towards cells. It was postulated that water structuring may indirectly affect the adsorption of adhesion proteins and may be used to explain cell adhesion characteristics of copolymer surfaces. Thus the presence of a monomer with higher proportions of non-freezing water may reduce the cell adhesion compared to a monomer with comparable total water binding ability, but lower proportion of non-freezing water.

The values of the water binding information illustrate the potential of AMO in the production of high water content hydrogels containing lower amounts of freezing water. The greater proportion of non-freezing water in AMO copolymers compared to NVP copolymers and NNDMA copolymers may also produce surfaces which are less adhesive towards cells and proteins due to the stronger interaction with water.

3.4 Effect Of Acryloylmorpholine On The Mechanical Properties Of The Copolymer Systems

3.4.1 Introduction

A significant factor in the development of hydrogels for biomedical applications has been the poor mechanical properties associated with these systems, particularly for applications where a high water content is required. In this Section the mechanical properties of the HEMA-AMO copolymer systems were investigated to assess the mechanical suitability of using high water content systems which contain acryloylmorpholine. A comparison was made with N-vinyl pyrrolidone, because it is widely used in many commercial hydrogel contact lens compositions and with N,N-dimethyl acrylamide because of its structural similarities.

3.4.2 Materials And Results

The mechanical properties of the series of HEMA-AMO, HEMA-NVP and HEMA-NNDMA hydrogel copolymers were determined using the tensile method described in Chapter 2.

Figures 3.10 - 3.12 illustrate the changes in elastic modulus, tensile strength and elongation at break for the HEMA copolymers containing increasing proportions of the nitrogen-containing monomers.

Figure 3.10 illustrates the effect of composition of the proportions of nitrogen containing monomers on the elastic modulus of the HEMA copolymers. The elastic modulus of the copolymers (tested under tensile conditions) provides an indication of the stiffness of the copolymer. The stiffness of the copolymer is in turn related to the chain mobility of the polymer network. AMO has a higher glass transition temperature than NVP and NNDMA which indicates that AMO polymers have a higher energy barrier to rotation than NVP or NNDMA polymers. The greater value of the glass transition temperature for AMO is reflected in the higher values of stiffness or elastic modulus for its copolymers compared to equivalent compositions of the NVP and NNDMA copolymers.

Overall in Figure 3.10 the elastic modulus undergoes an overall decrease over the whole composition range for each series of copolymers because of the flexibilising nature of the imbibed water which acts as an internal plasticiser.

Figures 3.11 and 3.12 show the effects of composition on the tensile strengths and elongations at break respectively, for each of the HEMA copolymer systems. The combination of these two mechanical properties provides an indication of the network integrity of the copolymer compositions. From both these figures it is evident that the greatest variation in values arises from the copolymers containing NVP and NNDMA. Whereas the AMO copolymers show a gradual decrease in tensile strength and elongation at break.

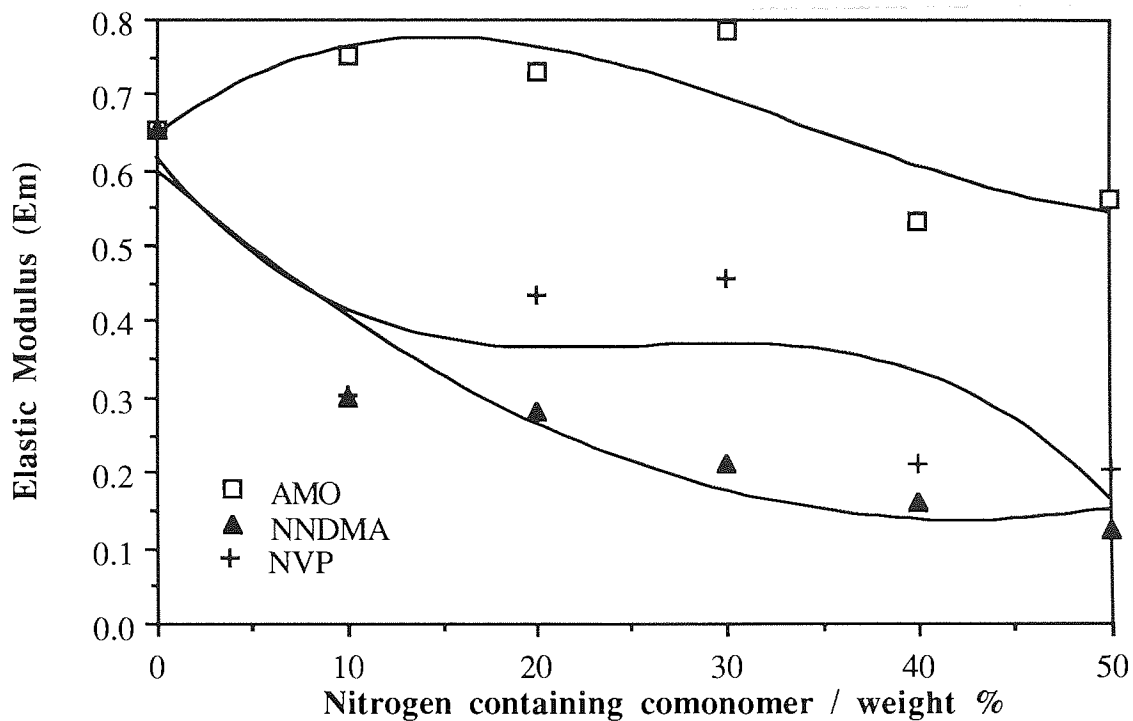


Figure 3.10 Effect of composition on the elastic modulus of the HEMA copolymers

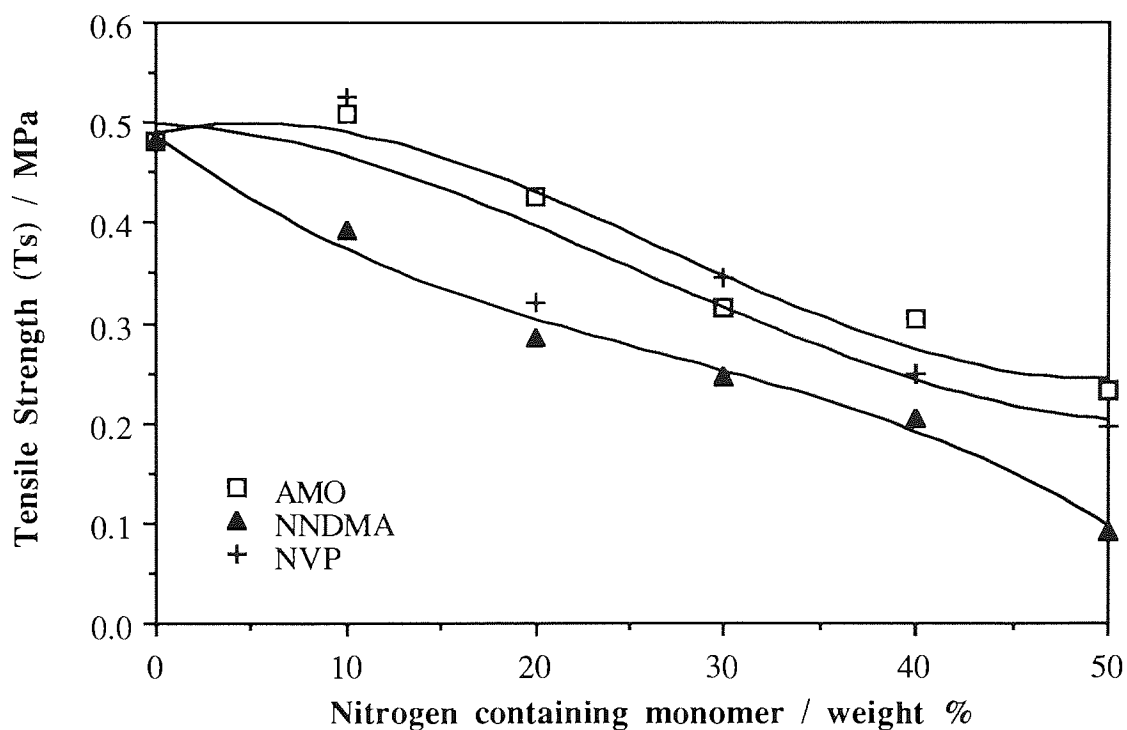


Figure 3.11 Effect of composition on the tensile strength of the HEMA copolymers

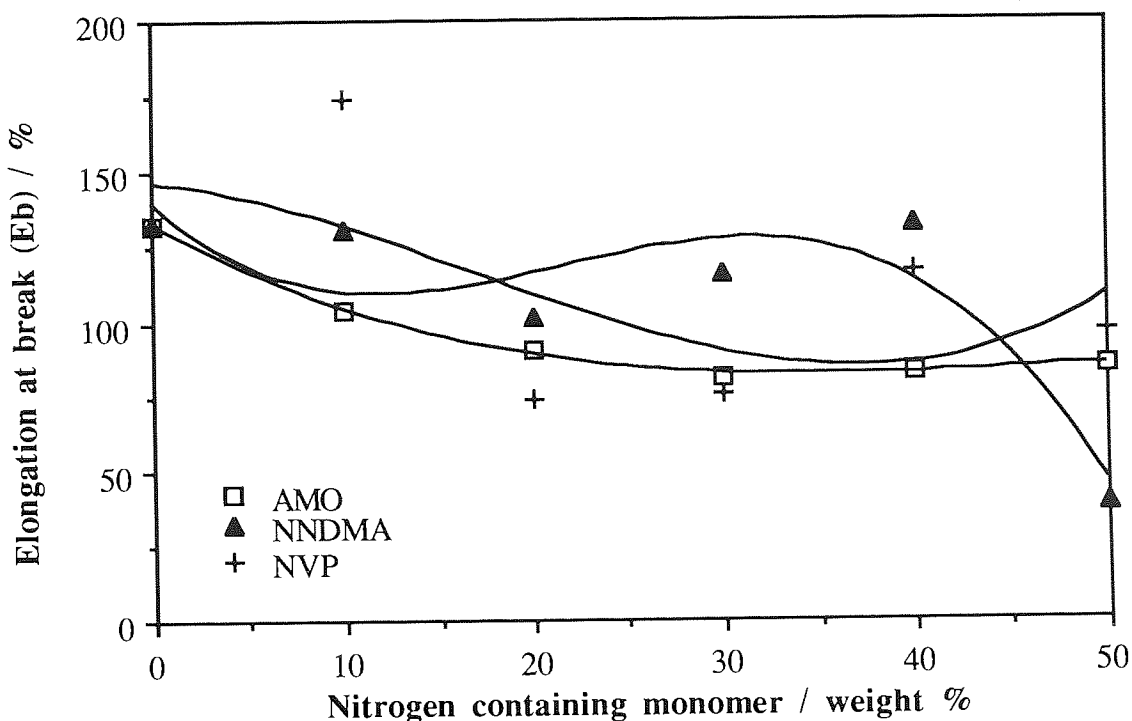


Figure 3.12 Effect of composition on the elongation at break of the HEMA copolymers

The observed variations that occurred in the HEMA-NVP and HEMA-NNDMA copolymers can be explained in terms of the polymerisation. HEMA and NVP monomers have very different free radical reactivity ratios and therefore there is a tendency to produce a block copolymer structure and a large disparity between the feed and actual copolymer compositions. Variation in copolymer structure and copolymer composition produce variability in the network characteristics⁴¹.

In the case of NNDMA copolymers, it is well known that NNDMA undergoes chain transfer reactions during its copolymerisation. The chain transfer reactions occur because of hydrogen abstraction from the pendant methyl groups of the amide group. The chain transfer reactions result in greater degree of variability in the copolymer network structure and is observed by a low tear strength⁴¹.

In the case of AMO monomer, firstly it has been shown to have a greater reactivity ratio towards HEMA than does NVP. The enhanced reactivity results in a copolymer which contains a more regular sequence of repeat units within its copolymer structure than the equivalent NVP systems and does not exhibit the large disparity between its feed ratio and actual copolymer composition. Secondly, due to the presence of a ring structure in its pendant group, compared to NNDMA, chain transfer reactions are sterically unlikely via hydrogen abstraction from a carbon adjacent to the amide group.

Variation in the mechanical properties may also be related to the EWC. Figures 3.13 - 3.15 show the changes in the elastic modulus, tensile strength and elongation at break of the copolymers with increasing equilibrium water content.

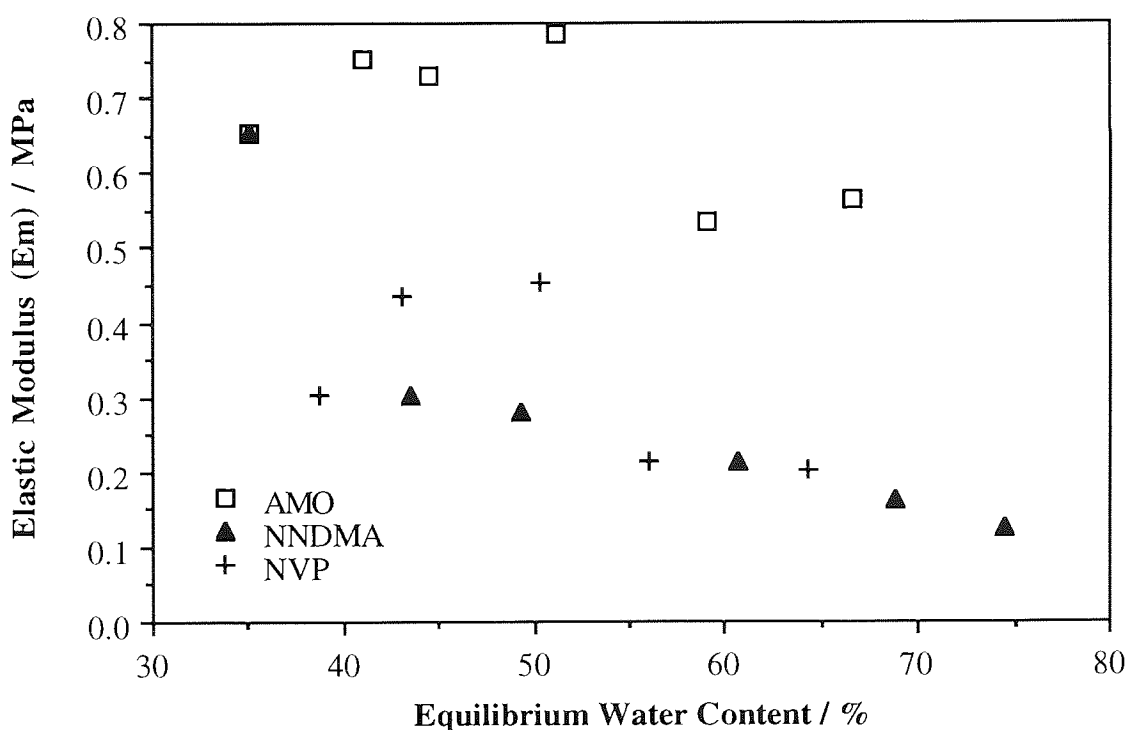


Figure 3.13 Effect of Equilibrium Water Content on the Initial Elastic Modulus of the HEMA copolymers

It can be observed from Figure 3.13 that for materials of equivalent equilibrium water content that the HEMA-AMO copolymers show the higher values of the elastic modulus. As mentioned previously, the higher value of the modulus is a reflection of the higher energy barrier to rotation of AMO compared to NVP and NNDMA. It is also clear from the figure that the overall trend is a decrease in the elastic modulus with increasing equilibrium water content. This was expected due to the plasticising nature of the imbibed water.

Figures 3.14 and 3.15 indicate that the tensile strength and elongation at break, decrease with increasing EWC. This would be expected, because as the proportion of water in the copolymer increases the hydrogel is plasticised to a greater extent.

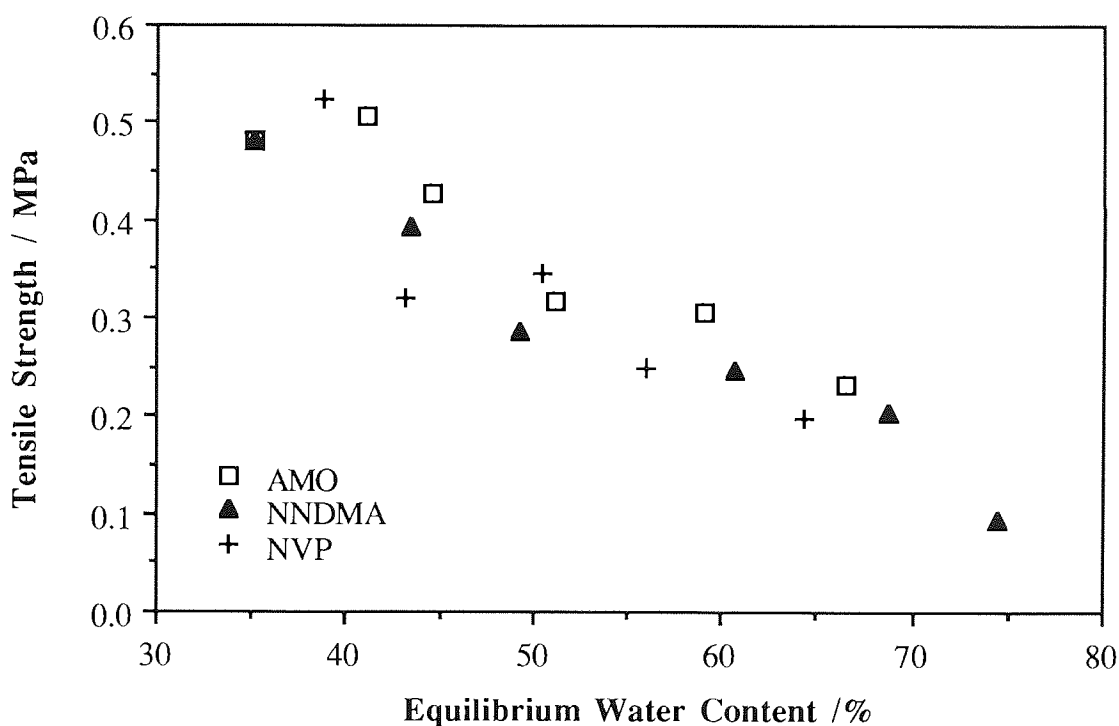


Figure 3.14 Effect of Equilibrium Water Content on the Tensile Strength of the HEMA copolymers

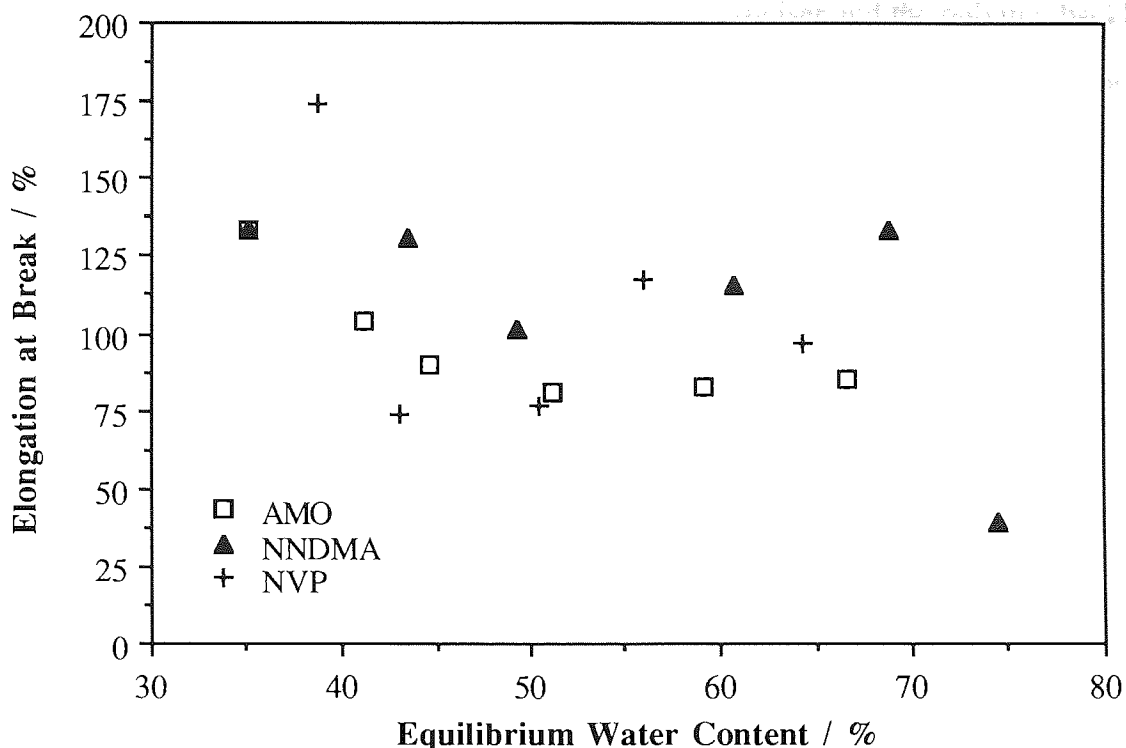


Figure 3.15 Effect of Equilibrium Water Content on the Elongation at Break of the HEMA copolymers

3.5 Surface Properties Of Modified HEMA Hydrogels

3.5.1 Introduction

The most successful application of hydrogels has been in the biomedical field, particularly in the development of contact lens materials. The nature of these applications requires the hydrogel to be in direct contact with its biological host and it is in part due to the unique surface characteristics of hydrogels that they have enjoyed this success. Previous workers have suggested that the nature of the surface governs its interactions with a biological environment and therefore the biotolerance of the surface within the environment^{145, 146}. It is clear that the surface characteristics of the hydrogel play an important role in determining the initial reactions and processes that will occur at the interface with a biological environment.

In water swollen polymer systems the water acts as a plasticiser and the polymer backbone and pendant chains will exhibit a high degree of rotational mobility at ambient temperatures thereby characterising the surface as one of high chain mobility. In 1975, Holly and Refojo¹⁴⁷ observed that the contact angles of fully hydrated poly(HEMA) measured in air were greater than 60°, which suggested that the surface was displaying a significant degree of hydrophobicity. Whereas the contact angles of the fully hydrated systems measured in water were low, indicating a greater degree of hydrophilicity than in the air situation. In characterising the behaviour of surfaces of this type, molecular mobility of the polymer chains was used to explain if a surface would display hydrophilic or hydrophobic character. This molecular mobility was dependant on the nature and polarity of the environment and the thermodynamic driving forces that attempt to minimise the interfacial energy.

3.5.2 Results

In the case of the copolymers studied in this work it is evident from the structures of the nitrogen-containing monomers that depending on the environment, either hydrophobic backbone groups or the hydrophilic nitrogen-containing pendant groups will be expressed at the interface. The surface properties of the copolymers of HEMA-AMO, HEMA-NVP and HEMA-NNDMA were studied in both the dehydrated and hydrated states and the results are presented here.

3.5.2.1 Surface properties of the dehydrated copolymers

Figures 3.16 - 3.18 show the experimental values of the individual polar and dispersive components, together with the total surface free energies of the dehydrated copolymer membranes for each series of copolymers.

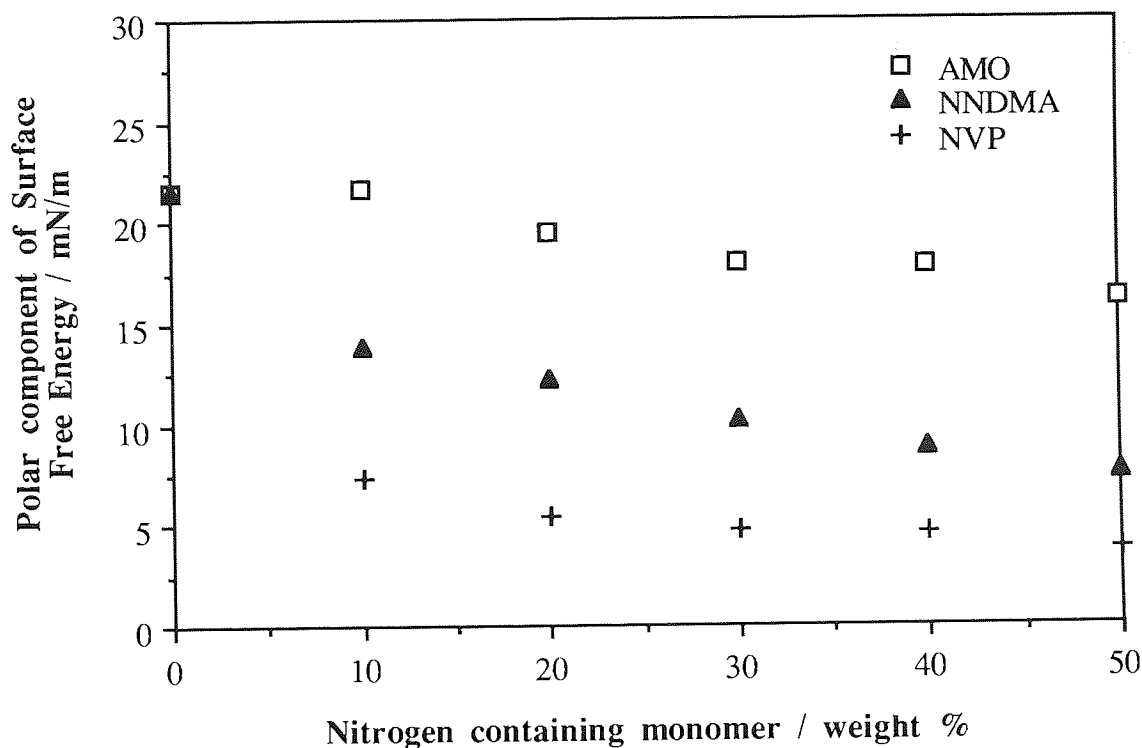


Figure 3.16 Effect of composition on the measured polar component of the surface free energy of dehydrated HEMA-AMO, HEMA-NNDMA and HEMA-NVP copolymers

Figure 3.16 shows the effect of composition on the polar component of the surface free energy of dehydrated HEMA-AMO, HEMA-NVP and HEMA-NNDMA copolymers. With increasing proportion of the nitrogen-containing monomers it was observed that the polar component decreased. The values obtained for the polar components of the HEMA-AMO, HEMA-NVP and HEMA-NNDMA copolymers are lower than the polar components of poly(HEMA), poly(AMO), poly(NVP) and poly(NNDMA). Therefore the polar component of the surface free energy of the nitrogen-containing copolymers must pass through a minimum value with increasing amount of nitrogen-containing monomer until the value of the polar component of the nitrogen-containing homopolymers is reached.

The reduction of the polar component as shown in Figure 3.16 is due to the formation of a molecular complex which is formed in each of the copolymers. The molecular complex

such that the orientation of the copolymers in the complex leads to the more hydrophobic sites being expressed at the surface of the copolymer. Therefore, complex formation causes the polar groups within the bulk of the copolymer and therefore the surface is rendered less polar.

The formation of a molecular complex with hydrophobic groups expressed at the surface is reflected in the increase in the dispersive component of the surface energy of the dehydrated HEMA-AMO, HEMA-NVP and HEMA-NNDMA copolymers shown in Figure 3.17.

Figure 3.16 also indicates that AMO is more polar than NNDMA and NVP. This is probably due to the presence of the ring oxygen atom.

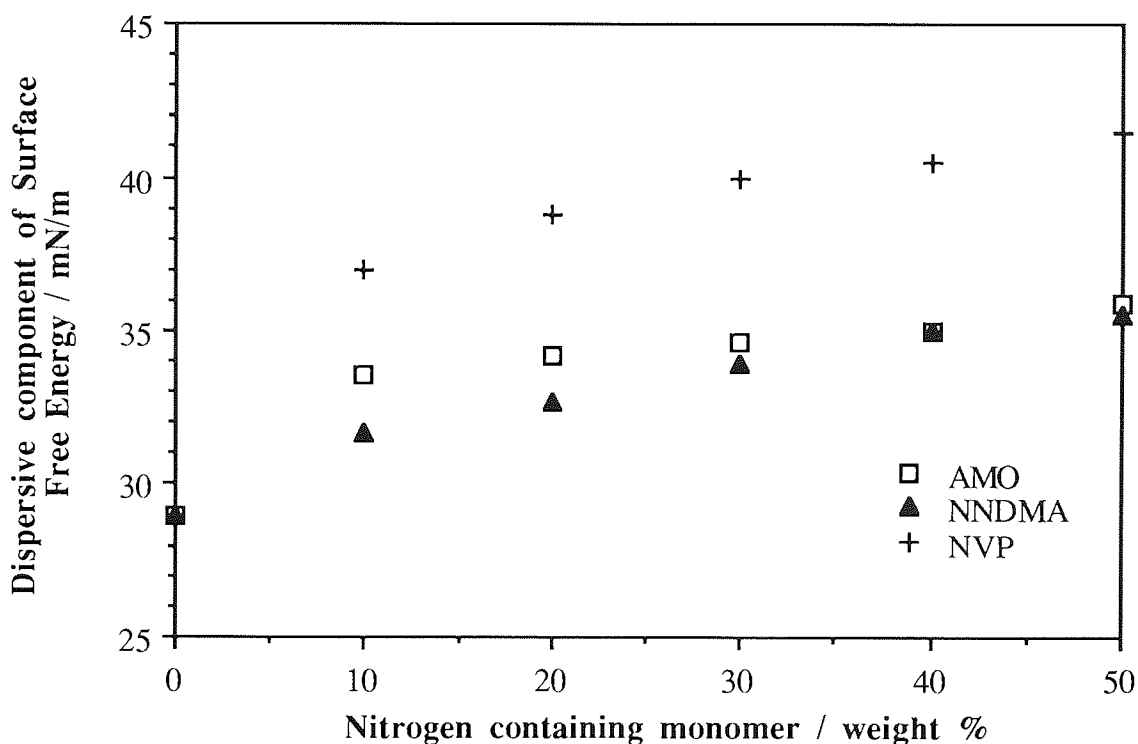


Figure 3.17 Effect of composition on the measured dispersive component of the surface free energy of dehydrated HEMA-AMO, HEMA-NNDMA and HEMA-NVP copolymers

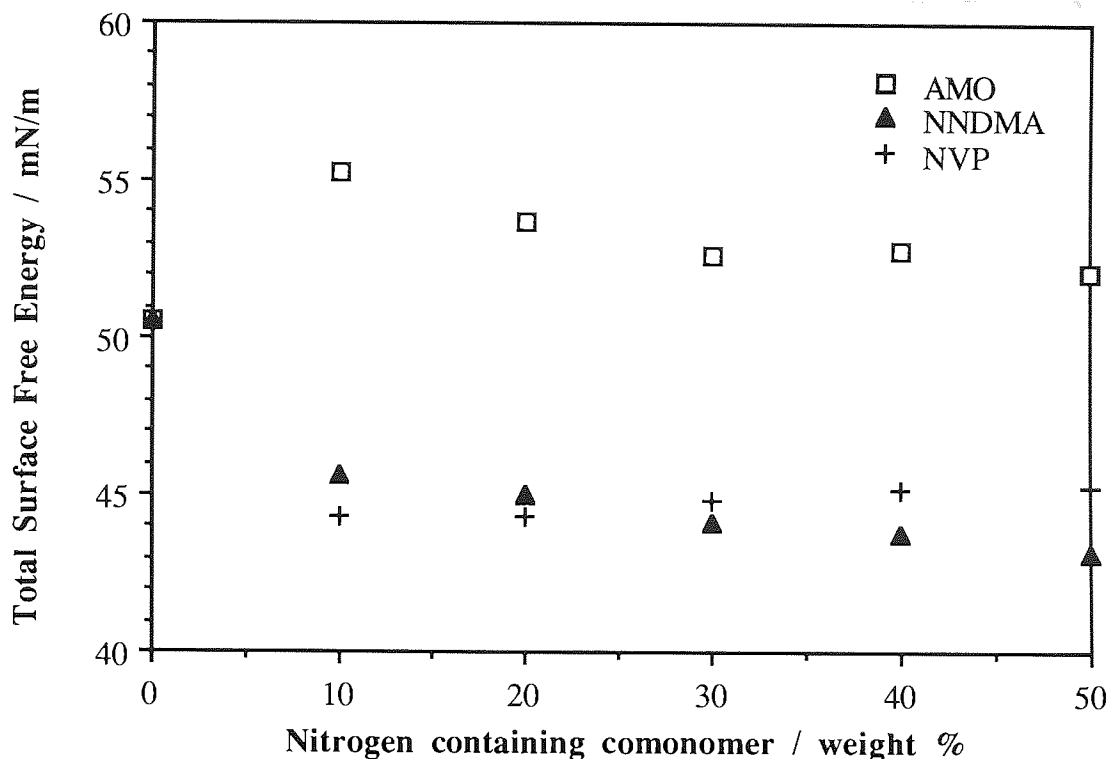


Figure 3.18 Effect of composition on the total surface free energy of dehydrated HEMA-AMO, HEMA-NNDMA and HEMA-NVP copolymers

3.5.2.2 Surface properties of the hydrated copolymers

The total surface free energies of the series of HEMA-AMO, HEMA-NVP and HEMA-NNDMA hydrated copolymers were determined from contact angle measurements obtained using both the Hamilton and captive air bubble techniques.

The values of the polar, dispersive and total surface free energies for each series of the copolymers mentioned above are shown in Appendix II. Figures 3.19 and 3.20 show the values of the polar and dispersive components of the hydrated surface free energies of the HEMA-AMO, HEMA-NVP and HEMA-NNDMA copolymers after the contribution to the total surface free energy due to the polar and dispersive components of water has been subtracted.

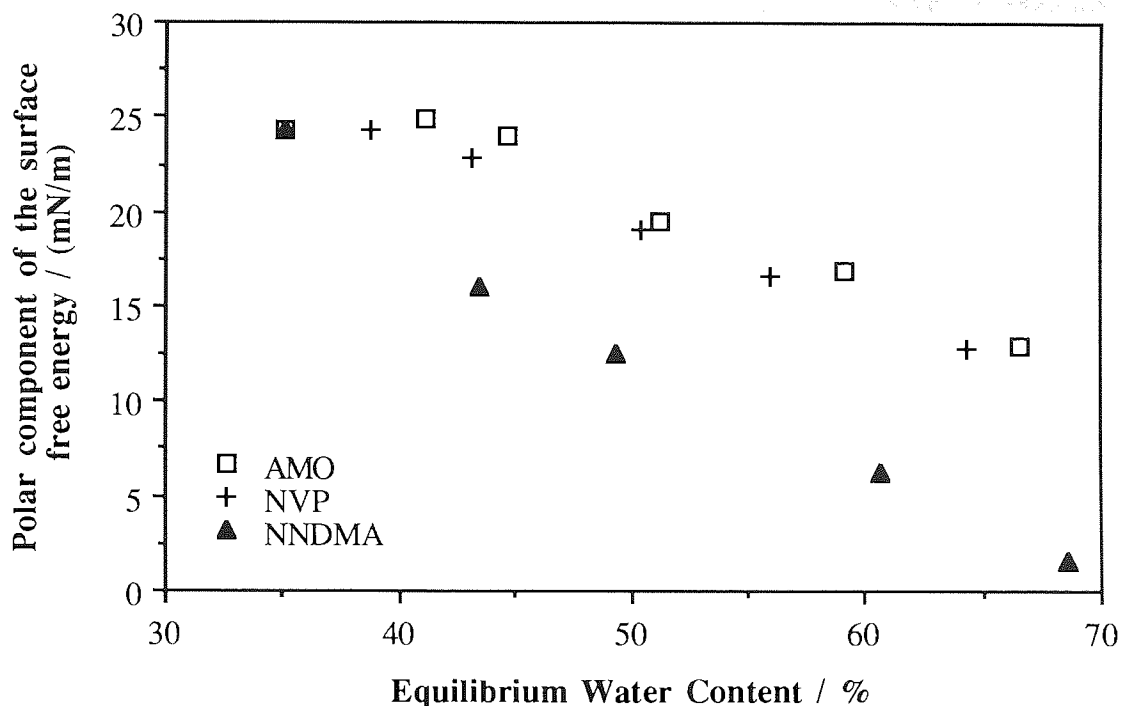


Figure 3.19 Variation in the polar component of the surface free energy with EWC for hydrated HEMA-AMO, HEMA-NNDMA and HEMA-NVP copolymers

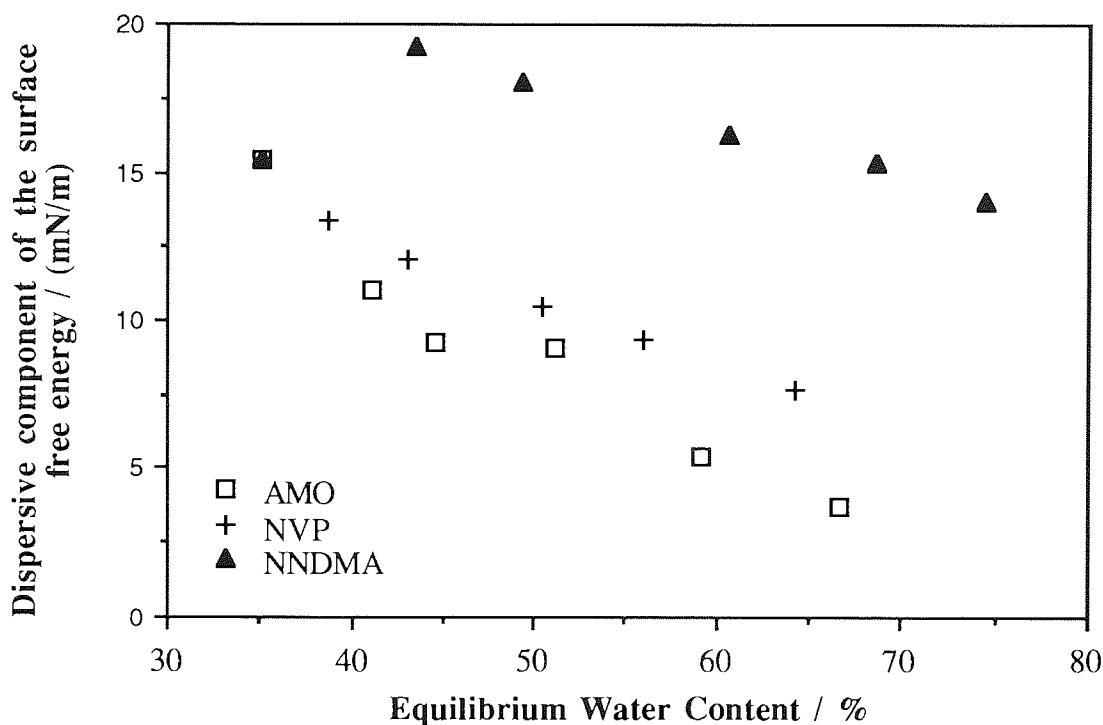


Figure 3.20 Variation in the dispersive component of the surface free energy of hydrated HEMA-AMO, HEMA-NNDMA and HEMA-NVP copolymers

Figures 3.19 and 3.20 illustrate that the value of the polar and dispersive components of the surface free energy decrease with increasing EWC for the series of HEMA-AMO, HEMA-NVP and HEMA-NNDMA copolymers. This observation would be expected because the amount of copolymer expressed as a proportion of the hydrogel (copolymer and water) decreases as the water content increases.

Comparison of Figures 3.19 and 3.20 indicates that the values of the polar component of the surface free energy for the series of HEMA-AMO, HEMA-NVP and HEMA-NNDMA copolymers is greater than the values of the dispersive component. This is because it is energetically more favourable for the polar groups of the copolymers to interact with water at the copolymer-water interface.

Also clear from Figure 3.19 is that the polar components for the series of HEMA-AMO copolymers is greater than the values for both the HEMA-NVP and HEMA-NNDMA copolymers. This indicates that the AMO monomer is more polar than NVP and NNDMA, which is probably due to an additional oxygen atom in the monomer structure of AMO.

3.5.3 Conclusions

The surface properties of the dehydrated HEMA-AMO, HEMA-NVP and HEMA-NNDMA copolymers are consistent with the formation of molecular complexes such that hydrophobic groups within the copolymers are expressed at the air interface and the polar groups are orientated towards the bulk of the polymer.

The surface properties of the hydrated HEMA-AMO, HEMA-NVP and HEMA-NNDMA copolymers are consistent with polar group expression at the water interface and the hydrophobic groups are orientated towards the bulk of the polymer.

The values of the hydrated and dehydrated surface properties indicate that AMO is the most polar of the three nitrogen-containing monomers studied in this work. This increase in the

polar character of AMO compared to NVP and NNDMA can be attributed to the extra oxygen atom in the pendant side group.

3.6 Protein Deposition Studies Of HEMA-NVP, HEMA-NNDMA And HEMA-AMO Copolymer Hydrogels

3.6.1 *In Vitro* Spoilation Procedures Of Membrane Materials 149

Copolymers to be tested were spoiled in "models" which mimic the tear/contact lens interaction. Four disks of sample were cut from each type of membrane using a size 7 cork borer. Three of the disks were used for each experiment and the fourth lens was run as a control. The control samples were run in saline and subjected to any disinfection or cleaning procedure used on the copolymers. No intermediate disinfection or surfactant treatment was used during this study. The procedure used for copolymer spoilation is referred to as the "shaker model" and uses a 1:2 (v/v) solution of foetal calf serum (FCS) diluted with phosphate buffered saline (PBS) as a tear solution substitute. This was then spiked with additional components such as lysozyme in order to mimic the tear lipid / protein composition.

The procedure involves placing a number of small glass beads in a vial, in order to provide an uneven surface on which the disks will sit. This allows contact with the air and tear solution, the latter being pipetted into a level just below the upper surface of the glass beads. The prepared vials were then placed on a shaker (flatbed rotary shaker used at 200 cycles per minute). This enhances the air - tear contact with the lenses. The tear solution in the vials was replaced every 24 hours to maintain the supply of undenatured protein and lipid components.

All the studies presented here were run for a total of 28 days. This produces an accelerated spoilation equivalent to several times this period of normal wear and is representative of extended wear profiles. Since spoilation is patient to patient, material and wear-regime dependent there is no single correlation factor. In our experience the lenses from 28 days *in*

vitro spoilation are equivalent to some six months *in vivo* wear, but for reasons stated above this cannot be used as a constant spoilation factor. Removal of patient to patient variability is a major reason for the use of an *in vitro* tear model in comparative studies of this type.

Prior to their exposure to the tear solution the fluorescence spectra of the copolymer disks were recorded after rinsing with sterile saline. Three disks of each copolymer sample were then exposed in the model and one disk of each sample in control saline. Their fluorescence spectra were monitored every 3 days.

3.6.2 Surface Fluorescence Analysis Of Gross Spoilation Profiles

Spectra (of the copolymer disks placed in the 8mm diameter cylindrical cell with the centre of the lens facing the light beam) were recorded with a modified Aminco-Bowman Fluorescence Spectrophotofluorimeter at excitation wavelengths of 360nm and 280nm since the emission from adsorbed proteinaceous and lipoidal components on the lens surface most commonly occur at these excitation wavelengths. The emission spectra are recorded between 200 and 800nm. Excitation at 280nm produces emission centred around 360nm, which provides the best measure of total gross protein whereas excitation at 360nm produces the best measure of gross lipid. An additional lipid peak is also determined at an excitation wavelength of 280nm which is indicative of the soluble aqueous phase lipid component. Examples of fluorescence spectra excited at 360nm and 280nm are shown in Figures 3.21 and 3.22 respectively.

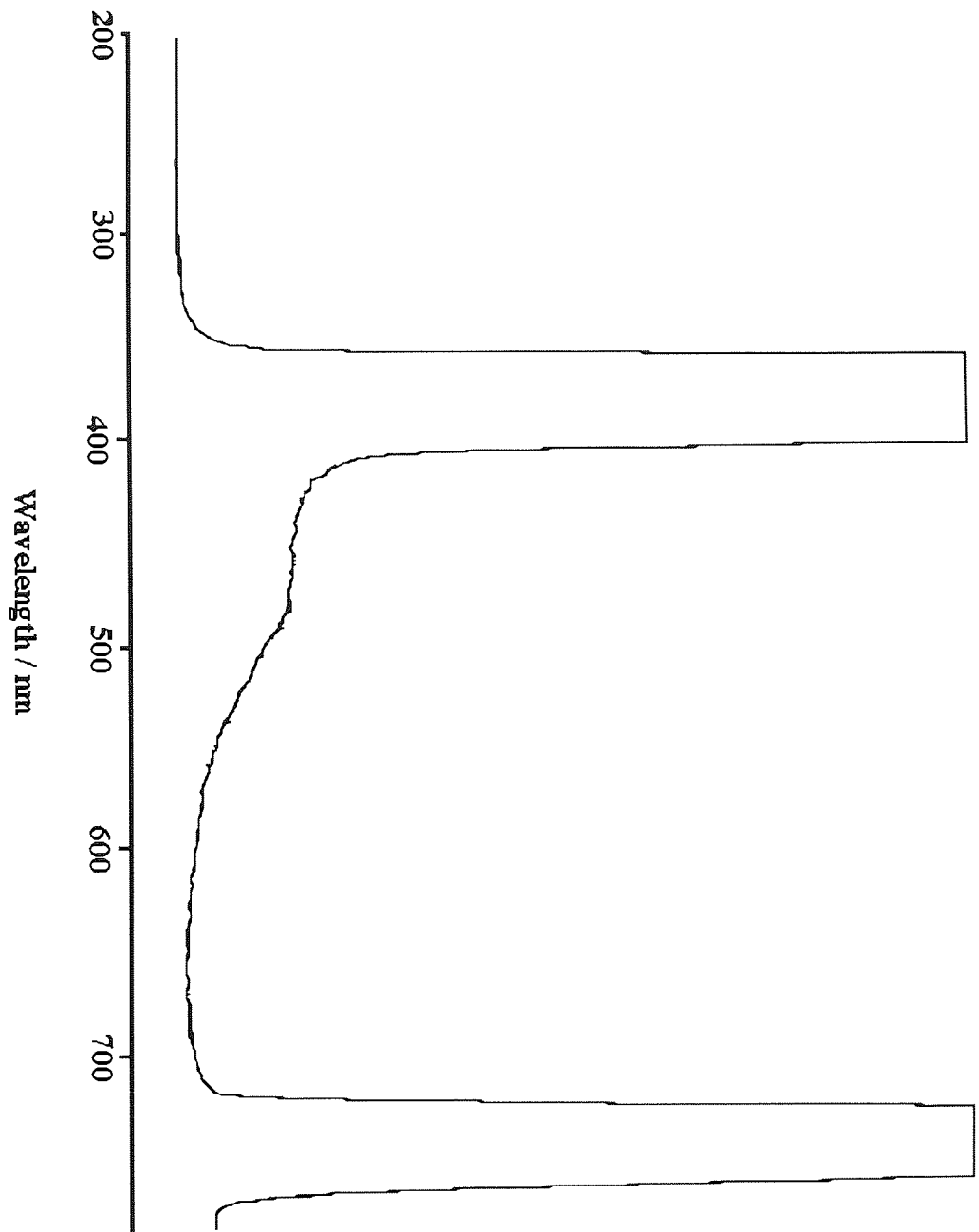


Figure 3.21 Fluorescence spectrum excited at 360 nm

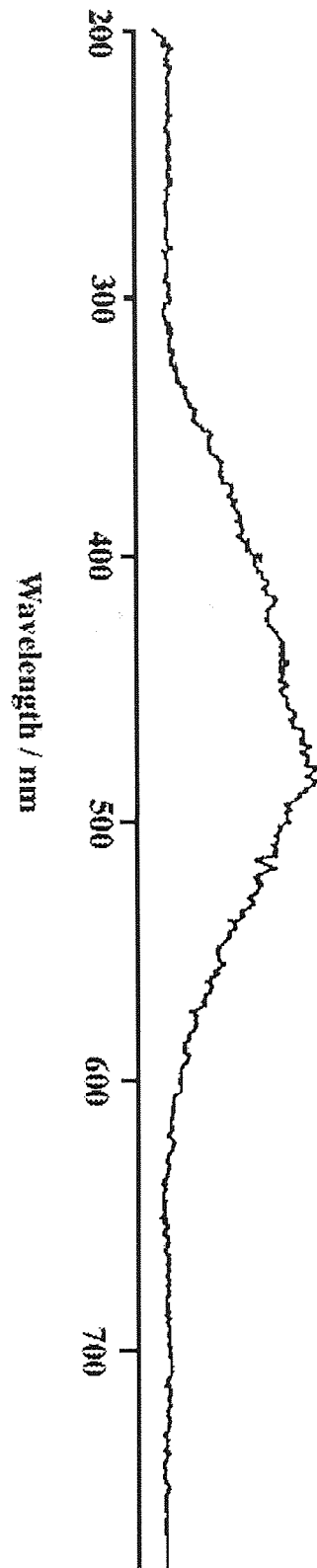


Figure 3.22 Fluorescence spectrum excited at 280 nm

3.6.3 Results

This investigation was designed to establish the effect of the type and amount of nitrogen-containing monomer on the protein and lipid deposition characteristics of HEMA copolymers.

The results of the protein and lipid deposition studies for the HEMA-NVP, HEMA-NNDMA and HEMA-AMO copolymer membranes are shown in Figures 3.23 - 3.37. Each deposition graph contains the results obtained for copolymers having equal amounts of the nitrogen-containing monomers. This is to show the effect of the type of nitrogen-containing monomer on the amount of deposition. The series of graphs are on common scales which enables the effect of the amount of nitrogen-containing monomer on the quantity of deposition to be established.

Figures 3.23 - 3.25 show the lipid and protein spoilation for the HEMA copolymer membranes containing 10 weight% of the nitrogen-containing monomer. These show that the amount of lipid and protein deposited on each of the copolymers increases with time. The amount of lipid deposition is greatest for the HEMA-NNDMA copolymers and least for the HEMA-AMO copolymers. The same trend is observed for the amount of protein deposited on the copolymers. The amount of protein deposited increases with time and the largest amount of protein is deposited on the HEMA-NVP copolymers and the lowest quantity on the HEMA-AMO copolymers.

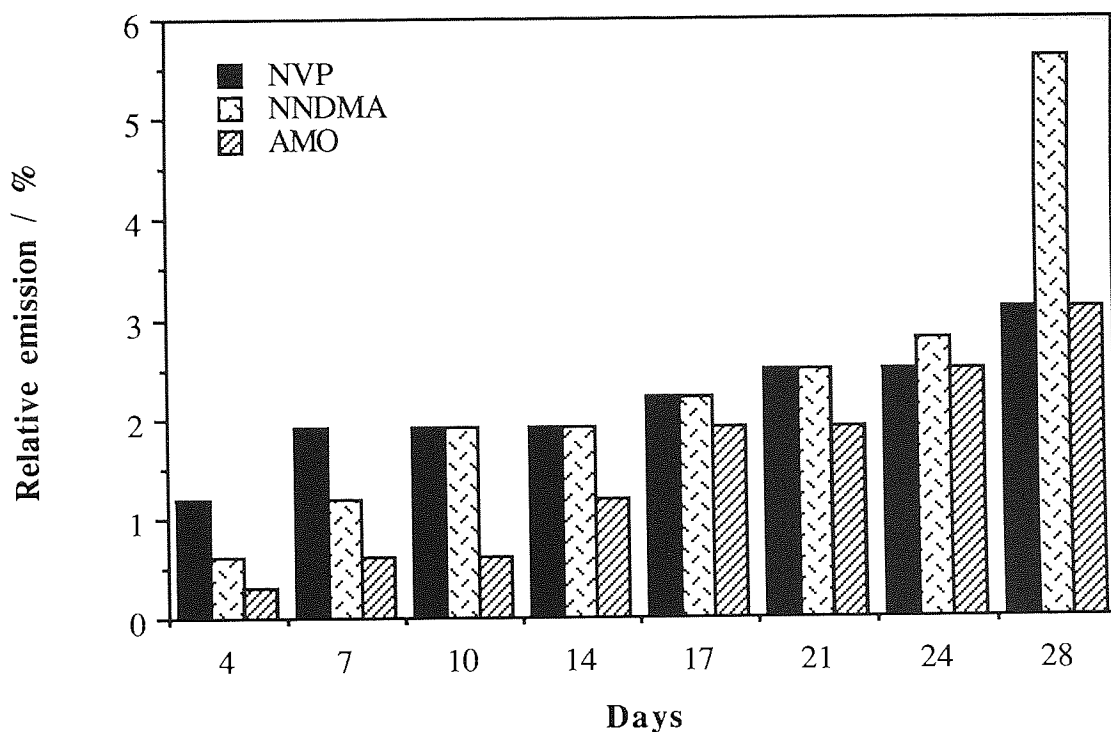


Figure 3.23 Progressive build-up of lipid spoilation, excited at 360 nm, of HEMA-NVP, HEMA-NNDMA, HEMA-AMO 90:10 membranes

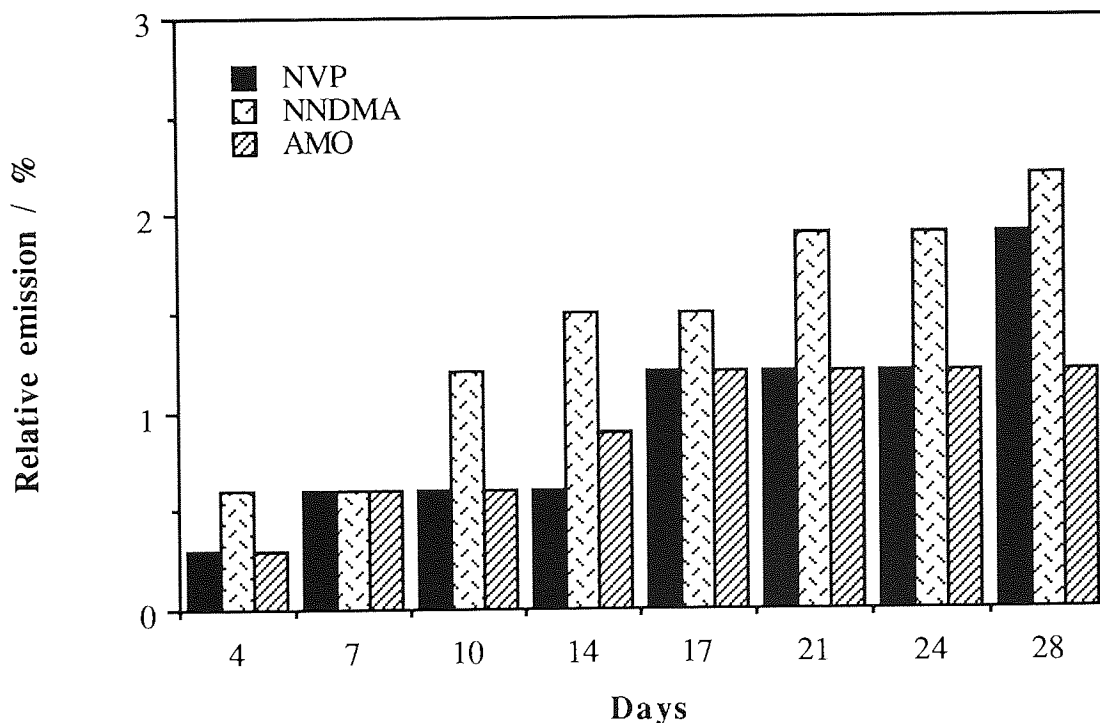


Figure 3.24 Progressive build-up of lipid spoilation excited at 280 nm of HEMA-NVP, HEMA-NNDMA, HEMA-AMO 90:10 membranes

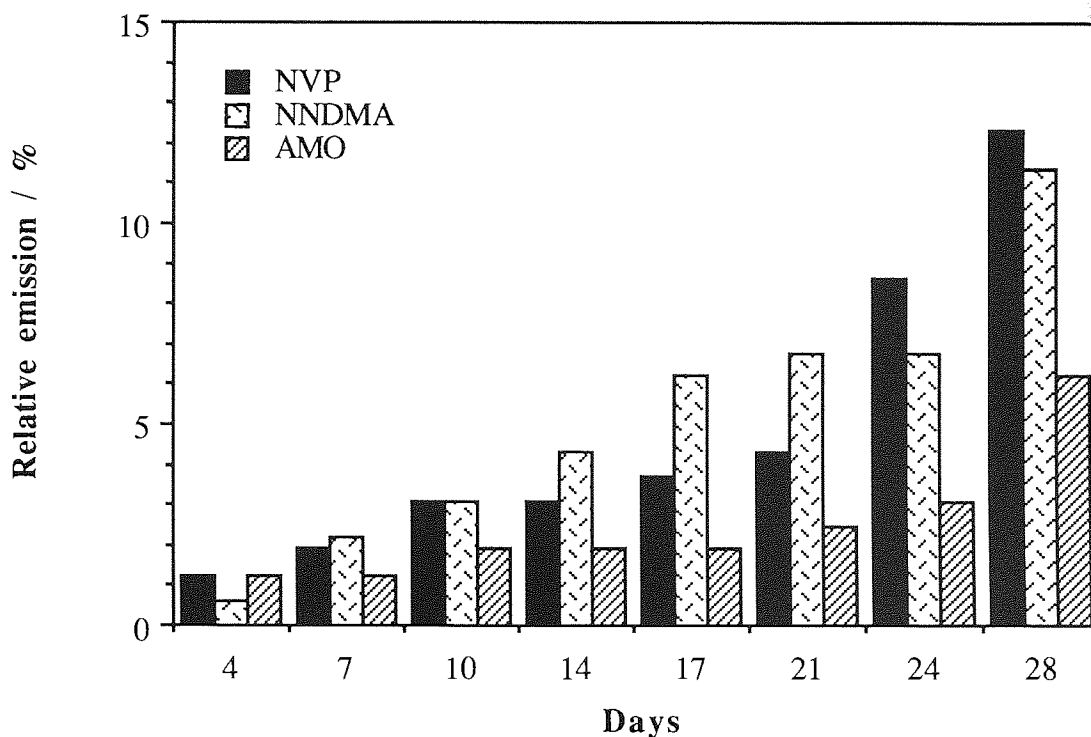


Figure 3.25 Progressive build-up of protein spoilation of HEMA-NVP, HEMA-NNDMA, HEMA-AMO 90:10 membranes

Figures 3.26 - 3.28 show the amounts of lipid and protein deposited on the HEMA copolymers containing 20 weight% of the nitrogen-containing monomers. These figures further support the fact that the amount of lipid and protein deposited increases with time. It is also further evidence that the least amount of lipid and protein is deposited on the HEMA-AMO copolymers.

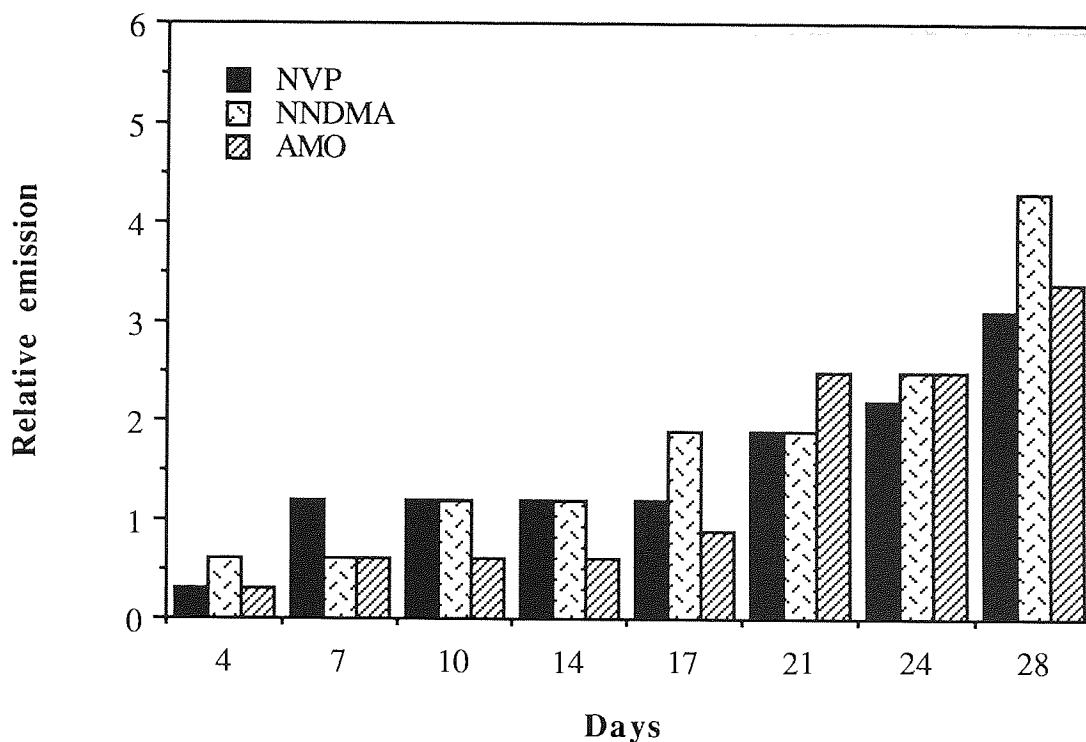


Figure 3.26 Progressive build-up of lipid spoilation excited at 360 nm of HEMA-NVP, HEMA-NNDMA, HEMA-AMO 80:20 membranes

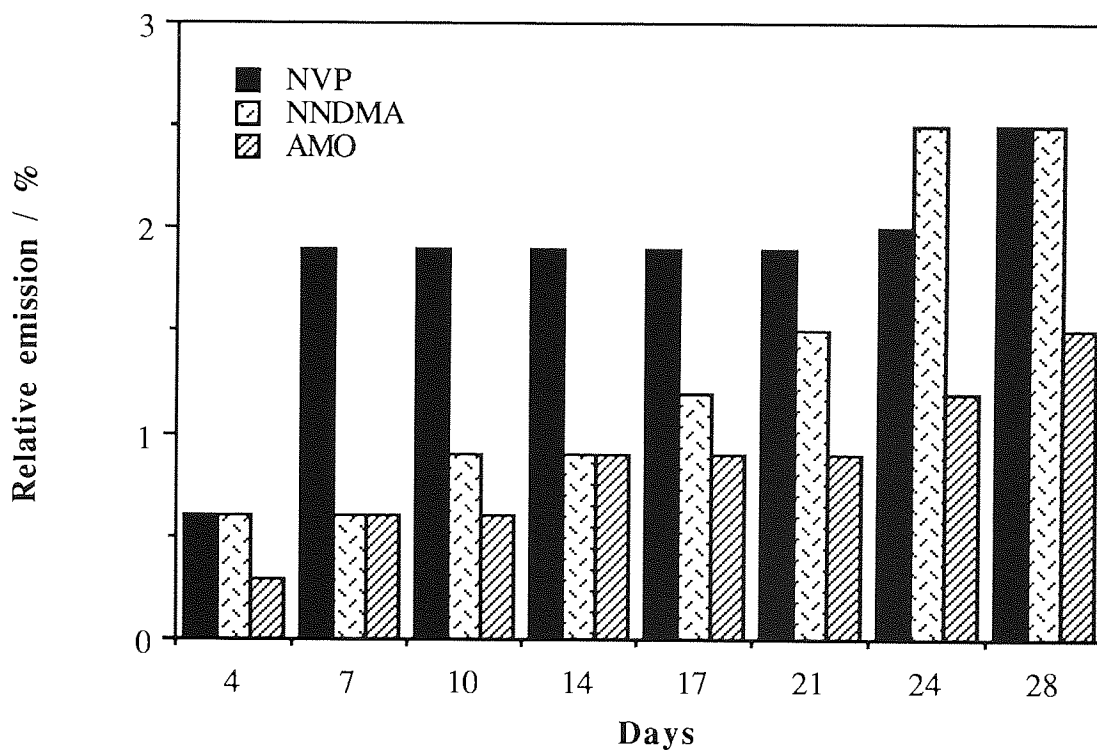


Figure 3.27 Progressive build-up of lipid spoilation excited at 280 nm of HEMA-NVP, HEMA-NNDMA, HEMA-AMO 80:20 membranes

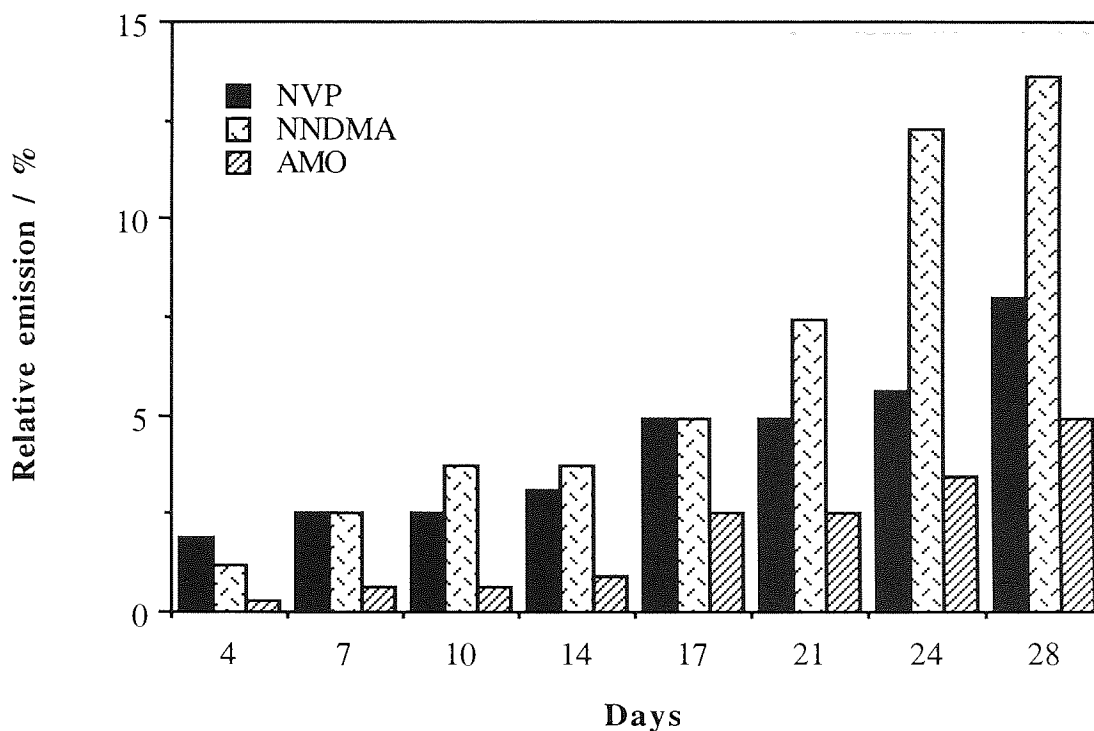


Figure 3.28 Progressive build-up of protein spoilation of HEMA-NVP, HEMA-NNDMA, HEMA-AMO 80:20 membranes

Figures 3.29 - 3.31 show the amounts of protein and lipid deposited on the HEMA copolymers containing 30 weight% of the nitrogen-containing monomers. While Figures 3.32 - 3.34 show the amounts deposited on the HEMA copolymers containing 40 weight% of the nitrogen-containing monomers. The remaining Figures 3.33 - 3.35 illustrate the amounts of protein and lipid deposited on the HEMA copolymers containing 50 weight% of the nitrogen-containing monomers. Some of the results were unobtainable as the materials broke during the course of *in vitro* spoilation procedure.

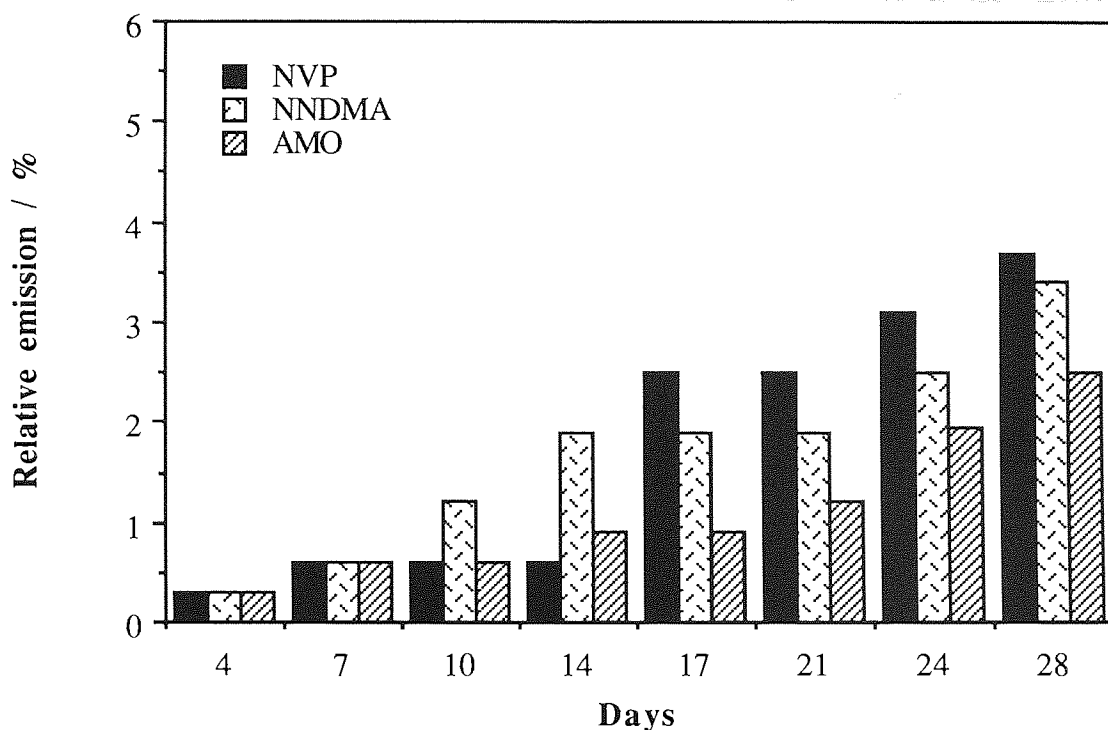


Figure 3.29 Progressive build-up of lipid spoilation excited at 360 nm of HEMA-NVP, HEMA-NNDMA, HEMA-AMO 70:30 membranes

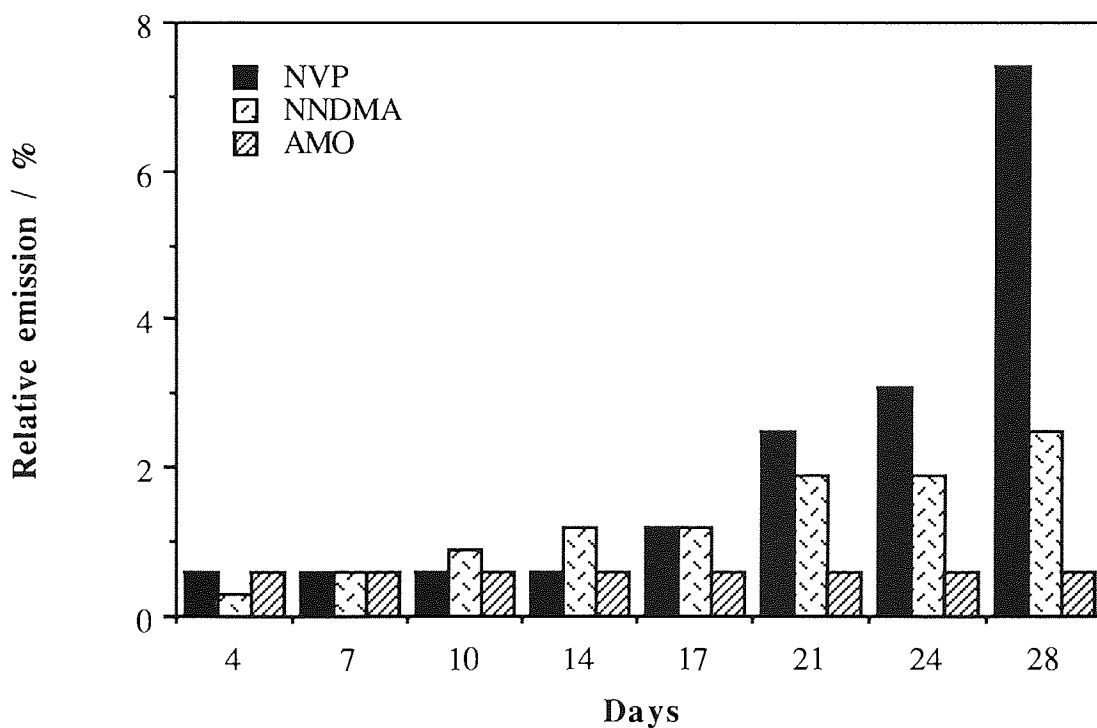


Figure 3.30 Progressive build-up of lipid spoilation excited at 280 nm of HEMA-NVP, HEMA-NNDMA, HEMA-AMO 70:30 membranes

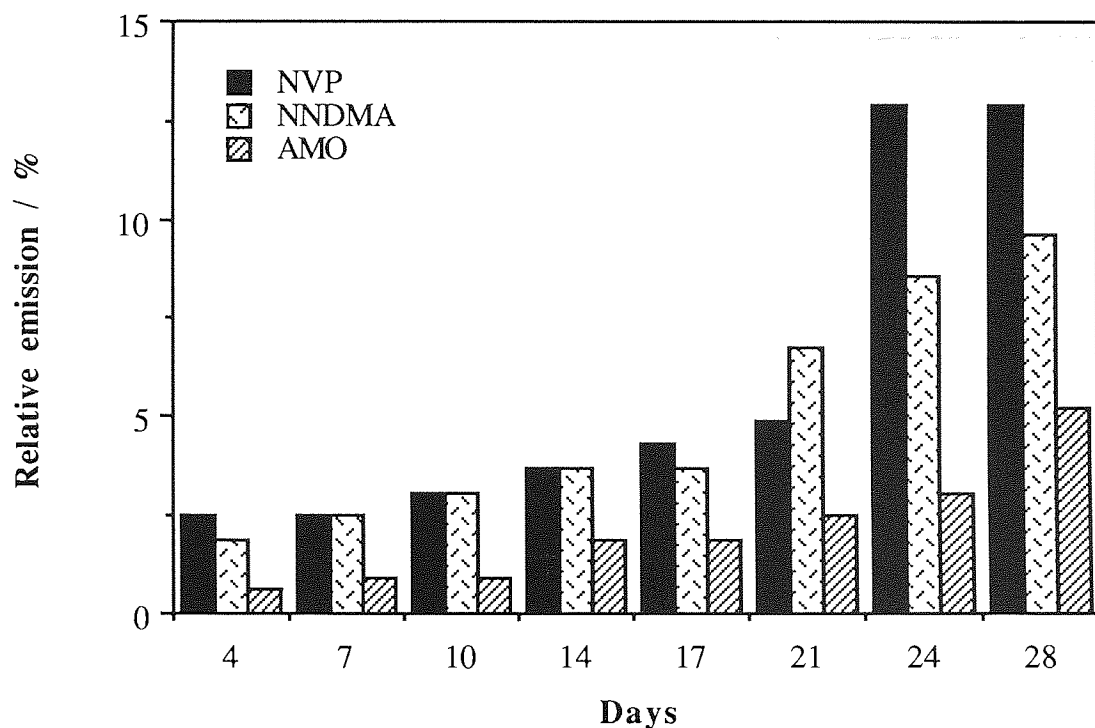


Figure 3.31 Progressive build-up of protein spoilage of HEMA-NVP, HEMA-NNDMA, HEMA-AMO 70:30 membranes

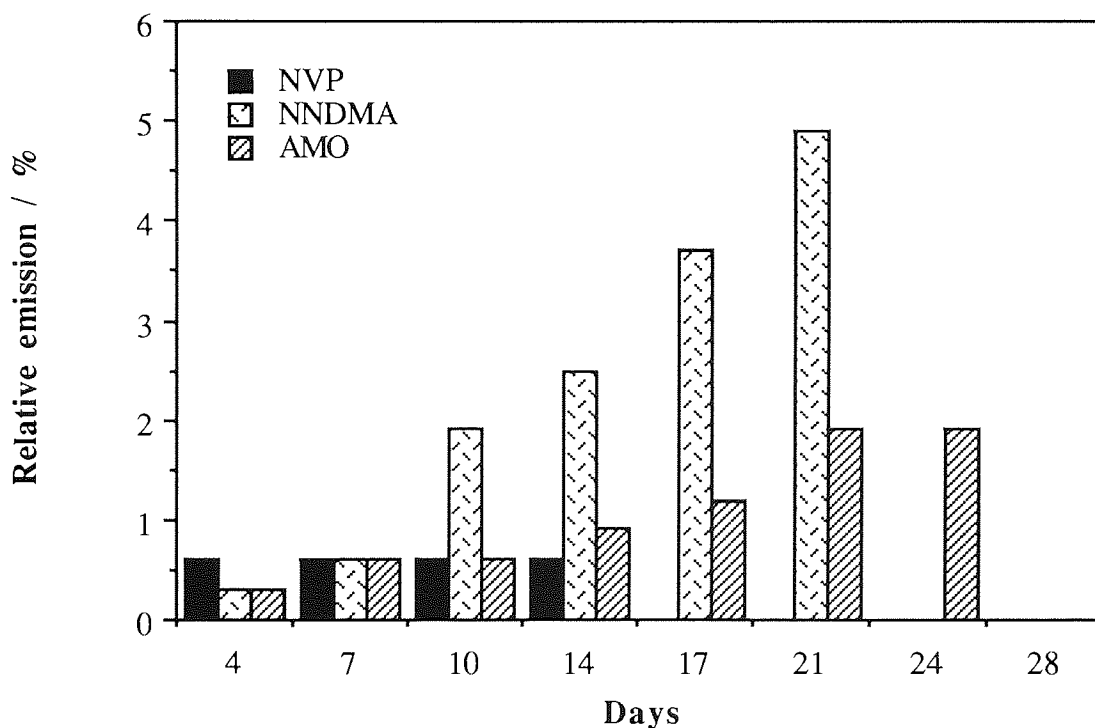


Figure 3.32 Progressive build-up of lipid spoilage excited at 360 nm of HEMA-NVP, HEMA-NNDMA, HEMA-AMO 60:40 membranes

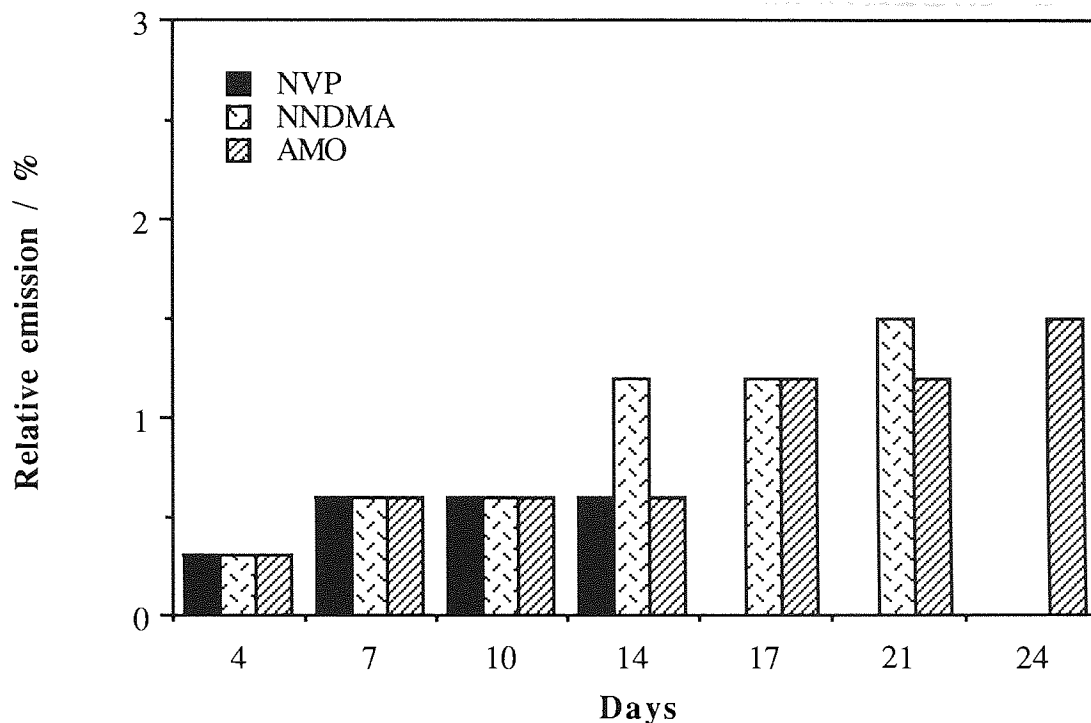


Figure 3.33 Progressive build-up of lipid spoilage excited at 280 nm of HEMA-NVP, HEMA-NNDMA, HEMA-AMO 60:40 membranes

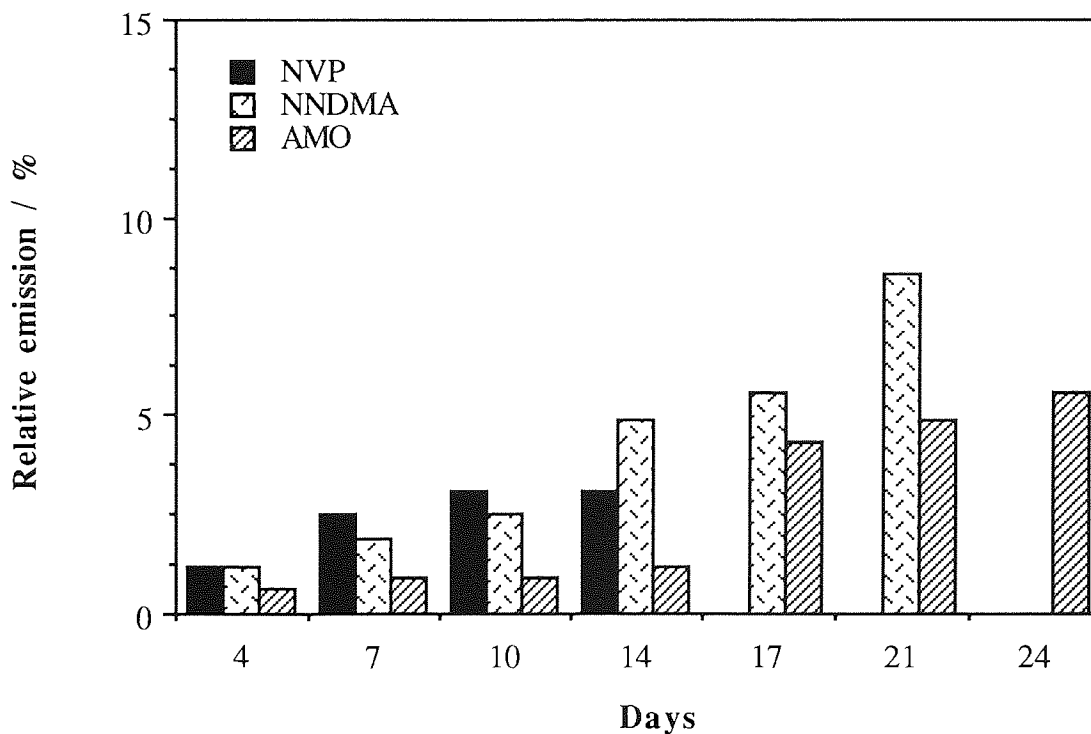


Figure 3.34 Progressive build-up of protein spoilage of HEMA-NVP, HEMA-NNDMA, HEMA-AMO 60:40 membranes

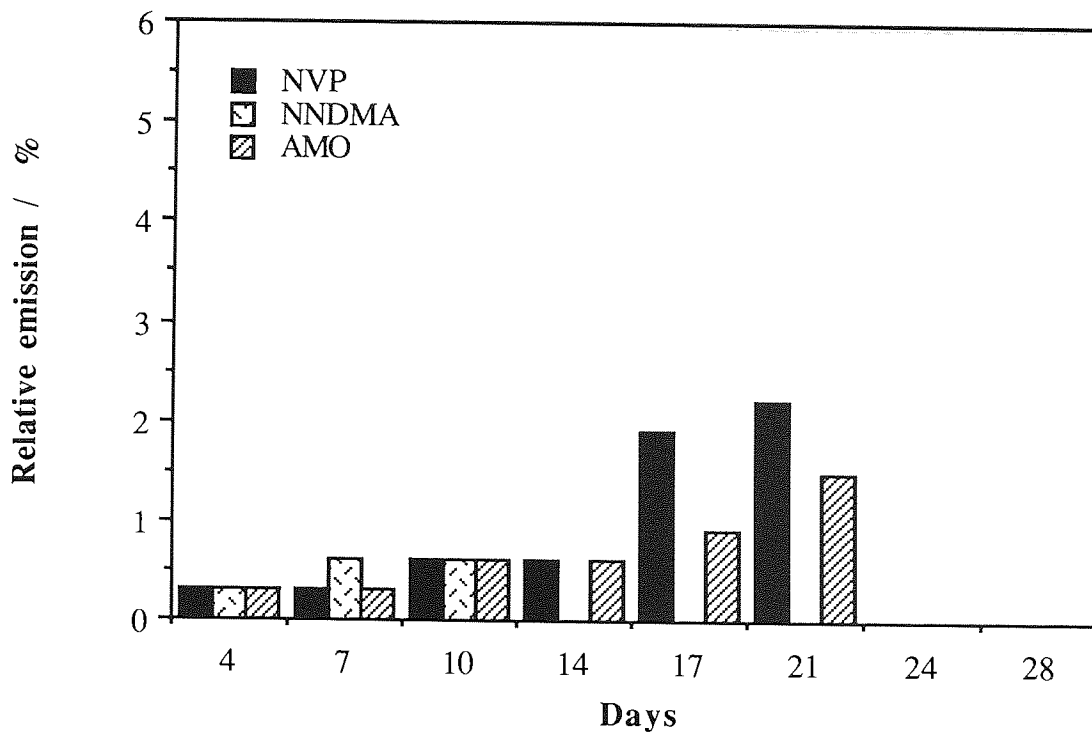


Figure 3.35 Progressive build-up of lipid spoilation excited at 360 nm of HEMA-NVP, HEMA-NNDMA, HEMA-AMO 50:50 membranes

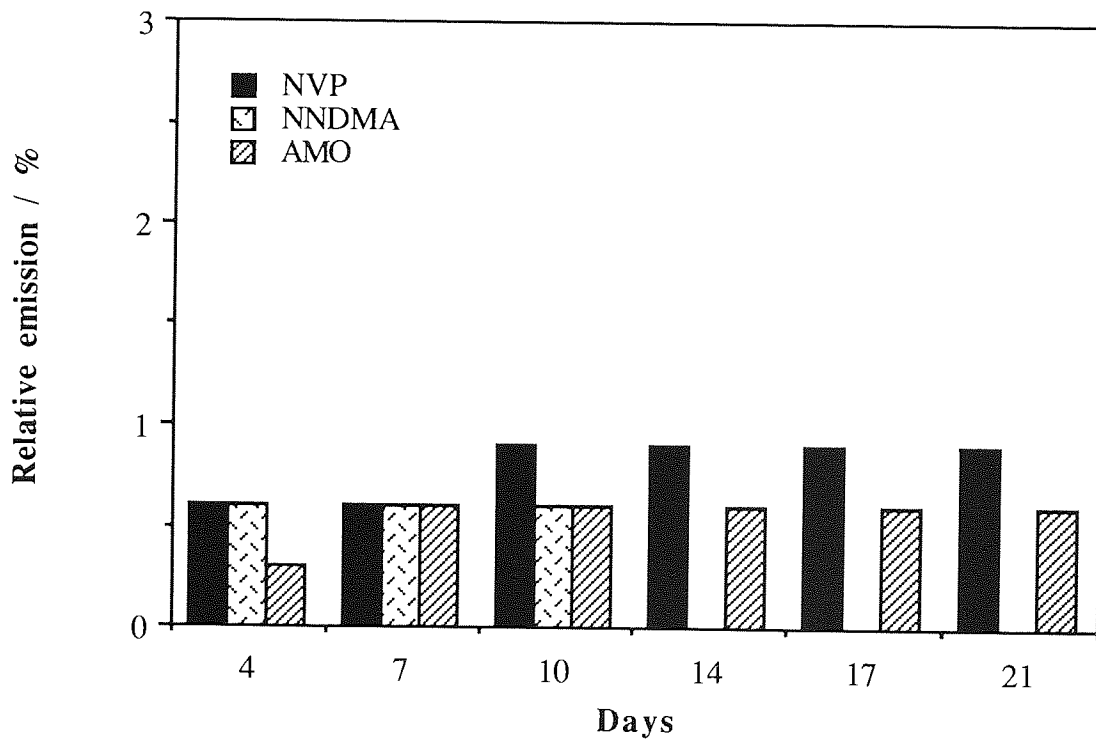


Figure 3.36 Progressive build-up of lipid spoilation excited at 280 nm of HEMA-NVP, HEMA-NNDMA, HEMA-AMO 50:50 membranes

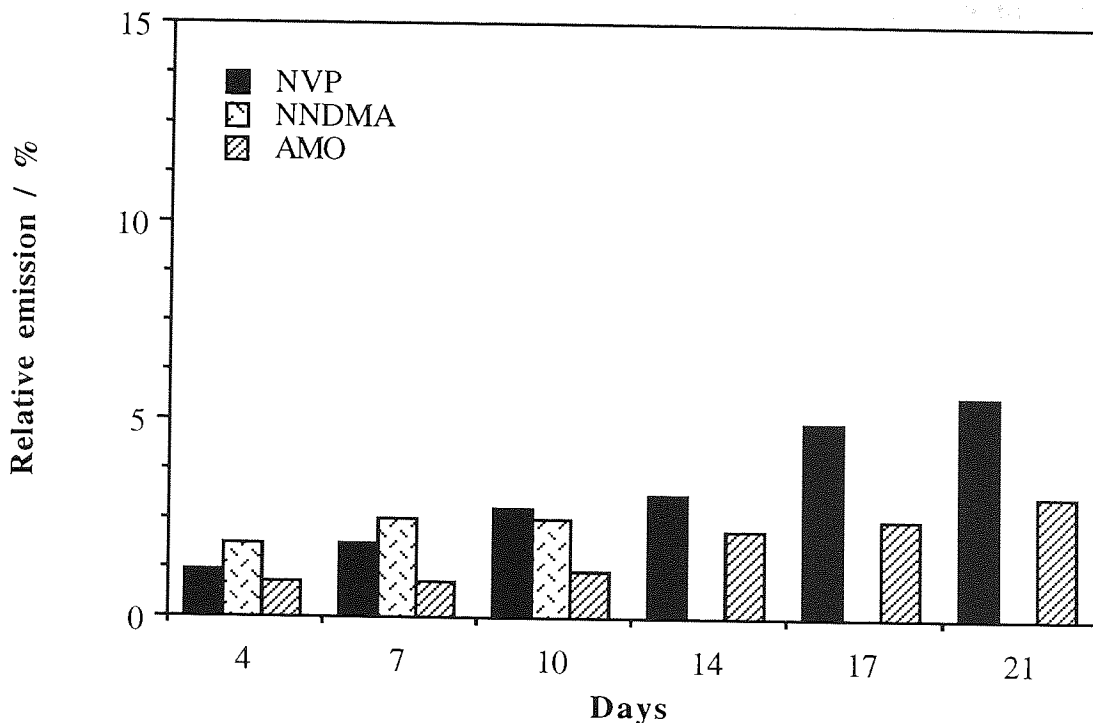


Figure 3.37 Progressive build-up of protein spoilation of HEMA-NVP, HEMA-NNDMA, HEMA-AMO 50:50 membranes

A number of factors have been shown to be important in affecting the amount of adsorption to hydrogels. These include the sequence distribution, the water structuring within the copolymer and the polar and dispersive character of the hydrogel surface.

The results presented in this Chapter suggest that lower levels of protein and lipid adsorption exhibited by the HEMA-AMO copolymers as compared to HEMA-NVP and HEMA-NNDMA copolymers may be attributed to the sequence distribution of the AMO, the strong water binding ability of AMO and the polar character exhibited by AMO surfaces.

3.6.4 Conclusions

These sets of Figures (3.23 - 3.37) support the conclusion that the amount of lipids and proteins deposited on HEMA-AMO copolymers was lower than the quantities deposited on HEMA-NVP and HEMA-NNDMA copolymers and that the amounts deposited increased

with time. Further comparison of Figures 3.23 - 3.37 indicates that the rate at which the lipid and protein is deposited onto the HEMA copolymers decreased with increasing proportion of the more hydrophilic nitrogen-containing monomer.

3.7 Summary

This Chapter has highlighted the potential of acryloylmorpholine as a novel hydrophilic monomer for hydrogel synthesis.

The reactivity ratio of AMO towards free radical polymerisations is greater than the reactivity of NVP and is comparable with the structurally similar NNDMA. The result of this increased reactivity is to produce a HEMA copolymer which has alternating short sequences of the two monomer types and an actual copolymer composition which is comparable to the values of the feed ratio.

AMO is hydrophilic and interacts with water very strongly, displaying non-freezing water contents which are greater than NVP or NNDMA.

HEMA-AMO copolymers show greater elastic moduli than the comparable HEMA-NVP and HEMA-NNDMA copolymers, because of the higher energy barrier to rotation of AMO compared to NVP and NNDMA. AMO produces alternating sequences with HEMA, unlike NVP which has a tendency to produce blocks and does not undergo chain transfer reactions which are characteristic of NNDMA.

The surface properties of AMO are typical of a hydrophilic monomer. In the dehydrated state copolymers containing AMO orientate the polar groups to the bulk of the polymer away from the copolymer-air interface. Whereas in the case of hydrated copolymers the polar groups are orientated towards the water. AMO has also been shown to be more polar than NVP and NNDMA.

The HEMA-AMO copolymers show lower levels of protein and lipid adsorption than HEMA-NVP and HEMA-NNDMA copolymers. This is probably due to a number of factors which have been shown to affect the amount of protein adsorption.

CHAPTER 4
High Water Content Systems
Incorporating Acryloylmorpholine
as the Hydrophilic Component

4.1 Introduction

The work presented in Chapter 3 highlighted the potential of AMO as a hydrophilic monomer in the production of high water content hydrogels. However, although AMO shows an improved sequence distribution with HEMA in comparison with the commercially used NVP, there is still the formation of a terminal block of some size. The terminal block will be composed of hydrophilic AMO and is water soluble. Therefore it may be possible that this terminal block may be leached out of the copolymer upon hydration of the membrane. However, should this not occur, then the presence of a block of one monomer unit may increase the amount of deposition on the copolymer surface.

It would therefore be preferable to use the advantages of acryloylmorpholine presented in the preceding chapter to their full potential by copolymerisation not with HEMA, but with another hydroxy monomer which possesses physical and chemical characteristics similar to HEMA, but produces a copolymer with a greater degree of alternation of the monomer repeat units.

In an attempt to produce a copolymer with an alternating copolymer structure of a narrower distribution of sequence lengths than HEMA-AMO, a further series of copolymers of AMO were characterised using other hydroxy monomers which possessed similar structural characteristics to HEMA. The hydroxy monomers used were 2-hydroxypropyl methacrylate (HPMA) and 2-hydroxypropyl acrylate (HPA). The polymerisation of HPMA-AMO and HPA-AMO copolymers enabled the structural factors of the hydroxy monomers which affected the reactivities and physical characteristics of the series of hydroxy monomer-AMO copolymers to be determined. From the results of the characterisations it would be possible to determine what characteristics of the hydroxy monomers could be exploited to allow production of an alternating copolymer structure with AMO and the desired water content, mechanical and surface characteristics.

4.2 Characterisation of the Sequence Distributions of the HEMA-AMO, HPMA-AMO and HPA-AMO copolymer systems

4.2.1 Introduction

It was necessary to study the reactivity and physical characteristics of HPMA-AMO and HPA-AMO hydrogel copolymers to determine the structural characteristics of the hydroxy monomers which affected the reactivity of the comonomer pairs and the physical characteristics of the copolymer membranes. By studying the elements which affect the reactivity characteristics it would be possible to determine which of the hydroxy monomers would produce a copolymer with AMO which possessed the narrowest distribution of sequence lengths. The next stage was to characterise the sequence distributions of the systems obtained when AMO was copolymerised firstly with hydroxypropyl acrylate which is a structural isomer of HEMA and secondly with hydroxypropyl methacrylate which is slightly less hydrophilic than HEMA.

4.2.2 Methods And Results

The sequence simulations of HEMA-AMO, HPMA-AMO and HPA-AMO copolymers were obtained using the computer program outlined in Chapter 2. Each of these copolymer simulations was obtained using reactivity ratio values which had been determined by the Q-e scheme. The values of the reactivity ratios for the HEMA-AMO, HPMA-AMO and HPA-AMO copolymers are shown in Table 4.1 and the sequence simulations for a 70:30 weight/weight composition of each of these copolymers are shown in Figures 4.1 - 4.3.

Table 4.1 Calculated reactivity ratios for the copolymer systems HEMA-AMO, HPMA-AMO and HPA-AMO

Copolymer System	r ₁	r ₂
HEMA-AMO	3.790	0.210
HPMA-AMO	0.409	0.102
HPA-AMO	0.120	0.096

70 mole % of Monomer A, HEMA

30 mole % of Monomer B, AMO

$r(AB) = 3.790$

$r(BA) = 0.210$

Polymerised to 100% conversion

In the simulated copolymer HEMA is represented by O and AMO is represented by X

```

OOXOOOOOOOOXOOOOOOXOXOOOOOOXOXOOOOOOXXOOOOOOOOOOOOXOOOOOOOOX
XOOOOOOOOOOOOXOOOOOOXOOOOOOOOXOXOOOOOOOOXOOOOOOXOOOXOOOOOOOOOX
OOXOOOOOOOOOOOOXOOXOOOOOOOOOOOOOOOOOOOOOOOOOOOOOOOOOOOOOOOOOO
OOOOOOOOOOOOOOOOXOOOOOXOOOOOOOOOOOOOOOOXOOOOOXOOOOOOOXOOOOOOXXO
OOOOXOOXOOOOXXOOOXOOOOOOXXOXOOOOOOXOXOOOOOOXOXOOOXOOOOOOOO
OXOOOOOOOOOOOOOOOOOOOOOOOOOOXOOOOOOOOOOXOXOOOOOXOOOOOOOOOXOOOXO
OOOOXOOOOOOOOOOOOOOOOOOOOOOOOOOXOOOXOOXOOOOOOOOOOOOOOOOOOOXOOOXO
XOOOOOOOOXOOOXOOOOOOOOOOXOOOOOOOOOOXOOOXOOOOOOXOOXOOOOOOOOOO
OOOOXOOOOOOOOOOOOXOOOXOOOXOOOOOOOOOOOOXOOXOOOOOOOOOOOOOOOOOOOO
OOOOOOOOOOOOOOOOXOOOOOOXOOOOOOOOOOOOXXXOXOOOOOOOOOXOXOXOOOXOO
OOOOOOOOOXOOOOOXOOOXOOXOXOOOXOOOOOOOOOOOOOOOOOOOOOOOOXOOOOOOOO
OOXOOOOXOOOXOOOXOOOXOOOXOOOXOOOXOOOXOOOXOOOXOOOXOOOXOOOXOOOXOO
OOOOOOXOOOXOOOXOOOXOOOXOOOXOOOXOOOXOOOXOOOXOOOXOOOXOOOXOOOXOOOX
OOOOOOXOOOXOOOXOOOXOOOXOOOXOOOXOOOXOOOXOOOXOOOXOOOXOOOXOOOXOOOX
OXOXOXOOOXOOOXOOOXOOOXOOOXOOOXOOOXOOOXOOOXOOOXOOOXOOOXOOOXOOOX
XOOXOOXOXOOXOXOOOXOOOXOOOXOOOXOOOXOOOXOOOXOOOXOOOXOOOXOOOXOO
OOOOOOOOOOOXOOOOOOXXXOXOOOOOOOOOOXOOOOOOXOXOOXOOOXOOXOOOXOOOXOO
OOOOOOOOOOOOXOOOXOOXOOOXOOXOOOXOOXOOOXOOXOOXOOXOOXOOXOOXOOXOO
XOXOOOOOXOOOXOOOXOOOXOOOXOOOXOOOXOOOXOOOXOOOXOOXOOXOOXOOXOOOXOO
OOXOOOXOOOXOOOXOOOXOOOXOOOXOOOXOOOXOOOXOOOXOOOXOOXOOXOOXOOOXOO
XOXOXOOOXOOOXOOOXOOOXOOOXOOOXOOOXOOOXOOOXOOOXOOOXOOOXOOOXOOOX
XOXOXOOOXOOOXOOOXOOOXOOOXOOOXOOOXOOOXOOOXOOOXOOOXOOOXOOOXOOOX
OXOOOOOXOOOXOOOXOOOXOOOXOOOXOOOXOOOXOOOXOOOXOOOXOOOXOOOXOOOXOO
OXXXXXOXOXOXOOXXXXXOOXOOXOOOXOOOXOOOXOOOXOOOXOOOXOOOXOOOXOOOX
XOOXOOOXOOXOOXOOXOOXOOXOOXOOXOOXOOXOOXOOXOOXOOXOOXOOXOOXOOXOO
OOOXOOOXOOXOOXOOXOOXOOXOOXOOXOOXOOXOOXOOXOOXOOXOOXOOXOOXOOXOO
XXXXXXXXXXXXXXXXXXXXXXXXXXXXXXXXXXXXXXXXXXXXXXXXXXXXXXXXXXXXXXXXXXXX
XXXXXXXXXXXXXXXXXXXXXXXXXXXXXXXXXXXXXXXXXXXXXXXXXXXXXXXXXXXXXXXXXXXX

```

The simulated copolymer contains 1400 HEMA units and 600 AMO units

Sequence Distributions

Sequence Length	HEMA	AMO
1	70	225
2	54	28
3	36	12
4	25	19
5	22	6
6	15	8
7	14	0
8	18	0
9	13	1
10	12	0
11	6	0
12	4	0
13	4	0
14	3	0
15	5	0
16	1	0
120	0	1

Figure 4.1 Sequence simulation of 70:30 wt/wt HEMA-AMO copolymer

70 mole % of Monomer A, HPMA

30 mole % of Monomer B, AMO

$r(AB) = 0.409$

$r(BA) = 0.102$

Polymerised to 100% conversion

In the simulated copolymer HPMA is represented by O and AMO is represented by X

```

OOXOOOXOOOXOOXOOOOOXOOOXOOXOXOXOXOXOOOXOXOXOXOOXOOOXOXOXOX
OOXOOXOXOXOXOXOXOXOXOOOXOXOOXOXOXOXOOXOXOOXOXOOOXOXOOOXOOOXO
XOOXOXOOOXOXOXOXOXOXOXOOXOXOXOXOXOXOOXOXOOXOXOXOOXOXOXOXOXOXO
OOXOOOOOOOXOOOXOOXOOXOOOXOXOXOXOOOXOXOOOXOXOOOXOXOXOXOXOXOXOO
OOXOXOXOXOXOXOXOXOXOXOXOXOXOXOXOXOXOXOXOXOXOXOXOXOXOXOXOXOXOX
OXOOOXOXOXOXOXOXOXOXOXOXOXOXOXOXOXOXOXOXOXOXOXOXOXOXOXOXOXOXOX
OXOOXOOXOOXOXOXOXOXOXOXOXOXOXOXOXOXOXOXOXOXOXOXOXOXOXOXOXOXOXOX
XOXOXOXOXOXOXOXOXOXOXOXOXOXOXOXOXOXOXOXOXOXOXOXOXOXOXOXOXOXOXO
OXOOOXOOXOXOXOXOXOXOXOXOXOXOXOXOXOXOXOXOXOXOXOXOXOXOXOXOXOXOXOX
OOXOXOOOXOXOXOXOXOXOXOXOXOXOXOXOXOXOXOXOXOXOXOXOXOXOXOXOXOXOXO
XOXOXOXOXOXOXOXOXOXOXOXOXOXOXOXOXOXOXOXOXOXOXOXOXOXOXOXOXOXOXO
XOXOXOXOXOXOXOXOXOXOXOXOXOXOXOXOXOXOXOXOXOXOXOXOXOXOXOXOXOXOXO
OXOXOXOXOXOXOXOXOXOXOXOXOXOXOXOXOXOXOXOXOXOXOXOXOXOXOXOXOXOXOX
OOOXOXOXOXOXOXOXOXOXOXOXOXOXOXOXOXOXOXOXOXOXOXOXOXOXOXOXOXOXOX
OOOXOXOXOXOXOXOXOXOXOXOXOXOXOXOXOXOXOXOXOXOXOXOXOXOXOXOXOXOXOX
OXOXOXOXOXOXOXOXOXOXOXOXOXOXOXOXOXOXOXOXOXOXOXOXOXOXOXOXOXOXOX
OXOXOXOXOXOXOXOXOXOXOXOXOXOXOXOXOXOXOXOXOXOXOXOXOXOXOXOXOXOXOX
XOXOXOXOXOXOXOXOXOXOXOXOXOXOXOXOXOXOXOXOXOXOXOXOXOXOXOXOXOXOXO
XOXOXOXOXOXOXOXOXOXOXOXOXOXOXOXOXOXOXOXOXOXOXOXOXOXOXOXOXOXOXO
OOXOXOXOXOXOXOXOXOXOXOXOXOXOXOXOXOXOXOXOXOXOXOXOXOXOXOXOXOXOXO
XOOXOXOXOXOXOXOXOXOXOXOXOXOXOXOXOXOXOXOXOXOXOXOXOXOXOXOXOXOXOX
OXOXOXOXOXOXOXOXOXOXOXOXOXOXOXOXOXOXOXOXOXOXOXOXOXOXOXOXOXOXOX
XXOOOXOXOXOXOXOXOXOXOXOXOXOXOXOXOXOXOXOXOXOXOXOXOXOXOXOXOXOXOX
OOOXOXOXOXOXOXOXOXOXOXOXOXOXOXOXOXOXOXOXOXOXOXOXOXOXOXOXOXOXOX
XOOXOXOXOXOXOXOXOXOXOXOXOXOXOXOXOXOXOXOXOXOXOXOXOXOXOXOXOXOXOX
OOOXOXOXOXOXOXOXOXOXOXOXOXOXOXOXOXOXOXOXOXOXOXOXOXOXOXOXOXOXOX
OOOXOXOXOXOXOXOXOXOXOXOXOXOXOXOXOXOXOXOXOXOXOXOXOXOXOXOXOXOXOX
OXOXOXOXOXOXOXOXOXOXOXOXOXOXOXOXOXOXOXOXOXOXOXOXOXOXOXOXOXOXOX
OXOXOXOXOXOXOXOXOXOXOXOXOXOXOXOXOXOXOXOXOXOXOXOXOXOXOXOXOXOXOX
XOOOXOXOXOXOXOXOXOXOXOXOXOXOXOXOXOXOXOXOXOXOXOXOXOXOXOXOXOXOXO
XOOOXOXOXOXOXOXOXOXOXOXOXOXOXOXOXOXOXOXOXOXOXOXOXOXOXOXOXOXOXO
OOOXOXOXOXOXOXOXOXOXOXOXOXOXOXOXOXOXOXOXOXOXOXOXOXOXOXOXOXOXO

```

The simulated copolymer contains 1400 HPMA units and 600 AMO units

Sequence Distributions

Sequence Length	HPMA	AMO
1	247	545
2	130	24
3	89	1
4	48	1
5	26	0
6	11	0
7	5	0
8	5	0
9	6	0
11	1	0
12	1	0
16	2	0
54	1	0

Figure 4.2 Sequence simulation of 70:30 wt/wt HPMA-AMO copolymer

Figure 4.1 shows the sequence simulation and distribution of sequence lengths obtained for the 70:30 weight/weight HEMA-AMO copolymer system. The most significant proportion of the AMO is consumed as short sequence lengths of the order of five consecutive monomer repeat units or less, the greatest proportion of AMO being in the form of single monomer units, diads and triads. However, because of the low reactivity of AMO towards HEMA, a terminal block composed of 120 AMO units which accounts for approximately 20% of the feed composition is formed. In this case it is likely that a significant proportion of this block is retained in the copolymer as earlier C, H, N results shown in Chapter 3 suggest that 90% of the feed quantity of AMO is incorporated in to the final copolymer for the 70:30 composition.

Figure 4.2 shows the sequence simulation and distribution of sequence lengths obtained for the 70:30 weight/weight HPMA-AMO copolymer system. For the HPMA-AMO copolymer the AMO is fully incorporated as monomer repeat units of 4 or less, the bulk of the monomer being incorporated as single monomer units. This is due to the lower reactivity ratios of HPMA-AMO compared to HEMA-AMO.

The nature of the reactivity of HPMA monomer compared to the reactivity of HEMA monomer towards AMO shows the effect of increasing the length of the side chain substituent with the presence of an extra methylene unit. The increased side chain length will not affect the reactivity of the radical by increased conjugation, which would stabilise the radical, but rather affects the reactivity of the monomer by changes in the polarity and the steric characteristics of the monomer structure compared to HEMA.

The presence of the extra methylene unit decreases the polarity of the vinyl bond and increases the steric hindrance of the side chain compared to that of HEMA. The overall effect is to decrease the total electron withdrawing ability of the side chain and sterically hinder the availability of the double bond. The HPMA monomer is therefore less reactive than HEMA monomer, but therefore the product of $r_1.r_2$ for HPMA-AMO is closer to zero

than the product of $r_1.r_2$ for HEMA-AMO and therefore the tendency to alternate is greater. This results in the narrower sequence lengths in the sequence distribution of a HPMA-AMO copolymer compared to that of HEMA-AMO.

Figure 4.3 shows the sequence simulation and distribution of sequence lengths obtained for the 70:30 weight/weight HPA-AMO copolymer system. This is an interesting system because the HPA monomer is a structural isomer of HEMA. Their chemical structures vary in the relative position of a methylene unit in the HPA side chain, which is found as an α -methyl moiety pendant to the vinyl group of the HEMA unit. The simulation shows that in this case the AMO would be consumed virtually all as single units within the copolymer structure, with perhaps a few diads. In this case the HPA monomer gives a broader distribution of sequence lengths than HEMA indicating that the monomer is much less reactive towards itself and has a greater tendency to alternate with the AMO.

A first comparison of the structures of HPA and HEMA indicates that the overall steric hindrance of HPA would be lower than that of HEMA. This is because the α -methyl group adjacent to the vinyl group has been transferred to the pendant side group. This reduces the vinyl group from a disubstituted monomer to a monosubstituted monomer and therefore reduces the steric hindrance at the radical centre during polymerisation. Therefore it might be expected that the HPA would have a higher reactivity ratio than HEMA. However, the values of the reactivity ratios and the copolymer sequence simulations show this not to be the case.

Mayo and Walling¹⁵⁰ found that as well as steric and polar effects, the monomer reactivity was found to increase with increasing resonance stabilisation of the radical formed. For methacrylates and acrylates it was found that the methacrylate radical is resonance stabilised to a greater extent than the acrylate due to hyperconjugation with respect to the α -methyl group. This is shown in Figure 4.4

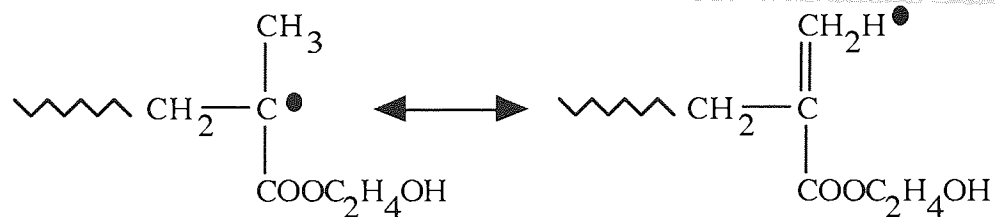


Figure 4.4 Resonance stabilisation via α -methyl substituent

However, HPA does not have the ability to be resonance stabilised via an α -methyl substituent and therefore according to the work by Evans *et al* ¹⁵¹ it is not energetically favourable for HPA to add to the growing polymer chain. HPA therefore has a lower reactivity ratio than HEMA and HPMA. The product of $r_1.r_2$ for HPA-AMO is almost zero which is a condition found to give the greatest degree of alternation and therefore the narrowest distribution of sequence lengths. This results in the sequence simulation shown in Figure 4.3.

4.2.3 Conclusions

By increasing the side chain length of HEMA to HPMA the reactivity ratio of the monomer is decreased. The product of the reactivity ratios for HPMA-AMO copolymers compared to HEMA-AMO copolymers is therefore closer to zero and the tendency to alternate is greater.

Removal of the α -methyl substituent, in the comparison of HPA and HEMA, reduces the reactivity ratio. The reduction in the reactivity ratio of HPA results in a narrower distribution of AMO sequence lengths in a HPA-AMO copolymer compared to a HEMA-AMO copolymer.

4.3 EWC's Of The HEMA-AMO, HPMA-AMO And HPA-AMO Copolymer Membranes

4.3.1 Materials And Methods

A series of HEMA-AMO, HPMA-AMO and HPA-AMO copolymer membranes containing increasing proportions of AMO were prepared by the polymerisation technique described in Chapter 2. The EWC's of each of these copolymer series was characterised by the gravimetric method and the results are presented here.

4.3.2 Results

Figure 4.5 illustrates the EWC's obtained for a series of HEMA-AMO, HPMA-AMO and HPA-AMO copolymer systems. For each of the series of copolymer membranes the EWC increases with increasing proportions of AMO. This was expected because AMO is more hydrophilic than HEMA, HPMA and HPA.

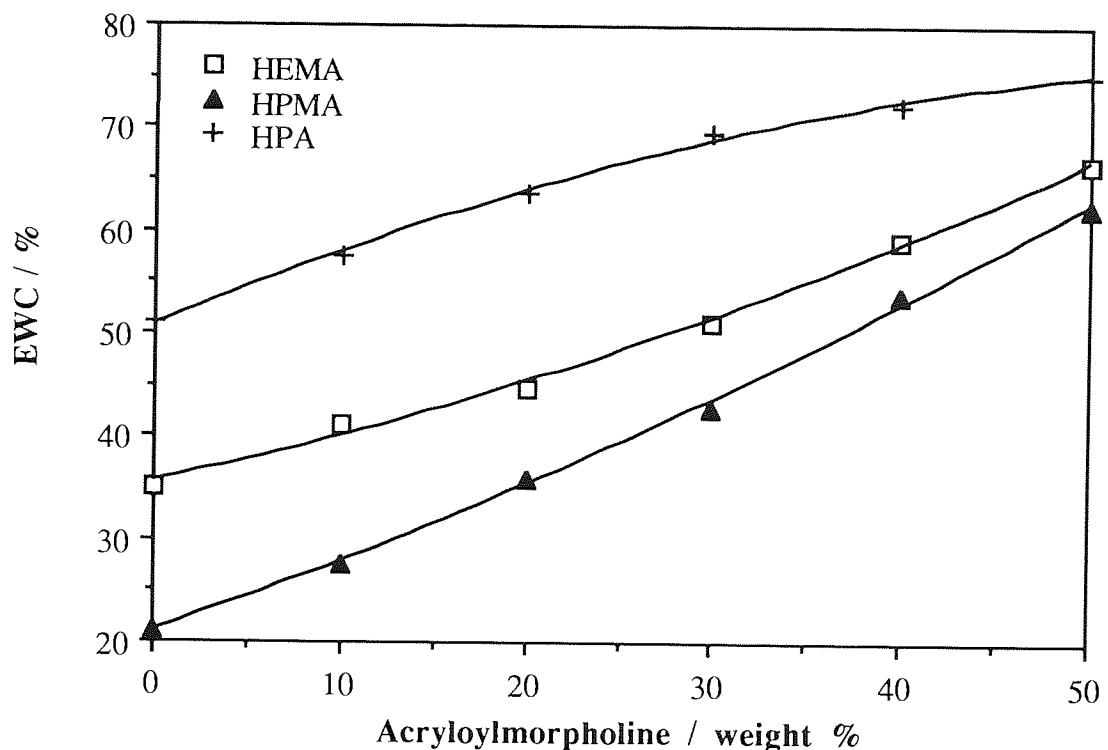


Figure 4.5 Effect of increasing proportion of AMO on the EWC of HEMA-AMO, HPMA-AMO and HPA-AMO copolymer membranes

Using the HEMA-AMO systems for comparison it can be seen that the HPMA-AMO copolymers have lower EWC's than their HEMA copolymer counterparts. This is due to the incorporation of an extra methylene unit into the side group which increases the hydrophobicity of HPMA monomer relative to HEMA.

In the case of HPA the results obtained for the HPA-AMO copolymers are interesting because HPA is a structural isomer of HEMA and HPA differs from HPMA only by the absence of the backbone α -methyl group. From the results of the EWC's it is possible to evaluate the effects of the structure of the monomer and the effects of a backbone α -methyl group on the EWC's of the copolymer membranes.

The HPA-AMO copolymers exhibit higher EWC's than the HEMA-AMO copolymers. These results indicate that the effect of the extra methylene unit in the side chain, as in HPA, has a smaller hydrophobic effect on the overall water binding capability of the monomer compared to the same moiety being in the α -methyl position of the monomer, such as in HEMA. This large increase in the hydrophobicity of the monomer by an α -methyl group on the polymer backbone is further displayed by the differences obtained between the HPA-AMO and HPMA-AMO copolymers. The EWC's of the HPMA-AMO are approximately 30% lower than the equivalent composition HPA-AMO copolymer because of the extra methyl group on the polymer backbone. These structural effects which affect the water binding ability of the hydroxy monomers were observed by Corkhill *et al*¹³³ who copolymerised HEMA, HPMA and HPA with a hydrophobic monomer, styrene.

The results presented here show that as the proportion of the more hydrophilic AMO is increased, the values of the EWC's for each series of the HEMA-AMO, HPMA-AMO and HPA-AMO copolymers begin to converge at higher proportions of AMO. This is because it is the water binding ability of AMO that governs the water absorption characteristics of

the copolymer. From the results it can also be seen that the relative hydrophilicity of the hydroxy monomers increases in the order HPMA < HEMA < HPA.

4.3.3 Conclusions

The hydrophilicity of the hydroxy monomers increases in the order HPMA < HEMA < HPA. Therefore higher values of the EWC can be obtained if AMO is copolymerised with HPA in preference to the other hydroxy monomers.

It may also be concluded from the results obtained that methyl insertion onto the polymer backbone reduces the water content to a greater extent than insertion into the monomer side chain.

4.4 Water Binding Characteristics of the HEMA-AMO, HPMA-AMO and HPA-AMO copolymers

4.4.1 Introduction

Although the results of the EWC's of the HEMA-AMO, HPMA-AMO and HPA-AMO copolymers indicate that the highest values of the EWC are obtained for the HPA-AMO copolymers it was also necessary to consider the water binding characteristics of these copolymers, because the water structuring within hydrogel copolymers has been shown to have an important role in the compatibility of the hydrogel within a biological environment¹⁴⁷.

4.4.2 Methods

The water binding characteristics of the HEMA-AMO, HPMA-AMO and HPA-AMO copolymers were obtained using differential scanning calorimetry, as described in Chapter 2. Figures 4.6 - 4.8 illustrate the effect of composition, for each of the copolymer series mentioned above, on the water binding characteristics over the range of compositions studied. The values were expressed as grams of water per gram of polymer to provide a clearer indication of the individual water binding potential of the monomers used.

The values obtained at a zero percentage of acryloylmorpholine gave the relative water binding potentials of the hydroxy monomers. This enabled a measure of the effect of the backbone α -methyl group and the effect of methylene insertion into the side chain on the water binding potential of a single monomer unit to be obtained.

The poly(HEMA) membrane at zero weight% of AMO binds 2.54 moles of water per mole of polymer, while poly(HPMA) binds only 1.95 moles of water per mole of polymer. This lower water binding potential is clearly due to the increased hydrophobicity of HPMA relative to HEMA. In the case of poly(HPA) the water binding potential rises to 4.20 moles of water per mole of polymer. The order of the water binding abilities, as expected, was the same as the order of the hydrophilicities of the hydroxy monomers given previously.

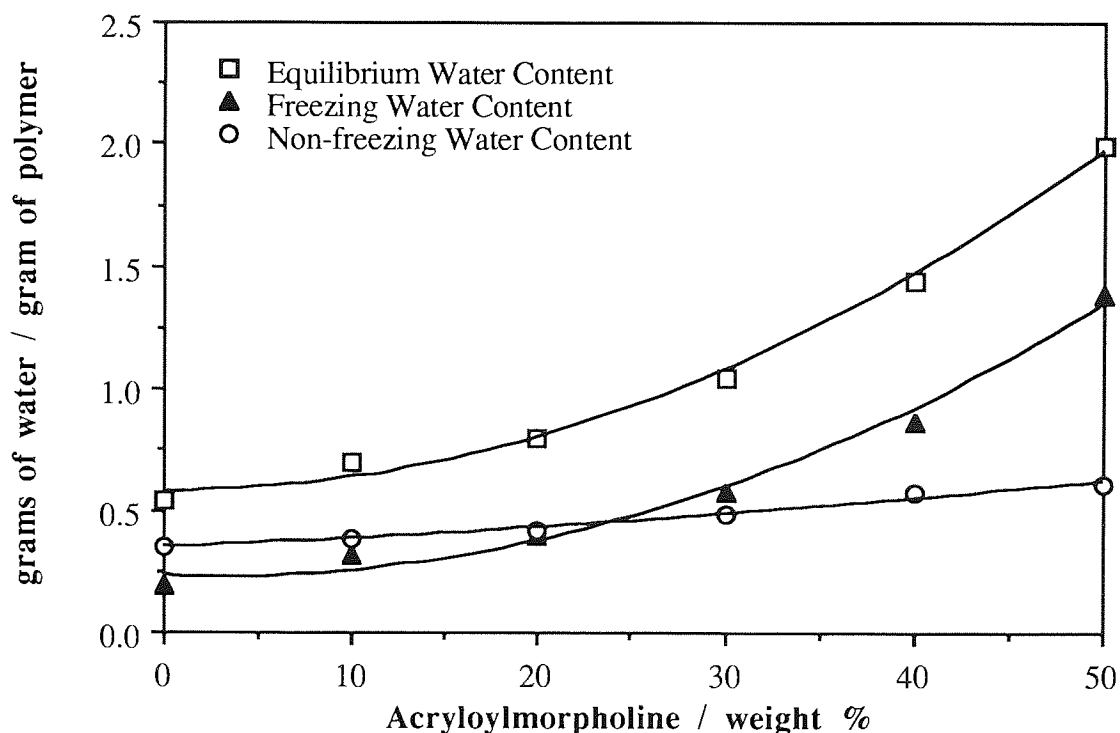


Figure 4.6 Effect of composition on the water binding ability of HEMA-AMO copolymers

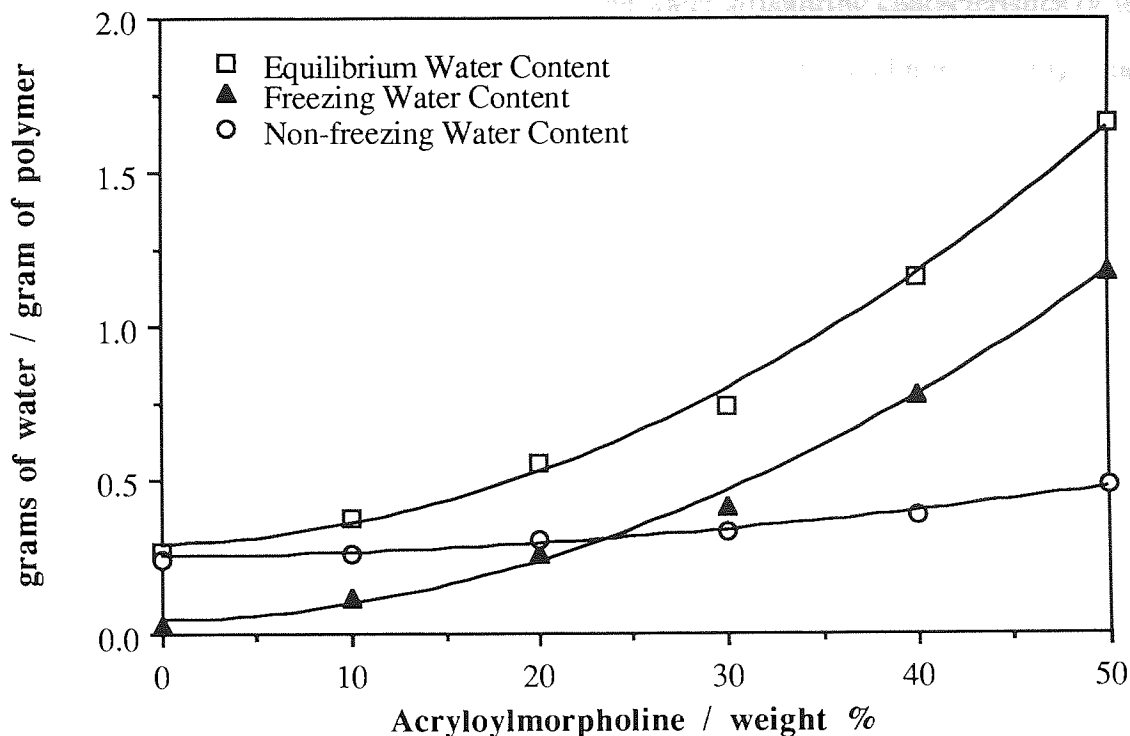


Figure 4.7 Effect of composition on the water binding ability of HPMA-AMO copolymers

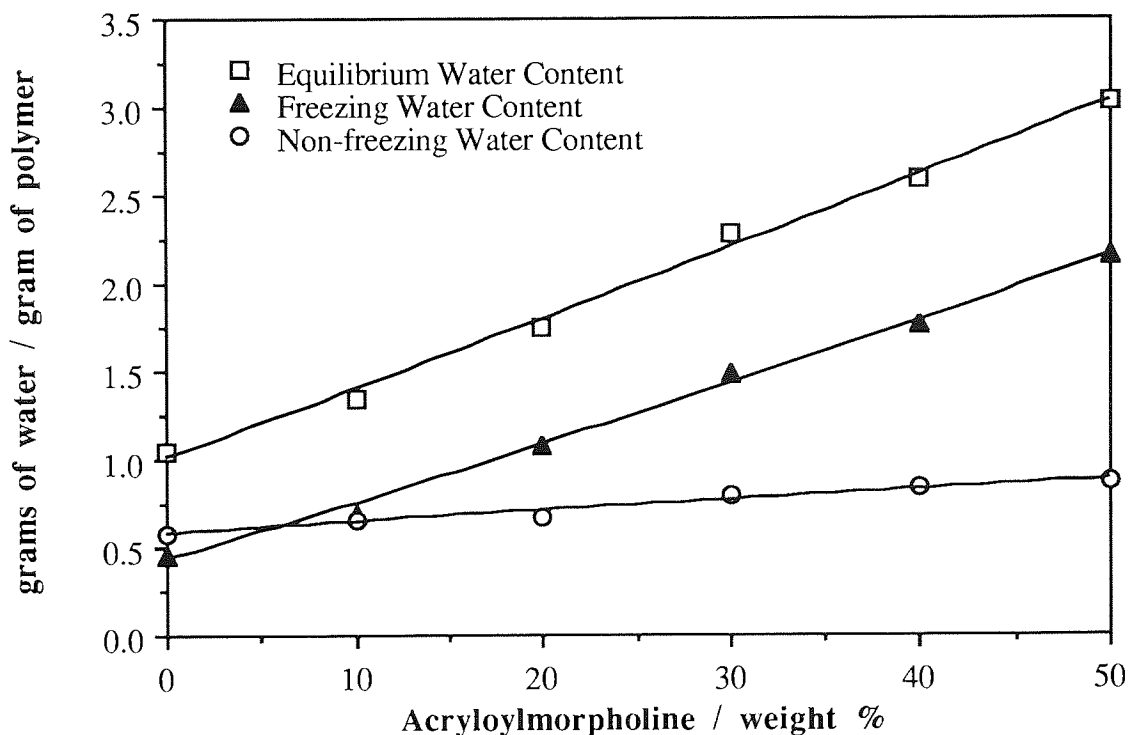


Figure 4.8 Effect of composition on the water binding ability of HPA-AMO copolymers

Figures 4.6 - 4.8 also provide an indication of the water structuring characteristics of the hydroxy monomers in terms of the relative proportions of freezing and non-freezing water in the zero weight% AMO copolymers. Previous work has shown that water structuring plays an important role in the adhesion of cells to a hydrogel surface⁷, with lower amounts of freezing water resulting in lower amounts of cell adhesion being observed.

If the ratio of freezing to non-freezing water is calculated for a series of copolymers then the lower the ratio the greater the relative proportions of non-freezing water within a particular hydrogel.

For the three series of copolymers presented in this work the freezing/non-freezing ratio was determined for the HEMA, HPMA and HPA homopolymers to provide an indication of the structural characteristics of these three monomers in terms of the proportions of freezing and non-freezing water.

For the HEMA homopolymer the value of the ratio calculated from the data presented in Figure 4.6 was 0.54. For the HPMA homopolymer this ratio falls to 0.10 which indicates that there is a greater proportion of non-freezing water in HPMA than HEMA. Therefore although increasing the side chain length of a HEMA monomer to a HPMA monomer reduces the total equilibrium water content, the proportion of non-freezing water is significantly increased. However, for the 50:50 weight/weight HEMA-AMO and HPMA-AMO copolymers the respective freezing non-freezing ratios are 2.23 and 2.47.

The HPMA copolymers exhibit a lower amount of non-freezing water than the equivalent HEMA copolymers. This is because the water binding of the copolymers is governed by the hydrophilic AMO and therefore the effect of the increased chain length of the HPMA side group compared to the HEMA side chain, is to increase the free volume between the polymer backbones available for water structuring. This results in the higher proportion of

freezing water of the 50:50 weight/weight HPMA-AMO copolymers indicated by the freezing/non-freezing ratio.

In the case of the HPA homopolymer the freezing/non-freezing ratio is 0.79. Comparison of this value with those of HEMA and HPMA indicates that the proportion of freezing water is greatest in the HPA homopolymer. HPA differs from HEMA only in the relative positions of a methyl group and therefore the effect of removing the α -methyl group from the backbone of the HEMA polymer and introducing the methylene unit into the HPA side chain is to increase the proportion of freezing water. This is because free volume swept out by backbone rotations of HPA is greater than that of HEMA and there is a greater volume between the polymer chains available for water structuring. Therefore although the EWC of the HPA polymer is increased the proportion of freezing water is significantly increased.

The overall trends of the water binding figures over the composition range are as expected for increasing incorporation of the more hydrophilic acryloylmorpholine, both values of non-freezing and freezing water increasing throughout the composition range.

4.4.3 Conclusions

The amounts of non-freezing and freezing water for the HEMA-AMO, HPMA-AMO and HPA-AMO copolymers increased with increasing proportion of the hydrophilic AMO, as expected.

The water binding results of the isomeric HPA and HEMA indicate that although HPA copolymers have a higher EWC than HEMA copolymers the relative proportion of freezing water is increased. Work elsewhere¹⁴⁷ has shown that copolymers with greater proportions of freezing water exhibit greater amounts of cell adhesion.

The use of HPMA in copolymers also increases the proportion of freezing water compared to the equivalent HEMA copolymers when the total water binding ability of the copolymers is dominated by a more hydrophilic monomer. This is because of the greater free volume between HPMA copolymer backbones which is available for water structuring.

4.5 Mechanical Properties of the HEMA-AMO, HPMA-AMO and HPA-AMO copolymer membranes

4.5.1 Methods

The mechanical properties of the HEMA-AMO, HPMA-AMO and HPA-AMO copolymer membranes were investigated using the tensile method described in Chapter 2. The examination of the mechanical behaviour of these copolymers showed the effects of monomer structure and water binding characteristics on the resulting mechanical properties.

A comparison of the properties of these systems was made with some commercially available contact lens materials to investigate their mechanical suitability for such an application.

4.5.2 Results

The results obtained for the initial modulus (E_m), tensile strength (T_s) and elongation at break (E_b), for the series of HEMA-AMO, HPMA-AMO and HPA-AMO copolymers are presented in Tables 4.2 - 4.4.

The results in Table 4.2 show that the initial incorporation of 10 weight% of AMO into the HEMA-AMO copolymers produced an increase in the elastic modulus and tensile strength, with a corresponding decrease in the elongation at break. The increase in stiffness or elastic modulus is a result of the higher energy barrier to rotation of AMO compared to HEMA which restricts the molecular mobility of the copolymer backbone. Further increases in the proportion of AMO in the HEMA-AMO copolymers resulted in a decrease

Table 4.2 Mechanical properties of HEMA-AMO copolymers

Ratio of HEMA:AMO / weight%	Initial Modulus (Em) / MPa	Tensile Strength (Ts) / MPa	Elongation at break (Eb) / %
100:0	0.654	0.481	133
90:10	0.753	0.508	104
80:20	0.729	0.427	90
70:30	0.785	0.316	81
60:40	0.533	0.305	83
50:50	0.564	0.233	85

Table 4.3 Mechanical properties of HPMA-AMO copolymers

Ratio of HPMA:AMO / weight%	Initial Modulus (Em) / MPa	Tensile Strength (Ts) / MPa	Elongation at break (Eb) / %
100:0	19.310	4.070	237
90:10	1.416	0.833	137
80:20	1.267	0.403	129
70:30	0.987	0.189	41
60:40	0.683	0.183	38
50:50	0.105	0.132	11

Table 4.4 Mechanical properties of HPA-AMO copolymers

Ratio of HPA:AMO / weight%	Initial Modulus (Em) / MPa	Tensile Strength (Ts) / MPa	Elongation at break (Eb) / %
100:0	0.524	0.238	81
90:10	0.422	0.208	60
80:20	0.338	0.201	70
70:30	0.258	0.065	41
60:40	0.300	0.211	76
50:50	0.356	0.152	56

in the mechanical characteristics. This was due to the increased amount of water in the copolymers which dominates the mechanical properties of the copolymers.

Barnes *et al*¹⁵² studied the mechanical properties of HEMA-Styrene copolymers and observed that at particular loadings of each monomer the mechanical characteristics became independent of changes associated with the modification of the backbone structure. It was found that the nature and quantity of water in the copolymer membrane controlled the mechanical properties of the copolymer.

The results in Table 4.3 show the effect of composition on the mechanical properties of the HPMA-AMO copolymers. A comparison of the results for the HPMA homopolymer with the HEMA homopolymer presented in Table 4.2 shows the effect of methylene insertion into the side group.

For poly(HPMA) the mechanical properties of the homopolymer are significantly greater than those obtained for poly(HEMA). This is due to the low freezing water content of the polymer and the low equilibrium water content.

Comparison of the glass transition temperatures of the homopolymers of HPMA and HEMA, obtained by DSC, indicates that the difference in mechanical properties was not due to steric and electrostatic differences. The glass transition temperature of 345K for poly(HPMA) was comparable to the value of 340K obtained for poly(HEMA). Values of 349K for poly(HPMA) and 328K, 359K and 311K for poly(HEMA) have been quoted¹⁵³. The differences in the glass transition temperatures of the two homopolymers suggested that it was not the energy barrier to rotation which increased the stiffness of the HPMA homopolymer compared to the HEMA homopolymer. This result further supported the importance of the equilibrium water content on the mechanical properties of a hydrogel.

Further increases in the proportion of AMO in the HPMA-AMO copolymers reduced the mechanical properties further because of the increasing amount of water in the copolymers.

Table 4.4 provides a comparison of the isomeric HPA and HEMA monomers and therefore the effect of the removal of a backbone methyl group. The value of 297 K obtained for the glass transition temperature of poly(HPA) indicates that the energy barrier to rotation of the homopolymer is lower than that of HEMA or HPMA homopolymers. Therefore combined with the fact that HPA has a higher EWC than HEMA or HPMA it would be expected that HPA was the most flexible (lowest modulus) of the three hydroxy type polymers. This was found to be the case.

Incorporation of AMO did not enhance the mechanical properties of HPA at any composition suggesting that the water binding characteristics of the HPA-AMO copolymers dominated the mechanical properties.

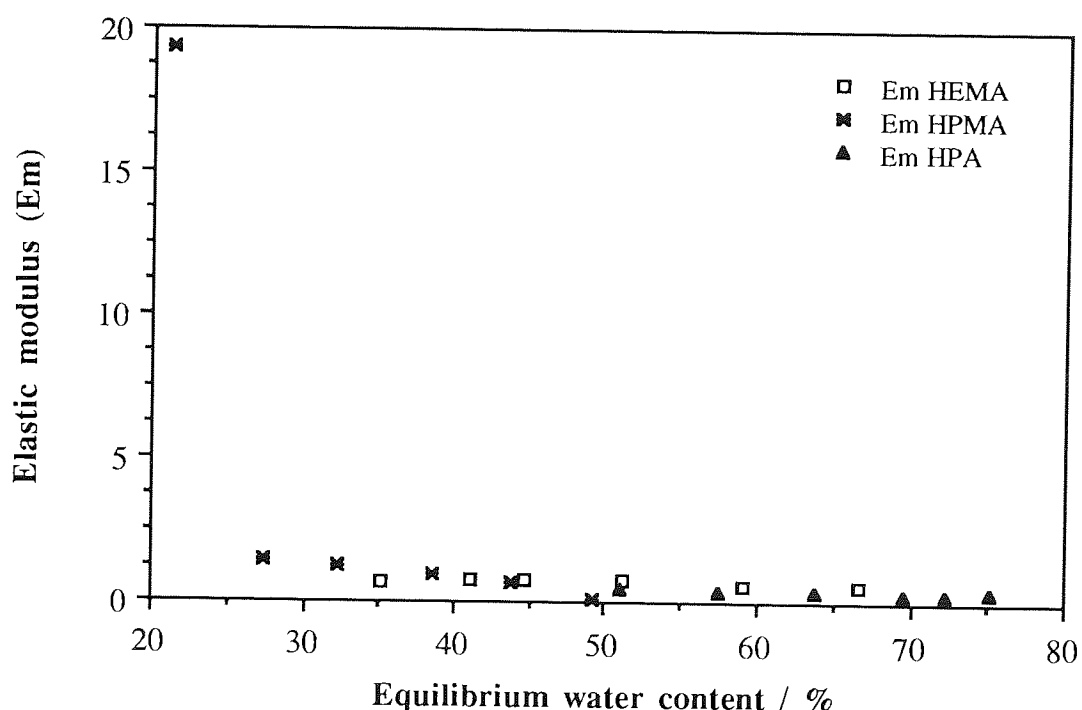


Figure 4.9 Effect of equilibrium water content on the elastic modulus of HEMA-AMO, HPMA-AMO and HPA-AMO copolymers

The domination of the elastic modulus of the HEMA-AMO, HPMA-AMO and HPA-AMO copolymers by the equilibrium water content is illustrated in Figure 4.9. Figure 4.9 shows that as the EWC increased the initial elastic modulus (or stiffness) decreased.

4.5.2 Conclusions

It can be seen from the results presented that for the HEMA-AMO, HPMA-AMO and HPA-AMO copolymer systems, with increasing equilibrium water content, the mechanical properties are decreased and that the water binding characteristics of the copolymers dominates their mechanical properties.

4.6 Surface properties of hydrated and dehydrated HEMA-AMO, HPMA-AMO and HPA-AMO copolymers

4.6.1 Methods

The surface properties of both the hydrated and dehydrated HEMA-AMO, HPMA-AMO and HPA-AMO copolymers were obtained using the contact angle methods described in Chapter 2. From the results obtained for the contact angles the polar, dispersive and total surface energies of the HEMA-AMO, HPMA-AMO and HPA-AMO copolymers were determined using the relevant theory outlined in Chapter 1.

4.6.1.1 Surface properties of dehydrated HEMA-AMO, HPMA-AMO and HPA-AMO copolymers

The results obtained for the dehydrated HEMA-AMO, HPMA-AMO and HPA-AMO copolymers are illustrated in Figures 4.10 - 4.11 respectively.

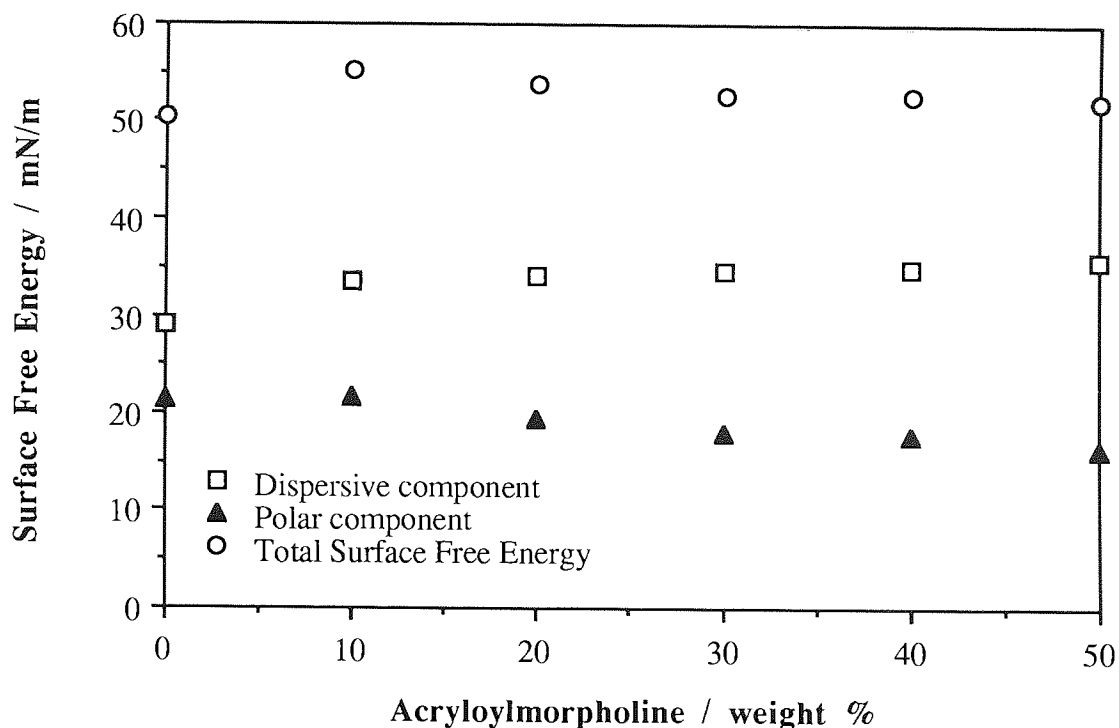


Figure 4.10 Effect of composition on the surface free energy of dehydrated HEMA-AMO copolymers

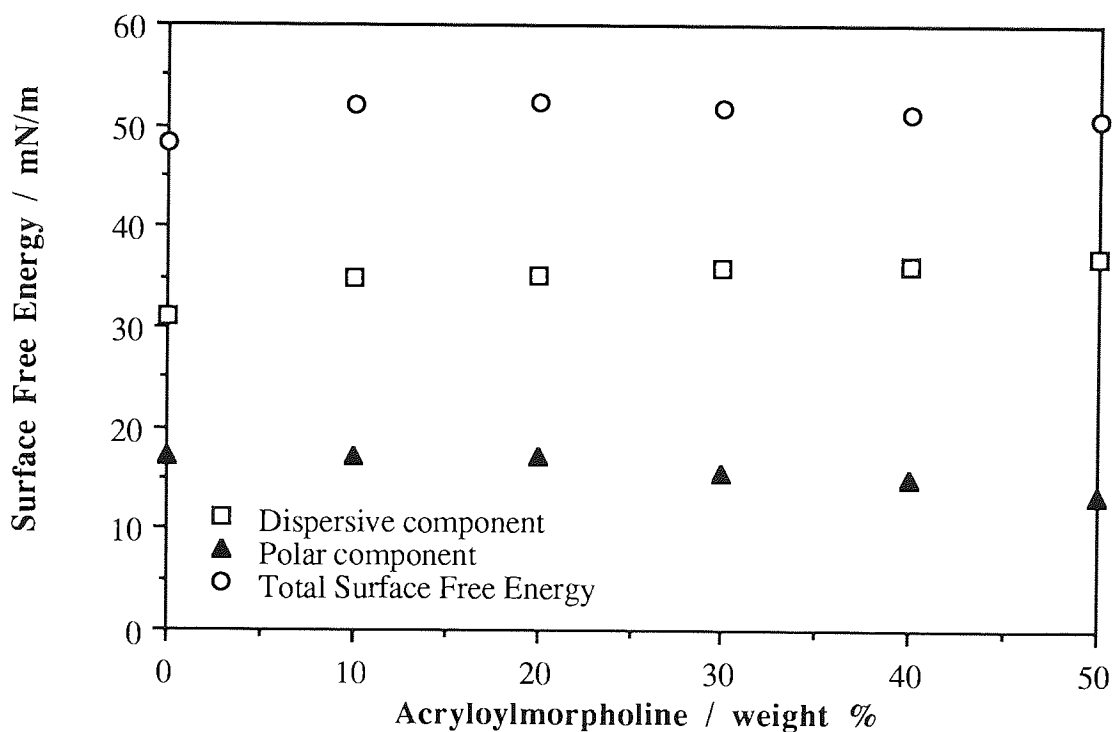


Figure 4.11 Effect of composition on the surface free energy of dehydrated HPMA-AMO copolymers

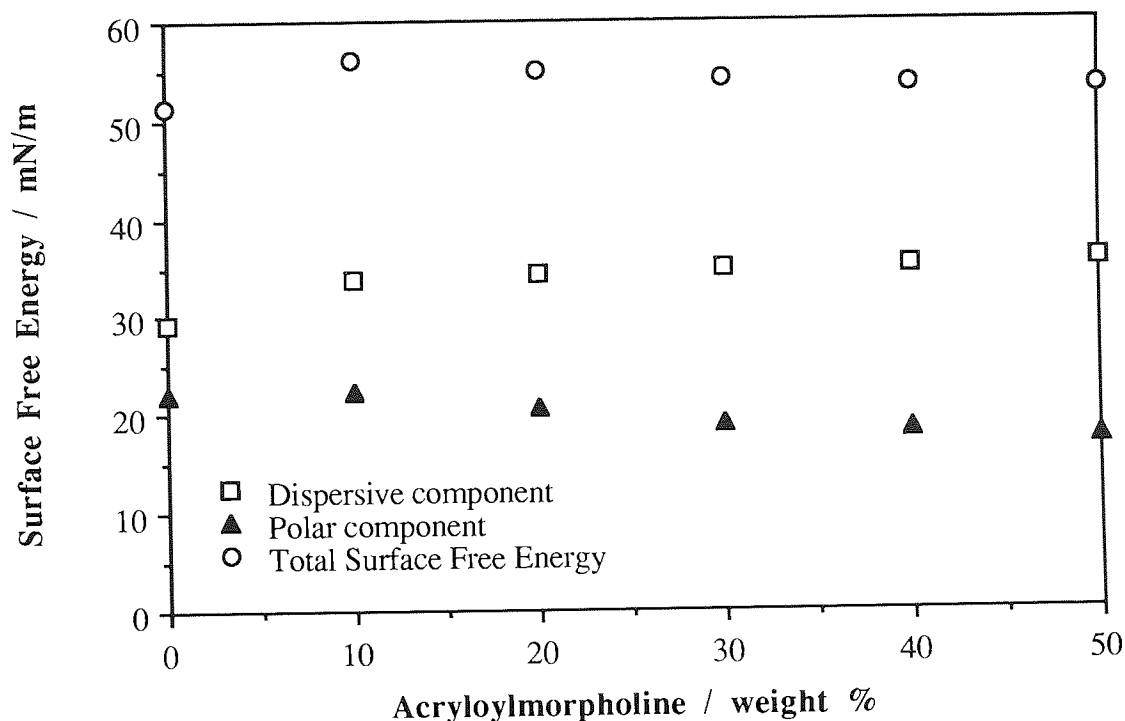


Figure 4.12 Effect of composition on the surface free energy of dehydrated HPA-AMO copolymers

Figures 4.10 - 4.12 show the effect of composition on the polar, dispersive and total surface energies of dehydrated HEMA-AMO, HPMA-AMO and HPA-AMO copolymers. With increasing proportion of AMO it was observed that the polar component of the surface energy decreased. The values obtained for the polar components of the HEMA-AMO, HPMA-AMO and HPA-AMO copolymers are lower than the polar components of poly(AMO) and therefore the polar component of the surface free energy of the HEMA-AMO, HPMA-AMO and HPA-AMO copolymers must pass through a minimum value with increasing amount of AMO until the value of the polar component of AMO homopolymers is reached.

The reduction of the polar components, as shown in Figures 4.10 - 4.12, are consistent with the formation of a molecular complex which is formed in each of the copolymers. The molecular complex is such that the orientation of the copolymers in the complex leads to the more hydrophobic sites being expressed at the surface of the copolymer. Therefore,

complex formation causes the polar groups to be orientated within the bulk of the copolymer and therefore the surface is rendered less polar.

The formation of a molecular complex with hydrophobic groups expressed at the surface is reflected in the increase in the dispersive component of the surface energy of the dehydrated HEMA-AMO, HPMA-AMO and HPA-AMO copolymers shown in Figures 4.10 - 4.12.

Figures 4.10 - 4.12 also indicate that there is very little difference in the individual polar and dispersive components and total surface energies of the HEMA-AMO, HPMA-AMO and HPA-AMO copolymers in the dehydrated state.

4.6.1.2 Surface properties of hydrated HEMA-AMO, HPMA-AMO and HPA-AMO copolymers

For the hydrated HEMA-AMO, HPMA-AMO and HPA-AMO copolymers it can be seen in Figures 4.13 - 4.15 that the magnitude of the total surface free energy is greater than the values of the surface energy of the dehydrated copolymers. This highlights the contribution which water plays in contributing to the surface energy of the copolymers.

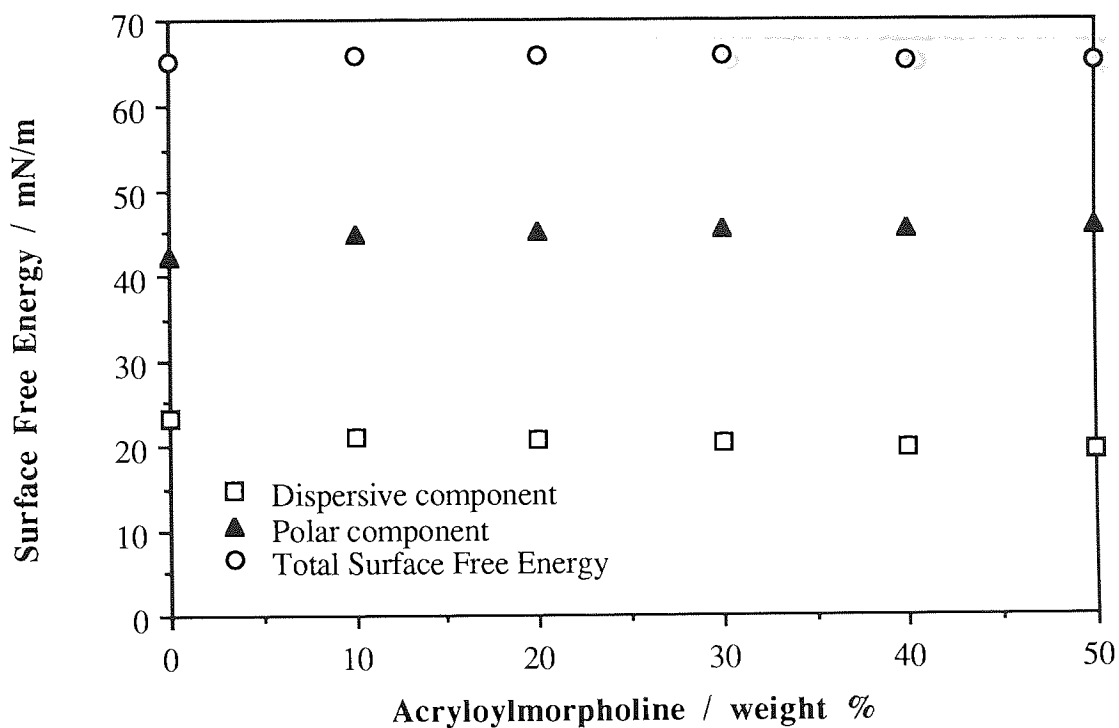


Figure 4.13 Effect of composition on the surface free energy of hydrated HEMA-AMO copolymers

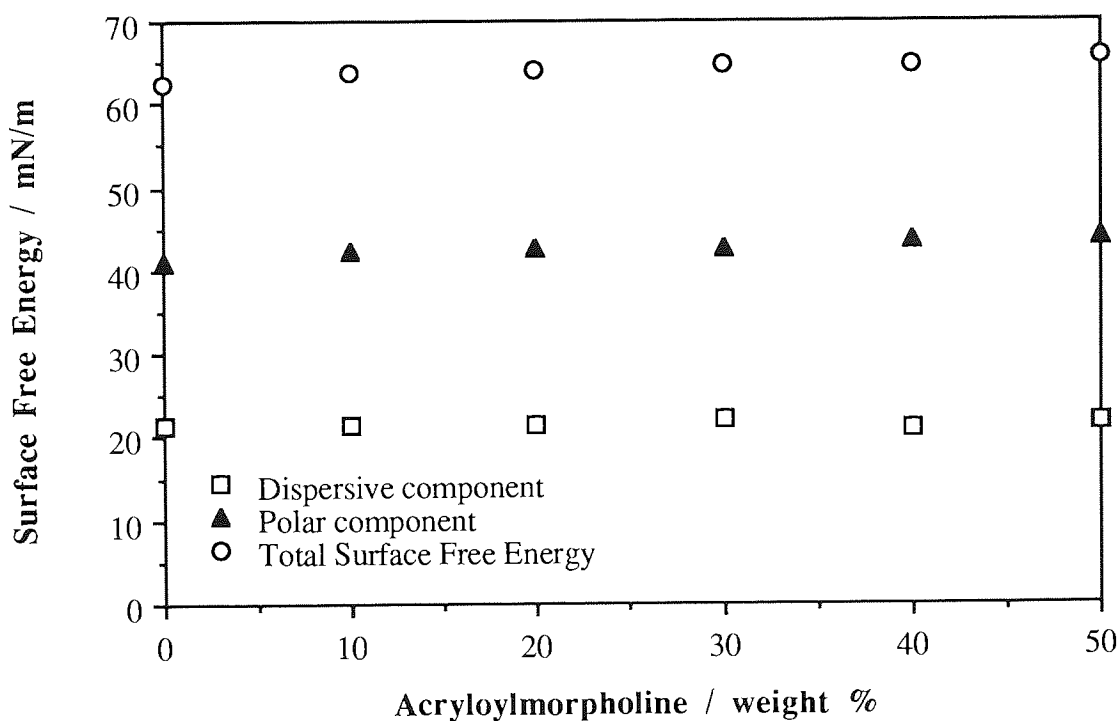


Figure 4.14 Effect of composition on the surface free energy of hydrated HPMA-AMO copolymers

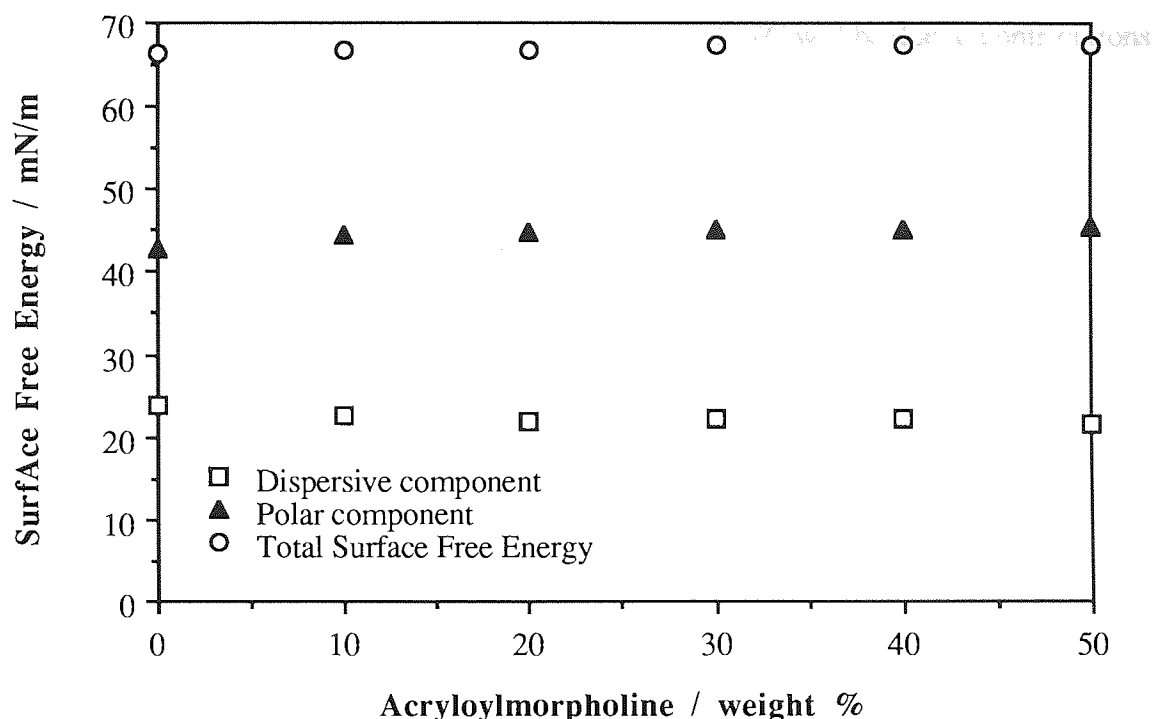


Figure 4.15 Effect of composition on the surface free energy of hydrated HPA-AMO copolymers

The values of the polar, dispersive and total surface free energies show little difference over the composition range for the HEMA-AMO, HPMA-AMO and HPA-AMO copolymers in Figures 4.13 - 4.15. This is because as the proportion of water in these copolymers increases with increasing amount of AMO, the components of the surface energies are dominated by the polar and dispersive components of water. Since water plays an integral part of the hydrogel structure and has a polar component of the surface free energy of 51mN/m and a dispersive component of 21.8mN/m the water therefore makes a significant contribution to the values of the surface energy of these hydrated copolymers.

However, the polar and dispersive components of the hydrogel copolymer can be determined by using the values of the equilibrium water contents of the copolymers to calculate the relative contributions of water to the values of the polar and dispersive components of the surface free energy. A plot of the polar, dispersive and total surface

free energies due to the copolymer structure versus the EWC can be obtained. Any deviations from linearity of these graphs with increasing EWC will be due to contributions to the polar and dispersive components of the copolymer structure.

Figures 4.16 - 4.18 show the polar, dispersive and total surface energies of the hydrated HEMA-AMO, HPMA-AMO and HPA-AMO copolymers, after the contribution to these components due to water has been removed.

It can be seen from Figure 4.16 that as the EWC increased the total surface free energy due to the copolymer decreased for each series of hydrated HEMA-AMO, HPMA-AMO and HPA-AMO copolymers. This would be expected because as the EWC of the copolymer increased the individual components of the surface free energy of water dominate the surface energies of the hydrogel copolymers.

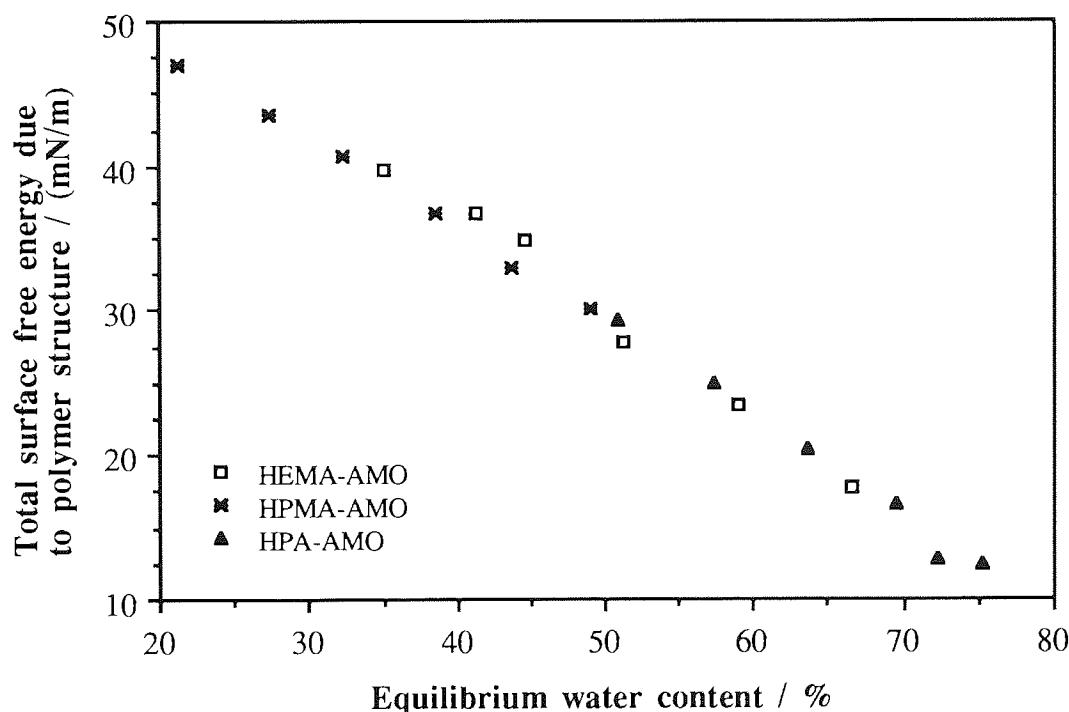


Figure 4.16 The variation in total surface energy versus EWC due to the contribution to the surface energy of the hydroxy monomer-AMO copolymers

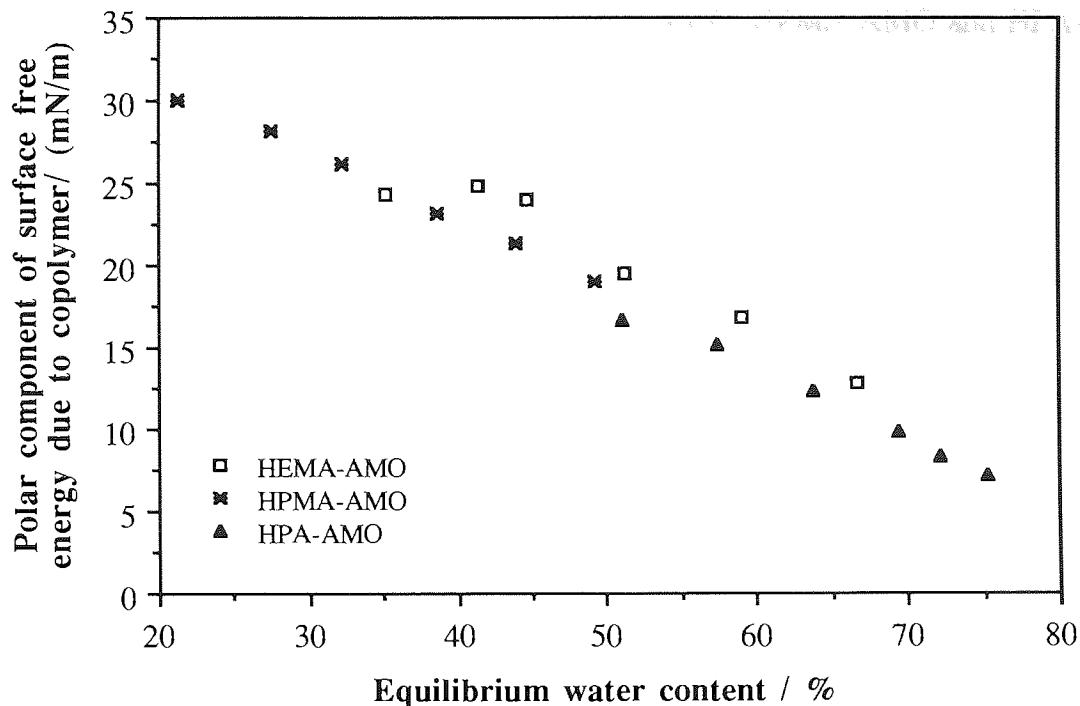


Figure 4.17 Variation in the polar component of the surface free energy with increasing EWC for the hydrated hydroxy monomer-AMO copolymers

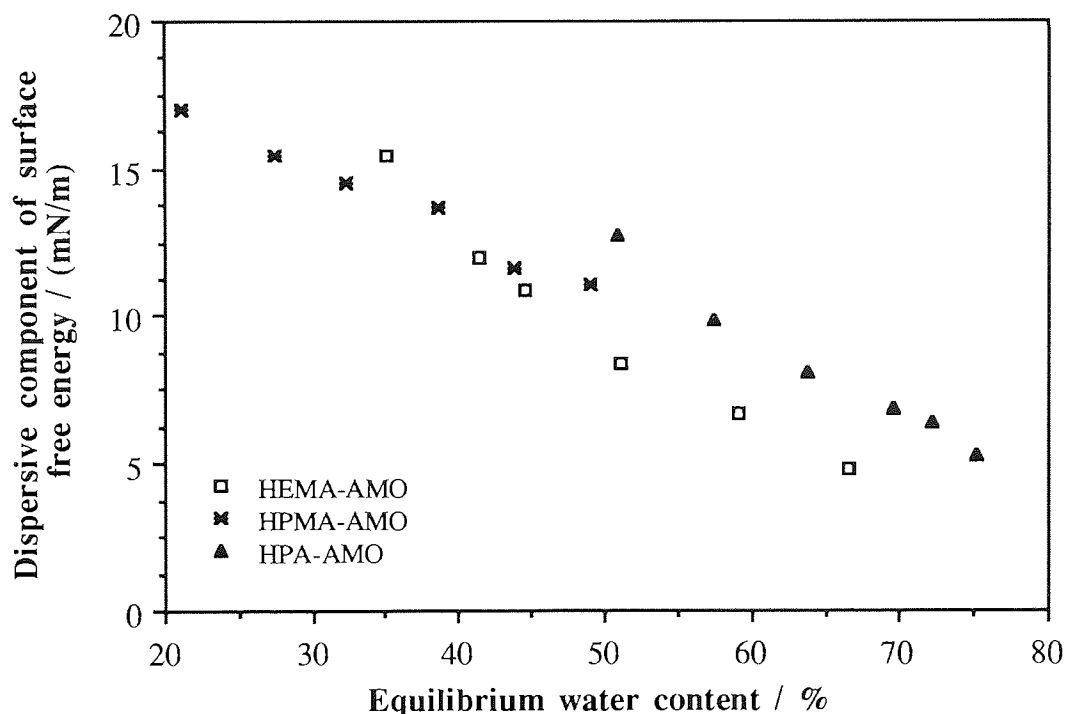


Figure 4.18 Variation in the dispersive component of the surface free energy with increasing EWC for the hydrated hydroxy monomer-AMO copolymers

Figure 4.17 and 4.18 indicate the polar and dispersive contributions with increasing water content to the surface free energy of the HEMA-AMO, HPMA-AMO and HPA-AMO copolymers.

It can be seen from Figure 4.17 that at equivalent water contents the HEMA-AMO copolymers are more polar than HPMA-AMO and HPA-AMO copolymers. This would be expected due to higher polar component of the hydroxyethyl group of HEMA compared to the hydroxypropyl group of the HPMA and HPA side chains.

Comparison of the values of the polar and dispersive components of the surface free energies shown in Figures 4.17 and 4.18 indicate that the polar component is greater than the dispersive component. This is because it is energetically more favourable for the polar groups to be orientated towards the hydrogel water interface and for the dispersive groups to be orientated away from the interface.

Figure 4.18 shows that at equivalent water contents the HEMA-AMO copolymers have a lower dispersive component of the surface free energy than the HPMA-AMO and HPA-AMO copolymers. Again this would be expected because the hydroxyethyl group of HEMA compared to the hydroxypropyl group of the HPMA and HPA side chains is more polar.

4.6.3 Conclusions

The surface properties of the dehydrated HEMA-AMO, HPMA-AMO and HPA-AMO copolymers are typical of the formation of a molecular complex which directs the polar components away from the hydrogel-air interface. There is very little difference in the values of the surface free energies of the HEMA-AMO, HPMA-AMO and HPA-AMO copolymers.

The surface properties of the hydrated HEMA-AMO, HPMA-AMO and HPA-AMO copolymers indicate that the HEMA-AMO copolymers are more polar than the HPMA-AMO and HPA-AMO copolymers because of the polarity of the side group.

4.7 Summary

The sequence distribution of acryloylmorpholine copolymers may be effectively optimised to produce a copolymer composed of narrow distributions of sequence lengths and therefore composed of alternating monomer units free from chemical domains of one molecular type. The tendency of the hydroxy monomers to alternate with AMO decreased in the order HPA > HPMA > HEMA.

Copolymer membranes with high water contents (>55%) can be attained by copolymerising a hydroxy monomer with AMO. It was found that the greatest proportions of non-freezing water were obtained in HEMA-AMO copolymers.

The mechanical properties of the HEMA-AMO, HPMA-AMO and HPA-AMO copolymers were dominated by the water contents. The HPA-AMO copolymers were the weakest mechanically at equivalent water contents to the HEMA-AMO and HPMA-AMO copolymer systems, because they possessed the largest proportions of freezing water which plasticised the copolymer network.

The surface properties of the dehydrated copolymers were consistent with the formation of a molecular complex which orientates the polar groups towards the bulk of the polymer and away from the air interface. The surface properties of the hydrated copolymers indicated that the HEMA-AMO copolymers were more polar than the HPMA-AMO and HPA-AMO copolymers.

The requirements for decreased adsorption of biological species requires a narrow distribution of sequence lengths, a higher proportion of non-freezing water and a polar

copolymer. No one of the three hydroxy monomers presented in this work satisfies all these criteria. The indication of the structural characteristics of the hydroxy monomers studied suggests 1, 2-dihydroxypropyl methacrylate as a potential monomer to meet these requirements.

1, 2-dihydroxypropyl methacrylate would be expected to have a reactivity more similar to HPMA than HEMA, because of the increased length of the side chain which would produce a narrower distribution of sequence lengths. However, 1, 2-dihydroxypropyl methacrylate would be expected to have a higher proportion of non-freezing water than HPA or HPMA because of the presence of an extra hydroxyl group. Therefore 1, 2-dihydroxypropyl methacrylate would be expected to exhibit the best compromise of the characteristics of sequence distribution, water binding, mechanical and surface properties exhibited by the hydroxy monomers presented in this work.

CHAPTER 5
THE EFFECT OF SEQUENCE DISTRIBUTION
ON THE MECHANICAL PROPERTIES
OF HYDROGEL COPOLYMERS

5.1 Introduction

Hydrogels have been considered for biomedical applications because of their ability to simulate the hydrated characteristics of natural tissue. The major disadvantage of hydrogels, which leads to limitations in the range of applications they may be considered for, is their relatively poor mechanical strength. This can theoretically be overcome to some extent by increasing the amount of crosslinking monomer within their structure or by forming interpenetrating networks within them. However, in employing either of these methods practically, problems are encountered; increasing the amount of crosslinker within them has been shown to increase the amount of biological debris deposited onto the hydrogel¹⁵⁴ and compositions for the formation of high water content interpenetrating networks (for contact lens applications) are limited because of the lack of compatible monomers that produce a transparent hydrogel membrane.

Consequently, another method of enhancing the mechanical properties of hydrogels has been used. This involves incorporating a hydrophobic monomer such as methyl methacrylate or styrene into the structure. Systems of this type have been investigated and the results show there is a significant increase in the mechanical properties of the hydrogels. However achieving this bears a cost; there is a corresponding decrease in the equilibrium water content of the system.

Corkhill *et al*¹⁵⁵ observed that by using monomers of different radical reactivities, the mechanical properties were enhanced without decreasing the equilibrium water content and suggested that this enhancement of mechanical properties was due to the sequence distribution.

The sequence distribution of copolymers has been shown to affect the interactions between hydrogel surfaces and the biological environment. This work was therefore designed to study the effect of the sequence distribution on the mechanical properties of hydrogel copolymers.

5.2 Materials

Polymer membranes were prepared by the membrane polymerisation method given in Chapter 2. Two sets of hydrogel copolymers were then prepared. The first were made of 70 weight% NVP copolymerised with 30 weight% hydrophobic monomer. The second set were composed of 70 weight% AMO copolymerised with 30 weight% hydrophobic monomer. 1 weight% of EGDMA was used as the crosslinking monomer for both sets of copolymers. The hydrophobic comonomers used to produce the two sets of copolymers are listed in Table 5.1.

Table 5.1 Hydrophobic monomers used

Hydrophobic Monomer	Abbreviation	M.Wt	Tg / K
Iso Bornyl Methacrylate	IsoBORNMA	222	383
Benzyl Methacrylate	BENZMA	175	327
Cyclohexyl Methacrylate	CHEXMA	168	324
tertiary-Butyl Methacrylate	tBUTMA	142	320
2-Phenylethyl Methacrylate	PhEMA	190	299
Phenoxyethyl Methacrylate	PhOEMA	206	290
Butyl Methacrylate	BMA	142	293
Hexyl Methacrylate	HMA	170	268
Methyl Methacrylate	MMA	100	311

Elimination of any variability in the EWC was a pre-requisite in selecting the hydrophilic and hydrophobic monomers, to ensure that any significant differences obtained in the mechanical properties of the systems could be attributed to the composition of the copolymer and the structure of the hydrophobic monomer. Consequently, hydrophobic monomers were selected for use on the basis of their homopolymer properties. Whereas NVP and AMO were selected as the hydrophilic monomers since these monomers have been shown to produce gels of a similar water content.

5.3 Effect Of Hydrophobic Monomer On EWC And Mechanical Properties

5.3.1 Introduction

Hydrogel membranes made from 30 weight% hydrophobic monomer copolymerised with 70 weight% NVP were prepared and their EWC's were determined to obtain a measure of the effect of the hydrophobic monomer on the EWC of the copolymer membranes.

5.3.2 Results Of The Effect Of Hydrophobic Monomer On The EWC Of NVP Copolymer Membranes

Figure 5.1 illustrates the EWC's obtained for the hydrogel copolymer membranes of NVP copolymerised with each of the hydrophobic monomers listed in Table 5.1. The crosslinking monomer was 1 weight% of EGDMA. The EWC's were determined using the gravimetric method described in Chapter 2.

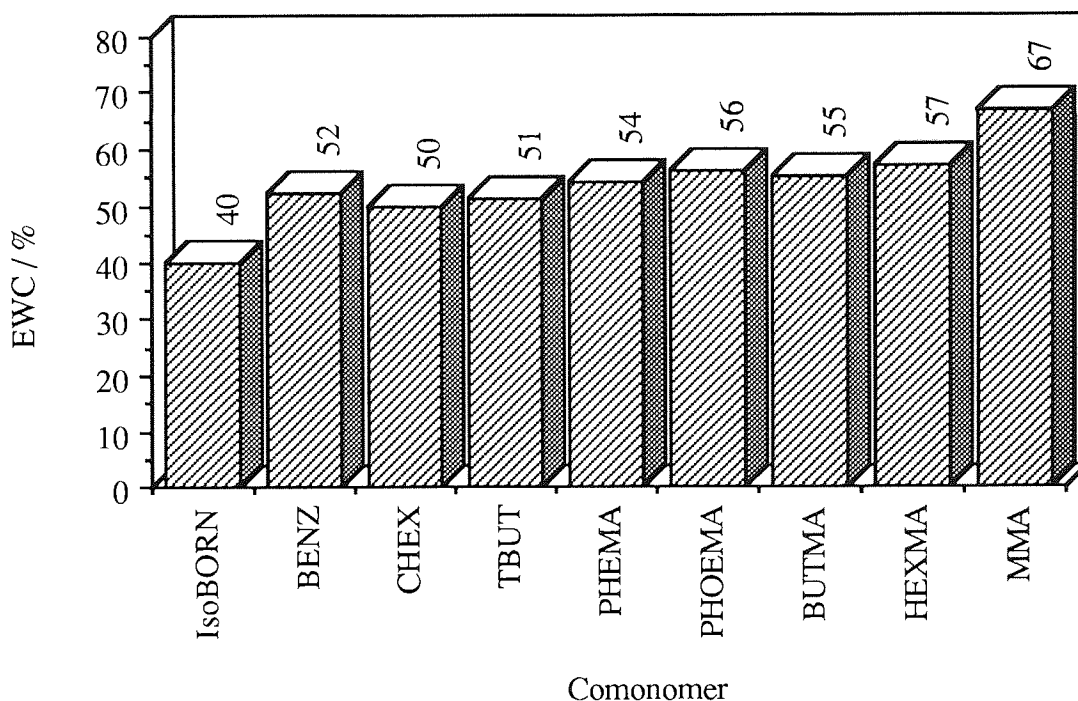


Figure 5.1 Effect of the hydrophobic monomer on the EWC's of NVP-hydrophobic monomer 70:30 weight/weight hydrogel membranes

The values of the EWC for all of the systems lies within the range $54\pm 3\%$ with the exception of isoBORNMA and MMA (Figure 5.1). It is well known that changes in EWC affect the mechanical properties of hydrogel copolymers. By producing copolymers with similar EWCs any large differences in the physical properties of each copolymer system could be attributed to copolymer structure and not EWC.

Before the effect of the sequence distribution on the mechanical properties of the copolymers can be considered it was necessary to consider the effect of comonomer structure on the mechanical properties.

5.3.3 Results Of The Effect Of The Structure Of The Hydrophobic Monomer On The Mechanical Properties Of The NVP Hydrogel Copolymers

The effects of the hydrophobic monomers on the tensile properties of the NVP copolymer membranes are clearly shown in the values obtained in Table 5.2. The profile of the load/extension curves obtained for each of the NVP-hydrophobic monomer membranes were found to show the same behaviour. A typical load/extension profile is illustrated in Figure 5.2.

The initial slope marked by a dotted line corresponds to the initial modulus of the copolymer. The greater the slope the stiffer the copolymer. As the extension or elongation increases the slope of the curve changes at the yield point of the copolymer and continues to the point of fracture whereupon the values of the tensile strength and elongation at break are calculated.

The results of the tensile tests are shown in Table 5.2. The observed differences are much greater than those which might have been expected for a set of copolymers with similar EWC's .

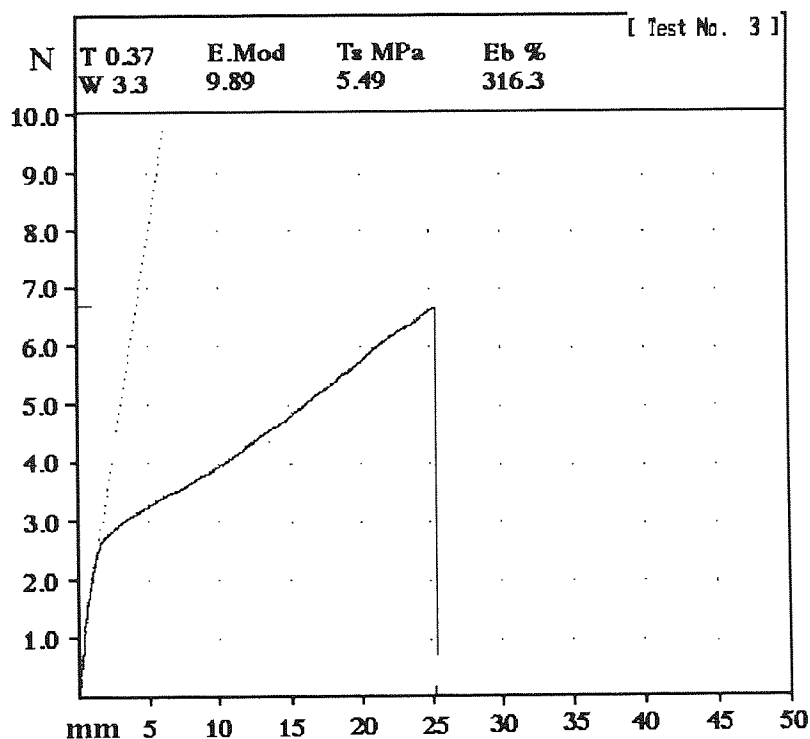


Figure 5.2 A typical load/extension profile for the NVP-hydrophobic monomer 70:30 weight/weight hydrogel membranes

Table 5.2 Mechanical properties of NVP-hydrophobic comonomer 70:30 weight/weight copolymer membranes

Hydrophobic comonomer	EWC / %	Em / MPa	Ts / MPa	Eb / %
IsoBORNMA	40	59.7	8.92	39
BENZMA	58	41.0	6.54	44
CHEXMA	50	37.3	5.70	51
tBUTMA	51	23.9	5.54	72
PhEMA	54	21.3	4.09	110
PhOEMA	56	9.9	3.48	118
BUTMA	55	6.2	2.83	151
HEXMA	57	1.5	1.66	171
MMA	67	0.6	0.81	145

Table 5.2 shows that, reading down from IsoBORNMA to MMA, the corresponding values for the initial elastic modulus (E_m) decreased, as did the values for the tensile strength (T_s) whilst there was an increase in the values of the elongation at break (E_b). The values for the EWC revealed an increase when reading from top to bottom of the table. This trend in the EWC of the hydrogel membranes would suggest that a less stiff, more flexible copolymer is produced with the monomers used at the bottom of the table which corresponds to the lower values observed for the mechanical properties within these copolymers.

However, the differences in mechanical property values are much larger than would be expected simply from changes in EWC alone. The differences must therefore be attributed to the structures of the monomers.

Monomer structure is clearly significant in the mechanical properties of the copolymer systems. The most marked effects are those illustrated by the isomeric pairs of butyl methacrylate (BUTMA) and tertiary-butyl methacrylate (tBUTMA) and by hexyl methacrylate (HEXMA) and cyclo-hexyl methacrylate (CHEXMA). Introduction of the branched tBUTMA and ring CHEXMA monomers increases the mechanical properties of the systems by decreasing the freedom of rotation of the polymer backbone. This is reflected in the physical characteristics of the films of tBUTMA and CHEXMA which are much stiffer and more brittle than their isomeric linear alkyl chain analogues of similar water content.

The effect of the freedom of rotation of the copolymer backbone is further emphasised by the introduction of benzyl methacrylate. The aromaticity of the ring compared to the cyclo-hexyl structure further increases the energy barrier to rotation, resulting in an increase in the elastic modulus of the copolymer. The results of the effect of the type of hydrophobic monomer on the elastic modulus of the NVP-hydrophobic monomer hydrogel membranes are more clearly shown in Figure 5.3.

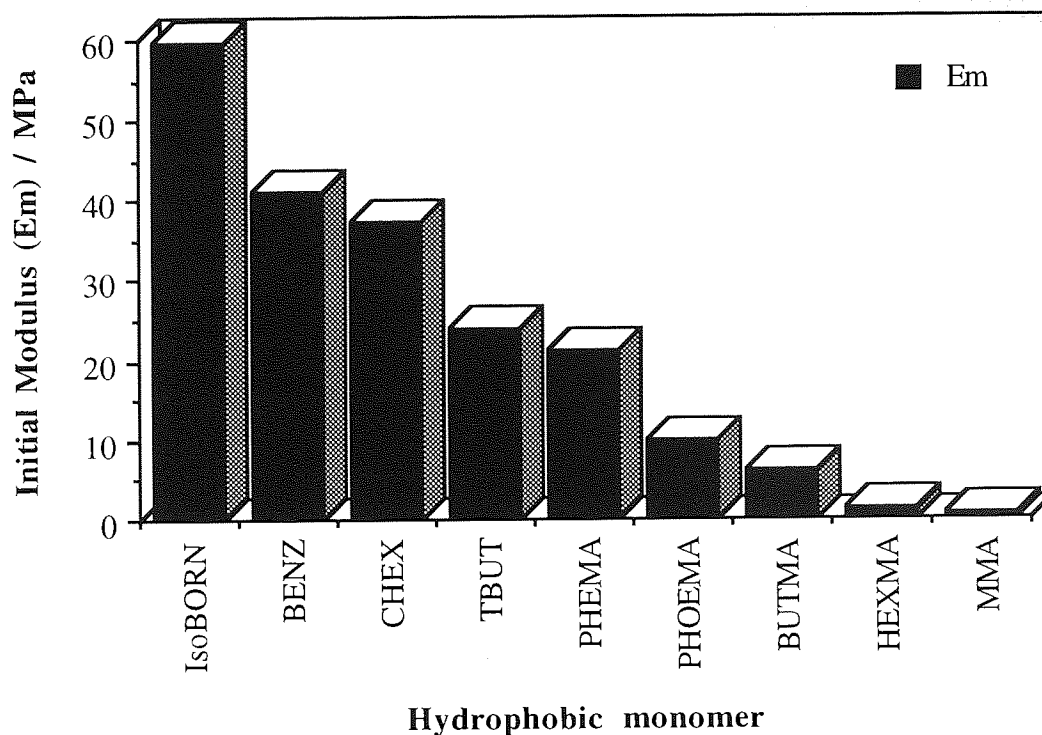


Figure 5.3 Effect of the type of hydrophobic monomer on the initial elastic modulus (E_m) of NVP-hydrophobic monomer 70:30 weight/weight hydrogel membranes

The steric and polar effects of the side group substituents hinder the rotation of the polymer backbone. The extent to which rotation is hindered is indicated by the glass transition temperature of the homopolymer. The glass transition temperature (T_g) is the temperature at which the molecular mobility of the polymer backbone increases such that the physical state of the polymer changes from glassy to rubbery. The T_g of polymers which contain pendant groups is increased by an increase in the steric hindrance and polar interactions produced by the chemical structure and nature of the pendant group. The order in which the T_g 's of the homopolymers of the hydrophobic monomers changes (see Table 5.1) is therefore reflected in the trend observed in the elastic modulus of the copolymer membranes. The T_g 's of the homopolymers of the hydrophobic monomers are listed in the right hand column of Table 5.1. The exception to the observed trend of T_g 's and mechanical properties is methyl methacrylate which is more flexible than its T_g

suggests. This is due to the much greater water content which makes the copolymer more flexible.

5.3.4 Conclusions

Equal amounts of the hydrophobic monomers used in this work produced copolymers with NVP that had EWC's within a narrow range. This enabled the differences between the mechanical properties of the copolymers studied to be attributed to the molecular structure of the comonomer. Increasing the energy barrier to rotation of the polymer backbone of copolymers with comparable EWC's increased the stiffness and the ultimate strength of the copolymer but decreased the elasticity.

5.4 The Effect Of Sequence Distribution On Hydrogel Copolymers

5.4.1 Introduction

NVP is relatively unreactive in free radical bulk polymerisation¹⁵⁶. Systems of this type have a tendency to form block copolymers, the structure of which mimic the characteristics of interpenetrating networks (IPNs). Corkhill *et al*¹⁵⁵ investigated a series of IPNs using NVP. They showed that higher tensile strengths and elastic moduli can be obtained for materials with a high water content by IPN formation.

The effect the hydrophobic monomer has on the mechanical properties of the copolymers listed in Table 5.2 can further be explained by the lack of reactivity of NVP. This would produce blocks of the hydrophobic monomer which would sterically exclude water from the hydrogel network. This type of block would be free from the plasticising effect of water and would essentially act as a large physical crosslink or reinforcing network. This would therefore result in the increased mechanical properties observed.

5.4.2 Comparison Of The EWC's Of The AMO Copolymers And NVP

Copolymers

A second set of hydrogel membranes made from 30 weight% hydrophobic monomer copolymerised with 70 weight% AMO were prepared and their EWC's were determined. The EWC's of the AMO copolymers were compared to the EWC's of the NVP copolymers. Figure 5.4 illustrates the EWC's of the two hydrophilic systems when copolymerised with 30 weight% of the hydrophobic monomers.

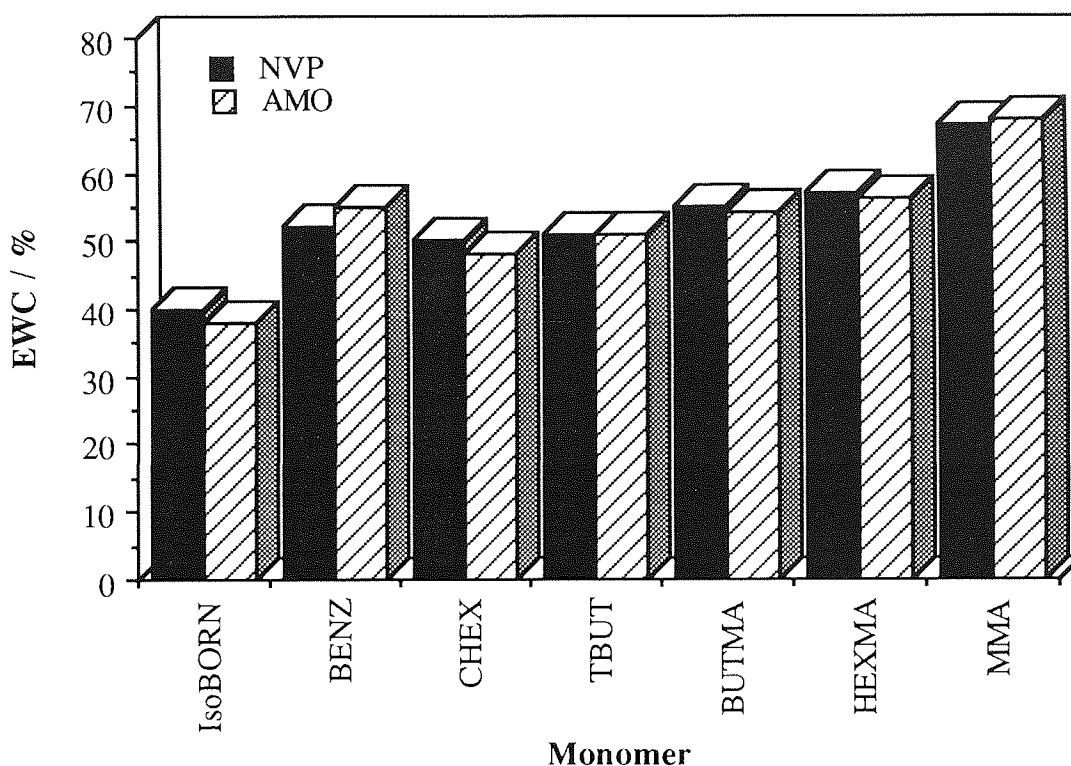


Figure 5.4 EWC's of equivalent NVP-hydrophobic monomer and AMO-hydrophobic monomer 70:30 weight/weight copolymer membranes

Figure 5.4 shows that the EWC's of the two sets of copolymer membranes are essentially equal. This is due to the similar water binding abilities of the hydrophilic monomers. The most significant difference between the hydrophilic monomers are their comparative reactivities in free radical polymerisations. AMO has a greater reactivity than NVP. It also has a greater tendency to alternate and therefore produce a copolymer with a greater number of short sequences. Of the homopolymers AMO has a moderately higher T_g than

number of short sequences. Of the homopolymers AMO has a moderately higher T_g than NVP. The contribution of the T_g to the mechanical properties has been mentioned previously. Therefore it was expected that the mechanical properties of the two sets of copolymers would be approximately equal.

5.4.3 Comparison Of The Mechanical Properties Of The AMO Copolymers And NVP Copolymers

The mechanical properties of the AMO were also determined using the tensile technique. It is observed from the results shown in Figure 5.5 that a marked difference occurred in the comparative mechanical properties of the two sets of copolymer membranes.

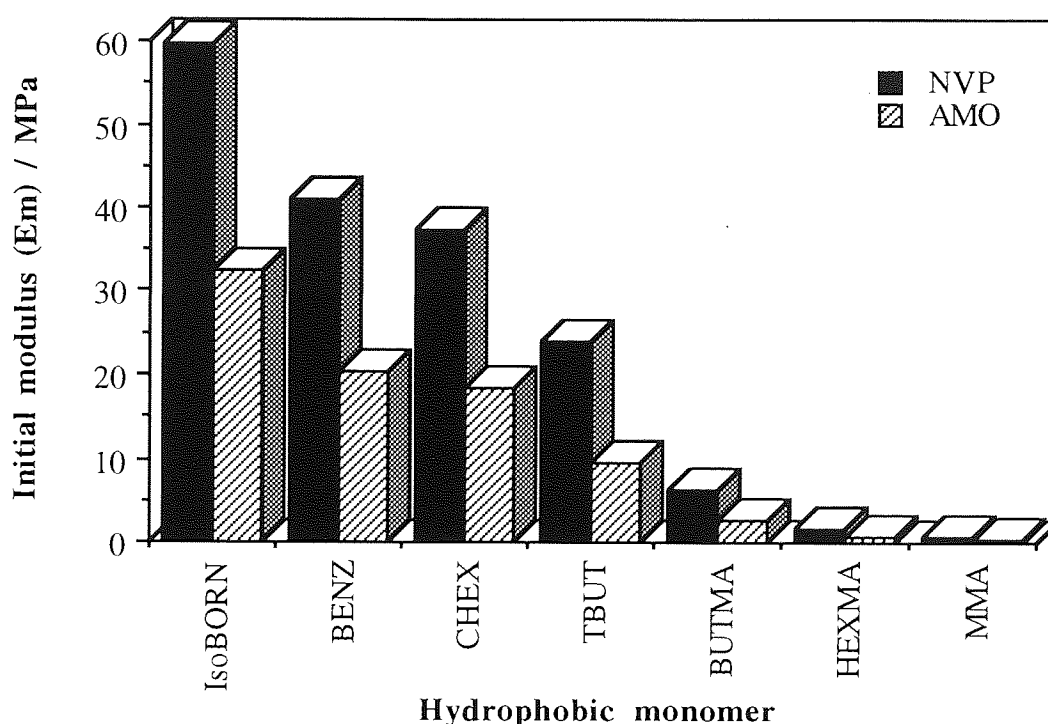


Figure 5.5 Initial elastic modulus of equivalent NVP-hydrophobic monomer and AMO-hydrophobic monomer 70:30 weight/weight copolymer membranes

It is evident from the results in Figure 5.5 that the elastic modulus of the AMO copolymers are approximately half of the values exhibited by the NVP systems. This difference is not due to any differences in EWC between the two sets of copolymers. In order to explain

this observation a closer inspection of the molecular architecture of the copolymers was required.

5.4.4 Sequence Simulation Experiments

Copolymer simulations of the AMO and the NVP systems were obtained using the copolymer simulation program described in Chapter 2. Reactivity data was obtained from the literature or determined by the Alfrey-Price Q-e scheme. Copolymer sequence simulations for the comparison of the AMO and the NVP copolymers are illustrated in Figures 5.6 - 5.9.

Direct comparison of the copolymer simulations of the AMO and NVP systems in Figures 5.6 to 5.9 immediately indicates that there was a more even distribution of AMO sequences throughout the copolymer than in the case of the NVP system due to the greater reactivity of AMO towards the hydrophobic comonomer. In the case of NVP, the monomer essentially formed a terminal end unit composed of approximately 70% of the feed composition of NVP which was preceded by what may be described as a predominantly hydrophobic block of the copolymer. Since hydrophobic polymer-water interactions are energetically unfavourable there was the potential for the hydrophobic dominated portion of the copolymer chain to interact with the same hydrophobic portion of other copolymer chains, therefore producing domains of hydrophobicity.

Huglin *et al* ¹⁵⁶ showed that the copolymer-water interaction was reduced by the inclusion of a hydrophobic monomer. These workers showed that the thermodynamics of the hydrophobic-hydrophobic interaction were greater than the thermodynamic force of dilution between the hydrophobic domain and water. The retractive force of the hydrophobic polymer chains were energetically more favourable than a hydrophobic-water interaction and therefore these domains aggregated. This type of aggregation or association (as a result of the dissimilar parts of the copolymer chain) is well known in the field of biological polymers and is referred to as *clustering*. In the systems prepared and described in this thesis, these aggregate domains are referred to as *hydrophobic clusters*. The hydrophobic clusters act as reinforcing domains and increase the mechanical characteristics of the copolymer.

In the AMO copolymers the distribution of the AMO resulted in a greater number of shorter hydrophobic sequences (shown in Figure 5.6). In this situation, because hydrophilic units were more evenly distributed between the hydrophobic units, the thermodynamics for copolymer-water interactions are more favourable than in the NVP systems. The type of hydrophobic clustering mentioned previously is therefore more likely in the NVP copolymers. This type of clustering results in the higher values of the

mechanical properties of the NVP copolymers compared to AMO copolymers of the equivalent composition and EWC.

5.4.5 Glass Transition Temperatures (Tg's) Of The AMO Copolymers And NVP Copolymers

Differential Scanning Calorimetry (DSC) and Thermal Mechanical Analysis (TMA) were used to determine the Tg's of dehydrated hydrogel disks of the AMO copolymers and the NVP copolymers. The methodology used is described in Chapter 2. The results obtained are shown in Table 5.3.

Table 5.3. Glass transition temperatures (Tg's) obtained by DSC for the series of NVP-hydrophobic monomer and AMO-hydrophobic monomer 70:30 weight/weight copolymer membranes

Hydrophobic comonomer	AMO copolymers	NVP copolymers	
	Tg / K	Tg1 / K	Tg2 / K
IsoBORNMA	375	380	342
BENZMA	355	325	300
CHEXMA	358	320	336
tBUTMA	355	318	325
BUTMA	340	290	316
HEXMA	334	270	306
MMA	351	308	320

The results in Table 5.3 show that only one glass transition temperature (Tg) was observed for the series of AMO copolymers. This is consistent with the formation of an alternating copolymer composition. However, the series of NVP copolymers show two clear Tg's indicating the presence of two domains within the copolymer. It is proposed that due to the low reactivity of NVP and the indication of a blocky copolymer from the sequence

simulation, that the formation of hydrophobic domains mentioned previously are responsible for the production of Tg₁ shown in Table 5.3.

5.4.6 Conclusions

These results provide evidence that not only the EWC and the comonomer structure affect the mechanical properties, but that sequence distribution is also important in determining how the mechanical properties of hydrophilic-hydrophobic copolymer membranes are affected. The display of two glass transition temperatures in the NVP-hydrophobic monomer hydrogel membranes indicated the presence of two different domains of copolymer. This evidence supports the theory of the production of hydrophobic domains, the formation of which reinforces the hydrogel copolymer.

5.5 Investigation Of The Minimum Quantity Of Hydrophobic Monomer Required To Produce Hydrophobic Clusters

5.5.1 Introduction

Work carried out within the Speciality Materials Research Group at Aston has shown that hydrogel copolymer membranes containing large blocks of one molecular type increase the amount of deposition of biological species onto the hydrogel surface. It was therefore necessary to determine the minimum amount of hydrophobic monomer required to produce reinforcement by the formation of hydrophobic clusters. This would enable a compromise on the effect of the sequence distribution on mechanical properties and the effect of the sequence distribution on the spoilation characteristics to be achieved.

5.5.2 Materials

At this stage only four of the hydrophobic monomers were selected for investigation. The remaining monomers were eliminated, as the hydrogels they formed were cloudy and translucent which would make them of little use in a contact lens application. The four monomers chosen were isobornyl methacrylate, benzyl methacrylate, cyclohexyl

methacrylate and tertiary-butyl methacrylate. They were also selected as they possessed a high strength combined with a high equilibrium water content.

Hydrogel copolymer membranes incorporating 5, 10, 15, 20, 25 and 30 weight% amounts of the hydrophobic monomer were prepared with the remainder of the composition being NVP. 1 weight% EGDMA was used as the crosslinking monomer.

5.5.3 Results

The EWC's and the mechanical properties of the membranes were determined by the techniques described in Chapter 2. The results for the mechanical properties are shown in Tables 5.4 - 5.7.

Table 5.4 Effect of increasing the amount of IsoBORNMA on the mechanical properties of NVP copolymers

weight% IsoBORNMA	EWC / %	Em / MPa	Ts / MPa	Eb / %
A				
5	84.2	1.4	0.24	78
10	72.7	2.9	0.52	55
15	64.6	21.2	3.17	40
20	57.2	29.5	4.35	29
25	47.6	40.4	6.05	31
30	40	59.7	8.80	27

Tables 5.4 - 5.7 show that there was a marked increase in the Em and Ts of the NVP copolymers at a proportion of 15 weight% of the hydrophobic monomer.

Table 5.5 Effect of increasing the amount of BENZMA on the mechanical properties of NVP copolymers

weight% BENZMA	EWC / %	Em / MPa	Ts / MPa	Eb / %
5	82.2	1.2	0.16	70
10	74.4	1.5	0.24	69
15	66.4	13.2	1.94	68
20	61.9	15.9	2.57	55
25	54.8	27.1	4.10	56
30	51.2	41.0	6.30	52

Table 5.6 Effect of increasing the amount of CHEXMA on the mechanical properties of NVP copolymers

weight% CHEXMA	EWC / %	Em / MPa	Ts / MPa	Eb / %
5	84.4	1.2	0.20	64
10	74.3	1.9	0.25	63
15	66.7	11.1	1.77	50
20	60.6	20.6	3.16	50
25	54.5	31.0	4.77	52
30	50	37.3	5.70	50

Table 5.7 Effect of increasing the amount of tBUTMA on the mechanical properties of NVP copolymers

weight% TBUTMA	EWC / %	Em / MPa	Ts / MPa	Eb / %
5	86.7	0.4	0.09	108
10	77.5	0.7	0.18	72
15	71.6	6.8	1.56	69
20	64.4	9.5	2.20	64
25	59.0	17.1	4.03	58
30	50.0	23.9	5.70	55

Graphs showing the variation in EWC with composition and the effect of the composition on the tensile strength of the copolymers are illustrated in Figures 5.10 - 5.13 for clearer comparison.

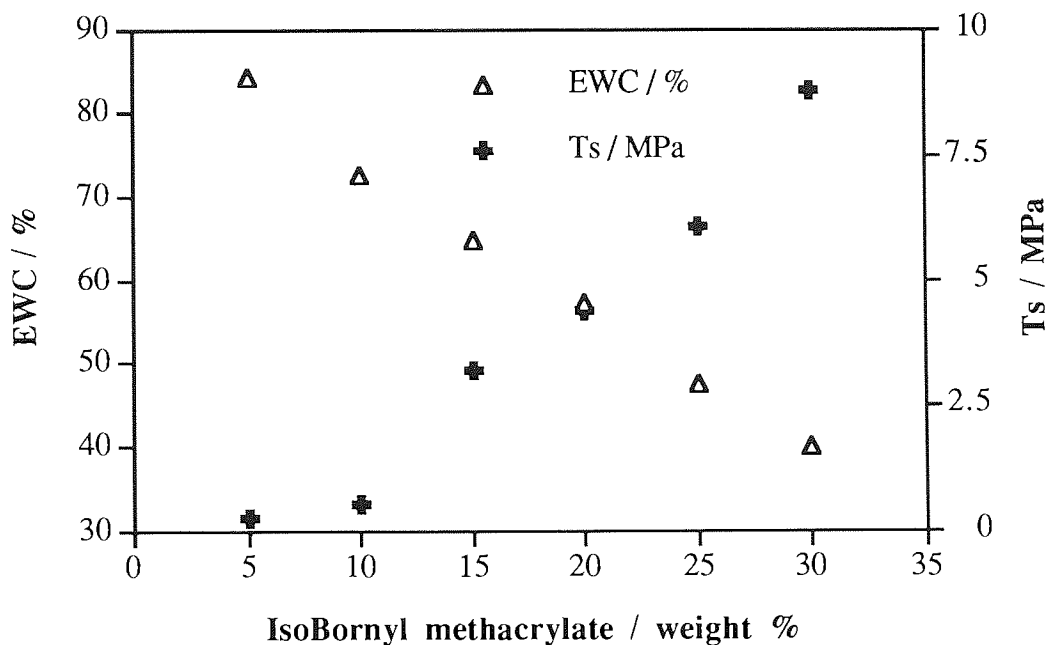


Figure 5.10 Effect of composition on the EWC and tensile strength of NVP-IsoBORNMA copolymers

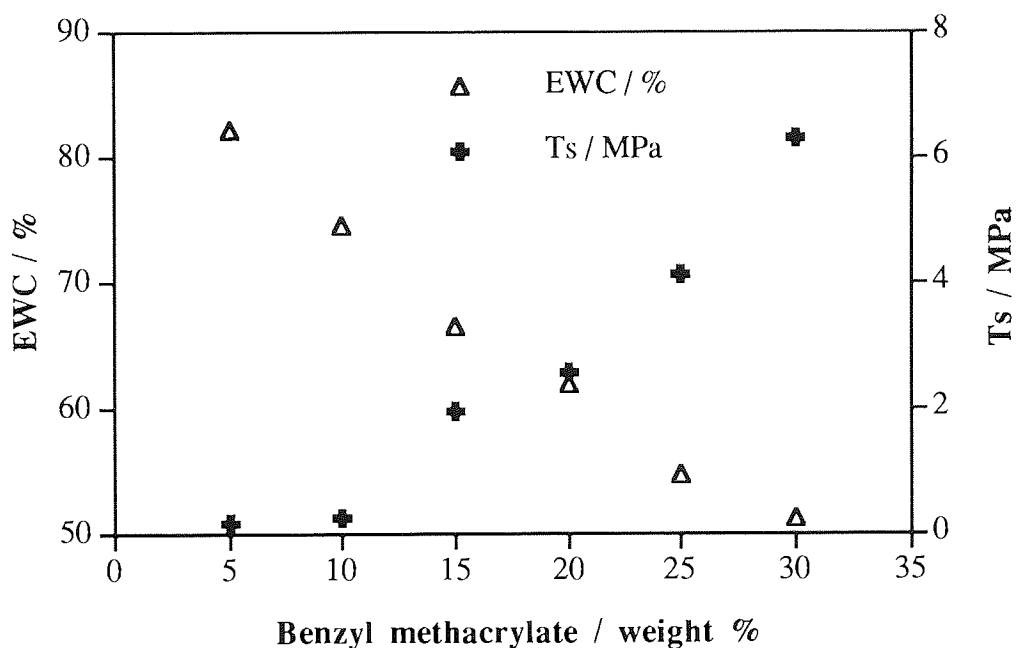


Figure 5.11 Effect of composition on the EWC and tensile strength of NVP-BENZMA copolymers

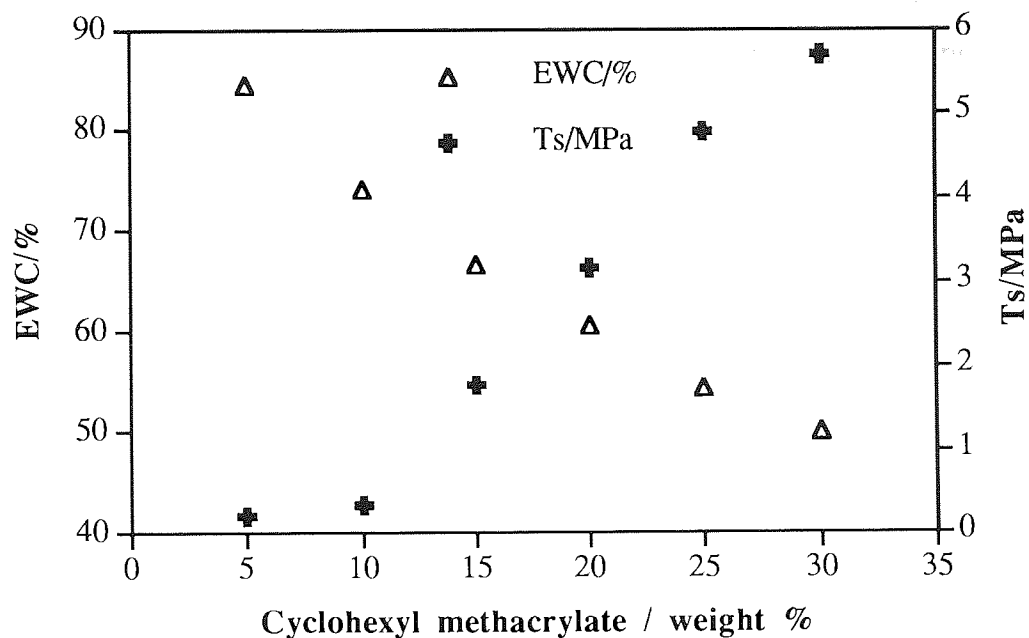


Figure 5.12 Effect of composition on the EWC and tensile strength of NVP-CHEXMA copolymers

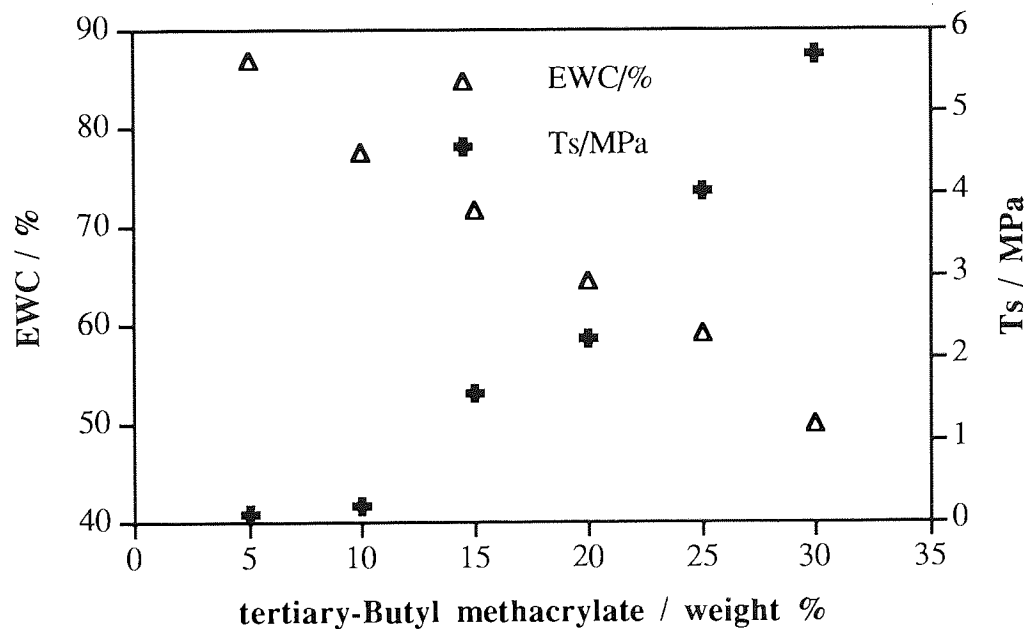


Figure 5.13 Effect of composition on the EWC and tensile strength of NVP-tBUTMA copolymers

The EWC's of the copolymers show the expected trend of a decrease in EWC with increasing proportion of hydrophobic monomer, this effect being well known in hydrophilic-hydrophobic systems^{155, 157}. In the case of the mechanical properties of the systems, the values of the elastic modulus (Em) and the tensile strength (Ts) increase with increasing amount of hydrophobic monomer, but a large increase in Em and Ts is observed at the compositions containing 15 weight% of the hydrophobic monomer. These results provide an indication of the minimum amount of hydrophobic monomer required to produce reinforcement by the formation of hydrophobic clusters. The amount of hydrophobic monomer and the existence of two domains is further quantified by the point at which two glass transition temperatures are observed for the series of copolymer hydrogels.

Glass transition temperatures were obtained for this series of NVP-hydrophobic monomer membranes using the DSC technique and the experimental values obtained are shown in Table 5.8.

Table 5.8 Effect of composition on the glass transition temperatures of each series of NVP:hydrophobic monomer dehydrated copolymer membranes

Weight%	IsoBORNMA		BENZMA		CHEXMA		tBUTMA	
	Tg1 /K	Tg2 /K	Tg1 /K	Tg2 /K	Tg1 /K	Tg2 /K	Tg1 /K	Tg2 /K
5	-	330	-	300	-	336	-	327
10	-	330	-	301	-	337	-	327
15	375	334	321	301	319	335	316	326
20	379	337	322	300	319	335	318	326
25	380	339	325	300	320	337	317	325
30	380	342	325	300	320	336	318	325

The hydrophobic aggregation within the copolymer corresponds to the glass transition temperature Tg1, the value of which is comparable to the Tg of the hydrophobic

homopolymer, (see values in Table 5.1). The value of T_{g2} was of the order expected for the glass transition temperature of the alternating copolymer.

Comparison of the T_g results with Figures 5.10 - 5.13 indicated that the marked increase in the mechanical properties occurs at a loading between 10 and 15 weight%. This point also corresponds to the appearance of the lower first glass transition temperature. The systems at loadings of 10 weight% and below of the hydrophobic monomer, exhibited one glass transition temperature only.

5.5.4 Conclusions

Preparation of hydrophilic-hydrophobic copolymers with pairs of monomers that produced sequence distributions containing large blocks dominated by the hydrophobic monomer, showed enhanced elastic moduli and tensile strengths. With hydrophilic-hydrophobic monomers that produce an alternating copolymer which is not dominated by one monomer type, these enhanced properties are not observed.

It has been suggested that hydrophobic aggregation of the hydrophobic-dominated domains produces clusters which reinforce the copolymer structure. The detection of two glass transition temperatures for copolymer compositions containing 15 weight% or greater of the hydrophobic monomer indicated two different regions within the copolymer thereby providing evidence for the formation of the afore-mentioned clusters.

5.6 The Reinforcement Of High Equilibrium Water Content Materials

5.6.1 Introduction

In Chapter 4 it was shown that high water content materials (EWC > 55%) with a controlled sequence distribution of the comonomers may be obtained using AMO copolymerised with HPA. However, at high water contents these systems are mechanically weak and unsuitable for contact lens applications.

Using the information collected about the molecular architecture of the hydrophilic-hydrophobic comonomer systems, hydrogels were prepared containing 50 weight% of the 50:50 weight / weight HPA-AMO systems copolymerised with 50 weight% of the 70:30 weight / weight NVP-hydrophobic monomer systems. This was performed in an attempt to maintain a high EWC and to enhance the mechanical properties of the HPA-AMO system by introducing a minimum quantity of the hydrophobic clusters required to reinforce the hydrogel membrane. The weight ratios selected corresponded to a hydrophobic proportion of 15 weight% which, from the previous results is equivalent to the minimum amount required to achieve the hydrophobic blocks.

5.6.2 Materials And Results

Three hydrogel membranes of the compositions described above were prepared incorporating firstly benzyl methacrylate, then cyclo-hexyl methacrylate and finally tertiary-butyl methacrylate monomers as the hydrophobic component. Membranes were prepared with 1% by weight of EGDMA as the crosslinking agent and cured as described in Chapter 2. The membranes were hydrated for the required period before any characterisation was performed.

The EWC's of the hydrated membranes were obtained and the mechanical properties determined. The results obtained for this series of membranes are shown in Table 5.9.

Table 5.9 EWC's and mechanical properties of the 50 weight% HPA-AMO (50:50) and 50 weight% NVP-hydrophobic monomer (70:30) copolymers

Hydrophobic monomer	EWC /%	Em / MPa	Ts / MPa	Eb / %
cHEXMA	58.6±0.3	1.212±0.001	1.722±0.073	339±28
tBUTMA	70.0±0.3	0.800±0.015	0.805±0.042	134±30
BENZMA	56.5±0.3	1.292±0.031	1.309±0.035	185±34

A comparison of the results obtained in Table 5.9 with the properties of the HPA:AMO compositions in Table 4.4 shows that the incorporation of the hydrophobic monomers significantly improved the mechanical properties with only a correspondingly small decrease in the equilibrium water content. The water content was maintained by copolymerising the two sets of copolymers which had previously been characterised as having high water contents. It was expected that the increase in the mechanical properties would be due to the formation of hydrophobic domains. The glass transition temperatures of the membranes were determined in order to identify the presence of such domains.

The glass transition temperatures of the dehydrated *composite* copolymers were determined by differential scanning calorimetry (DSC). The values obtained are shown in Table 5.10.

Table 5.10 Glass transition temperatures of composite materials obtained by DSC

Hydrophobic monomer	Tg1 /K	Tg2 /K
BENZMA	181	287
CHEXMA	175	285
tBUTMA	147	270

The observation of two glass transition temperatures Tg1 and Tg2 suggests the presence of two regions of polymer formation. Tg1 is characteristic of the value obtained for the hydrophobic homopolymer and would correspond to the volume of hydrophobic aggregation. Tg2 is characteristic of the value which would be obtained for a polymer composed of HPA, AMO and NVP.

5.6.3 Conclusion

It could therefore be expected that Tg₁ arose from a hydrophobic cluster and Tg₂ from the sequence-controlled copolymer. As a result it was the hydrophobic cluster which reinforced the mechanical characteristics of the hydrogel.

5.7 Summary

The work presented in this chapter supports the effect of monomer structure on the mechanical properties of hydrogel copolymers. It further revealed the effect of the sequence distribution of the copolymer on the mechanical characteristics.

Two series of copolymer membranes composed of firstly NVP, then AMO hydrophilic monomers copolymerised with a series of hydrophobic monomer produced sets of copolymers which had comparable equilibrium water contents. However, a dramatic difference was discovered in the values obtained for the mechanical properties. Observation of the copolymer sequences showed that the NVP copolymers had less tendency to produce an alternating copolymer structure. This led to the production of hydrophobic domains. These domains were impenetrable by water and therefore reinforced the hydrogel structure, increasing the tensile strength when compared to systems with equal water contents.

It was possible to detect these hydrophobic domains by observation of their glass transition temperatures using DSC. The hydrophobic domains appeared not to be formed once the level of hydrophobic monomer was less than 15 weight% of the hydrophobic monomer and the level of hydration along the copolymer chain was then thermodynamically unfavourable for hydrophobic-hydrophobic interactions to produce these domains.

CHAPTER 6

Novel Biomaterials Possessing Charged Monomer Units

6.1 Introduction

Hydrogels have been widely investigated for their use in biomedical applications because of their unique mechanical and surface characteristics. There are numerous publications on the preparation, structure and applications of hydrogels and it is evident from the literature that one of the most significant problems in the design of a biomaterial are the reactions that occur at the interface between the synthetic device and the biological environment. An example of this can be seen in the design of artificial arteries; if surface interactions cause the deposition of debris from the blood, this may lead to thrombus formation within the artery which may result in a potentially fatal sequence of events. Another example of this can be seen in the case of a contact lens; surface interactions may lead to the deposition of tear proteins and lipids which will reduce the quality and comfort of vision experienced by the wearer and subsequently may lead to eye infections. This deposition of biological components onto a synthetic material is generally referred to as "spoilation".

It is therefore necessary to have an understanding of the underlying surface chemistry which may contribute to these type of interfacial reactions. By applying this knowledge to the design of subsequent biomaterials, appropriate surface characteristics which do not produce spoilation can be incorporated.

Due to the potential use of hydrogels within systems which interact with the blood, many theories have been proposed relating to the factors which render a surface non-thrombogenic. These include the moderate surface energy hypothesis suggested by Baier and co-workers⁸⁷ and the minimum interfacial energy hypothesis proposed by Andrade⁸⁰. More recently research has been centred on ion-containing polymers for blood contacting applications and the role of the ions in the surface interactions between the host environment and the surface of the biomaterial.

Studies along this line have found that the incorporation of ion-containing pendant groups within the material is one method of improving the blood contacting properties of a variety

of polymers^{108, 110, 113, 158-160}. Previous studies investigating the blood contacting properties have shown that carboxylate or sulphonate ionic groups improve antithrombotic activity, reduce complement activation and give lower platelet deposition and activation^{110, 112}. Although if too great a concentration of charged monomer is combined with other polar molecules at the hydrogel surface, the thrombogenicity of the polymer is enhanced. Further studies investigated the use of sulphobetaine monomers¹¹¹. Sulphobetaines are macromolecules which contain a zwitterion or 'inner salt' in the polymer side chain. The potential of sulphobetaine polymers as hydrogels was suggested by Salamone *et al*¹¹¹ who prepared polymers from vinylimidazolium sulphobetaines by free radical polymerisations. It was found that the incorporation of such ion containing groups onto a polymer backbone improved the blood contacting properties and increased their wettability. The incorporation of ions also gave rise to coagulant behaviour. Jozefonwicz¹¹³ evaluated the anticoagulant behavior of carboxylate and sulphonate derivatized polymers and concluded that the carboxylate polymers had a lower anticoagulant behavior than the sulphonate containing analogues. These studies illustrated the dependence of the ionomer's biological activity on the polymer backbone structure, the ion type and the ion content.

As well as enhancing the blood contacting properties, ion incorporation affects the mechanical properties of the polymers. The modified materials have greater tensile strength and modulus in the dehydrated state than the underivatized polymer. This is believed to be due to the clustering of the ionic groups which serve to act as physical crosslinks. However, upon swelling, ion incorporation increases the equilibrium water content; the water acts as a plasticiser thereby reducing the mechanical properties of the hydrated polymer. This can prove to be a major problem because hydrogels in general have poor mechanical properties. Therefore, the ion content must be optimized to balance the surface and mechanical properties.

Very little published literature has investigated the use of ion containing monomers in hydrogel contact lenses. This is somewhat surprising because to date the most widely used monomer for soft contact lens production is HEMA. It is also well known that one of the side products in HEMA monomer and poly(HEMA) production is methacrylic acid (MAA). Methacrylic acid causes the surface of the material to be negatively charged at physiological (7.4) pH, which makes the surface susceptible to spoilation by proteins; more specifically those proteins which are positively charged. Recent work at Aston has examined the interactions of ion containing polymers with different charged tear protein; Sariri¹⁶⁵ has detailed the role of tear protein interactions with hydrogel contact lenses containing methacrylic acid.

The work presented in this chapter was concerned with the physical characteristics of a series of poly(HEMA)-based hydrogels possessing progressively increasing quantities of negative and / or positive charge. The results show the effect of the amount and type of charge on the equilibrium water content and the relative proportions of freezing and non-freezing water. The mechanical properties of the hydrogels were studied in order to gain an understanding of the effect of different types of charge and to provide an indication of the suitability of ion containing hydrogels for contact lens applications.

The surface properties of the hydrogels were investigated to determine surface group expression. To this end surface energy values (obtained by contact angle measurements) were used. This was performed to provide an indication of the significance of charged groups at the surface of the polymer. This was followed by a characterisation of the interaction of these materials with tear proteins of different charges to further understand and emphasise the role of the charged groups upon the protein deposition characteristics of the polymers produced.

6.2 The Effect of the Incorporation of Charged Monomers on the Water-Binding Characteristics of HEMA Copolymers

6.2.1 Introduction

The properties of a hydrogel are strongly influenced by its water content. There is evidence that the water in hydrogels exists in more than one state and that the state of the water has important consequences on its properties such as the permeability and surface characteristics of the hydrogel. The water binding characteristics of the polymers were therefore studied to establish the effect of the charged groups upon the equilibrium water contents and also the relative proportions of freezing and non-freezing water in the polymers produced.

6.2.2 Materials and Methods

Hydrogel polymer membranes were prepared as described in Chapter 2. The membranes used in this work were made of HEMA copolymerised with increasing proportions of the charged monomer. The monomers used to introduce charge into the hydrogel membrane were methacrylic acid (MAA), itaconic acid (ITC), N-vinyl imidazole (NVI) and N-(3-sulfopropyl)-N-methacryloxyethyl-N,N-dimethylammonium betaine (SPE). The structures of these monomers are illustrated in Chapter 2. Ethylene glycol dimethacrylate (EGDMA) was used as the crosslinking agent at a proportion of 1 weight%, with 0.5 weight% of azo-bis-isobutyronitrile (AZBN) used as the free radical initiator.

The equilibrium water contents of the charged hydrogel membranes were determined using the gravimetric method described in Chapter 2. A minimum of 5 disks of sample were used to obtain the value of the equilibrium water content. The water-binding capability of the charged monomers can be derived from the relative proportions of freezing and non-freezing water. Consequently, the values of freezing and non-freezing water were determined using DSC as described in Chapter 2.

6.2.3 Results

The values of the equilibrium water contents obtained for the series of hydrogels which possessed increasing amounts of the charged monomers are illustrated in Figure 6.1. The results show that the equilibrium water content increased when the proportion of the charged monomer increased. This was expected because the charged monomers are more polar than HEMA.

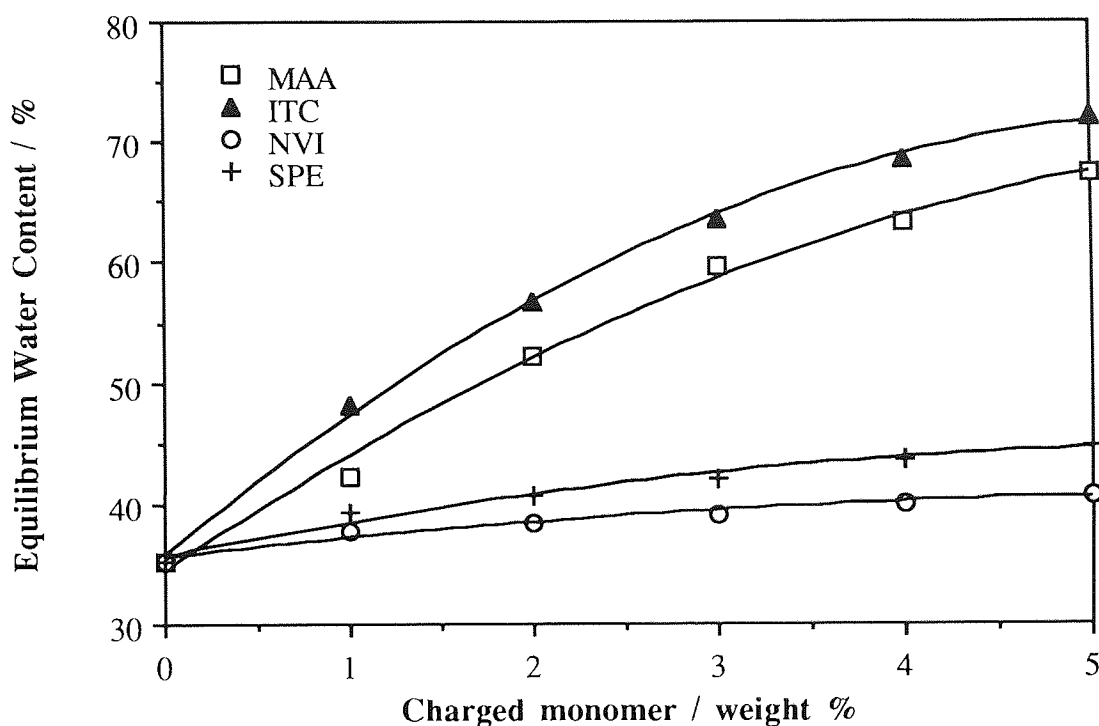


Figure 6.1 Effect of increasing proportion of charged monomer on the equilibrium water contents of HEMA copolymer membranes

The water binding abilities for a given composition are not due to the nature of the charge alone, but are dependant upon the balance of the contribution of polar and steric factors. In the case of the itaconic acid (ITC) monomer the polar contribution is predominantly due to the two carboxyl groups and steric effects are due to the presence of the two side chains. A comparison of the structures of ITC and MAA shows that one of the carboxyl groups has been replaced by a hydrogen to produce an α -methyl group. Although the steric contribution has been decreased in MAA when compared to ITC, the number of polar

are reflected in the values of the EWC obtained for these two series of hydrogels which are shown in Figure 6.1 . The values of the EWC are reflective of the balance of polar and steric factors. For copolymers containing ITC the polar character and not the steric characteristics of the extra acid group are the dominant factor controlling the water absorption of the copolymer. This result indicates that values of the EWC can be significantly increased by incorporating monomers with two polar side chains.

The effect of positive charge in the form of N-vinyl imidazole was not as great as the negative charge introduced by the acid groups upon the EWC. This is due to the weaker ionic strength of the quaternary ammoniums compared to the carboxylate group.

Incorporation of N-(3-sulfopropyl) -N-methacryloxyethyl -N,N- dimethylammonium betaine (SPE) increases the EWC. This was due firstly to the strongly water binding sulphonate group which has a higher ionic strength than the carboxylate group and secondly to the presence of a quaternary nitrogen. It might be expected that the higher ionic strength of the combination of these ionic groups causes the SPE comonomer to produce EWC's of the order of those observed when equal amounts of MAA are used. However, although there are a number of polar groups present in SPE it is the steric contribution of the alkyl side chain which dominates the total water binding ability of this monomer. This results in lower values of the equilibrium water content than would be expected for a monomer containing such ionic groups. This further supports the significance of polar and steric effects on the EWC of the polymer.

A more detailed picture of the water-binding capability of the charged monomers can be derived from the relative proportions of freezing and non-freezing water. The results from this study are shown in Figures 6.2 - 6.4. The values are expressed as grams of water per gram of polymer to provide information on the relative water binding capabilities of these charged systems.

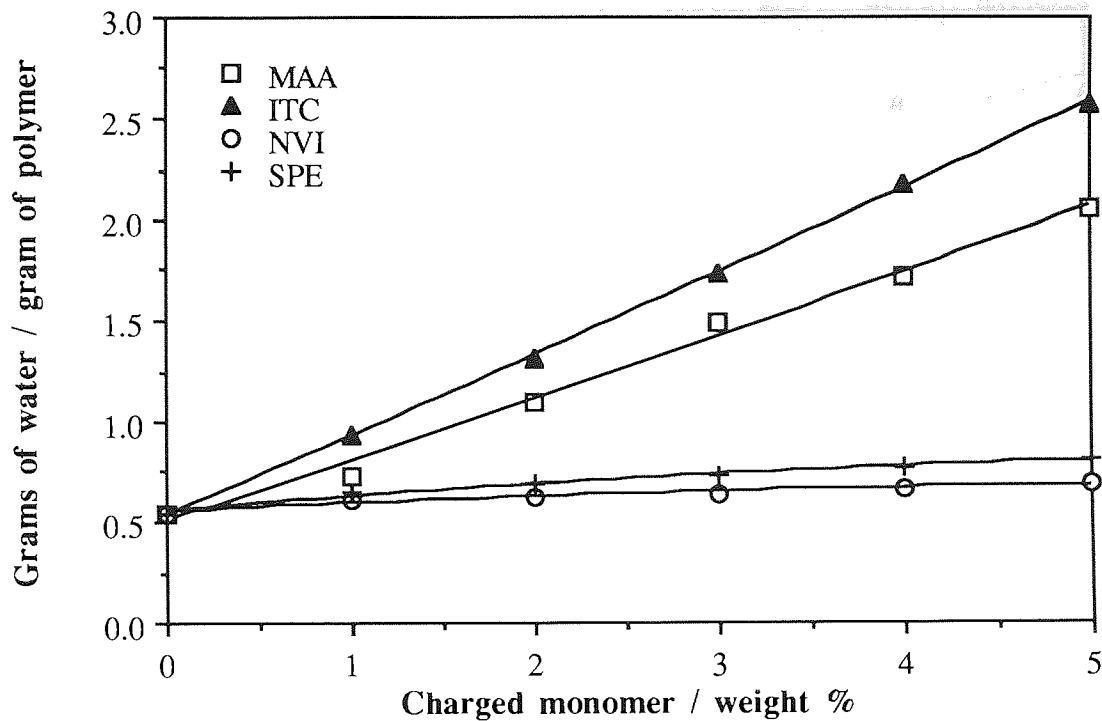


Figure 6.2 Effect of increasing proportion of charged monomers on the total water binding capability of HEMA copolymer membranes

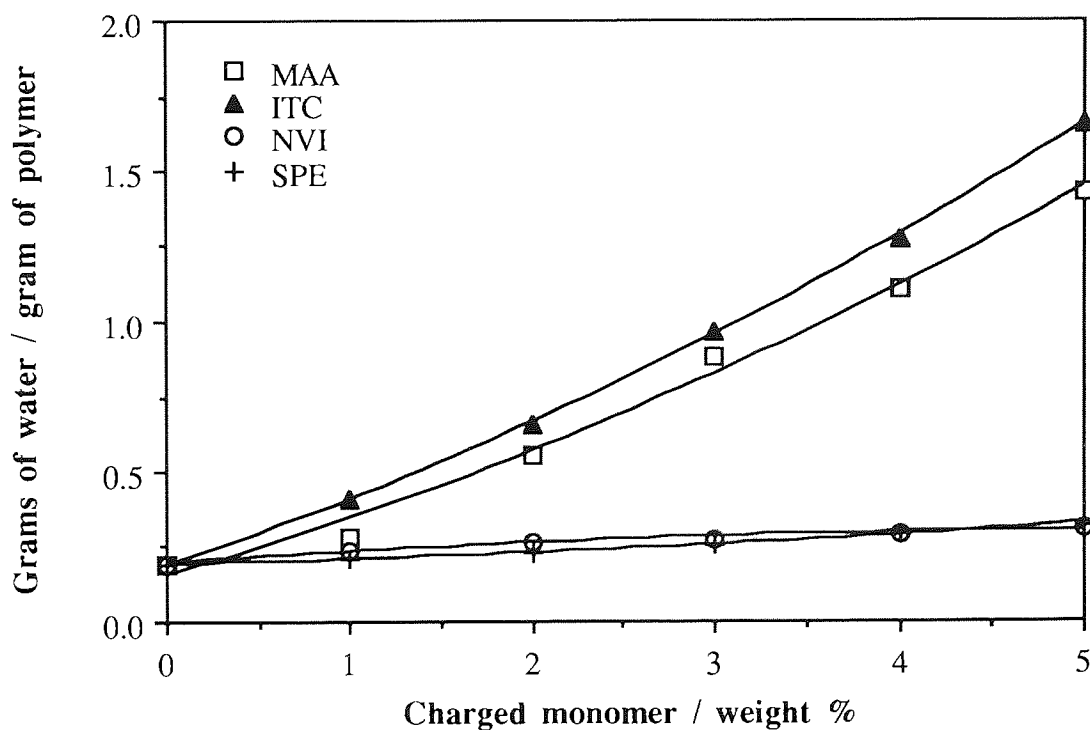


Figure 6.3 Effect of increasing proportion of charged monomers on the freezing water content of HEMA copolymer membranes

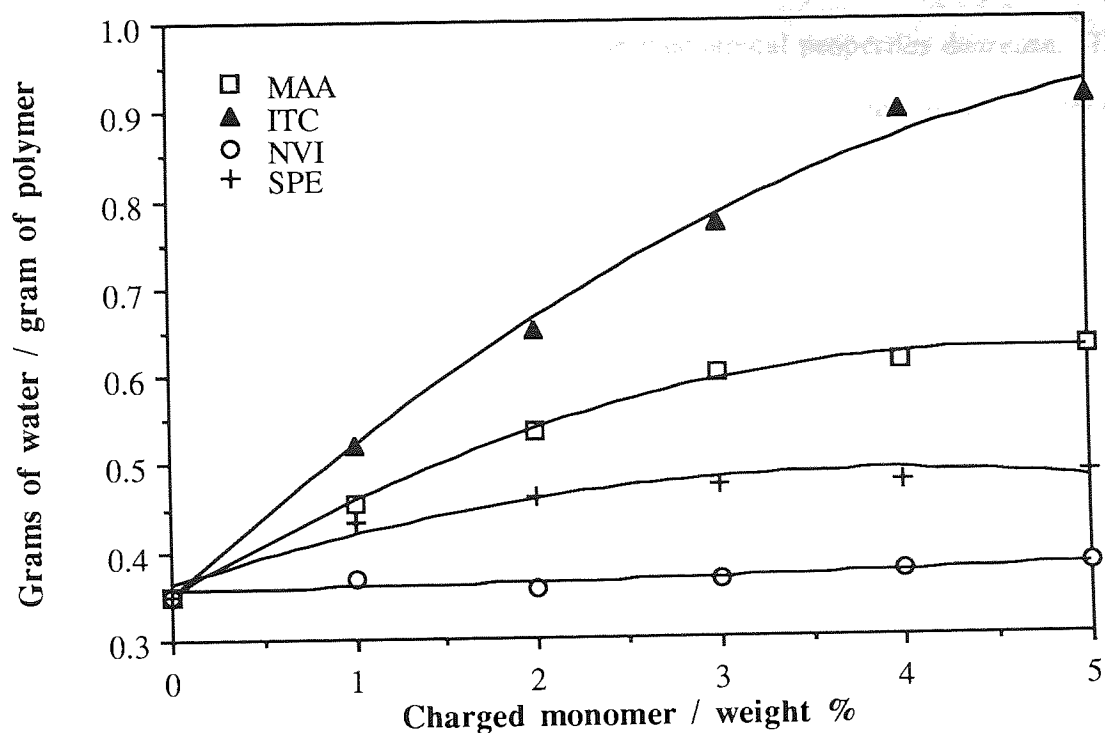


Figure 6.4 Effect of increasing proportion of charged monomers on the non-freezing water content of HEMA copolymer membranes

Figure 6.2 provides an indication of the relative water binding capabilities of the charged monomers and it was shown that the total water binding capabilities of the charged monomers increase in the order $NVI < SPE < MAA < ITC$. This indicates that negative charge was more effective than positive charge in increasing the EWC of the polymer.

Figures 6.3 and 6.4 show the effects of the proportion of charged monomer upon the relative proportions of freezing and non-freezing water respectively. From the results in Figures 6.3 and 6.4 it was calculated that the proportion of non-freezing water in the HEMA copolymer containing 5 weight% of MAA was approximately 31%. For the comparable HEMA copolymer containing 5 weight% of ITC the proportion of non-freezing water was approximately 36%. This result indicates that using a monomer containing two pendant groups as opposed to one, increased both the EWC and the proportion of non-freezing water. Therefore, the proportion of freezing water in the polymer was reduced. This is useful because it has been shown that the mechanical

properties of hydrogels are dependant upon the proportion of freezing water. That is, as the proportion of freezing water increases, the mechanical properties decrease. This is because the freezing water has been correlated to a plasticising effect upon the mechanical properties of the polymer. Therefore the incorporation of monomers with two pendant polar groups increases the EWC and decreases the relative proportion of freezing water.

From Figures 6.2 - 6.4 the results obtained for the copolymers containing NVI and SPE indicate the effect of the type of charge on the water binding abilities of the copolymers. When charged, NVI carries positive charge due to the formation of two quaternary ammonium groups whereas the charge present in SPE is negative due to a quaternary ammonium structure and the sulphonate ion. The freezing and non-freezing water contents (observed in Figures 6.3 and 6.4) for HEMA copolymers containing these monomers indicates that the amount of non-freezing water is greater for the SPE containing copolymers (approximately 60% compared to 55%). This suggests that water is more strongly associated with negatively charged groups than it is with positive groups.

6.2.4 Conclusions

The results show that the effect of incorporation of charge into HEMA copolymers was to increase the EWC and to this end, that negative charge appeared to be more effective than positive charge. The values of the EWC shown in Figure 6.1 and the structures of the monomers used further highlight the significance of the polar and steric contributions to the total water binding ability of the monomers.

The results also show the effect of the amount and type of charge upon the EWC of copolymers. Increasing the amount of charge in the copolymer increased the EWC. The use of negative charge produced copolymers with lower proportions of freezing water than copolymers with positive charge. This is useful because it is the amount of freezing water which plasticises the copolymer. The use of two pendant groups compared to one also decreased the amount of freezing water because of the increased number of polar sites per monomer, which water molecules may be associated with. These results should be useful

in the designing of high water content copolymers which possess smaller amounts of freezing water, so that their mechanical properties are not adversely affected.

6.3 Mechanical Properties of Hydrogel Polymers Containing Charge

6.3.1 Introduction

It is known that as the EWC of a copolymer increases the mechanical properties decrease due to the plasticising effect of the imbibed water. The previous results in this chapter have shown that the EWC increases with increasing amounts of charged monomer. It is therefore necessary to determine what effect the increased proportion of water and also the effect of the type and amount of charge have upon the mechanical properties of the copolymers.

The results presented earlier in this chapter show that with increasing amounts of ionic charge in the hydrated copolymer there is a corresponding increase in the EWC's. It would be expected that an increase in the water content, particularly the freezing water which acts as an internal plasticiser, would reduce the mechanical properties of the hydrogel copolymers.

This observation has been explained by the theory of polymer networks which predicts the following about the modulus G:-

$$G = (1-2/f) \cdot \nu RT \cdot \langle r^2 \rangle / \langle r^2 \rangle_0 \quad \text{Equation 6.1}$$

where f is the functionality of crosslinks

ν is the molar number of elastically effective network chains per unit volume

R is the gas constant

T is the temperature

$\langle r^2 \rangle$ is the mean square end to end distance of the chains in the network

$\langle r^2 \rangle_0$ is the corresponding quantity for the chains in the uncrosslinked state, under the same conditions¹⁶¹.

When the EWC, expressed as the degree of swelling q is increased, v varies inversely proportionally and correspondingly the modulus G decreases. However, it must be noted that the ionic charges would be expected to produce deviations from these theoretical predictions. In fact, attempts have been made to take account of the modifications that would occur in the behaviour of the charged polymer network¹⁶². Opperman *et al*¹⁶³ examined the behaviour of both ionic and non-ionic poly(acrylamide) gels, in order to understand the consequences of ionisation between 2 and 10 weight% of the charged monomer. Mechanical measurements of the resulting gels did not show the predicted decrease when the swelling ratio was increased. On the contrary values of the modulus were observed to increase up to five fold.

6.3.2 Materials and Methods

The effect of increasing the quantities of methacrylic acid (MAA), itaconic acid (ITC), N-vinyl imidazole (NVI) and N-(3-sulfopropyl)-N-methacryloxyethyl-N,N-dimethyl-ammonium betaine (SPE) were investigated upon the mechanical properties of the HEMA copolymers. The properties of the hydrated copolymer membranes were determined using the tensile method previously described in Chapter 2.

6.3.3 Results

The results obtained for the initial elastic modulus, tensile strength and elongation at break, together with the type and amount of charge are shown in Table 6.1.

Table 6.1 Effect of the type and amount of charged monomer on the mechanical properties of HEMA copolymers

Comonomer	Weight%	Initial modulus Em / MPa	Tensile Strength Ts / MPa	Elongation at break, Eb / %
MAA	0	0.654	0.726	133
	1	0.587	0.646	169
	2	0.615	0.745	176
	3	0.502	0.455	122
	4	0.462	0.360	91
	5	0.435	0.333	86
ITC	0	0.654	0.726	133
	1	0.731	0.567	122
	2	0.636	0.510	121
	3	0.548	0.579	133
	4	0.603	0.569	99
	5	0.708	0.420	77
NVI	0	0.654	0.726	133
	1	0.672	0.639	141
	2	0.555	0.837	218
	3	0.583	0.717	197
	4	0.574	0.692	199
	5	0.600	0.701	179
SPE	0	0.654	0.726	133
	1	0.674	0.788	181
	2	0.636	0.707	151
	3	0.617	0.700	162
	4	0.564	0.700	200
	5	0.570	0.730	203

From Table 6.1, which shows the results of the investigation into the effect of the type and amount of the charge upon the mechanical properties of the HEMA copolymers, it can be seen that for the copolymers containing increasing proportions of methacrylic and itaconic acid the mechanical properties increased at low levels; 1-2 wt % of the charged monomer. These copolymers showed a slight overall decrease at the upper proportions of the

comonomer. Even at the highest levels of ion incorporation the mechanical properties of the copolymers were greater than those of hydrogel systems with comparable water contents (refer to 3.2.4; EWC's of nitrogen containing monomers). Therefore, it was concluded that the enhanced mechanical properties of these copolymers must have been due to the effect of the charged monomer.

The remaining copolymers incorporating N-vinyl imidazole and N-(3-sulfopropyl)-N-methacryloxyethyl-N,N-dimethylammonium betaine showed a marked increase in the mechanical properties over the composition range, resulting in a far more elastic gel being produced. The role of the charge is clearly more evident in these two systems because the water contents are of a much narrower range than the methacrylic and itaconic systems and the effect of the water is kept to a minimum.

6.3.4 Conclusions

These results indicate that increasing ionic charge gave higher swelling ratios. This is in line with the conclusions derived by Oppermann¹⁶³ in their studies upon poly(acrylamide) gels. Oppermann also observed that when the swelling ratio increased, the modulus did not follow the predicted decrease; it was concluded that this observation was due to increasing chain extension with increasing ionic charge. The polymer chains therefore no longer obey the statistics associated with normal network theory. It is therefore reasonable to assume that introducing charge into the copolymers used in this chapter may increase the chain extension within the network due to electrostatic repulsion of like charges. Therefore the proportion of elastically ineffective rings within the network will be lower. This enables the network to maintain its mechanical integrity with increasing EWC.

6.4 Surface Properties of Charged Hydrogel Materials

6.4.1 Materials and Methods

The surface properties of the copolymers were obtained in both the dehydrated and hydrated states using the techniques described in Chapter 2.

6.4.2 Results

The values of the total surface free energies with their individual polar and dispersive components are shown in Figures 6.5 - 6.12. It can be seen that the total surface free energies for the hydrated materials were lower than the values for the hydrated materials. This was expected due to the contribution and modification of the surface by the water present within hydrated systems.

In Figures 6.5, 6.7 and 6.8 the results show that increasing the amount of ionic charge decreased the polar component of the surface free energy. This observation was consistent with the effect of hydrophobic group expression at the air interface and the orientation of the hydrophilic groups towards the polymer bulk. However, in Figure 6.6 the results show that the polar component of the surface free energy increased. This is explained in terms of the charged monomer structure; itaconic acid possesses two carboxyl groups and produces a copolymer with one carboxyl group on each side of the polymer backbone. Therefore there is always a polar group expressed at the air interface, which will contribute to the polar component of the surface free energy. This effect would be particularly useful in applications where some degree of dehydration of the biomedical device occurs *in vivo*; for example contact lenses. It is well known that lens dehydration occurs during wear periods. Dehydration causes the polymer molecules to orientate such that the polar groups are not expressed at the lens-air interface and therefore the surface of the lens becomes more hydrophobic; a more hydrophobic surface results in increased adsorption of proteins. However, using the monomers containing two pendant groups it is evident that some degree of polar component is maintained at a dehydrated surface.

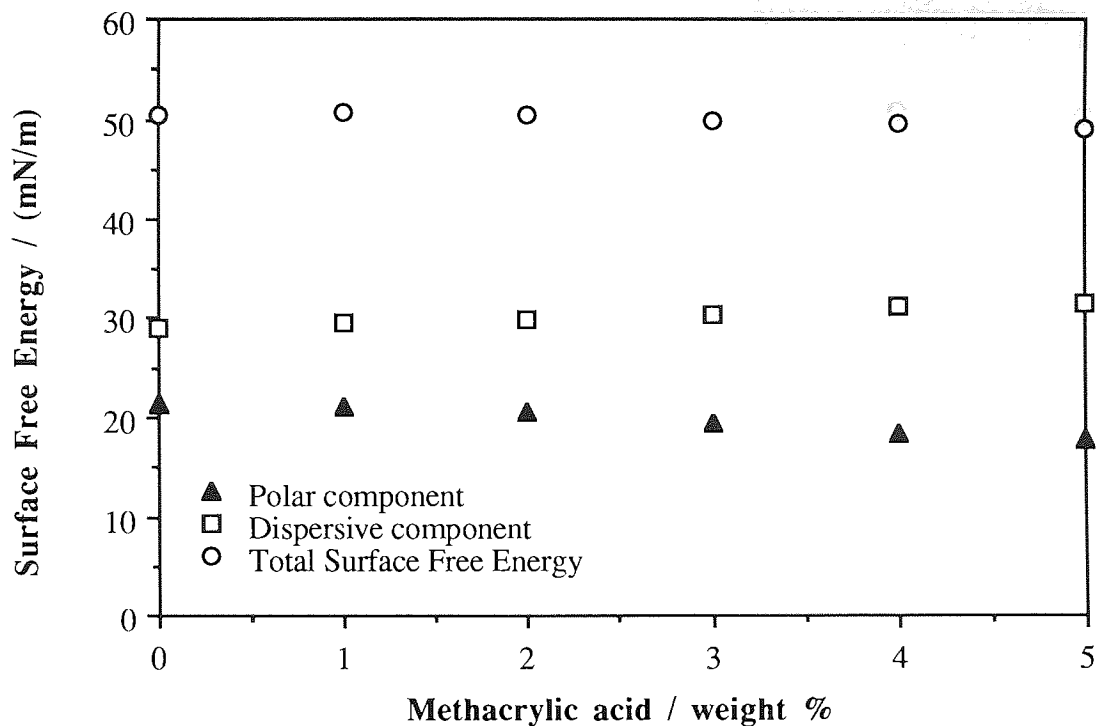


Figure 6.5 Effect of composition on the surface free energy of dehydrated HEMA-MAA copolymers

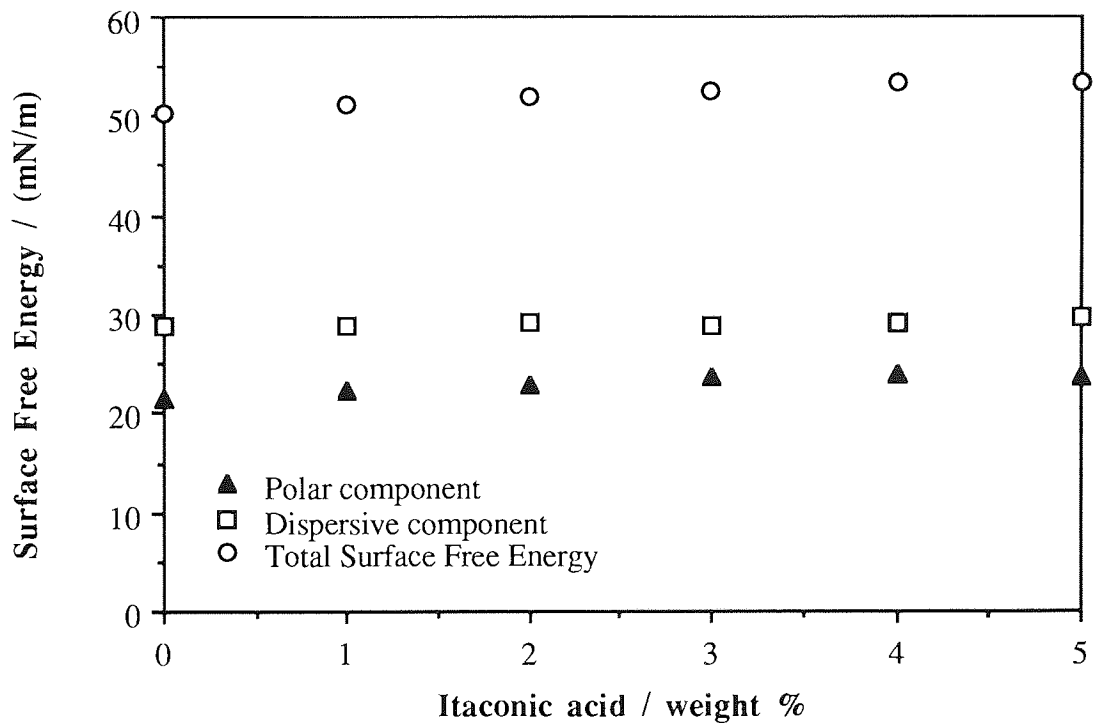


Figure 6.6 Effect of composition on the surface free energy of dehydrated HEMA-ITC copolymers

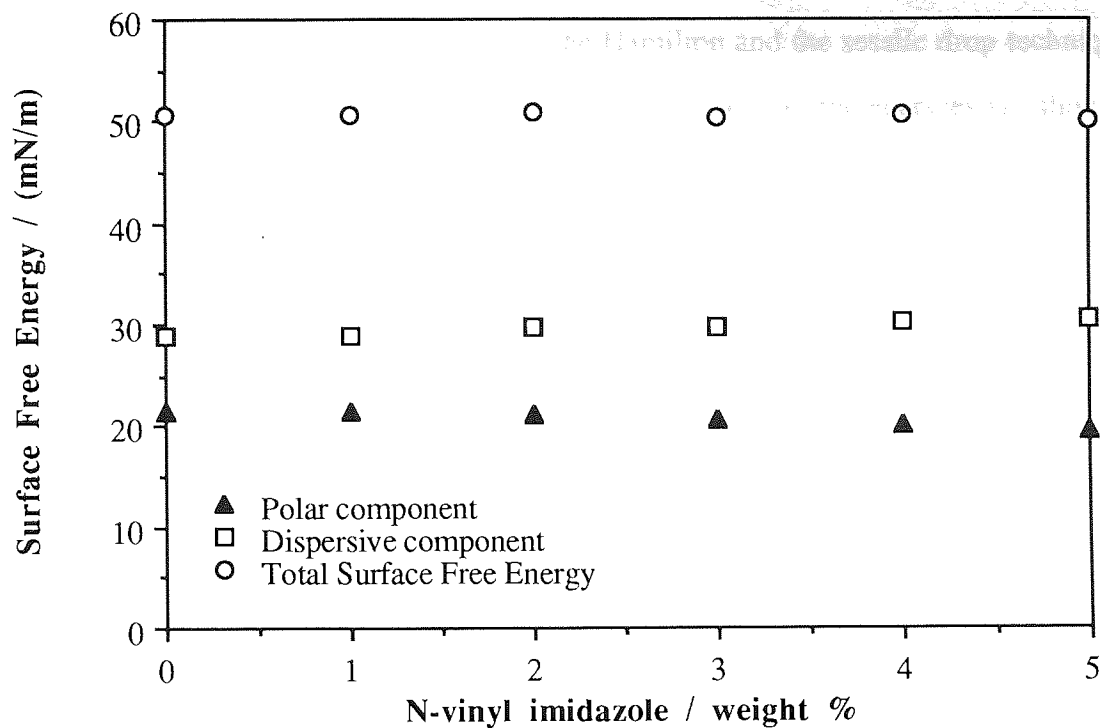


Figure 6.7 Effect of composition on the surface free energy of dehydrated HEMA-NVI copolymers

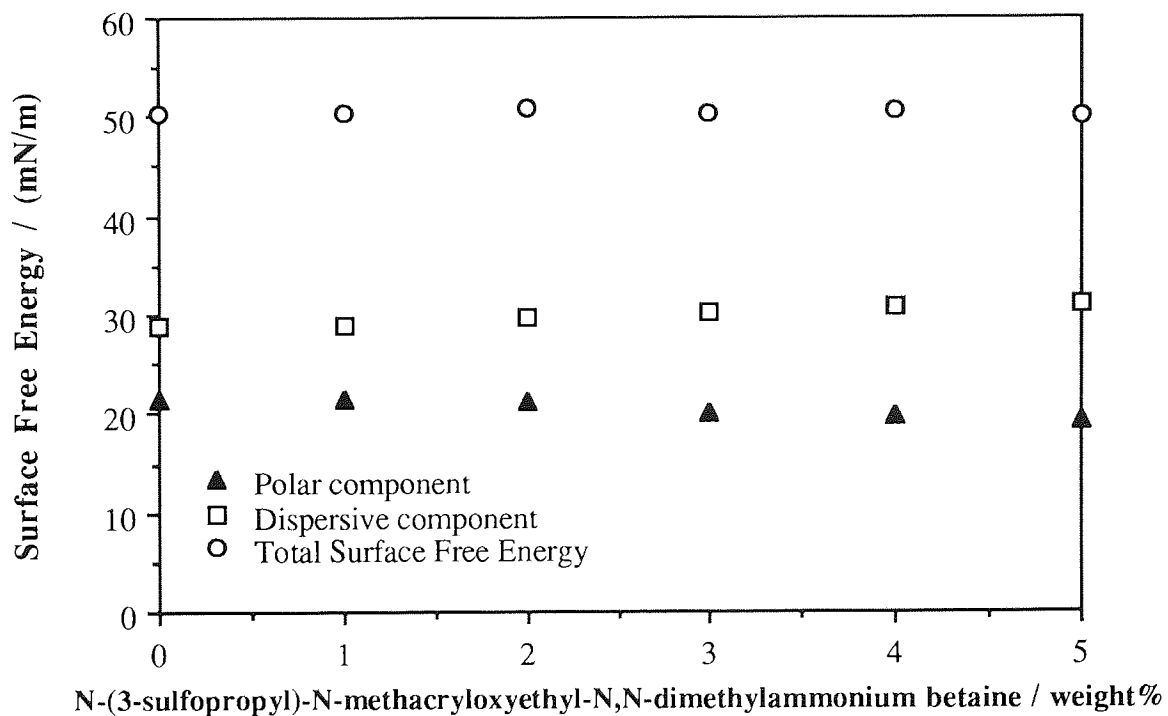


Figure 6.8 Effect of composition on the surface free energy of dehydrated HEMA-SPE copolymers

The total surface free energies and the individual polar and dispersive components of the hydrated materials were determined using the Hamilton and the sessile drop techniques. The values of the individual components and the total surface free energies are shown in Appendix III. The contributions of the individual polar and dispersive components of the surface free energy of the polymer are plotted against the values of the EWC together with the contribution of the polar and dispersive components of water. This enables a measure to be obtained for the contribution of the polymer structure to the surface characteristics of the hydrogel.

The results shown in Figures 6.9 - 6.12 reveal evidence that the polar component of the surface energy due to the polymer was greater than the dispersive component due to the polymer. This result is consistent with the theory that the molecular orientation of the polymer backbone is such that the polar groups within the copolymer are expressed at the interface with water. This molecular re-orientation results in an increase in the polar component and a decrease in the dispersive component of the surface free energy.

Figure 6.9 shows what the contributions to the surface free energy were by the polar and dispersive components due to both the polymer and the imbibed water with respect to the equilibrium water content for the series of HEMA-MAA copolymers. As was expected, the polar and dispersive components of the surface free energy due to water increased with increasing equilibrium water content. This was because water plays an integral part of the hydrogel structure; it has a polar component of the surface energy of 51mN/m and a dispersive component of 21mN/m. Therefore it would be expected that the results would indicate, that as the proportion of water increased within the copolymer, the polar and dispersive components of the surface energy would approach the values for the individual components for pure water.

In contrast, the polar and dispersive contributions to the surface energy of the hydrogel due to the polymer decreased with increasing equilibrium water content. This was expected

expected because the proportion of polymer within the hydrogel decreased as the proportion of water increased. However, it is the ratio of the polar and dispersive components due to the polymer which provide information on the effect the polymer structure has on the balance of polar and dispersive forces. For the HEMA-MAA copolymers the polar/dispersive ratio at zero weight% MAA (corresponds to EWC = 35.1) was 1.5. This ratio rose to 1.8 for the HEMA-MAA copolymer containing 5 weight% of MAA (corresponding to an EWC = 67.3%). This latter ratio indicates that the polymer structure becomes increasingly polar with the addition of the polar MAA.

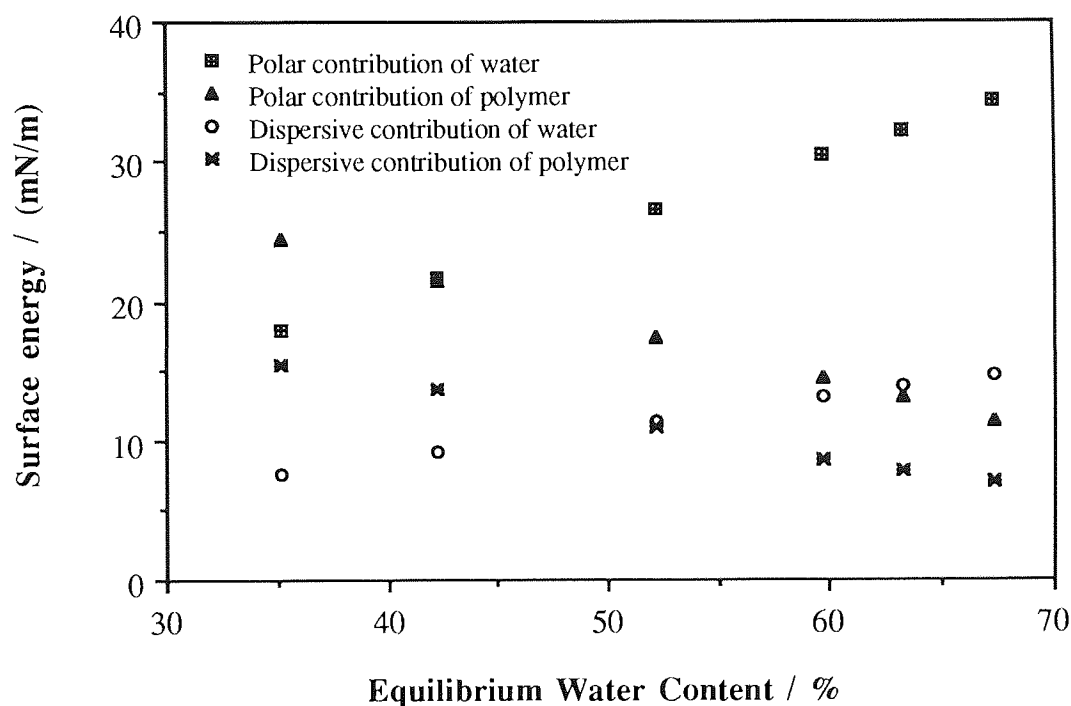


Figure 6.9 Variation in the polar and dispersive components of the surface energy with increasing EWC for hydrated HEMA-MAA copolymers

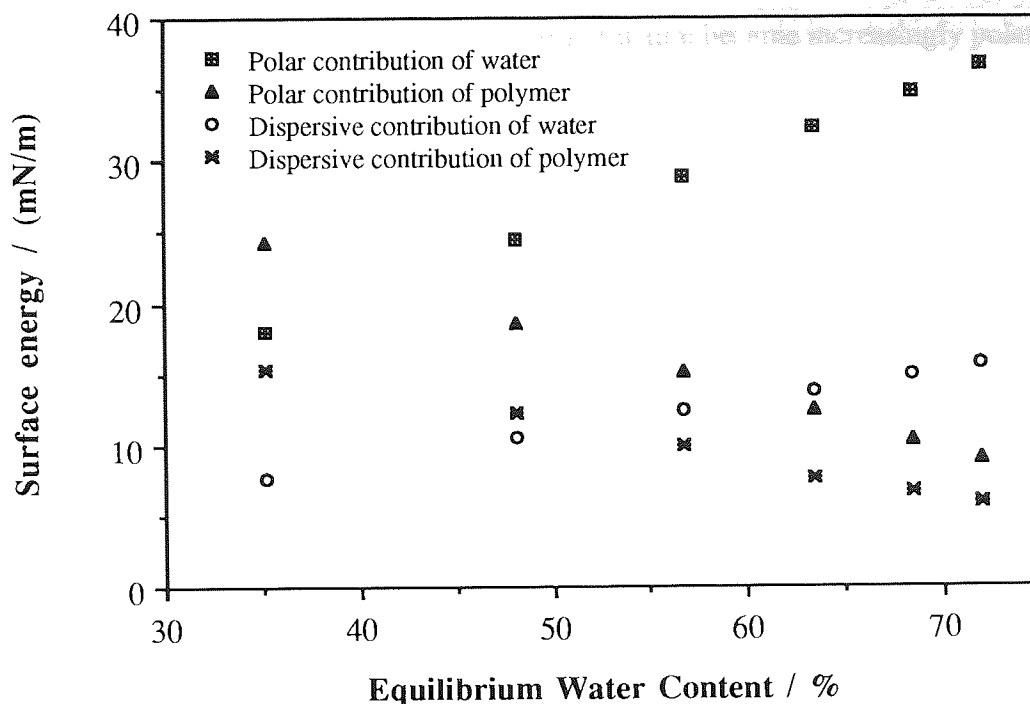


Figure 6.10 Variation in the polar and dispersive components of the surface energy with increasing EWC for hydrated HEMA-ITC copolymers

Figure 6.10 shows what contributions to the surface free energy were made by the polar and dispersive components due to both the polymer and the imbibed water with respect to the EWC for the series of HEMA-ITC copolymers. As was the case for the structurally similar HEMA-MAA copolymers, the polar and dispersive components of the surface free energy due to water, increased with increasing EWC. This was again due to the water being an integral part of the hydrogel structure.

In contrast, the polar and dispersive contributions to the surface energy of the HEMA-ITC copolymers due to the polymer, decreased with increasing EWC. Again this would be expected because the proportion of polymer within the hydrogel decreased as the proportion of water increased. In the case of the HEMA-ITC copolymers the ratio of the polar and dispersive components due to the polymer rose from the polar/dispersive ratio at zero weight% ITC (corresponds to EWC = 35.1) of 1.5 to approximately 1.8 for the

HEMA-ITC copolymer containing 5 weight% of ITC (corresponding to an EWC = 72.3). Once again this ratio indicates that the polymer structure became increasingly polar with the addition of ITC.

Comparison of the MAA and the ITC structures (Chapter 2) indicates that ITC contains two polar acid groups compared to the one in MAA. It might therefore be expected that the addition of ITC would further increase the polar component of the surface energy, yielding a higher polar/dispersive ratio. However, for each molecule of ITC only one acid group may be expressed at the surface, because each group is pendant to opposite sides of the backbone and therefore its surface energies reflect the trend and contributions observed for MAA containing copolymers.

Figures 6.11 and 6.12 show the contributions of the polar and dispersive components of the surface energy, with variation in the EWC, made by the HEMA-NVI and HEMA-SPE copolymers respectively. The contribution to the surface energy due to water does not undergo a large change because the range of water contents studied are narrow. The incorporation of NVI into HEMA copolymers increases the polar character of the surface due to the polymer as the polar dispersive ratio increases from 1.5 for HEMA-NVI containing zero weight% of NVI (corresponding to EWC = 35.1%), to 2.0 for the HEMA-NVI copolymer containing 5 weight% NVI.

For the HEMA-SPE copolymers the changes in polar and dispersive contributions to the surface energy are studied over a broader range of water contents. Therefore the magnitude of the effect of the water polar and dispersive contributions are more clearly observed than for the series of HEMA-NVI copolymers. The polar dispersive ratio increases from 1.5 to 1.9 for the copolymers containing zero and 5 weight% of SPE respectively. This indicates that as the proportion of SPE is increased the polar character of the copolymer is increased.

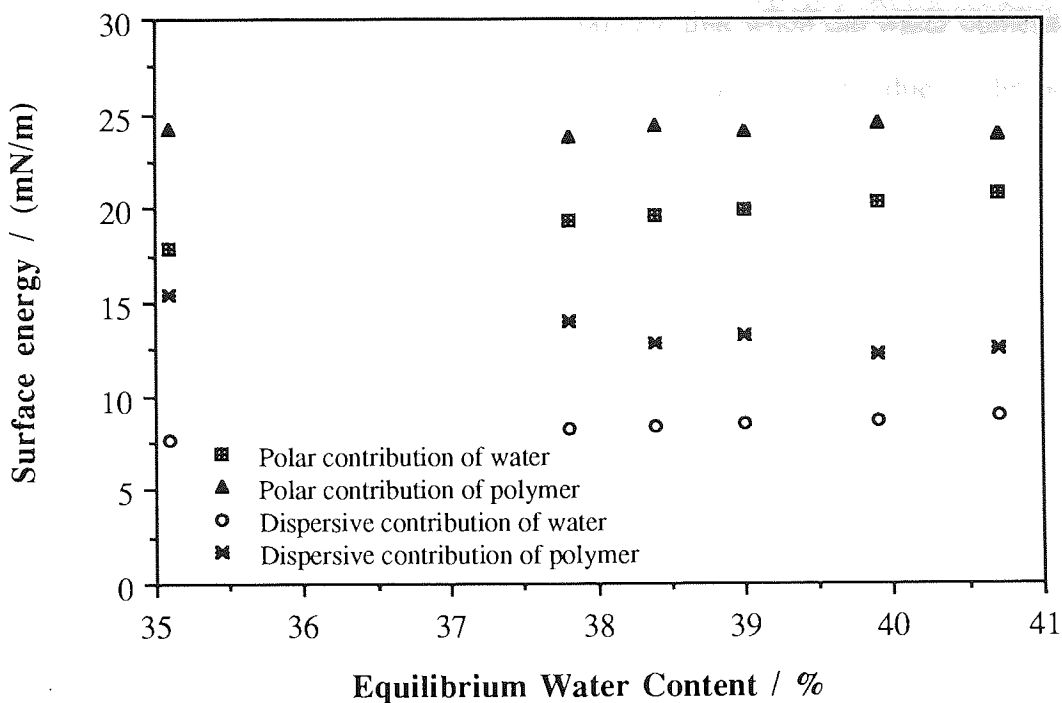


Figure 6.11 Variation in the polar and dispersive components of the surface energy with increasing EWC for hydrated HEMA-NVI copolymers

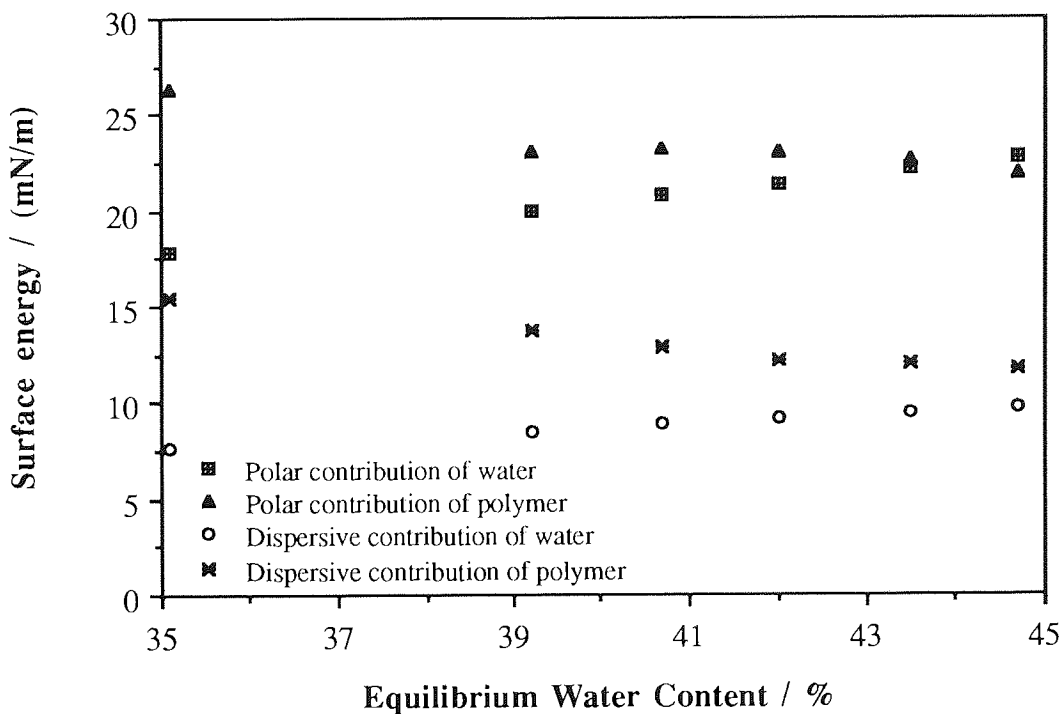


Figure 6.12 Variation in the polar and dispersive components of the surface energy with increasing EWC for hydrated HEMA-SPE copolymers

6.4.3 Conclusions

The results for the four sets of copolymers indicate that when the water content of the copolymers was increased, the contribution to the surface energy due to the polymer decreased. This was expected because the copolymer becomes a smaller percentage of the total system as the equilibrium water content is increased.

For each of the copolymer series, it was shown that, as the proportion of charged monomer increased the polar character of the copolymer increased. This trend was indicated by the change in the polar/dispersive ratio for each of the copolymer series studied. It appears that positive charge has the greatest effect on the polar character of the polymer because it increases the polar/dispersive ratio to a larger extent than the equivalent proportions of negative charge. It would therefore be expected that the most marked changes in surface interactions at an interface due to the polar character of the polymer would be occur for polymers containing positive charge.

Although surface energy measurements provide a useful insight into the changes of polar and dispersive characters of the polymer structure, no information can exactly be projected to the implications this holds for the polymer interactions with biological species. It was therefore necessary to characterise the interactions of the polymer with biological species in order to attempt to correlate changes in the charge, polar and dispersive characters and water contents of the polymers with changes in the amounts of adsorption to the polymer.

6.5 Protein Interactions with Charged Hydrogel Polymers

6.5.1 Introduction

Proteins are an important part of tear chemistry and are well known for their role in the spoilage of hydrogels. Such spoilage is undesirable, for example in the case of contact lens materials, since this would cause impairment in the quality of vision experienced by the wearer and likely discomfort also. The interaction of tears and synthetic materials leads to the virtually instantaneous process of protein adsorption¹⁶⁴ and once adsorbed, the

protein is very difficult to remove from the material surface. It is also well known that the most abundant tear protein, lysozyme, is able to diffuse into the matrix of some high water content lenses thereby rendering the protein more difficult to remove. The interactions that govern the mechanism of protein adsorption are complex. It is believed that primary migration of the protein to the synthetic material occurs, which forms the basis of surface deposition and that diffusion of the protein into the bulk of the material can occur in particularly high water content materials which are able to accommodate this diffusion process. The complexity of the processes are beyond the scope of this thesis, but work here at Aston has looked at the processes involved in protein deposition; Sariri¹⁶⁵ describes in detail the effect of hydrogel structure on the nature and quantity of protein absorbed into the lens matrix. This coworker concluded that both the size and charge of proteins are influential in their deposition onto contact lenses.

It is apparent from the work of Sariri that the size and charge of proteins in the biological environment are influential to the interactions occurring at an interface. Consequently, the next investigation was designed to study the effect of monomers with negative and/or positive charge upon the protein deposition onto the series of HEMA copolymers and the effect of this charge upon the interactions with charged biological proteins.

6.5.2 Materials and Methods

The protein under examination was used as a protein solution; solutions were prepared as stock solutions with the concentration of protein in the range of 1-2 mg/ml distilled water. The proteins used for the studies were lysozyme, albumin, lactoferrin, ferredoxin and lactalbumin. The working solutions used for the protein interaction studies were prepared by diluting the stock solutions when required. The hydrogel polymers were cut into 14mm diameter disks using a size 7 cork borer in order to study the protein spoilation.

Each of the protein-containing solutions were used to spoil the polymers in 2ml single-solutions at a concentration of 0.5 mg protein/ml. The materials were incubated at room

temperature, ($22 \pm 2^\circ\text{C}$) over a time period of five days and were constantly shaken on a slow speed shaker.

The quantities of the protein on the surface of the material were measured using a direct U.V. absorption technique, at a wavelength of 280 nm. This application of the technique as a quantitative method for determining the amount of protein deposition is described in detail by Sariri¹⁶⁵. To avoid error when making the measurements, (arising from the polymer absorption), a background reading was taken for the absorption values of a control piece of blank material prior to the measuring the spoilation value for the material. Each spoilation process was carried out on three individual samples and the results were taken as a mean value of three readings.

6.5.3 Results

Tables 6.2 - 6.5 show the quantities of protein deposited onto the range of polymers, together with the type and amount of charged monomer used.

Table 6.2 Quantities of protein deposited on HEMA-MAA copolymers

MAA /wt%	Protein deposited (mg/disk) \pm 0.002				
	Lysozyme	Albumin	Lactoferrin	Ferredoxin	Lactalbumin
0	0.062	0.032	0.021	0.029	0.025
1	0.311	0.034	0.194	0.032	0.027
2	0.412	0.038	0.223	0.033	0.028
3	0.435	0.043	0.263	0.034	0.028
4	0.482	0.046	0.282	0.035	0.028
5	0.493	0.046	0.297	0.036	0.029

Table 6.3 Quantities of protein deposited on HEMA-ITC copolymers

ITC / wt%	Protein deposited (mg/disk) \pm 0.002				
	Lysozyme	Albumin	Lactoferrin	Ferredoxin	Lactalbumin
0	0.060	0.034	0.021	0.026	0.026
1	0.145	0.042	0.098	0.023	0.024
2	0.342	0.049	0.264	0.021	0.022
3	0.446	0.054	0.286	0.019	0.020
4	0.496	0.067	0.298	0.018	0.018
5	0.562	0.069	0.301	0.017	0.019

Table 6.4 Quantities of protein deposited on HEMA-NVI copolymers

NVI / wt%	Protein deposited (mg/disk) \pm 0.002				
	Lysozyme	Albumin	Lactoferrin	Ferredoxin	Lactalbumin
0	0.065	0.030	0.021	0.025	0.024
1	0.068	0.032	0.021	0.028	0.028
2	0.054	0.031	0.018	0.029	0.029
3	0.046	0.028	0.017	0.034	0.031
4	0.042	0.026	0.012	0.038	0.041
5	0.040	0.026	0.009	0.041	0.042

Table 6.5 Quantities of protein deposited on HEMA-SPE copolymers

SPE / wt%	Protein deposited (mg/disk) \pm 0.002				
	Lysozyme	Albumin	Lactoferrin	Ferredoxin	Lactalbumin
0	0.063	0.032	0.023	0.024	0.024
1	0.065	0.032	0.045	0.026	0.027
2	0.062	0.033	0.047	0.027	0.029
3	0.057	0.035	0.049	0.027	0.029
4	0.054	0.036	0.052	0.029	0.030
5	0.054	0.036	0.055	0.031	0.032

The effect of the type and amount of charged monomer on the quantity of protein deposited on the series of HEMA copolymers is more clearly illustrated in Figures 6.13 - 6.16. Tables 6.2 - 6.5 are referred to in more detail in Section 6.6.1.

Figure 6.13 illustrates that the deposition of positively charged proteins increased when the proportion of the negatively charged methacrylic acid (MAA) increased whereas the negatively charged proteins, such as ferredoxin and lactalbumin, deposited to a lesser extent when the proportion of MAA increased. This was expected due to the electrostatic attraction of unlike charges and the electrostatic repulsion of like charges.

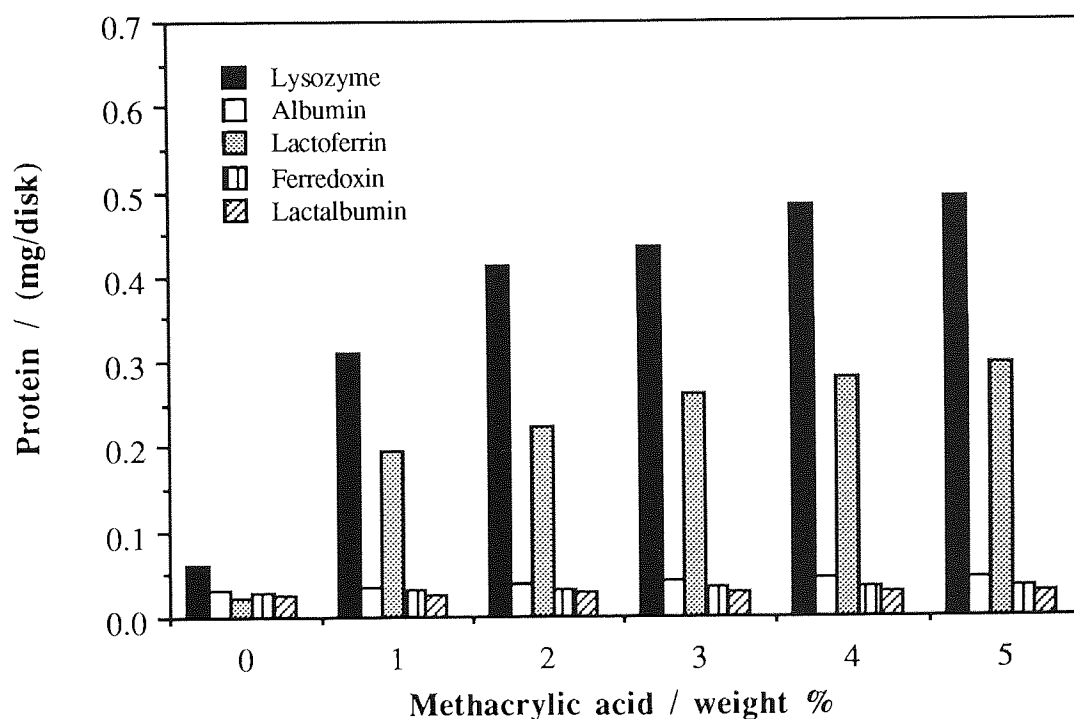


Figure 6.13 Effect of methacrylic acid content on the absorption of positively and negatively charged proteins to HEMA copolymers

Similarly, Figure 6.14 shows that the same trend was observed for copolymers containing the negatively charged itaconic acid (ITC). However, the quantities of positively charged proteins deposited are greater than those observed for the methacrylic acid copolymers. Also the quantities of negatively charged proteins were lower. A comparison between the

chemical structures of these two charged monomers, (illustrated in Chapter 2) shows that for every molecule of itaconic acid there are two carboxyl groups introduced into the copolymer whereas for every molecule of methacrylic acid, there is only one carboxyl group introduced. The itaconic acid copolymers will therefore contain a greater proportion of carboxylate anions at physiological pH and therefore a greater proportion of negative charge. This increase in the amount of negative charge increases the interaction of the copolymer with positively charged proteins and increases the repulsion with negatively charged proteins when compared to copolymers containing methacrylic acid.

These results support the significance of charge at the surface of a material and the influence it has upon protein interactions.

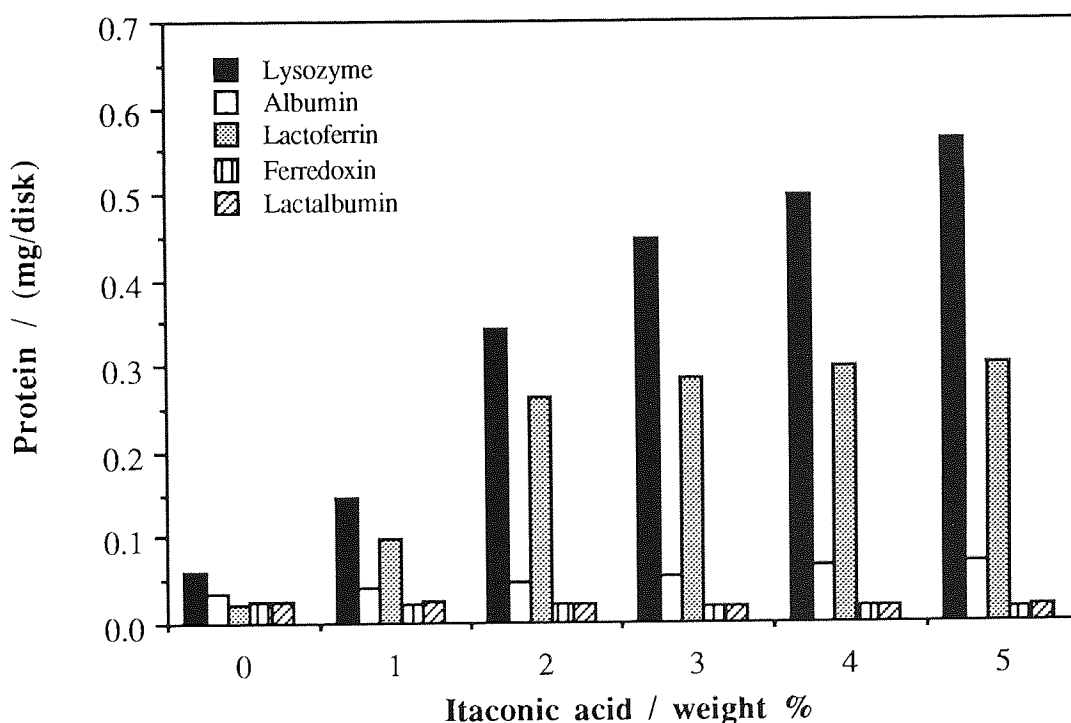


Figure 6.14 Effect of itaconic acid content on the uptake of positively and negatively charged proteins on HEMA copolymers

The significance of the type of charge on the quantities of protein deposited upon the copolymers is further reinforced by the use of positive charge in the form of N-vinyl

imidazole (NVI) and positive and negative charge present in N-(3-sulfopropyl)-N-methacryloxyethyl-N,N-dimethylammonium betaine (SPE).

It can be seen from Figure 6.15 that the N-vinyl imidazole containing copolymers showed a decrease in the absorption of positively charged proteins (such as lysozyme), but showed an increase in the absorption of negatively charged proteins (such as ferredoxin) when the proportion of charged monomer was increased. This situation was expected for a monomer which would be positively charged, because it is the opposite of the trend and type of interactions observed for polymers containing negative charge.

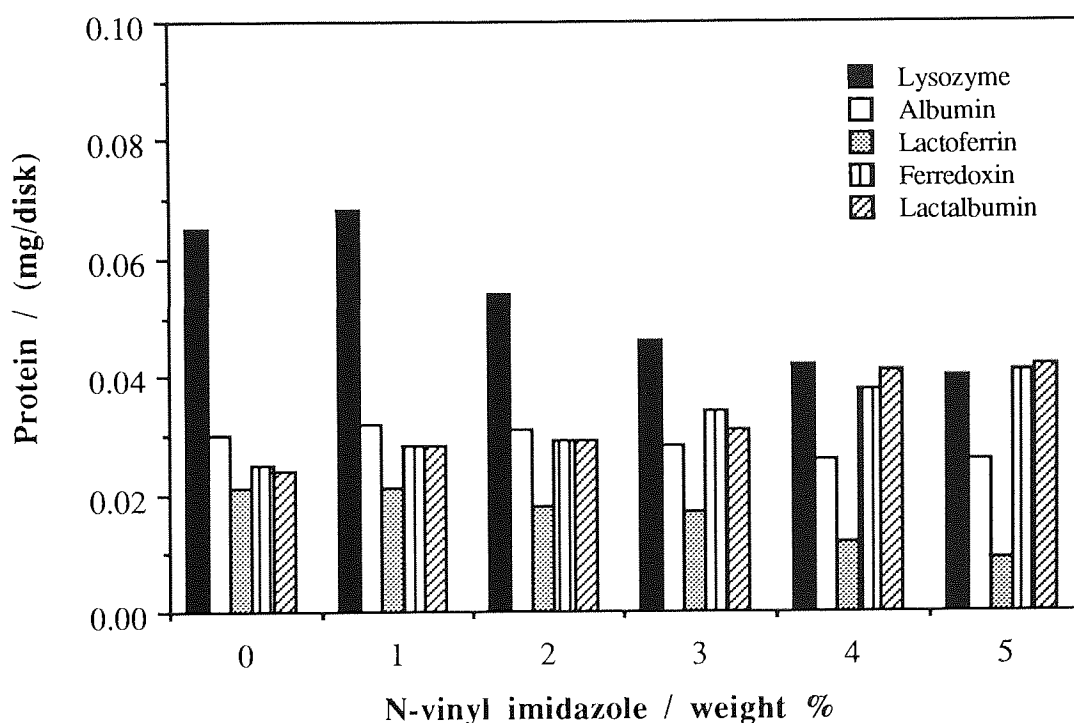


Figure 6.15 Effect of N-vinyl imidazole content on the uptake of positively and negatively charged proteins on HEMA copolymers

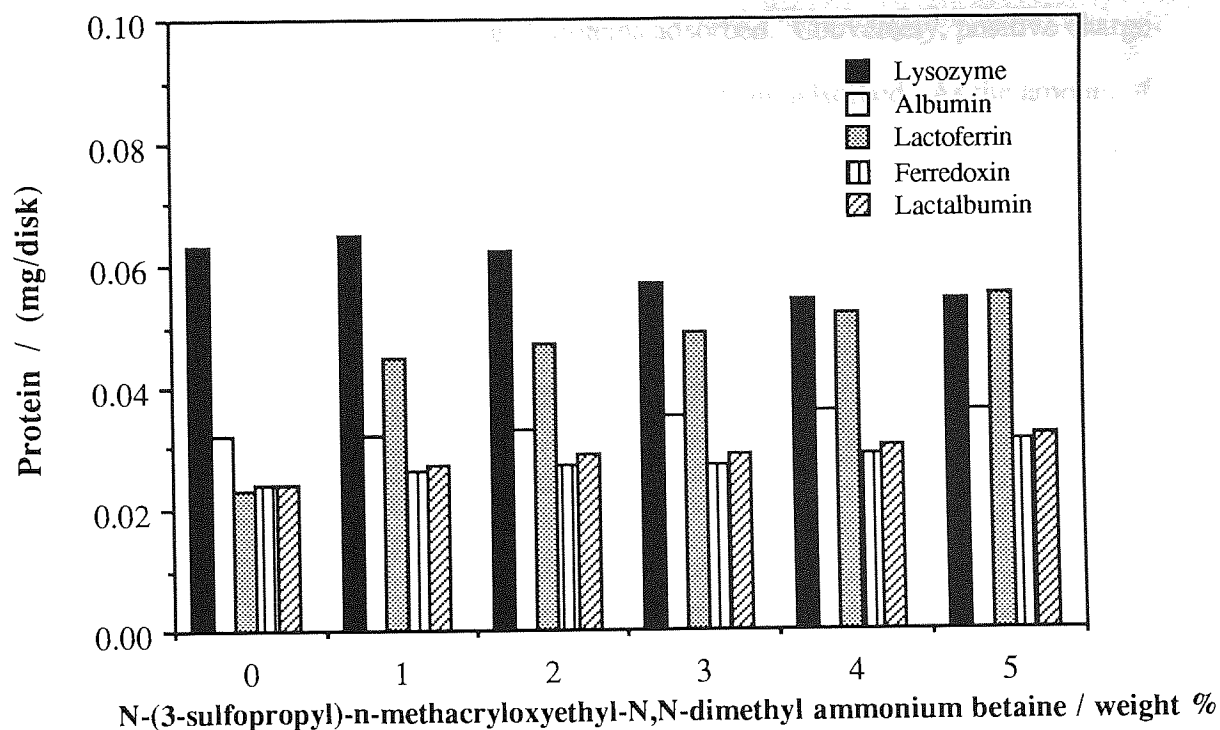


Figure 6.16 Effect of N-(3-sulfopropyl)-N-methacryloxyethyl-N,N-dimethyl ammonium betaine content on the uptake of positively and negatively charged proteins on HEMA copolymers

In the case of the N-(3-sulfopropyl)-N-methacryloxyethyl-N,N-dimethyl ammonium betaine containing copolymers its structure reveals (Chapter 2) that the monomer contains a zwitterionic structure possessing both a positive and negative charge. It might be expected therefore that the introduction of this monomer into a copolymer would reduce the adsorption of both negative and positively charged proteins. However, the results illustrated in Figure 6.16 show an increase in the adsorption of positive and negative charged proteins when the quantity of the charged monomer increased. This was because of the increasing amount of positive and negative charge within the copolymer.

6.5.4 Conclusions

The results presented in this work indicate that the interactions of HEMA copolymers with proteins may be significantly modified by copolymerisation with small amounts of charged monomers. The type and amount of charged monomer governs the type and quantity of

protein deposited upon the copolymer. It is evident from the results that negative charge increases the amount of positively charged proteins adsorbed. Conversely, positive charge increases the amount of negatively charged proteins which are adsorbed. As the amount of charge increases within the copolymer, the amount of adsorbed protein increases. Further support was provided by the incorporation of both negative and positive charge into the copolymer, which resulted in an increase in the amount of both positively and negatively charged proteins which were adsorbed.

6.6 The Effect of EWC on Protein Up-take

6.6.1 Introduction

With reference to the results in Tables 6.2 - 6.5, a comparison of the quantity of protein deposited onto the materials indicates that the copolymers containing methacrylic and itaconic acid (which are negatively charged), adsorb a greater quantity of protein than those containing the N-vinyl imidazole and the N-(3-sulfopropyl)-N-methacryloxyethyl-N,N-dimethylammonium betaine (which are positively charged). First indications would suggest that this difference was caused by the differences in the types of charge introduced in to the copolymer. However, when considering the interaction of a protein solution with a hydrated polymer network the EWC would be expected to have an effect on the protein uptake, because the water content affects the permeability of the polymer network and therefore the mobility of solute and solution that interact with the material. It was therefore necessary to study the effect of EWC for materials containing the same type and amount of charge.

6.6.2 Materials

To investigate this observation two sets of materials, which possessed the same type and amounts of methacrylic acid were prepared. However, the first set contained 1% of ethyleneglycol dimethacrylate (EGDMA) as opposed to 10% in the second set. It is well known that an increase in the crosslink density decreases the EWC⁹ because the mobility and the hydrophilicity of the network is decreased. With this in mind, the EWC's for the two sets of materials were obtained.

6.6.3 Results of the Effect of Crosslinker Concentration on the EWC of HEMA-MAA Copolymers

The results for the EWC's for the two sets of materials are shown in Table 6.6.

Table 6.6 Effect of composition on the EWC's of HEMA-MAA copolymers containing 1 and 10 weight% EGDMA

Methacrylic acid / weight%	EWC with 1% EGDMA / %	EWC with 10% EGDMA / %
0	35.1	18.1
1	42.3	30.1
2	52.2	33.4
3	59.7	35.4
4	63.2	37.2
5	67.3	39.3

6.6.4 Results of the Spoilation of the Copolymers Containing 1 and 10% weight% EGDMA

Disks of the hydrogel membranes containing the two levels of crosslinking agent were spoiled as described in Section 6.5.3 and the protein uptake was measured using the U.V absorption technique. The materials were allowed to incubate at room temperature, ($22\pm 2^{\circ}\text{C}$) over a time period of five days and were constantly shaken on a slow speed shaker.

The results obtained for the materials containing methacrylic acid and possessing 1% crosslinking agent are shown in Table 6.2 whilst those possessing 10% crosslinking agent are shown in Table 6.7.

Table 6.7 Quantities of protein deposited on HEMA-MAA copolymers with 10% crosslinking agent

MAA /wt%	Protein deposited (mg/disk) \pm 0.002				
	Lysozyme	Albumin	Lactoferrin	Ferredoxin	Lactalbumin
0	0.040	0.021	0.025	0.035	0.028
1	0.081	0.019	0.065	0.032	0.026
2	0.089	0.017	0.081	0.031	0.025
3	0.135	0.016	0.097	0.028	0.025
4	0.157	0.016	0.115	0.025	0.022
5	0.174	0.015	0.125	0.024	0.021

From Table 6.7 it is observed that protein adsorption exhibited the same trend as it did when 1% crosslinker was present. In effect, both sets of results show that there was an increase in the adsorption of positively charged protein and a decrease in the adsorption of negatively charged protein when the amount of negative charge within the copolymer structure was increased. However, the actual amounts of protein deposited were lower on the material of lower EWC.

Figures 6.17 and 6.18 show more clearly that when crosslinker concentration was increased (with a corresponding decrease in EWC) there is a reduction in the amount of the positively charged proteins adsorbed. This was due to the decrease in the network mobility and the decrease in the mobility of the proteins in and around the polymer network.

6.6.5 Conclusions

It was again evident that the inclusion of charge into a hydrogel polymer membrane modified its interaction with proteins. Control over the quantity and type of charge may optimise the preference for or against the absorption of negatively or positively charged proteins, however it must be noted that the EWC of the copolymers obtained by the inclusion of charged monomers affects the amount of adsorption that occurs.

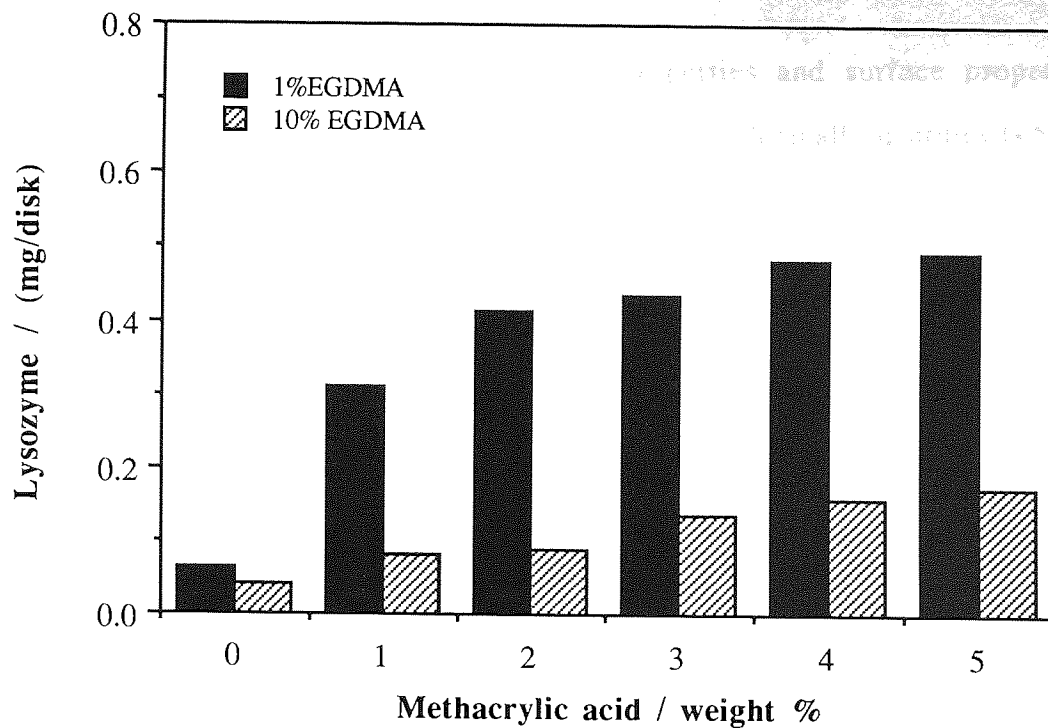


Figure 6.17 Effect of MAA content on lysozyme uptake with HEMA-MAA copolymers, at crosslinker concentrations of 1 and 10 weight%

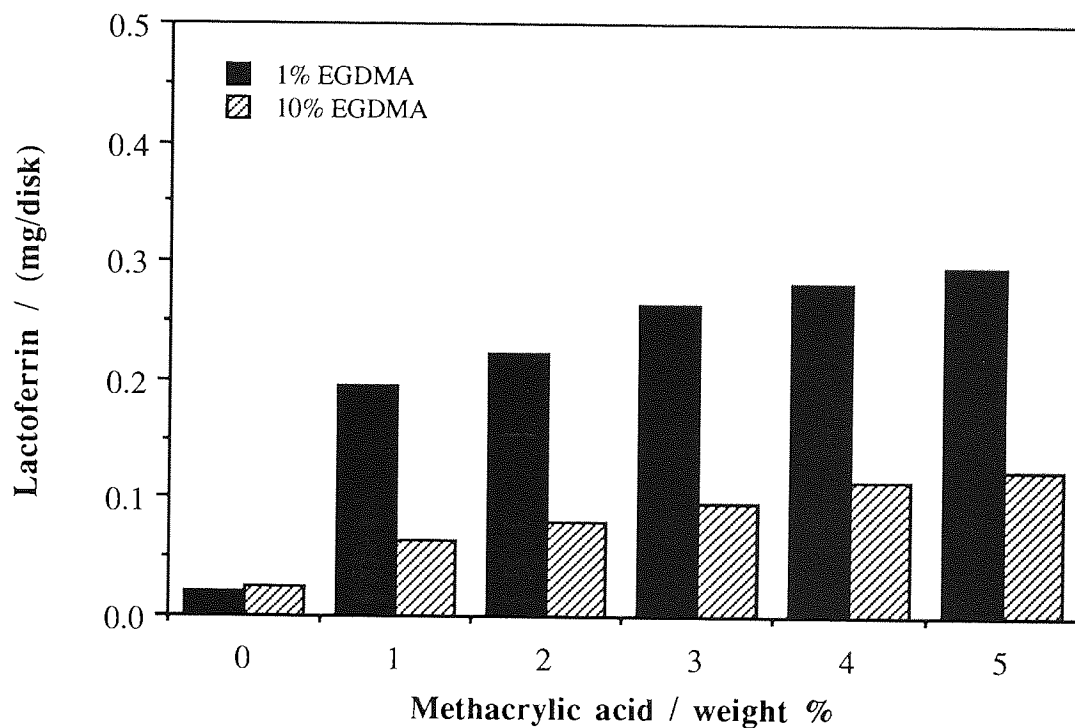


Figure 6.18 Effect of MAA content on lactoferrin uptake with HEMA-MAA copolymers, at crosslinker concentrations of 1 and 10 weight%

6.7 Summary

The water binding properties, mechanical properties and surface properties of poly(HEMA) hydrogel membranes may be modified with small quantities (<5%) of a charged monomer. In general, the effect of incorporating charge has two effects. The first is to increase the EWC, because of the increased polar nature of the material and the second is to decrease the the mechanical properties due to the plasticising effect of the imbibed water, although low levels (<5 weight%) of charged monomer have been shown to enhance the mechanical characteristics of the material by reducing the proportion of elastically ineffective chains.

The dehydrated surface properties are typical of the behaviour of hydroxyalkyl methacrylates; exhibiting polar group orientation towards the bulk of the polymer and hydrophobic group expression at the copolymer/air interface. However, this behaviour may be modified by the inclusion of monomers with pendant groups on both sides of the backbone, as backbone rotation still produces a polar group at the surface.

The hydrated surface properties were typical of polar group expression at the surface. Expression of the charged monomer at the surface governs the interaction of the materials with charged species such as proteins. The incorporation of negative charge into HEMA copolymers causes positively charged proteins (such as lysozyme) to be adsorbed to a greater degree, while the incorporation of positively charged monomers enhances the adsorption of negatively charged proteins to the surface of the copolymer. This type of behaviour enables hydrogel copolymers to be designed which preferentially adsorb proteins of a particular charge.

CHAPTER 7

Effect of Crosslinker Type and Concentration on the characteristics of Hydrogel Membranes

7.1 Introduction

Since the advent of hydrogels and the discovery of their potential biomedical properties, a wide range of hydrophilic polymers have been investigated for their suitability in biomedical applications. The degree of biotolerance of hydrogels has been attributed to their unique surface characteristics which impart upon them the ability to mimic the highly hydrated characteristics of natural tissue. The broad range of monomer systems available to the synthetic chemist makes these materials more versatile, because the proportion of imbibed water in the synthetic hydrogel may be controlled by its chemical composition. However, the major disadvantage of these materials is their relatively poor mechanical properties, particularly at high values of the equilibrium water content.

In Chapter 5 it was shown that the role of the sequence distribution of the comonomers affected the mechanical properties of the copolymer. Values for the mechanical properties well above those expected at high EWC's may be obtained by the production of hydrophobic blocks of one monomer type, which reinforce the mechanical properties of the network. This method of reinforcement has been widely used in commercial applications, but materials composed of large molecular domains of one chemical type are more prone to the deposition of biological species¹¹⁴. Consequently, alternative methods for increasing the mechanical strength include the formation of interpenetrating networks (IPNs) and to increase the amount of crosslinking monomer within the material. The lack of miscible monomers and polymers which can be used to form transparent interpenetrating networks which have a high EWC eliminates the use of this method for strength improvement at present. Increasing the amount of crosslinking monomer in the form of ethyleneglycol dimethacrylate (EGDMA) which is widely used, serves to increase the mechanical properties of the material and decrease the EWC, but has been shown to increase the amount of protein and lipid deposition onto the surface of hydrogel copolymers¹⁵⁴

Ethyleneglycol dimethacrylate (EGDMA) is essentially a polyether-type crosslinker, containing only one ethylene oxide repeat unit. The use of polyethers has been considered in attempting to reduce the amount of protein and lipid deposition (spoilation) which occurs on the surfaces of copolymers. Okano *et al* ¹⁶⁶ studied copolymers which contained microphases of polyethers and found that the microdomains controlled the thrombogenicity of the copolymers.

This chapter will investigate some possibilities for improving the mechanical properties of hydrogels by incorporating an increasing proportion of chemical crosslinking within them, whilst attempting to maintain the water content of the material. The effect that both the crosslinking monomers have on the surface properties of the hydrogel copolymers and the effect on the interaction of the copolymers with biological species will be considered.

The effects of increasing the length of the polyether chain of EGDMA in the form of poly(ethylene glycol) dimethacrylates 200, 400 and 1000, upon the water content and the mechanical and surface properties of hydrogel copolymers was studied and characterised. It was hoped that the incorporation of these more hydrophilic crosslinkers would not adversely affect the EWC, but would improve the mechanical properties of the material. It was also hoped that the use of the polyether crosslinkers would mimic the action of polyether microdomains; controlling the depositon of debris upon the surface. The latter was studied by interacting the copolymers with biological species. The reactivity of the crosslinkers was also considered in order to try and obtain some information regarding their efficiency in crosslinking. Two other crosslinkers were also studied; 2,4,6-triallyloxy-s-triazine (TAC) and N,N-diallyltartaramide (TAR). These were investigated because they have been shown to decrease cell adhesion to hydrogels, in comparison to the cell adhesion characteristics exhibited by EGDMA¹¹⁴.

7.2 Reactivity Of The Crosslinking Agents

7.2.1 Introduction

Ashraf¹¹⁴ examined the reactivity of crosslinking agents in terpolymers and quoted values for the reactivity of the first and second vinyl bonds of ethylene glycol dimethacrylate, 2,4,6-triallyloxy-s-triazine and N,N-diallyltartaramide with hydroxyethyl methacrylate and N-vinyl pyrrolidone. The values quoted by Ashraf for the reactivity of the 1st and 2nd vinyl groups of the crosslinking agent with 2-hydroxyethyl methacrylate are listed below

Table 7.1 Reactivity ratios of 1st and 2nd vinyl groups for HEMA:crosslinking agent copolymer system

Cross-linking agent	HEMA: crosslinker reactivity ratio			
	1st vinyl bond		2nd vinyl bond	
	r ₁	r ₂	r ₁	r ₂
ethylene glycol dimethacrylate	1.882	0.388	2.834	0.023
2,4,6-triallyloxy-s-triazine	9.670	0.065	74.750	0.013
N,N-diallyltartaramide	4.266	0.007	47.780	0.020

The reactivity of the crosslinking monomer is clearly important because the degree of conversion of the crosslinker and the number of effective crosslinks will affect the properties of the final network. Tian *et al*¹⁶⁷ examined the reactivity of ethylene glycol dimethacrylate in free radical bulk polymerisation. These workers discovered that the termination rate of crosslinking radicals (the 2nd vinyl group) was low and that as the ethylene glycol dimethacrylate concentration was increased, diffusion of the 2nd vinyl group, or macroradical as it may be considered, was hindered at high degrees of conversion. Examination of the electron spin resonance spectra (E.S.R.) for high conversion polymers gave signals which were characteristic of radical species. They concluded that many double bonds remained unreacted, because pendant double bonds were not able to diffuse through the dense polymer matrix and if such macroradicals were formed they would be unlikely to terminate. A comparison of the reactivities of the

crosslinkers used in this work provides an indication as to whether the crosslinkers were more or less efficient than EGDMA

7.2.2 Methods And Results

Sequence simulations using the quoted reactivity ratios for the reactivity of the 1st and 2nd vinyl groups of ethyleneglycol dimethacrylate (EGDMA), 2,4,6-triallyloxy-s-triazine (TAC) and N,N-diallyltartaramide (TAR) were obtained. Figures 7.1 - 7.6 illustrate the reactivity simulations for the polymerisation of 2-hydroxyethyl methacrylate with the 1st and 2nd vinyl groups of ethylene glycol dimethacrylate, 2,4,6-triallyloxy-s-triazine and N,N-diallyltartaramide respectively.

Many studies and review articles have examined the polymerisation of macromonomers¹⁶⁸⁻¹⁷⁷ and each has concluded that the copolymerisation rates significantly depended upon the chain length of the macromonomer. The general trend was that increasing the chain length revealed a corresponding decrease in the polymerisation rate which was due to steric hindrance caused by the macromonomer. Suzuki *et al*¹⁶⁸ copolymerised poly(ethylene glycol) macromonomers and observed that a marked decrease in the polymerisation rate occurred above 500 molecular weight due to the steric hindrance of the side chain.

Consequently, for the work in this investigation it was therefore assumed that the reactivity of the 200 and 400 dimethacrylates would be directly comparable with ethylene glycol dimethacrylate and that only the 1000 dimethacrylate would show a lower reactivity towards the copolymerisations. Suzuki *et al*¹⁶⁸ suggested that the polymerisation rate would be a thousand times less reactive for macromonomers with a molecular weight of a thousand or above and therefore it was considered that the 1000 dimethacrylate would be the most unreactive of the crosslinking systems studied.

It can be seen from Figures 7.1 - 7.6 that the reactivity of the crosslinking monomers at a loading of 10 mole% was very low compared with the reactivity of the HEMA monomer. Consumption of the crosslinker would appear to be as single units, but because of the low reactivities of the crosslinker, the HEMA monomer was consumed before the crosslinking monomer. This resulted in a terminal block of the crosslinker, even in the case of the more reactive 1st vinyl group of the crosslinker. For the second vinyl groups it was expected that the terminal block would consist of unreacted and radical vinyl groups which would be typical of the experimental crosslinking mechanism¹⁶⁸. However, it was expected that the use of comonomers with a lower reactivity than HEMA, (NVP for example) would result in more rapid consumption of the 1st vinyl group of the crosslinking monomer, that it would be distributed as single units and that the terminal block of unreacted and radical

2nd vinyl groups would be reduced. This characteristic was shown and discussed previously by Ashraf¹¹⁴.

The minimisation of unreacted crosslinks can be achieved by using low levels of crosslinking monomer. For example 1 mole% is the most widely used proportion, but this level of crosslinking results in the poor mechanical characteristics of high water content hydrogels.

The order of the reactivity of the crosslinking monomers used in this work decreased in the order EGDMA \geq PEG200DMA \geq PEG400DMA > TAC > TAR \geq PEG1000DMA. It might therefore be expected that the efficiency of crosslinking would follow the same order, which in turn would affect the mechanical properties of the copolymers produced. The degree of crosslinker inefficiency would adversely affect the properties of the hydrogel copolymers because the less efficient the degree of crosslinking the lower the mechanical properties. It was anticipated that by increasing the amounts of the crosslinking monomers studied, improvement or maintenance of both the mechanical characteristics and the EWC of the hydrogels could be obtained and that at increased proportions of crosslinking monomer, these properties would not be adversely affected by their relatively low radical reactivities compared to EGDMA.

7.3 Effect Of Amount And Nature Of Crosslinking Monomer On The Equilibrium Water Content (EWC) Of HEMA Copolymers

7.3.1 Materials And Methods

Hydrogel copolymer membranes were prepared from 2-hydroxyethyl methacrylate with increasing proportions of one of the crosslinking monomers. A series of HEMA copolymers were made for each of the crosslinkers. The resultant membranes were hydrated and their EWC's characterised.

7.3.2 Results

Table 7.2 below shows the results for the range of compositions studied:-

Table 7.2 Effect of crosslinker type and concentration on the EWC of HEMA copolymers

Wt % of crosslink	Equilibrium Water Content / %					
	EGDMA	PEG200 DMA	PEG400 DMA	PEG1000 DMA	TAC	TAR
1.0	35.1	37.6	38.6	39.8	39.9	41.3
2.5	34.7	36.5	37.3	40.6	38.7	-
5.0	33.0	35.3	37.0	41.4	38.0	-
7.5	29.6	31.9	36.7	41.8	37.2	-
10.0	27.9	29.7	34.7	42.3	36.7	-

The effects of increasing the concentration of EGDMA, PEG200DMA, PEG400DMA and TAC was to decrease the EWC and are more clearly illustrated in Figure 7.7.

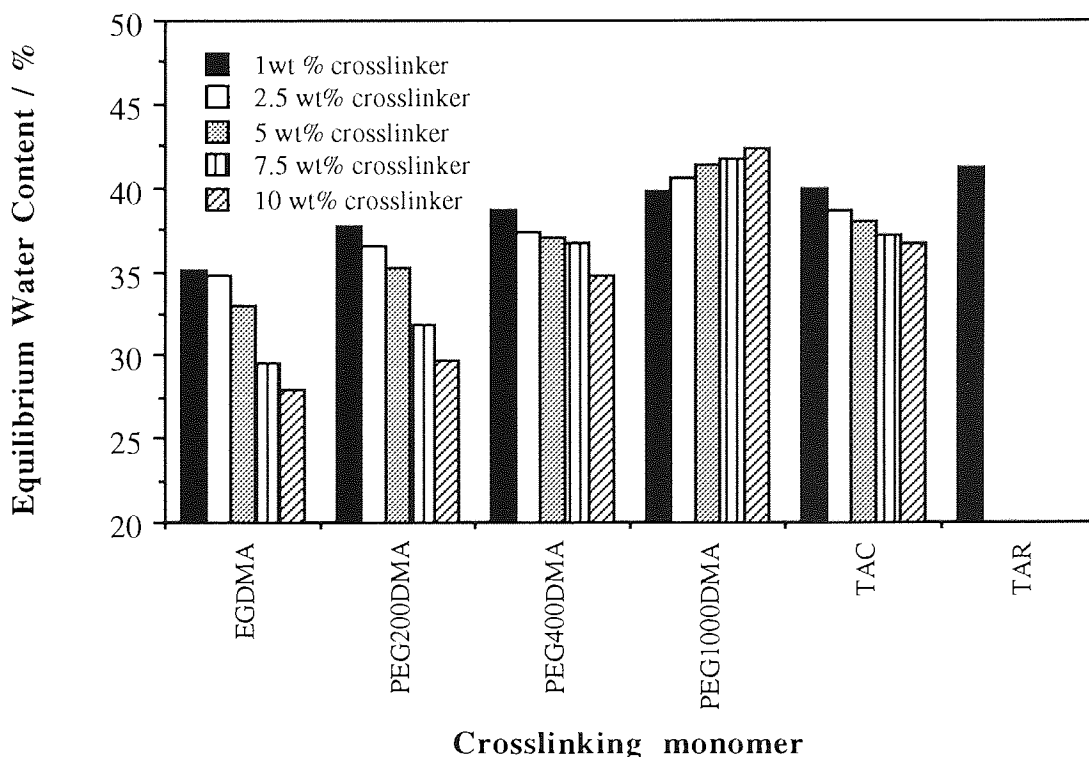


Figure 7.7 Effect of the nature and proportion of the crosslinking monomer on the EWC of HEMA copolymers

This observed decrease in EWC was expected because increasing the crosslink density of the network decreases the mobility and hydrophilicity of the network structure. Therefore, the free volume of the network available for water binding was decreased. This steric exclusion effect is not offset by the increased hydrophilicity of the crosslinker.

However, for PEG1000DMA the EWC increased proportionally with crosslinker concentration. This may have been due to the fact that the increase in the number of crosslinks was compensated for by the length and hydrophilicity of the polyether chain between the crosslinker end groups. However, it may also have been due to the low reactivity of PEG1000DMA which may have resulted in a large number of ineffective crosslinks; therefore the network mobility was not decreased with the corresponding increase in crosslinker concentration. The resulting effect is that the copolymer behaves like one which contains a proportion of monocapped polyether, such as those characterised in Chapter 8. If this was the case then the expected behaviour of the PEG1000DMA copolymers would be to display the same trends in EWC and mechanical properties as those systems containing a monocapped polyether. There was an inability to investigate the properties of the TAR crosslinker as its solubility in HEMA was found to be limited to 1 weight%.

Comparison of the EWC's of the HEMA copolymers containing 1 weight% of the crosslinkers shows that they increased in the order EGDMA < PEG200DMA < PEG400DMA < PEG1000DMA < TAC < TAR. The ethylene glycol derivatives would be expected to show this order because of their increasing chain length. TAC and TAR would be expected to be more hydrophilic than EGDMA because of the greater number of hydrophilic elements within their compositions.

7.3.3 Conclusions

For each of the crosslinking systems except PEG1000DMA, the EWC decreased as increasing amounts of crosslinking monomer were used because the network mobility and overall hydrophilicity of the network was decreased.

Increasing the amount of PEG1000DMA resulted in an increase in the EWC. This may have been due to the low reactivity of the 2nd vinyl group which results in the crosslinker behaving as a monocapped polyether; monocapped linear polyethers have been shown to increase the EWC of HEMA copolymers¹⁵⁴.

It was therefore necessary to investigate the mechanical properties of the copolymers in order to determine the mechanical integrity of the crosslinked systems.

7.4 Effect Of Crosslinker Type And Concentration On The Mechanical Properties Of HEMA Copolymers

7.4.1 Materials And Methods

The mechanical properties of the hydrated HEMA-crosslinker copolymer hydrogels were obtained using the tensile method described in Chapter 2. The results obtained are shown in Tables 7.3 - 7.8.

7.4.2 Results

Table 7.3 shows the effect of increasing the concentration of ethylene glycol dimethacrylate crosslinker. It can be seen that when the concentration was increased (EDMA/weight), the elastic modulus (E_m) and tensile strength (T_s) also increased, whilst the elongation at break (E_b) decreased. This was because the increasing proportion of crosslinker decreased the molecular weight of the polymer backbone between crosslinks, which in turn increased the crosslink density and therefore the retractive force between the polymer chains. The result was the formation of a stiffer, less elastic copolymer. This effect of increasing the crosslink density and decreasing the EWC was previously studied

by Raab and Janacek¹⁷⁸ who investigated the effect of increasing the ethylene glycol dimethacrylate concentration in poly (HEMA).

Table 7.3 Effect of proportion of EGDMA upon the mechanical properties of HEMA copolymers

EDMA / weight %	Em / MPa	Ts / MPa	Eb / %
1.0	0.654	0.726	133
2.5	0.838	0.766	109
5.0	1.654	1.310	87
7.5	3.410	2.210	76
10.0	7.740	4.230	69

Table 7.4 shows the effect of increasing the concentration of poly(ethylene glycol) 200 dimethacrylate on the mechanical properties of poly (HEMA).

Table 7.4 Effect of proportion of PEG200DMA upon the mechanical properties of HEMA copolymers

PEG200DMA / weight%	Em / MPa	Ts / MPa	Eb / %
1.0	0.500	0.790	186
2.5	0.670	0.800	151
5.0	1.120	0.910	73
7.5	1.980	1.010	56
10.0	3.180	1.480	52

The same trend was observed as for ethyleneglycol dimethacrylate incorporation; similarly the increase in elastic modulus (Em) and tensile strength (Ts) and the decrease in elongation at break (Eb) was explained by the increase in retractive force between the polymer chains. A comparison of equivalent weight percents of ethylene glycol dimethacrylate and poly(ethylene glycol) 200 dimethacrylate revealed that the poly(ethylene glycol) 200 dimethacrylate copolymers had lower values of elastic modulus (Em) and

tensile strength (Ts). This was due to the increased length of the crosslink in the PEG200DMA compared to EGDMA which resulted in a decreased retractive force achieved by the crosslinks between the polymer chains.

Table 7.5 contains the results for the HEMA-poly(ethylene glycol) 400 dimethacrylate copolymers. These results show the same trend as for the previous two copolymers; a resultant increase in elastic modulus (Em) and tensile strength (Ts) when the amount of crosslinker was increased. This was also due to the corresponding increase in retractive force between the polymer chains. However, once again the effect of crosslink chain extension was to reduce the order of magnitude of the retractive force achieved by the crosslinking monomer.

Table 7.5 Effect of proportion of PEG400DMA upon the mechanical properties of HEMA copolymers

PEG400DMA / weight%	Em / MPa	Ts / MPa	Eb / %
1.0	0.490	0.617	196
2.5	0.543	0.786	153
5.0	0.835	0.915	127
7.5	1.174	0.680	69
10.0	1.428	0.864	69

Table 7.6 shows the effect of a further increase in the length of the crosslink with the incorporation of poly(ethylene glycol) 1000 dimethacrylate. When the amount of crosslinking monomer was increased, the expected increase in elastic modulus (Em) and tensile strength (Ts) were observed, but to a much lesser extent than for the previous copolymers. This was because of the increased length of the crosslink.

If only one vinyl group had been incorporated into the material (because of the low reactivity of the crosslinker), then the effect of the PEG1000DMA would have been expected to parallel the behaviour of monocapped linear polyethers. This is not the case.

Indeed, the results shown in Table 7.6 suggest that both vinyl groups of the PEG1000DMA were incorporated, with some degree of efficiency. The hydrogels showed an increase in mechanical properties which was associated with an increase in the amount of crosslinker.

Table 7.6 Effect of proportion of PEG1000DMA upon the mechanical properties of HEMA copolymers

PEG1000DMA / weight%	Em / MPa	Ts / MPa	Eb / %
1.0	0.350	0.608	252
2.5	0.454	0.631	186
5.0	0.618	0.721	159
7.5	0.752	0.733	119
10.0	0.917	0.819	90

Tables 7.7 and 7.8 show the result of incorporating a nitrogen-containing ring structure and an amide-containing crosslinking monomer into the material.

Table 7.7 Effect of proportion of TAC upon the mechanical properties of HEMA copolymers

TAC / weight%	Em / MPa	Ts / MPa	Eb / %
1.0	0.276	0.874	514
2.5	0.331	0.862	478
5.0	0.451	0.907	449
7.5	0.596	0.956	416
10.0	0.674	0.924	379

Table 7.8 Effect of TAR incorporation on the mechanical properties of HEMA copolymers

TAR / weight%	Em / MPa	Ts / MPa	Eb / %
1.0	0.333	0.887	599

For the TAC the expected increases in elastic modulus (E_m) and tensile strength (T_s) were observed, but it was noted that this was to a lesser extent than for poly(ethylene oxide)-type crosslinkers. The most significant difference between the effects observed with this type of material was the increase in elongation at break (E_b) when comparable weight percents of crosslinker were used; for example TAC and EGDMA. This can be explained, since with the nitrogen-based system there would be a large increase in electrostatic interaction between the polymer chains compared to one containing oxygen alone. This effect was also observed for the TAR crosslinking monomer. However, investigations into the effect of crosslinker concentration for this monomer were not permitted due to its limited solubility in HEMA.

7.4.3 Conclusions

In general, increases in the crosslinking monomer concentration were associated with a corresponding increase in the elastic modulus and tensile strength of the HEMA copolymers, but a decrease in the elongation at break. This is attributed to an increase in the crosslink density and therefore an increase in the retractive force between the polymer chains. Consequently, these characteristics manifest as a stiffer, less flexible hydrogel.

Cross-linkers of the same chemical type, but with increasing crosslink chain lengths have a different effect upon the magnitude of the retractive force. This applied when equal amounts of crosslinker were used with the result that as the chain length increased, the retractive force decreased. As a consequence of this, a smaller increase in the mechanical properties was observed when the chain lengths increased. For almost all the copolymers, an increase in the crosslink density improved the mechanical properties and decreased the EWC. The exceptions to this were those copolymers containing poly(ethylene glycol) 1000 dimethacrylate. This result therefore enables the mechanical properties of the hydrogel to be enhanced without decreasing the EWC. The hydrophilic component of the crosslink also played a role in the effects upon the mechanical properties and EWC of the copolymers. When the hydrophilic chain length was increased to a minimum polyether

chain length of approximately 20 ethylene oxide units an increase in the amount of crosslinking monomer produced an increase in both these properties. This was achieved by the use of a crosslinker which was sufficiently hydrophilic to offset the decrease in network mobility attained by the increased amount of crosslinking monomer, in this case PEG1000DMA. This effect of increasing the mechanical properties while increasing the mechanical properties is more clearly illustrated in Figure 7.8 which shows the elastic modulus (E_m) versus equilibrium water content (EWC).

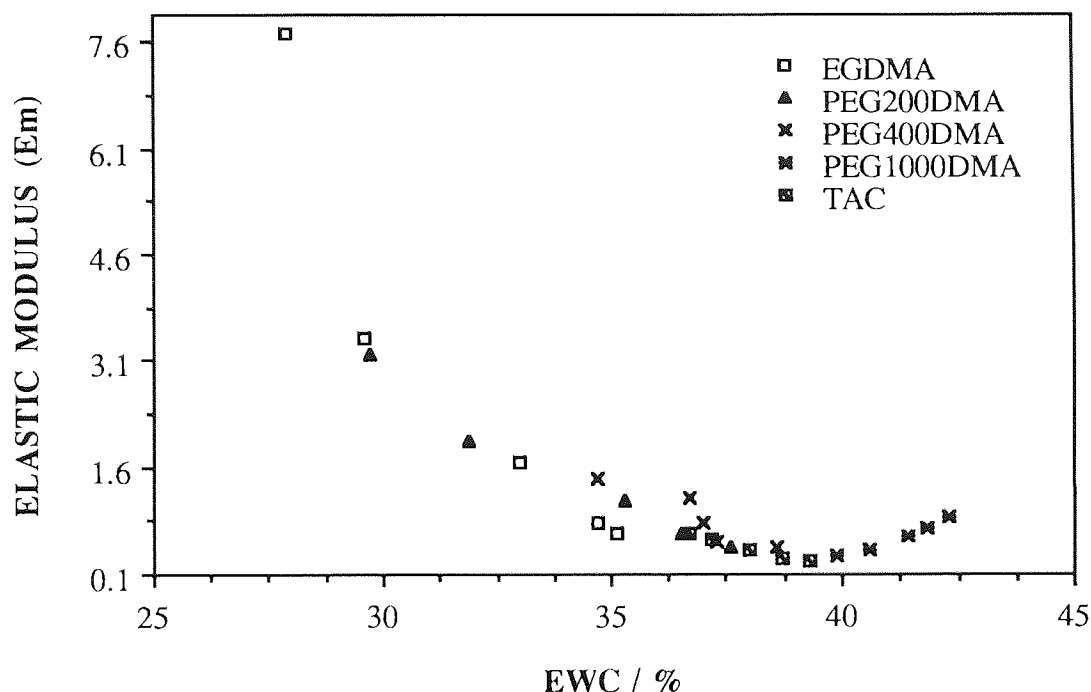


Figure 7.8 Variation in E_m and EWC for the HEMA copolymers with the series of crosslinkers studied

Only the PEG1000DMA copolymers exhibit the trend for increasing water content and tensile strength. For the mechanical properties of the copolymers containing increasing amounts of PEG1000DMA, these increases suggest that both vinyl groups were polymerised, thereby causing the crosslinker to be incorporated effectively. If this was not the case and the PEG1000DMA was acting like a monocapped poly(ethylene oxide) then an expected decrease in tensile properties with increasing EWC might have been exhibited as there would have been insufficient crosslinks to hold the network together.

7.5 Effect Of Crosslinking Monomer Concentration And Type On The Surface Properties Of HEMA Hydrogels

7.5.1 Introduction

The surface properties of the hydrogels are also an important area for study. This is because many biomedical applications, for example contact lenses, require the hydrogel surface to be in intimate contact with biological fluids. Consequently, the nature of the hydrogel surface and the biological environment govern whatever chemical and physical processes occur at the interface between the two.

7.5.2 Materials And Methods

Hydrogel membranes were used which contained increasing amounts of the polyether crosslinking monomers outlined in the previous sections. The surface properties of these materials were determined in their hydrated state using the Hamilton and captive air bubble contact angle techniques described in Chapter 2.

The polar and dispersive components of the surface free energies were plotted against the EWC to provide an indication of the contribution of the polymer structure and the imbibed water to the surface energy of the hydrogels studied.

7.5.3 Results

Figure 7.9 gives the change in polar and dispersive components of the surface energy as a function of the equilibrium water content (EWC). The polar and dispersive components are due to the water and the polymer structure of the hydrated HEMA-EGDMA copolymers. It was shown in Table 7.3 that increasing the EGDMA concentration decreased the EWC of the HEMA copolymers. It can be seen in Figure 7.9 that as the EWC decreased the polar component of the surface energy due to the polymer was decreased, whereas the dispersive component of the surface energy due to the polymer increased. The observed decrease in the polar component and increase in the dispersive component is due to the increased hydrophobicity of the HEMA copolymers. The increase in hydrophobicity corresponds to the increase in the amount of EGDMA within the copolymer. The incorporation of increasing amounts of EGDMA decreased the EWC of the copolymers and evidently decreases the polar component of the surface energy of the polymer and increases the dispersive component of the polymer.

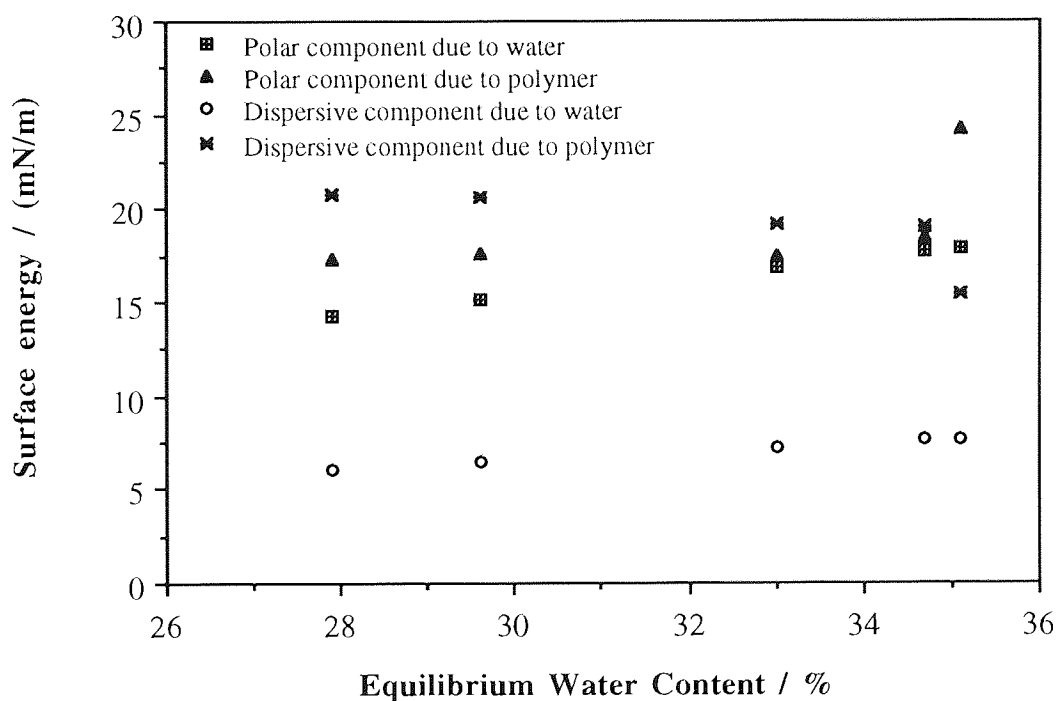


Figure 7.9 The polar and dispersive components of the surface energy due to water and the polymer structure of hydrated HEMA-EGDMA copolymers

Figure 7.10 shows the change in polar and dispersive components of the surface energies as a function of the equilibrium water content (EWC). It was shown in Table 7.3 that increasing the concentration of PEG200DMA decreased the EWC of the HEMA copolymers, but this decrease was to a lesser extent than those copolymers containing EGDMA. It can be seen in Figure 7.10 that as the EWC decreased the polar component of the surface energy due to the polymer was decreased, whereas the dispersive component of the surface energy due to the polymer was increased. The observed changes in the polar and dispersive components was due to the increased hydrophobicity of the HEMA copolymers. The increase in hydrophobicity corresponded to the increase in the amount of PEG200DMA within the copolymer. The results are evidence that the incorporation of increasing amounts of PEG200DMA decreased the polar component of the surface energy of the polymer and increased the dispersive component of the polymer of the HEMA copolymers.

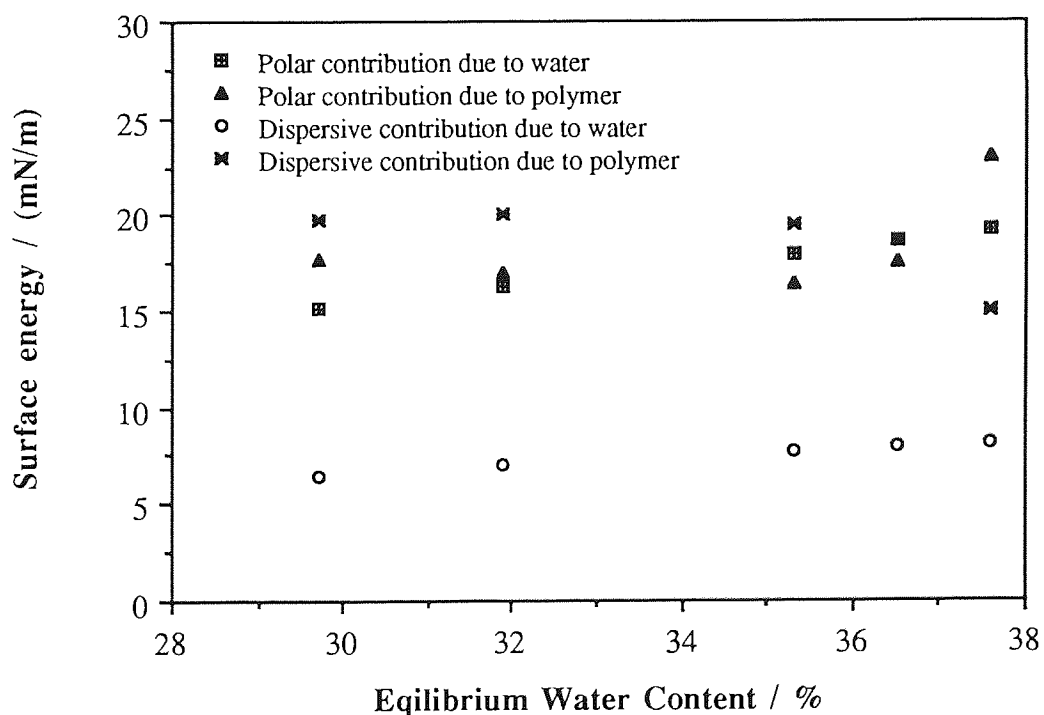


Figure 7.10 The polar and dispersive components of the surface energy due to water and the polymer structure of hydrated HEMA-PEG200DMA copolymers

Figure 7.11 illustrates the change in polar and dispersive components of the surface energies as a function of the EWC for the series of HEMA-PEG400DMA copolymers. As was the case for the HEMA-EGDMA and HEMA-PEG200DMA copolymers increasing the proportion of crosslinking monomer decreased the EWC. This was due to the hydrophobic character of the crosslinking monomer. It can be seen in Figure 7.11 that as the EWC decreased the polar component of the surface energy due to the polymer was decreased, whereas the dispersive component of the surface energy due to the polymer was increased. This was due to the increased hydrophobicity of the HEMA-PEG400DMA copolymers. The increase in hydrophobicity corresponded to the increase in the amount of PEG400DMA within the copolymer. It is therefore reasonable to assume that the incorporation of increasing amounts of PEG400DMA decreased the polar component of the surface energy of the polymer and increased the dispersive component of the polymer of the HEMA-PEG400DMA copolymers.

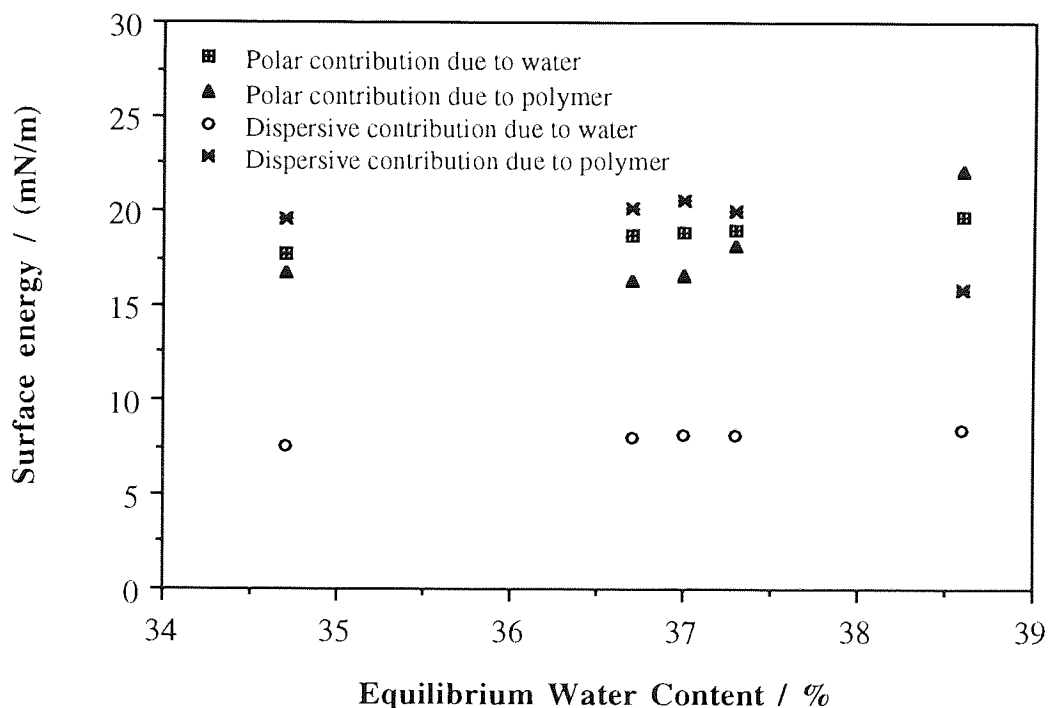


Figure 7.11 The polar and dispersive components of the surface energy due to water and the polymer structure of hydrated HEMA-PEG400DMA copolymers

Figure 7.12 shows the change in polar and dispersive components of the surface energies as a function of the equilibrium water content (EWC) for the series of HEMA-PEG1000DMA copolymers. It was shown previously in this work that increasing the concentration of PEG1000DMA increased the EWC of the HEMA copolymers. It can be seen in Figure 7.12 that as the EWC increased the polar component of the surface energy due to the polymer was increased, whereas the dispersive component of the surface energy due to the polymer was decreased. These observed changes in the polar and dispersive components were due to the increased hydrophilicity of the HEMA copolymers. The increase in hydrophilicity corresponded to the increase in the amount of PEG1000DMA within the copolymer. Previous results showed that increased amounts of PEG1000DMA increased the mechanical properties of the HEMA copolymers. The results presented here show that the polar component of the surface energy increased with increased EWC which corresponds to increased mechanical properties.

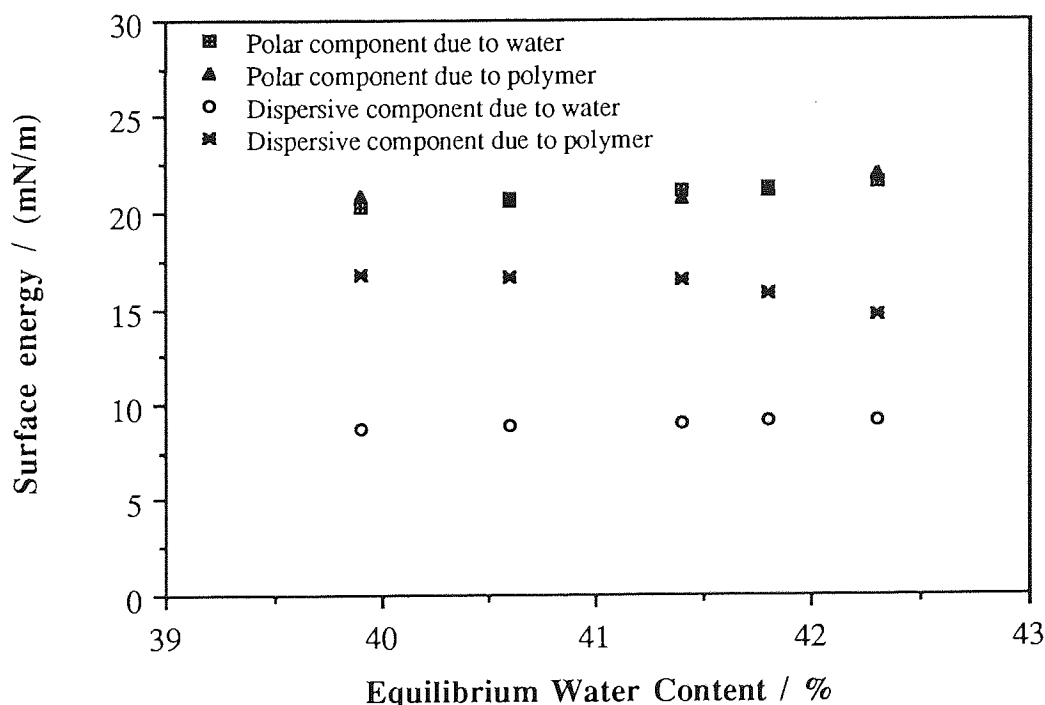


Figure 7.12 The polar and dispersive components of the surface energy due to water and the polymer structure of hydrated HEMA-PEG1000DMA copolymers

Figure 7.13 shows the change in polar and dispersive components of the surface energies as a function of the EWC for the HEMA-TAC copolymers. It was shown in Table 7.3 that increasing the concentration of TAC decreased the EWC of the HEMA copolymers this was due to the hydrophobicity of the crosslinker. It can be seen in Figure 7.12 that as the EWC decreased the polar component of the surface energy due to the polymer was decreased, whereas the dispersive component of the surface energy due to the polymer increased. This was because the hydrophobicity of the HEMA copolymers was increased with increased amounts of the crosslinker, TAC. As the proportion of TAC in the copolymer was increased, which corresponded to a decrease in the EWC, the polymer structure was dominated by dispersive forces.

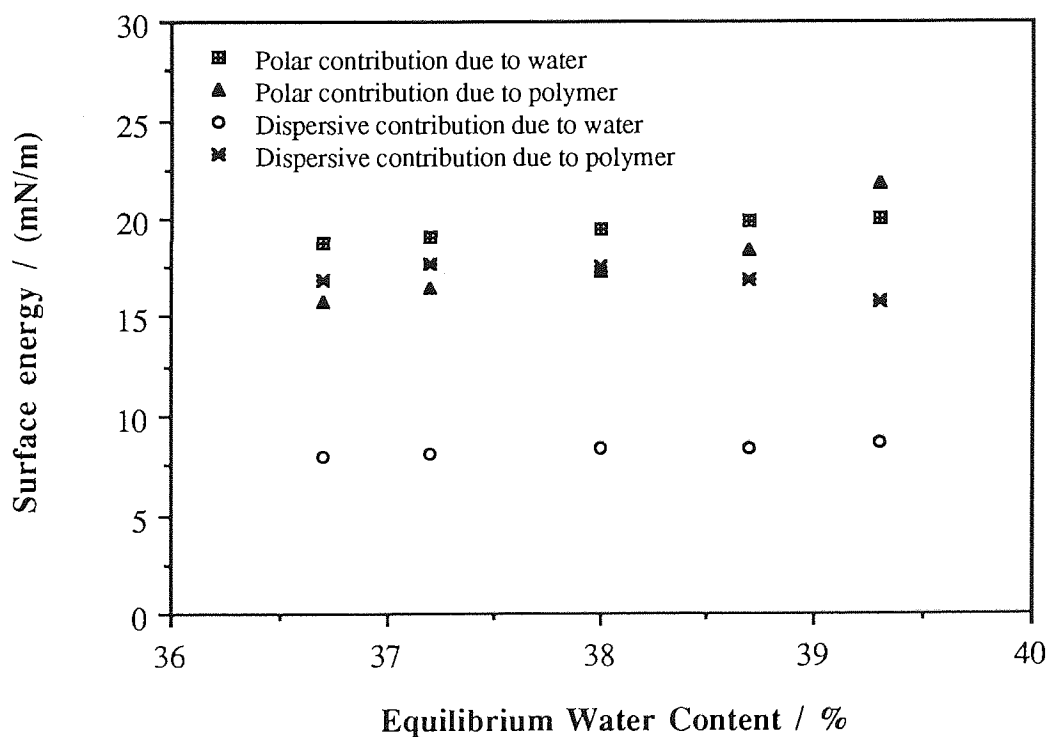


Figure 7.13 The polar and dispersive components of the surface energy due to water and the polymer structure of hydrated HEMA-TAC copolymers

7.5.4 Conclusions

In summary, Figures 7.9 - 7.13 show that the polar components of the surface energy increased and the dispersive components decreased with increasing EWC. This was due to the increased hydrophilicity of the copolymers. However, for the HEMA-PEG1000DMA copolymers these observed trends corresponded to increased proportions of the crosslinking monomer.

The results presented in this Chapter show that for HEMA-EGDMA copolymers the EWC decreased, the mechanical properties increased and the copolymer became less polar with increasing amounts of EGDMA. However, increasing the length of the crosslink and the hydrophilicity of the crosslinker by using longer chain polyethylene oxides which are known to be hydrophilic, to a crosslink length of 20 ethylene oxide repeat units, it was possible to enhance the mechanical properties of the copolymers studied, at the same time increasing the EWC and the polar component of the surface energy.

Work has shown that surfaces which become less polar are more prone to deposition of biological species. To be able to maintain the polar component of the surface energy the interactions with biological species would not be expected to be adversely affected.

7.6 Ion Permeability of Poly(ethylene oxide) Crosslinked Hydrogel Copolymers

7.6.1 Introduction

Studies in the ocular environment have indicated that calcium plays a significant role in the formation of discrete elevated deposits¹⁷⁹ and the formation of white surface film deposits¹⁸⁰ on hydrogel contact lenses.

Linear polyethers are well known for their ability to complex with alkali and alkaline earth metal cations such as calcium. It was necessary therefore, to study the interaction of salts containing group I and II ions, to detect whether the polyether crosslinkers used in this

work would interact with cations, particularly group II metal cations such as calcium and magnesium, because this may lead to biointolerance in the biological environment.

The effect of linear monocapped polyethers on the transport of group I and II metal ions through hydrogels containing polyethers has been studied in detail by Oxley¹⁵⁴. Oxley examined the effect of monocapped polyethers of different chain lengths on cation transport. It was found that the longer chain polyethers with greater than 10 ethylene oxide repeat units interacted with calcium ions and it was concluded that the complexation of the cation by the polyether occurred at the free chain end of the polyether. This was because complexation at the chain end attached to the polymer backbone was sterically hindered by the backbone.

In this investigation it was expected that using polyethers as crosslinking monomers the complexation of a cation with the free chain end of a polyether would be eliminated and complexation should not occur because of the restricted polyether chain mobility. Consequently the ion permeability of HEMA-PEGDMA crosslinker membranes at 90:10 weight% proportions respectively, were studied in order to detect whether ion permeability was hindered by interaction with the polyether crosslinkers used.

7.6.2 Materials And Methods

The materials studied were the HEMA membranes containing 10 weight% of the polyether crosslinkers which were polymerised by the method described in Chapter 2. The permeability of different ions was measured using three separate salt solutions, NaCl, MgCl₂ and CaCl₂.

The permeability studies were performed using the method described in Chapter 2. Hydrated circular membranes of equal thickness were placed in the centre of the two-compartment cell. The paddles were stirred at the surface of the membrane to prevent a stagnant layer of charged species and the cell was placed into a 37°C water bath. One side

of the cell was filled with deionized water and the other side with one of the three salt solutions at a 0.25M concentration. The study was timed from the introduction of the solutions into the cell. The concentration of the permeant species was analysed by conductivity. This was achieved by connecting a conductivity flow-through cell on the deionized water side of the two-compartment cell. This enabled the ion concentration to be measured at 30 minute intervals. A conductivity and ion concentration calibration graph was obtained by measuring the conductivity of metal chlorides at concentrations from 1 μ M to 0.25 M.

7.6.3 Results

Figure 7.14 shows the transport data obtained for the permeation of NaCl across the HEMA membranes which contained 10 weight% of the polyether dimethacrylates. Data was obtained for each of the polyether crosslinkers used. The data presented earlier in this Chapter shows that the EWC of the HEMA-polyether membranes increased when the polyether crosslink chain length increased. Previous work has shown that ion transport is enhanced by increasing the water content^{181, 182}. Therefore for the NaCl solution, if no complexation of the Na occurred it would be expected that the permeation of NaCl would be enhanced by the increased crosslink length. This enhancement of the ion permeability with increasing polyether chain length is observed in Figure 7.13. The permeability increased linearly with time and therefore the permeability coefficients may be calculated from the gradients of the graph. The values obtained for the permeability coefficients, (P), for the permeation of NaCl, MgCl₂ and CaCl₂ across the polyether crosslinked membranes are presented in Table 7.9

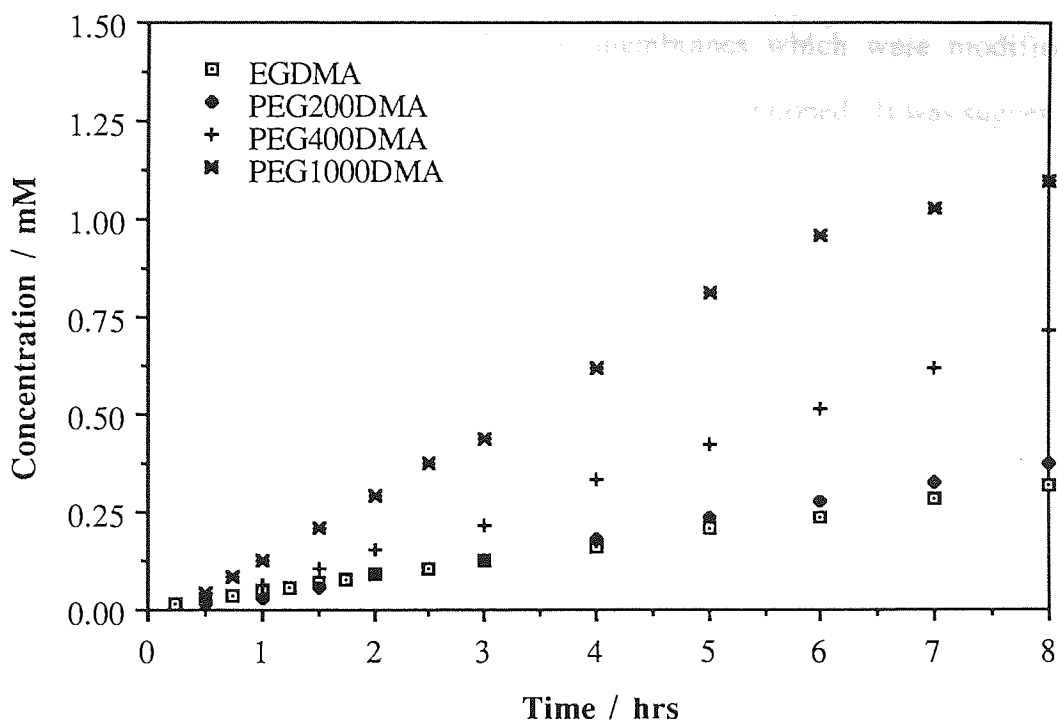


Figure 7.14 Effect of poly(ethylene oxide) crosslink chain length on the permeation of NaCl across a HEMA membrane

Figure 7.14 shows that the amount of permeation of NaCl across the polyether modified HEMA membranes increased when the polyether chain length was increased. This increase in the amount of permeation was reflected in the magnitude of the permeability coefficients obtained for NaCl transport across the hydrogel materials. Complexation of the cations with the polyethers would be expected to produce a suppression of the ion permeability and a decrease in the permeability coefficient because the ions would not permeate through the membrane because of interaction with the polyethers.

As an increase in the polyether chain length increased the equilibrium water of the polyether modified copolymers, as shown in Table 7.3 it might be expected that there is a relationship between the water content and the permeability coefficient. This theory would correspond with observations in the published literature^{181, 182} and was considered more closely later in this Chapter.

Suppression in ion permeability was observed by Oxley¹⁵⁴ who studied the transport of group I and II metal salts across HEMA membranes which were modified with monomethacrylate poly(ethylene oxides) as previously mentioned. It was suggested that complexation occurred at the free poly(ethylene oxide) chain end. This suggestion corresponds with the results presented in this Chapter, because for the materials used in the work here both chain ends of the polyether were incorporated into the polymer backbone by crosslinking and complexation of the metal cations by the polyether chains did not occur.

Table 7.9 Effect of polyether crosslink chain length on the permeability coefficients, P, for the permeation of 0.25M solutions of NaCl, MgCl₂ and CaCl₂ across crosslinked HEMA membranes

Membrane Composition	EWC / %	P x 10 ⁸ / cm ² s ⁻¹		
		NaCl	MgCl ₂	CaCl ₂
HEMA-EGDMA, 90:10	27.9	2.70	0.08	0.14
HEMA-PEG200DMA, 90:10	29.7	3.40	0.80	0.44
HEMA-PEG400DMA, 90:10	34.7	4.40	3.10	1.14
HEMA-PEG1000DMA, 90:10	42.3	6.20	7.70	2.14

As was observed for the permeation of NaCl across the HEMA membranes, the transport of MgCl₂ across the poly(ethylene oxide) crosslinked membranes, illustrated in Figure 7.15, was linear. However, for the HEMA membranes which were crosslinked with EGDMA and PEG200DMA it appeared that the ion permeability was suppressed over the time period studied. Taking into account previous work^{181, 182} which examined the effect of the degree of hydration of the membrane, (H), which is the reciprocal of the EWC, upon the permeability coefficient, (P), for a series of salts. It was found that there was a cut off point in the permeability which occurred at a minimum degree of hydration for each

of the salts studied. This minimum degree of hydration was found to be $H=0.30$ for $MgCl_2$ and explains why the ion transport for the EGDMA and PEG200DMA membranes used in this investigation, which have degrees of hydration less than 0.30, appeared to be suppressed. When the degree of hydration was increased above this level, as was the case for the HEMA membranes crosslinked with PEG400DMA and PEG1000DMA which have respective EWC's of 34.7% and 42.3%, permeation of the metal salt was observed. The slopes of the graphs were linear, therefore suggesting that complexation did not occur.

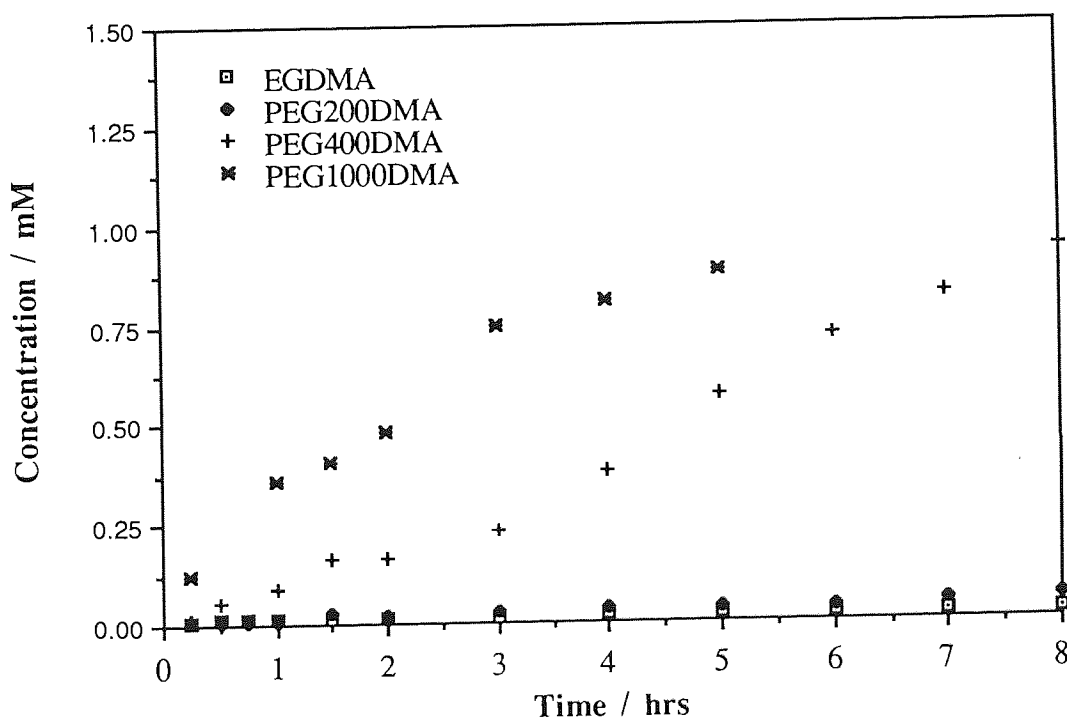


Figure 7.15 Effect of poly(ethylene oxide) crosslinker chain length on the permeation of $MgCl_2$ across a HEMA membrane

Figure 7.16 shows the data obtained for the transport of $CaCl_2$ across the HEMA membranes. Once again a linear trend was observed for each of the membranes which suggests that the transport of calcium is uninhibited by the use of poly(ethylene oxide) crosslinkers of the chain lengths studied.

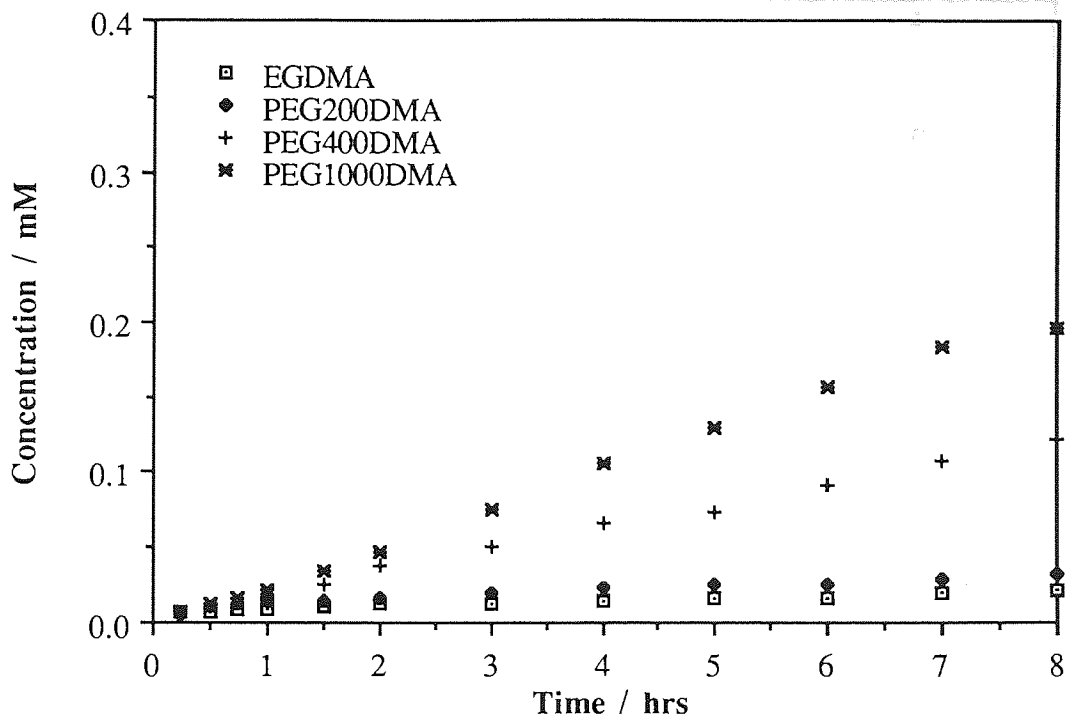


Figure 7.16 Effect of poly(ethylene oxide) crosslink chain length on the permeation of CaCl_2 across a HEMA membrane

It was apparent from the permeability results presented in this work that a possible relationship exists between the ion permeability coefficients and the degree of hydration of the polymer membranes. This has been examined in previous studies^{181, 182} and a plot of P versus H for the results obtained in this work is illustrated in Figure 7.17. This plot was surprisingly linear and it suggests that the transport of metal chlorides is directly proportional to the degree of hydration for the membranes studied in this work. The linearity of this graph is further evidence that the group I and II metal ions were not complexed by the polyether crosslinkers. However, it does not take account of any changes in EWC which might occur due to the transported ions.

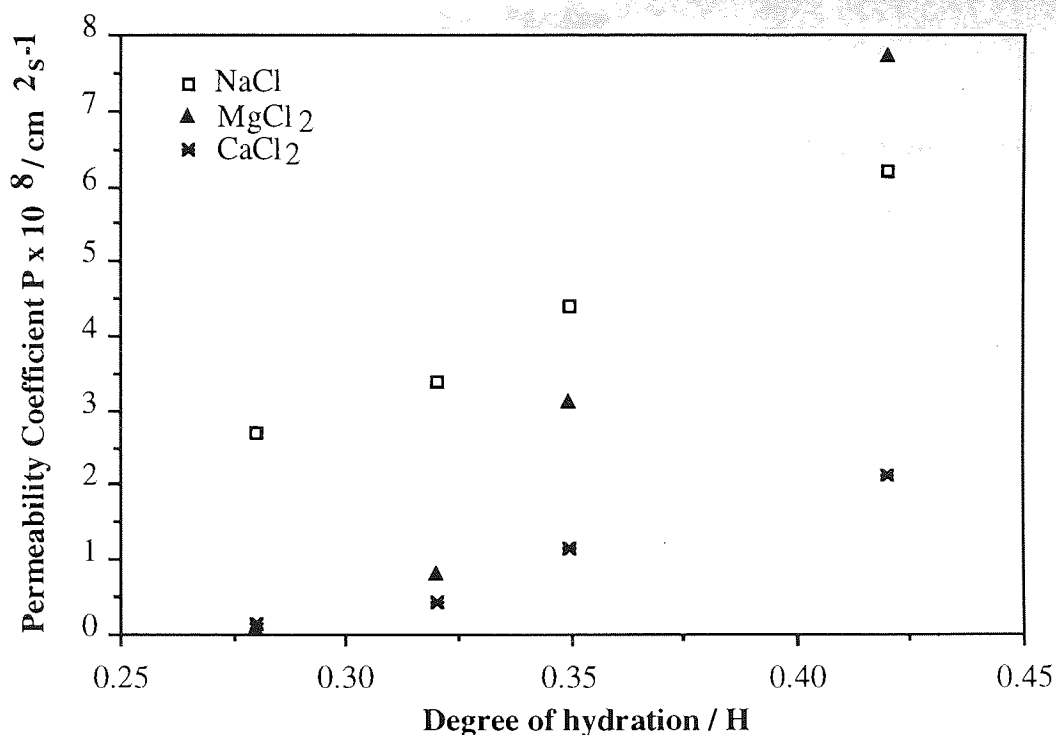


Figure 7.17 Plot of P versus H for the transport of metal chlorides across poly(ethylene oxide) crosslinked HEMA membranes

7.6.4 Conclusions

The results indicate that HEMA membranes modified with polyether crosslinking monomers upto a chain length of approximately 20 ethylene oxide repeat units do not interact with group I and II metal cations.

As it is apparent that HEMA copolymers modified with polyether crosslinkers would not be expected to interact with metal ions, which might lead to biointolerance, then it was of further use to investigate the interaction of the materials used in this work with other biological species.

7.7 Protein And Lipid Deposition Studies

7.7.1 Introduction

Perhaps the most successful commercial application of hydrogels has been in the production of soft contact lenses. The ease of access to the eye has enabled a wide range of material compositions and their interactions with a complex biological environment to be studied. Tear chemistry is very complex, it varies from person to person and is also influenced by external factors. For example the chemistries of emotional tears, or tears stimulated from exposure to onions are very different from the unstimulated tear film. The differences in tear chemistry manifest themselves in the large variations and inconsistencies obtained with *in vivo* results. Consequently, in an attempt to overcome these difficulties in comparing subtle changes in the material chemistry, an *in vitro* spoilation model was developed at Aston within the Biomaterials Research Group. The details of this model and its development are beyond the scope of the work presented here, but are described in detail by Franklin¹⁴⁹.

The model attempts to mimic the interactions of the spoilation process. This is achieved by using a standard artificial tear solution based on a foetal calf serum and phosphate buffered saline of pH = 7.4. This solution is similar to natural tears, but it is also possible to add additional tear components such as lysozyme, lactoferrin and mucin. As mentioned previously in Chapter 3 the deposition of proteins and lipids can be monitored using fluorescence spectroscopy, which is a non-destructive technique. Additionally, excitation at 360nm and 280nm and observation of the protein and lipid peaks at 400-600nm, enables further information about the spoilation process to be obtained. Due to the greater consistency of the model compared to individual variation, it is possible to test many more material compositions with very small changes in the material chemistry.

Previous studies have shown that the deposition of proteins and lipids onto hydrogel surfaces increases with increasing crosslinker concentration¹⁵⁴. In contrast the use of monocapped poly(ethylene oxides) was shown to decrease the quantity of deposition¹⁵⁴.

Therefore, the effect of polyethers as crosslinkers on the amount of deposition was studied to determine which of these effects would be observed.

7.7.2 Methods

Samples of each of the polyether modified HEMA membranes were cut into disks using a size 7 cork borer. Each individual sample was spoiled using the tear model. The amount of deposition of proteins and lipids from the artificial tear solution was monitored for a period of 28 days using fluorescence spectroscopy. Examples of sample emission spectra obtained using this technique are illustrated in Chapter 2.

7.7.3 Results Of Protein And Lipid Spoilation Characteristics

Using the *in vitro* spoilation model the protein and lipid deposition characteristics of the series of crosslinked HEMA membranes were obtained. The results obtained for the amount of protein and lipid deposited onto the crosslinked HEMA membranes are illustrated in Figures 7.18 and 7.19.

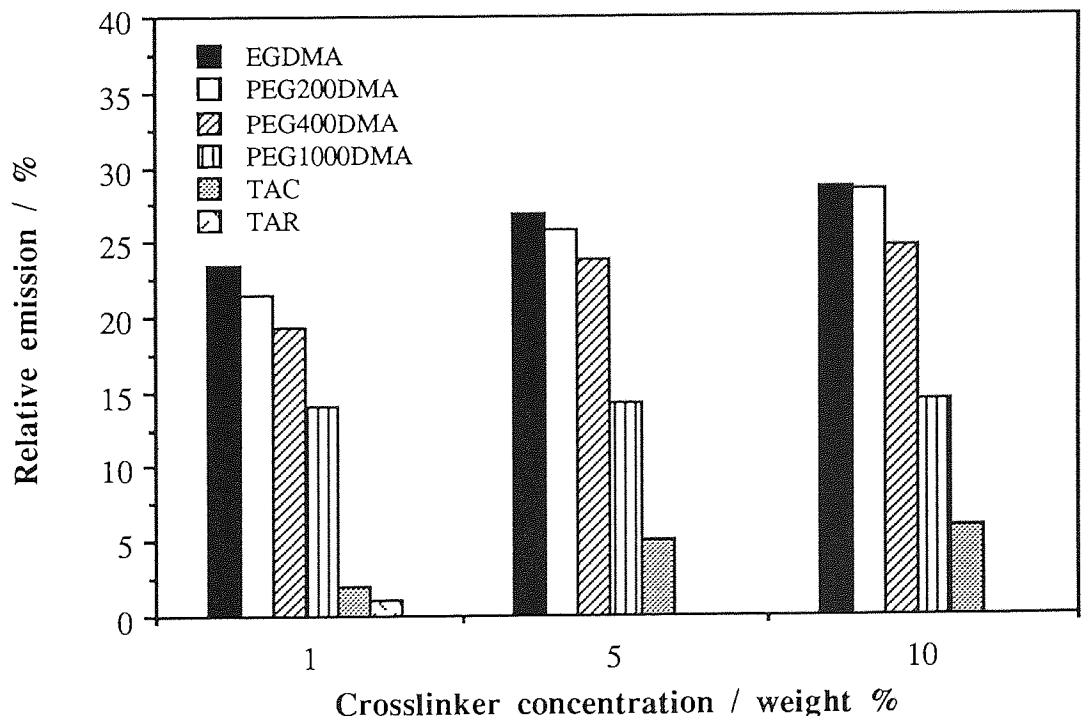


Figure 7.18 Effect of crosslinker type and concentration on the protein deposition of modified poly (HEMA) membranes after 28 days

Figure 7.18 shows the effect of crosslinker type and concentration on the protein deposition of modified HEMA membranes. The amount of deposition has been shown to be dependant on the hydrophilicity/hydrophobicity of the hydrogel surface¹⁸³. It can be seen in this instance that the amount of protein deposited onto the hydrogel surface decreased with increasing hydrophilicity of the crosslinking monomer. EGDMA is the least hydrophilic monomer and TAR is the most hydrophilic.

Increasing the crosslinker concentration for each of the crosslinker series (except those membranes modified with PEG1000DMA) increased the amount of protein and lipid deposited. This was because the increase in crosslinker concentration decreased the chain mobility of the network and restricted polar group expression at the surface. The decreased mobility results in an increase in the hydrophobicity of the surface.

For the HEMA membranes crosslinked with PEG1000DMA the amount of deposition was decreased. This was because the length and hydrophilicity of the polyether chain offset the increase in hydrophobicity caused by a decrease in network mobility as a result of the increased amount of crosslinker.

Figure 7.19 shows the effect of crosslinker type and concentration on the lipid deposition characteristics of the HEMA modified membranes. The general trend was that lipid deposition decreased with increasing hydrophilicity of the crosslinker. Again the effect of increasing the crosslink chain length was to decrease the levels of deposition that occurred. This is because the mobility of the network was decreased and therefore the amount of polar group expression was decreased resulting in a more hydrophobic surface.

Once again it was apparent that for PEG1000DMA the levels of deposition did not increase with increasing amount of crosslinker. This was again due the length and hydrophilicity of the polyether chain offsetting any increase in hydrophobicity due to the increased number of crosslinks.

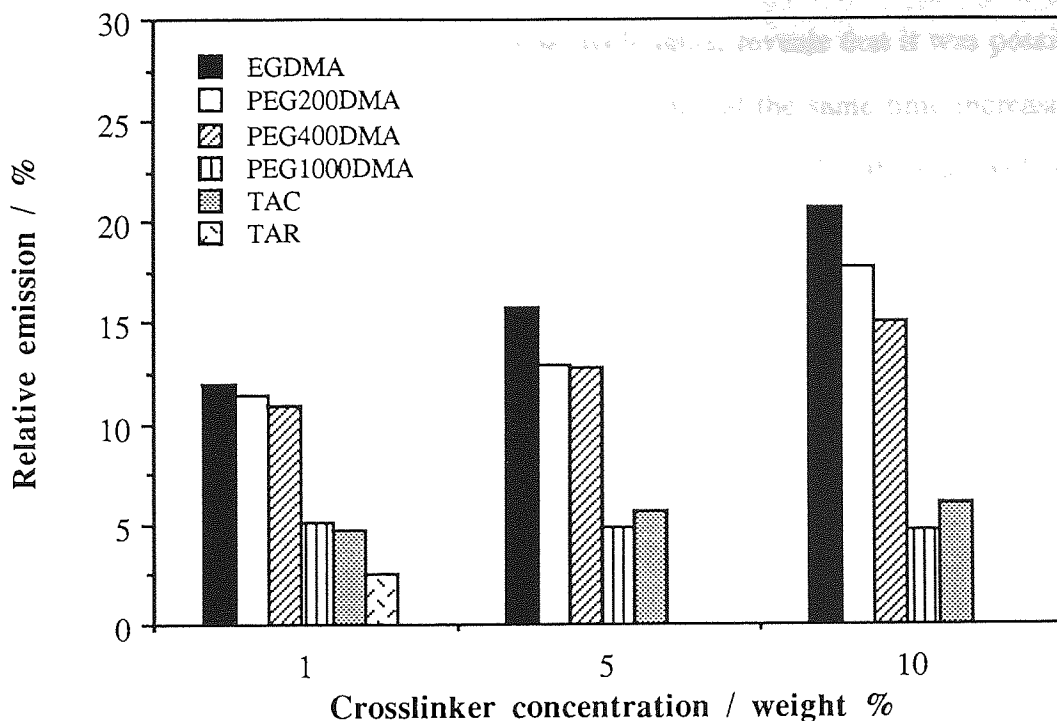


Figure 7.19 Effect of crosslinker type and concentration on the lipid deposition of modified poly (HEMA) membranes after 28 days

7.7.4 Conclusions

The amount of protein and lipid deposited on the HEMA membranes decreased with increasing hydrophilicity of the crosslinker. However, the amount of deposition occurring was observed to increase with increasing concentration of crosslinker for each series of HEMA membranes except those containing PEG1000DMA. This was because the length and hydrophilicity of the polyether chain offset the decrease in chain mobility which is normally associated with an increase in the amount of crosslinker.

7.8 Summary

The mechanical properties of hydrogels with high EWC's are in general poor for many applications. Increasing the amount of EGDMA crosslinker increases the mechanical properties, but decreases the EWC.

The results presented in this work indicate that an increase in the polyether chain length of EGDMA to a minimum number of ethylene oxide units, reveals that it was possible to increase the mechanical properties of a hydrogel while at the same time increasing its EWC. This effect was observed for a minimum chain length of 20 ethylene oxide repeat units, which corresponds to PEG1000DMA.

However, poly(ethylene oxides) are known to sequester metal cations which could lead to biointolerance of the materials, but ion permeability studies suggest that at the crosslinker chain lengths up to and including PEG1000DMA, interaction of the metal cation and the polyether did not occur. This result supports the theory proposed by Oxley¹⁵⁴ which suggests that for polyether chains of upto 20 ethylene oxide repeat units complexation occurs at the free chain end.

Initial deposition studies of the HEMA membranes which were modified with polyether crosslinkers show that the quantity of proteins and lipids deposited decreased with increasing polyether chain length. It was also evident that for the HEMA-PEG1000DMA copolymers that the amount of deposition did not increase with increasing amount of the crosslinking monomer.

The results presented in this Chapter suggest that the mechanical properties of a hydrogel membrane can be increased while at the same time increasing the EWC. This can be achieved by the use of polyether crosslinkers of a minimum chain length, nominally 20 repeat units. Permeability measurements and protein and lipid interaction studies indicated that the PEG1000DMA used to achieve the increase in strength and water content did not adversely interact with biological species.

CHAPTER 8

Hydrogels modified with Monocapped Linear Polyethers

8.1 Introduction

Poly(ethylene glycols) (PEG) and poly(ethylene oxides) (PEO) are both terms for materials with the general formula, $\text{HO}(\text{CH}_2\text{CH}_2\text{O})_n\text{H}$. The subscript n refers to the total number of ethylene oxide repeat units in the molecule and is referred to as the degree of polymerisation. For example, for PEG400MA $n=9$ and PEG1000MA $n=22$. In recent years poly(ethylene oxides) have been assessed for their potential in biomedical applications and they have been found to be relatively inert towards biological species.

It has been observed that the incorporation of PEO segments into hydrogels and increasing the PEO chain length, reduced the adsorption of plasma proteins and adherent platelets. Several studies have studied PEO containing copolymers and have produced materials with PEO side groups and materials with segments of PEO as the soft phase component in segmented polyurethanes^{166, 184, 185}. In all situations the PEO containing materials exhibited reduced activity towards biological species.

Recent work at Aston has revealed that polyethers used in hydrogels may form regions of crystallinity. Polyethers are well known for crystallising, because of their regular structure. The formation of domains of crystallinity may lead to biointolerance in applications such as contact lenses. The work at Aston has highlighted the fact that the combination of mechanical and physical trauma caused by such material characteristics produces disturbance of the mucin layer which covers the cornea. The resultant effect is to produce "stranding" and "balling" of mucin on the hydrogel surface. Examples of mucins on hydrogel surfaces are shown in Figure 8.1.

This work was therefore designed to further investigate the use of polyethers for modifying hydrogel polymers and to investigate the possible formation of crystalline domains of polyethers. Firstly, the reactivities of the polyethers being investigated were considered. If the reactivity of the polyethers is such that the sequence distribution of polyether sequences within a copolymer contains domains or blocks of polyether then

crystalline formation will be a more significant possibility than a sequence distribution where the polyether is more evenly distributed along the backbone of the copolymer. An overview of the effects of polyethers on the EWC's, mechanical and surface properties will be provided, together with scanning electron microscope (SEM) and X-ray diffraction (XRD) examination of the hydrogels surfaces.

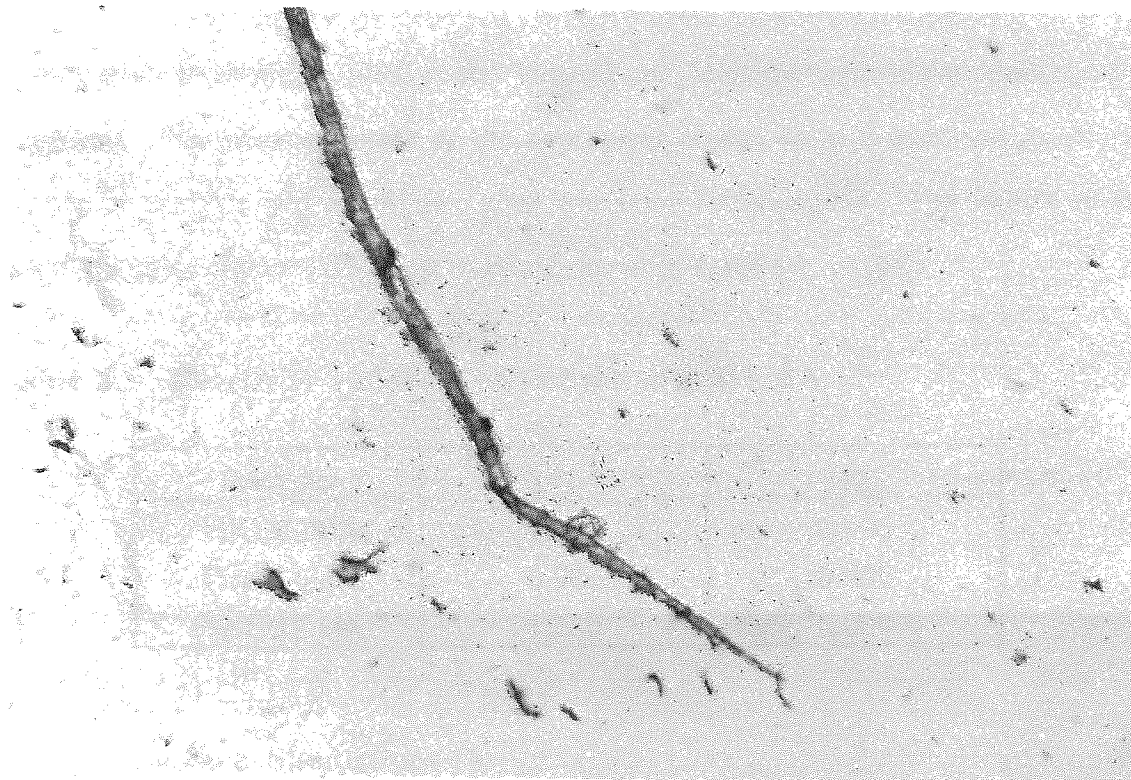


Figure 8.1 SEM micrograph of mucin on a hydrogel surface

8.2 The Reactivity of Long Chain Polyethers in Hydrogel Synthesis

8.2.1 Introduction

The literature to date shows that there is no agreement as to the relative importance of the factors that govern the reactivity of macromonomers. However, there appears to be a consensus that the following factors are important in determining the reactivity:

- (i) the chemical nature of the polymerisable end group,
- (ii) the degree of compatibility of the macromonomer with the propagating chain,
- (iii) the molecular weight of the macromonomer,
- (iv) the polymerisation medium,

(v) the degree of conversion.

Considering these elements the experimental reactivity ratios have been determined previously¹⁸⁶ for the reactivity of the polyether monomers used in this work with 2-hydroxyethyl methacrylate. The authors prepared copolymers with varying degrees of conversion and calculated the reactivity ratios using the Fineman-Ross and Kelen-Tudos linearisation methods, as well as the Tidwell and Mortimer non-linear least squares treatment. The microstructure of the copolymer chains were determined by NMR, elemental analysis and copolymer glass transition temperatures. The values of the reactivity ratios obtained from this work are shown in Table 8.1.

Table 8.1 Reactivity ratios of polyethers with HEMA

Polyether	r ₁	r ₂
PEG200MA	1.020	0.990
PEG400MA	0.980	0.090
PEG1000MA	1.280	0.009

8.2.2 Sequence Simulations

Using the reactivity ratios listed in Table 8.1, sequence simulations were obtained using the copolymer simulation program. The resulting simulations are illustrated in Figures 8.2 - 8.4.

80 mole % of monomer A, HEMA

20 mole % of monomer B, PEG1000MA

$r(AB) = 1.280$

$r(BA) = 0.009$

Polymerised to 100 % conversion

In the simulated copolymer HEMA is represented by O and PEG1000MA by X

```

OOOOOOOOOOOXOOOXOOOXOOOOOXOOOOOOOOOOOOOOOOOOOOOOOOOOOOOOOOOXOOXOO
OOXOOOOOOOOOOOOOOOOOOOOOOOXOOOOOOOOOOOOOOOOOOOOOXOOOXOOOOOOOOOOOXOOO
OOOOOOOOOOOOOOOOOOOOOOOOOOOOOOOOOOOOOOOOOOOOOOOOOOOOOOOOOXOOOOOOOXOO
OOOOOOOOOOOXOOOOOOOXOOOOOOOOOOOOOOOOOOOOOXOOOOOOOOOOOOOOOOOOOXOOOO
OOOXOOOOOOXOOOOOOOXOOXOOOOOOOOOOOOOOOOOOOOOOOOOOOOOOOXOOOOOOOOOO
OOOOOXOOOOOOOOOOOOOOOOOOOOOXOOOOOOOOOOOOOOOXOOOOOOOOOOOOOOOOOOOOOO
OOOOOOOOOOOOOOOOOOOOOOOOOOOOOXOOOOOOOOOOOOOOOOOOOOOOOXOOOOOOOOOO
OOOOOOOOOOOOOOOOOOOOOOOOOOOOOXOOOOOOOOOOOOOOOOOOOOOXOOOOOOOOOOOO
OOOOOOOOOXOOOOOOOOOOOOOOOOOOOOOOOOOOOOOXOOOOOOOOOOOOOOOOOOOOOO
OXOXOOOOOOXOOOOOOOOOXOXOOOOOOOOOOOOOXOXOOOXOOOOOOOOOOOOOOOXO
OOOOOXOXOXOOOOOXOOOOOOOOOOOOOXOXOOXOOOOOOOOOXOOOOOOOXOXOOOOO
XOOOOOOOOOOOOOXOOOOOOOOOOOOOXOOOOOXOOOOOOOXOXOOOOOXOXOOOOOOO
OOOOOOOOOXOOOOOOOOOOOXOOOOOOOXOOOOOOOOOOOOOOOOOOOOOXOOOOOOOOOOOX
OOOOOOOOOOOXOOXOOOOOOXOOOOOOOXOOOOOOOOOOOOOOOOOOOOOOOOOOOXOXXO
OOOOOOOOOXOXOOOOOOOOXOOXOOXOOOOOXOXOXOOOOXOOOOOOOOOOOOOOOOOO
XOXOOOOOXOOOOOOOXOOOXOXOXOOOOOOOXOOOOOOOOOOOOOOOOOOOOOOOXOOXOO
OOXOOXOOOOOOOOOOOOOOOOOOOOOOOOOOOOOOOXOOXOOXOOOXOXOOOXOOOOOOXXO
OXOOOOOOOOOOOOOOOOOOOOOOOXOOXOOXOOOXOOOXOOOXOOOOOOOXOOOXOOOOOOXOO
XOOOXOOOOOOOOOOOXOOOXOOOOOOOXOOXOOXOOOXOOOXOOOXOOOXOOOXOOXXOO
OOOOOOOXOXOOOOOXOOOOOXOOOXOOOXOOOXOOOXOOOXOOOXOOOXOOOXOOOXOOOX
XOOOXOOOXOOOOOOOOOXOOXXOOXOOXOOOXOOXXOOOXOOOXOOOXOOOXOOOXOOXXOXX
OOXXOXOOOXOOOXOOOXOOXXOXOOXXOOXOOXOOXOOXOOXXOOOXOOOXOOOXOOOXOO
OOXOXOXOXOOOOOOOXOOOXOXOXOOOXOXOOOXOOOXOOOXOOOXOOOXOOOXOOOXOX
OXOXOXOOXXOOOOOXOOXOXOXOOOXOOOXOOOXOOXXOXOOOXOOOXOOOXOOOXOOXX
XOOOXOOOXOOXXOOXXOXOOXXOOOXOOOXOOOXOOOXOOOXOOOXOOOXOOOXOOOXOOXX
XXXXXXXXXXXXXXXXXXXXXXXXXXXXXXXXXXXXXXXXXXXXXXXXXXXXXXXXXXXXXXXXXXXX
XXXXXXXXXXXXXXXXXXXXXXXXXXXXXXXXXXXXXXXXXXXXXXXXXXXXXXXXXXXXXXXXXXXX

```

The simulated copolymer contains 1600 HEMA units and 400 PEG1000MA units

Sequence Length	Number of Sequences		Sequence Length	Number of Sequences	
	HEMA	PEG1000MA		HEMA	PEG1000MA
1	39	174	18	4	0
2	31	23	19	5	0
3	27	6	21	1	0
4	18	3	22	3	0
5	14	2	23	2	0
6	8	0	24	1	0
7	11	0	27	1	0
8	6	0	28	2	0
9	4	0	29	4	0
10	6	0	31	1	0
11	3	0	35	1	0
12	2	0	38	2	0
13	4	0	43	1	0
14	2	0	46	1	0
15	2	0	53	1	0
16	1	0	140	0	1
17	1	0			

Figure 8.4 Sequence simulation of a HEMA and PEG1000MA copolymer

8.2.3 Results

It is evident from the sequence simulations and the values of the reactivity ratios between HEMA and the series of PEGMA's that the reactivity of the polyether is decreased with increasing polyether chain length. The reactivity ratios for each system indicate that the reactivity of a growing polymer chain ending in a HEMA radical has a greater propensity to add to a successive HEMA unit. The value of r_2 for each of the polyethers indicates that a growing polymer chain ending with a PEGMA radical will also be more likely to react with a HEMA monomer unit. These characteristics result in the sequence simulations presented in Figures 8.2 - 8.4.

It is apparent in Figure 8.2 that the reactivity of the PEG200MA is not very different from that of HEMA. This may be expected when considering the two structures. The HEMA may be considered as a methacrylate end group possessing one ethylene oxide unit and the PEG200MA as a methacrylate end group possessing 4 or 5 ethylene oxide units. It would therefore appear that the increase in chain length of only 3 or 4 ethylene oxide units does not adversely affect the reactivity by steric hindrance and is not sufficiently long enough to affect the reactivity via a decreased rate of diffusion in the polymerisation system or the formation of polyether complexes within the polymerisation. The relative proportions of each monomer and their similar reactivities give an alternating copolymer, the HEMA blocks being larger due to their dominance of the feed ratio.

In the case of the PEG400MA in Figure 8.3 it is evident that the increase in poly(ethylene oxide) chain length suppresses the reactivity of this monomer and the addition of HEMA units to the growing polymer chain ending in either a HEMA or a PEGMA radical is the most likely scenario. However, the reactivity of the PEG400MA is great enough for approximately 93% of the feed ratio to be consumed as singular units distributed evenly throughout the copolymer. This result enables copolymers incorporating PEG400MA to be evenly distributed throughout the copolymer as single monomer units at high degrees of copolymer conversion.

Figure 8.4 illustrates the reactivity simulation of HEMA with PEG1000MA. The simulation illustrates that the PEG1000MA produces a terminal block of polyether. This would be expected from its low reactivity. In the case of PEG1000MA addition to a growing polymer chain, successive addition would be a HEMA unit, because of the low rate of reaction between two PEG1000MA units.

The simulated low reactivity is consistent with Suzuki *et al* ¹⁸⁷ who suggested that the polymerisation rate would be a thousand times less reactive for macromonomers with a molecular weight of a thousand or above.

8.2.4 Conclusions

Simulations of the reactivity of polyethers up to a molecular weight chain length of 400 units indicates that the polyether units will be potentially distributed evenly throughout the polymer backbone of HEMA copolymers. It is therefore likely that incorporation of polyethers upto a molecular weight of 400 will be unlikely to crystallise with each other, because they are kept distant from each other.

In the case of PEG1000MA the reactivity simulation indicates that the reactivity of the polyether is so low that a terminal block composed of polyether monomer units is produced. The formation of blocks of polyether will increase the possibility of crystallisation of adjacent polyether chains.

8.3 Effect of PEG Incorporation on the EWC

8.3.1 Materials and Methods

Polymer membranes of 2-hydroxyethyl methacrylate crosslinked with one weight percent of ethylene glycol dimethacrylate were prepared with increasing amounts of methoxy and hydroxy poly(ethylene oxide) monomethacrylates using the method described in Chapter 2. Prior to their use the molecular weight distributions of the PEGMA's were determined using gel permeation chromatography. This was to ensure that the characteristics of the

resulting hydrogels could be attributed to individual polyethers. The resulting traces are illustrated in Figures 8.5 - 8.7.

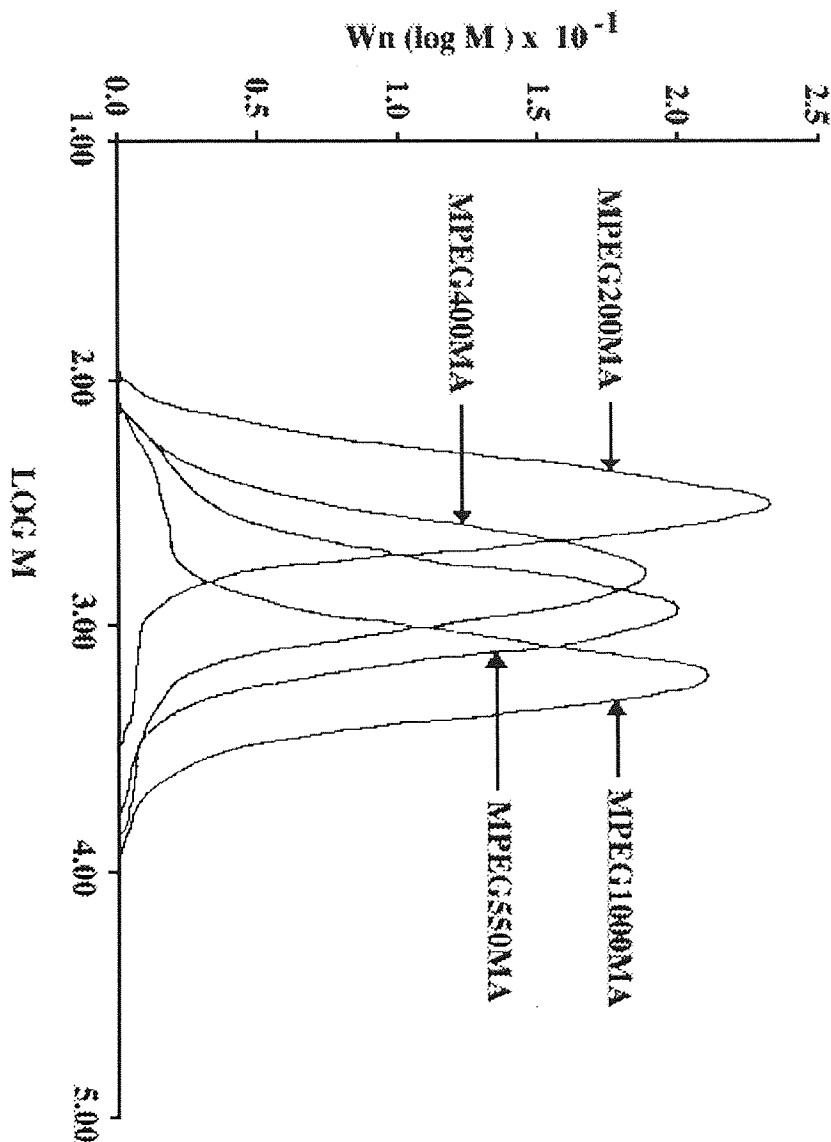


Figure 8.5 Gel permeation chromatograms for the methoxy terminated polyethylene glycol methacrylates, (MPEG MA's)

The molecular weights are polystyrene equivalent molecular masses. The column used was a PL gel 2 x mixed gel, the solvent used was THF at a flow rate of $1\text{ml}\cdot\text{min}^{-1}$ and a concentration of $2\text{mg}\cdot\text{ml}^{-1}$ with a refractive index detector.

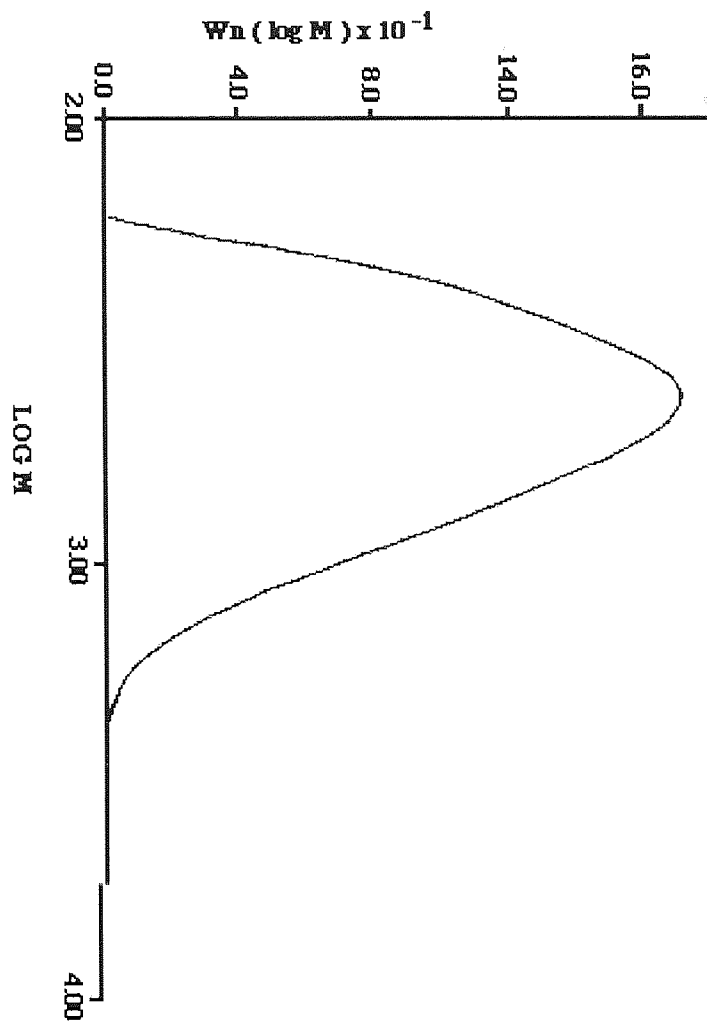


Figure 8.6 Gel permeation chromatograms for polyethylene glycol methacrylate 10 ethylene oxide units, (PEGMA 10 EO)

The molecular weight is a polystyrene equivalent molecular mass. The column used was a PL gel 2 x mixed gel, the solvent used was DMF at a flow rate of $1\text{ml}\cdot\text{min}^{-1}$ and a concentration of $2\text{mg}\cdot\text{ml}^{-1}$ with a refractive index detector.

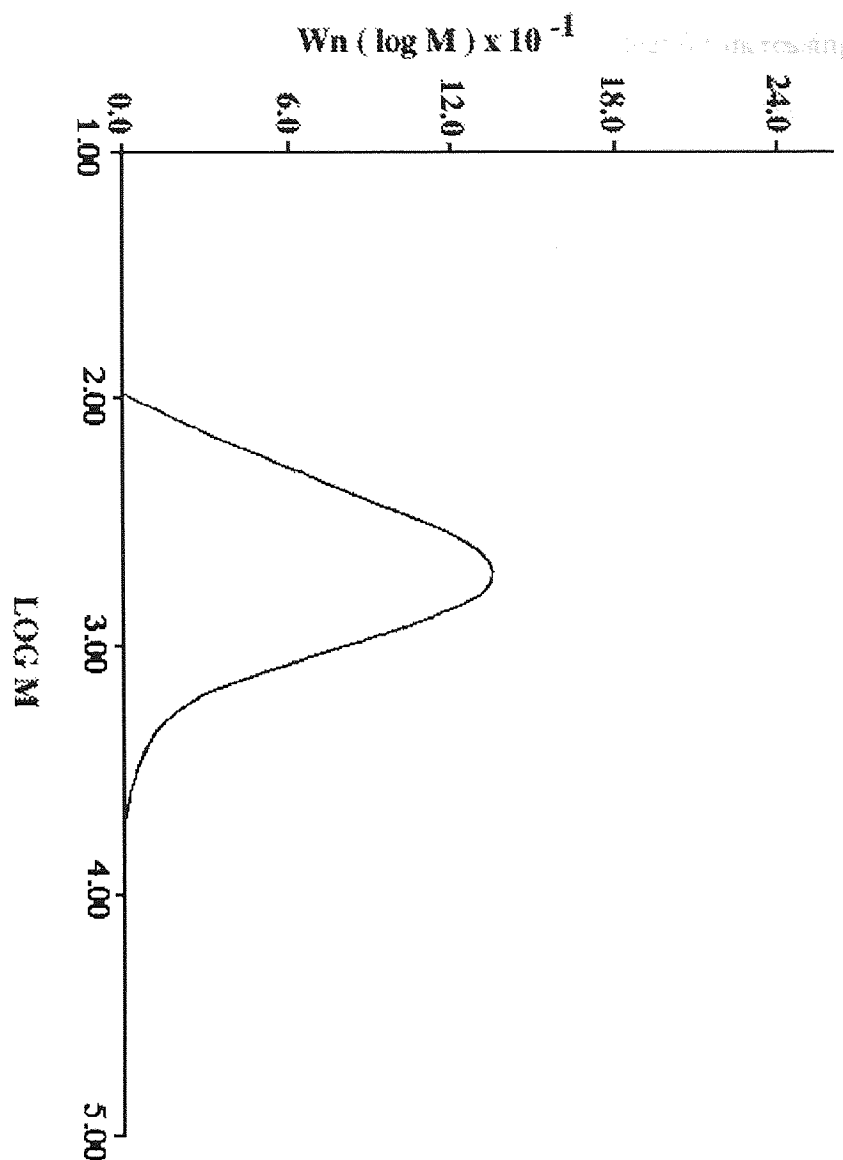


Figure 8.7 Gel permeation chromatograms for ethoxylated hydroxyethyl methacrylate, (HEMA 4,5 EO)

The molecular weight is a polystyrene equivalent molecular mass. The column used was a PL gel 2 x mixed gel, the solvent used was THF at a flow rate of $1\text{ml}\cdot\text{min}^{-1}$ and a concentration of $2\text{mg}\cdot\text{ml}^{-1}$ with a refractive index detector.

8.3.2 Results

The equilibrium water contents of the membranes were obtained by the method described in Chapter 2 and are presented in Table 8.2. It can be seen that for increasing amounts and chain length of the poly(ethylene oxide) the EWC increases. This is expected, because of the greater hydrophilicity of poly(ethylene oxide) compared to HEMA and the increasing degree of hydrophilicity induced by an increasing chain length. These effects have previously been reported⁷.

Of further significance is the fact that the hydroxy terminated poly(ethylene oxides) give a lower EWC than the methoxy terminated derivatives of an equal chain length, because it would be expected that the methoxy group is more hydrophobic than the hydroxyl group. The difference between the methoxy and hydroxy terminated derivatives is more clearly illustrated in Figure 8.8. Oxley⁷ attributed this anomaly to the formation of an internal complex between the hydroxyl group and the polyether chain, thereby forming an internal ring structure in preference to water binding. Preference for the formation of such a ring type structure produces a lower water binding capacity than a fully extended polyether chain.

Table 8.2 Effect of poly(ethylene oxide) incorporation on the EWC of polyether modified HEMA membranes

PEO	Weight% of PEO	EWC / %
None	0	35.1
MPEG200MA	10	37.8
	20	43.5
MPEG400MA	10	42.6
	20	50.4
MPEG1000MA	10	45.6
	20	56.6
HEMA 4,5 EO	10	37.4
	20	40.7
HEMA 10 EO	10	40.2
	20	42.4

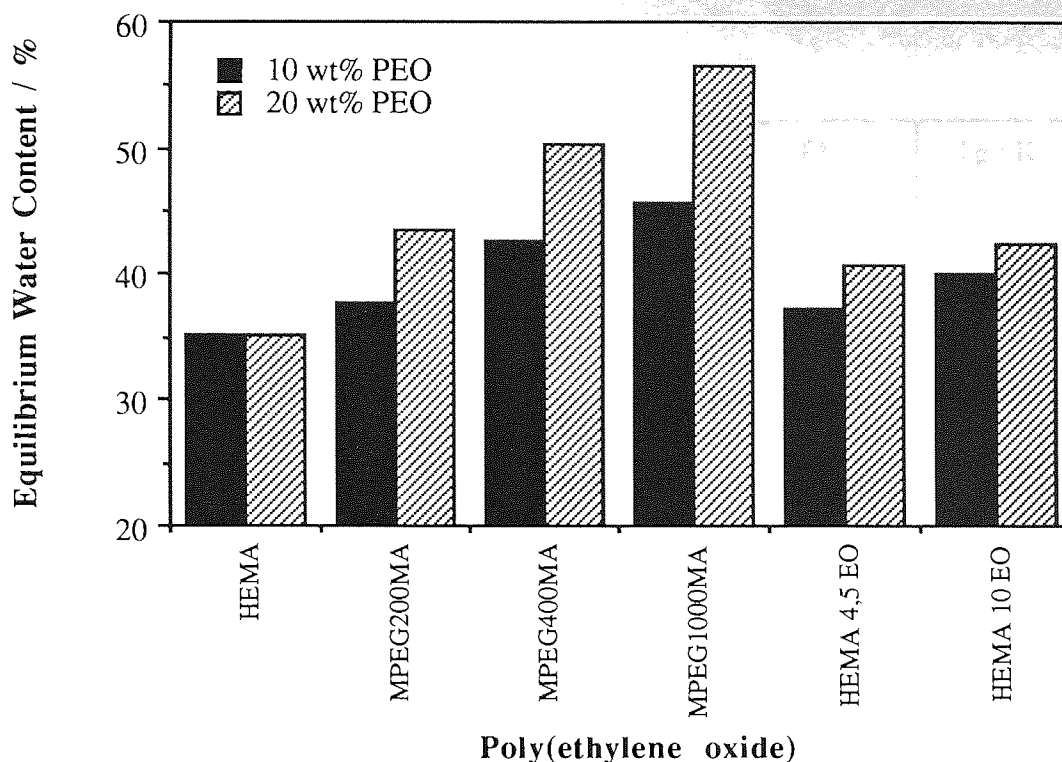


Figure 8.8 Effect of the amount and chain length of poly(ethylene oxide) on the EWC of HEMA-EGDMA, (99:1), hydrogel membranes

8.4 Effect of Poly(ethylene oxide) Incorporation on the Mechanical Properties of HEMA Modified Hydrogels

8.4.1 Materials and Methods

The mechanical properties of the HEMA membranes modified with polyethers were obtained using the tensile method described in Chapter 2. Secondly, the glass transition temperatures (T_g 's), of the membranes were obtained by differential scanning calorimetry (DSC), which is also described in Chapter 2.

8.4.2 Results

Table 8.3 shows the results obtained for the elastic modulus (E_m), tensile strength (T_s), elongation at break (E_b) and T_g 's for the HEMA copolymers modified with linear polyethers.

Table 8.3 Mechanical properties of HEMA membranes modified with poly(ethylene oxide)s

PEO	Weight% of PEO	Em / MPa	Ts / MPa	Eb / %	Tg / K
None	0	0.654	0.726	133	393
MPEG200MA	10	0.522	0.630	143	356
	20	0.400	0.478	153	348
MPEG400MA	10	0.460	0.545	157	345
	20	0.378	0.474	153	340
MPEG1000MA	10	0.406	0.478	141	349
	20	0.288	0.369	139	352
HEMA 4,5 EO	10	0.631	0.599	113	359
	20	0.537	0.480	86	353
HEMA 10 EO	10	0.555	0.509	109	348
	20	0.337	0.410	75	355

It is evident from Table 8.3 that incorporation of either a methoxy or hydroxy terminated polyether lowers the mechanical strength of the modified HEMA membranes. It was shown in Section 8.3.1 that the addition of the hydrophilic polyether chain is to increase the EWC of the hydrogels, therefore it would be expected that the higher water contents would plasticise the hydrogel network resulting in a lowering of the stiffness or elastic modulus of the hydrogels and an increase in the flexibility of the polymer chains, indicated by a fall in the value of the glass transition temperature. This was the trend observed upon the introduction of a polyether into a HEMA hydrogel. Further increases in the amount and length of the polyether chain indicated a further reduction in the elastic modulus of the hydrogel membrane.

Comparison of the reduction in mechanical properties due to the introduction of hydroxy terminated polyethers compared to methoxy terminated polyethers with an equivalent chain length, for example MPEG200MA and HEMA 4,5 EO, indicate that the reduction due to the hydroxy terminated polyethers is less than that due to the methoxy terminated polyethers. This is probably due to the moderately lower EWC's, which is believed to be due to the formation of an internal ring structure via the polyether chain and the hydroxyl terminus, which would plasticise the structure to a lesser extent than a higher water content system. Secondly, the formation of an internal ring structure would increase the energy barrier to rotation of the polymer backbone. This is reflected in the higher values of the glass transition temperatures observed for hydroxy over methoxy terminated polyethers of equal chain length which indicates that the chain mobility is lower in the hydroxy terminated copolymers. This lower chain mobility results in a stiffer copolymer and therefore higher values of the elastic modulus.

Also apparent from Table 8.3 are the anomalies that occur in the value of the glass transition temperatures T_g 's of the hydrogel copolymers as the amount and chain length of the polyethers are increased. The incorporation of the polyether chain with molecular weight 200, lowers the glass transition temperature of the modified HEMA membrane. This would be expected, because the introduction of a lengthy pendant side chain is to increase the free volume between polymer backbone chains. This results in a decrease of the steric and electrostatic interactions and therefore lowers the energy barrier to rotation for the polymer backbone producing a lower T_g . Further increases in the proportion of the flexibilising polyether results in a further decrease in the glass transition temperature.

The observed decrease in glass transition temperature is further exaggerated with the introduction of the 400 molecular weight polyether chain because the energy barrier to rotation is further reduced by another increase in the free volume between polymer backbone chains. However, a further increase in polyether chain length to molecular

weight 1000 does not reduce the glass transition further and an increase in the proportion of the 1000 molecular weight polyether results in a small increase in the glass transition.

A possible explanation for this observation can be made from the sequence distribution of PEG1000MA units and the length of the polyether chain. The sequence simulation indicates that the PEG1000MA will be incorporated into a HEMA copolymer as large domains. It is possible that due to the regularity of the polyether structure, the formation of domains of polyether and a polyether chain of sufficient length that crystallisation of the polyether occurs. However, although the T_g is a characteristic of the amorphous region, it has been found that the steric constraint of a crystalline region adjacent to an amorphous domain is to decrease the mobility of the polymer chains^{188, 189}. Hence, possible crystalline formation would result in the increase in the T_g observed by an increase in the molecular weight of the polyether to 1000.

8.4.3 Conclusions

The mechanical properties follow the expected trend of decreasing stiffness, because of the corresponding increase in water content and flexibilising characteristics due to hydrophilic, long chains of polyether.

The glass transition results provide further evidence that crystallisation of the polyethers occurs at a molecular weight of 1000 units.

8.5 Surface Properties of Polyether Modified HEMA Membranes

8.5.1 Introduction

The surface properties of HEMA copolymers modified with linear polyethers have been investigated in the dehydrated state previously by Oxley¹⁵⁴. Oxley observed that the dispersive component of the surface free energy was lowered with the incorporation of polyethers into HEMA membranes and that the value of the polar component increased. It was concluded that the polar ether groups must express themselves at the surface, since as

the dispersive component arises predominantly from contributions to the surface energy from non-polar groups it was reasonable to assume that the suppression in the dispersive component was a result of the shielding effect of the polymer chains.

It is well known that contact angle measurements provide an insight into the hydrophilicity of hydrogel surfaces. The Wilhelmy technique, which is the basis of dynamic contact angle measurement, detects changes in the surface properties brought about by reorientation of polymer chains or segments at the polymer surface. In a further attempt to clarify the expression of linear polyether chains at the hydrogel surface the dynamic advancing, θ_a , and receding, θ_r , contact angles were measured.

8.5.2 Materials

The hydrogels to be studied were prepared from HEMA containing increasing amounts of either a methoxy or hydroxy terminated poly(ethylene glycol) methacrylate. The proportions of polyether used were 5, 10, 15 and 20 weight%. A series of membranes corresponding to these compositions was prepared for each of the polyethers. The polyethers used were PEG200MA, PEG400MA, PEG1000MA, HEMA 4,5 EO and PEGMA 10 EO. The membranes were polymerised using the technique described in Chapter 2. Following polymerisation the membranes were hydrated in distilled water, which was changed daily, for the required period of two weeks.

Upon completion of the required hydration period the dynamic advancing and receding contact angles for each series of membranes were measured using the dynamic contact angle technique described in Chapter 2.

8.5.3 Results

Table 8.4 shows the values of the advancing, θ_a , and receding, θ_r , contact angles, together with the contact angle hysteresis, for the range of modified HEMA samples prepared. The type and amount of polyether used to modify the HEMA membrane is also included in the table.

Table 8.4 Advancing and receding contact angles for HEMA copolymers modified with linear polyethers

Sample	Contact angle / degrees		
	θ_a	θ_r	Hysteresis
HEMA	75	33	42
HEMA + 5wt% PEG200MA	74	29	45
HEMA + 10wt% PEG200MA	73	25	48
HEMA + 15wt% PEG200MA	71	22	49
HEMA + 20wt% PEG200MA	70	19	51
HEMA + 5wt% PEG400MA	74	28	46
HEMA + 10wt% PEG400MA	72	25	47
HEMA + 15wt% PEG400MA	71	21	50
HEMA + 20wt% PEG400MA	70	18	52
HEMA + 5wt% PEG1000MA	74	25	49
HEMA + 10wt% PEG1000MA	72	23	49
HEMA + 15wt% PEG1000MA	70	19	51
HEMA + 20wt% PEG1000MA	70	17	53
HEMA + 5wt% HEMA 4,5 EO	73	30	43
HEMA + 10wt% HEMA 4,5 EO	73	28	45
HEMA + 15wt% HEMA 4,5 EO	73	27	46
HEMA + 20wt% HEMA 4,5 EO	71	22	49
HEMA + 5wt% PEGMA 10 EO	75	30	45
HEMA + 10wt% PEGMA 10 EO	70	25	45
HEMA + 15wt% PEGMA 10 EO	70	23	47
HEMA + 20wt% PEGMA 10 EO	69	21	48

The effects of the type and amount of polyether on the values of the advancing and receding contact angles is more clearly illustrated in Figures 8.9 - 8.11.

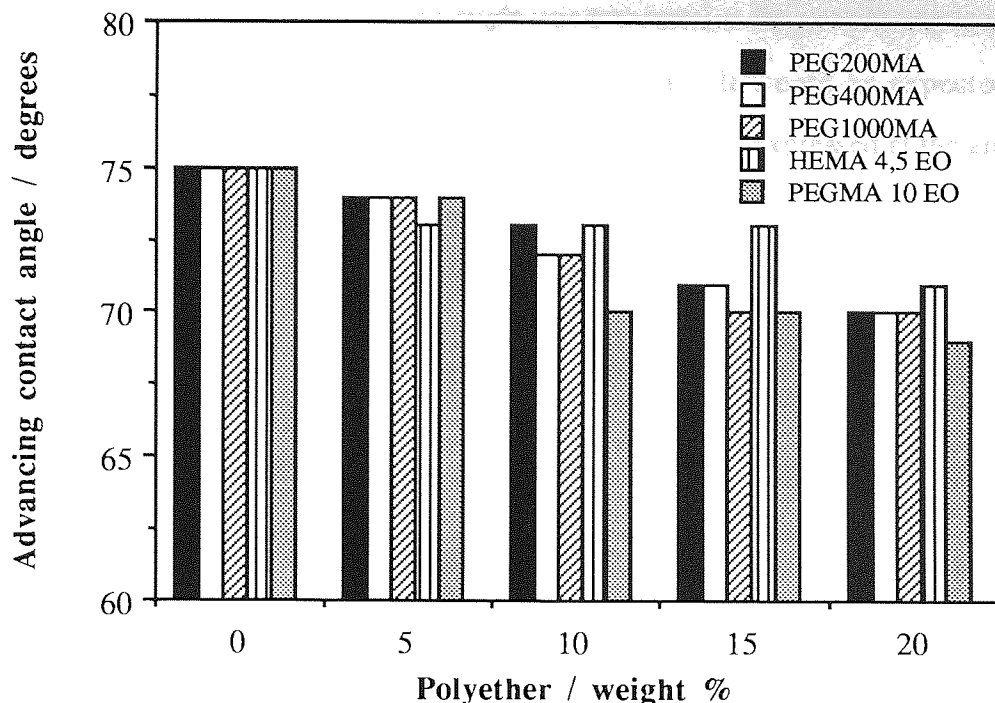


Figure 8.9 Advancing contact angles for HEMA membranes modified with increasing amounts of polyethers

Figure 8.9 shows that the value of the advancing contact angle decreases with increasing amount of polyether and Figure 8.10 shows that the value of the receding contact angle decrease with increasing amount of polyether. The nett result of these two effects is to increase the contact angle hysteresis with increasing amount of polyether.

During dynamic contact angle measurements the water forms an interface with the polymer surface. Hydrophilic chains such as polyethers thermodynamically favour water over an air interface. If the interface is allowed to relax in air the hydrophilic chains will attempt to bury themselves within the bulk of the polymer and the hydrophobic groups of the polymer will be expressed at the interface. If allowed to relax in water, the hydrophilic chains will expose themselves preferentially at the water interface.

Figure 8.9 shows that the advancing contact angle decreases with increasing proportion of the polyether. The advancing contact angle was measured as the sample was lowered from being in an air environment to a water environment. It would be expected that the hydrophobic α -methyl group of the methacrylates would be expressed at the air interface and that the observed decrease in the advancing contact angle would not be observed. The decrease in the value of θ_a suggests that the hydrophilic polyether chains are expressed at the interface. This observation would be consistent with the conclusion of Oxley¹⁵⁴ who observed that in the dehydrated state the dispersive component of the surface energy was suppressed with increasing polyether content.

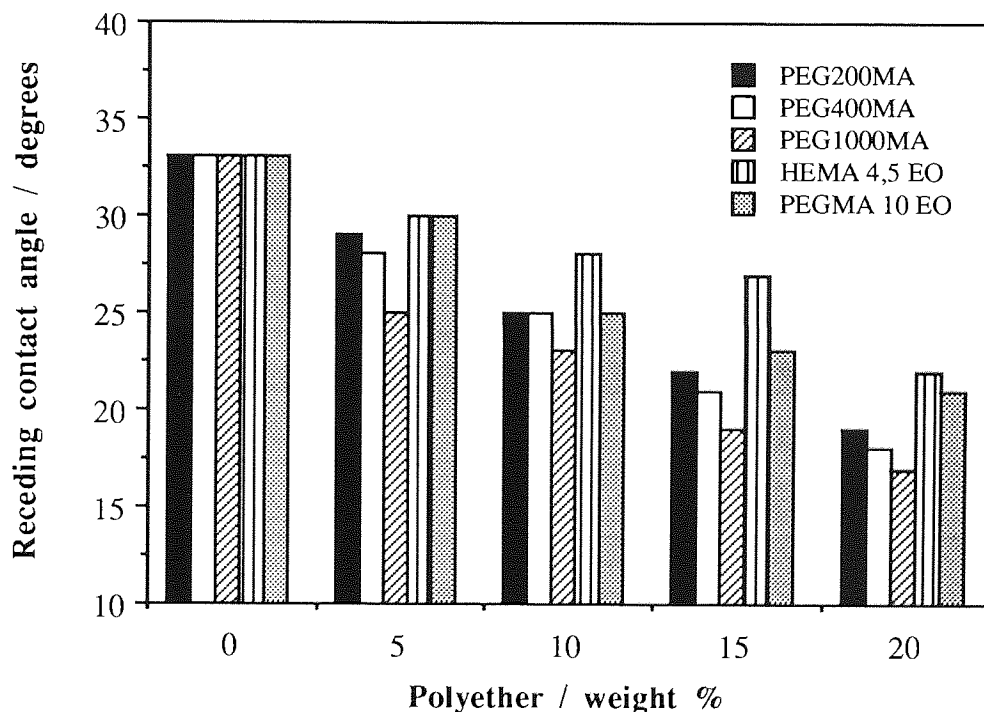


Figure 8.10 Receding contact angles obtained for HEMA membranes modified with increasing amounts of polyethers

Figure 8.10 further substantiates the evidence that the polyether chains are expressed at the surface of the copolymer. It is shown in Figure 8.10 that the receding contact angle decreases with increasing amount of polyether and that the receding contact angle also decreases with increased polyether chain length. The observed decrease in θ_r corresponds

to an increasingly hydrophilic surface. The surface becomes more hydrophilic with an increase in the chain length of hydrophilic polyethers and an increase in the polyether concentration.

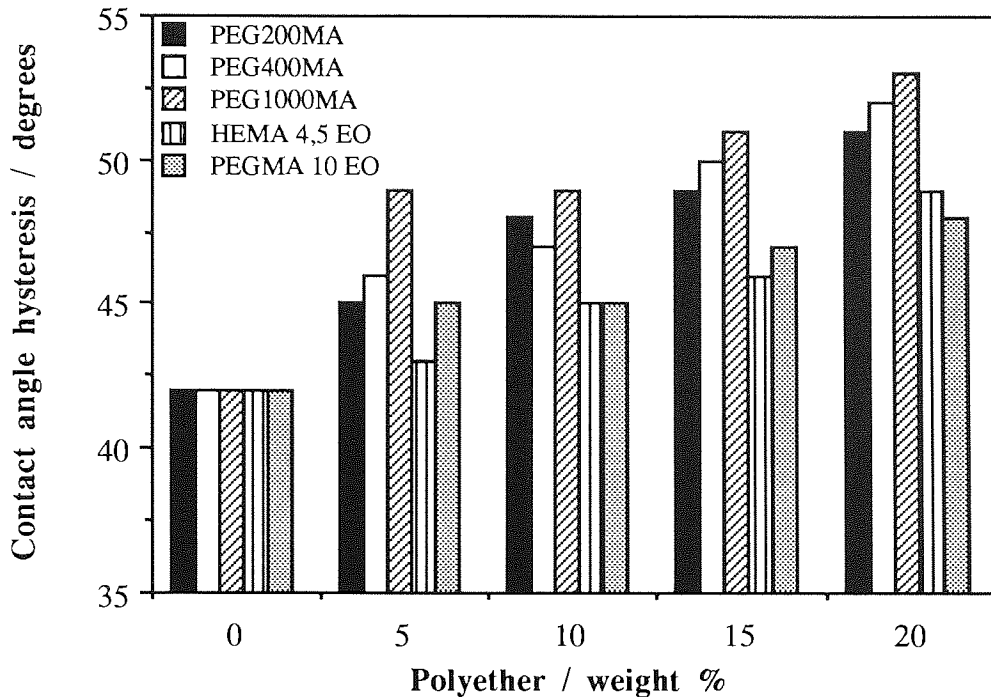


Figure 8.11 Contact angle hysteresis for HEMA membranes modified with polyethers

Figure 8.11 shows the contact angle hysteresis for HEMA copolymers modified with increasing concentrations of polyethers of increasing chain length. The hysteresis increases with increasing polyether concentration.

8.5.4 Conclusions

If the schematic representation of polyether chains at an interface is considered, as in Figure 8.12, it can be seen that in the hydrated state, such as in the case of polymer-water interface the polyether chains would be in an extended conformation. The hydrated extended conformation would result in the low receding contact angles observed in this work. Increases in the polyether chain length and concentration would further increase the hydrophilicity of the surface which would result in a lowering of the receding contact

angle. At an air interface the polyether chains thermodynamically favour water and would preferentially attempt to bury themselves within the bulk polymer and therefore the chains would be in a collapsed conformation. The collapsed conformation decreases the hydrophilicity of the polymer surface and results in the observed moderately high values of the advancing contact angle. Due to the collapsed conformation of the polyether chains some shielding of the bulk polymer would occur. The amount of shielding in the collapsed state would increase with increasing concentration and chain length of the polyether. This results in the decrease observed in the value of the advancing contact angle. The results obtained for the values of the dynamic advancing and receding contact angles are consistent with the model of polyether chains at the polymer surface presented in Figure 8.12

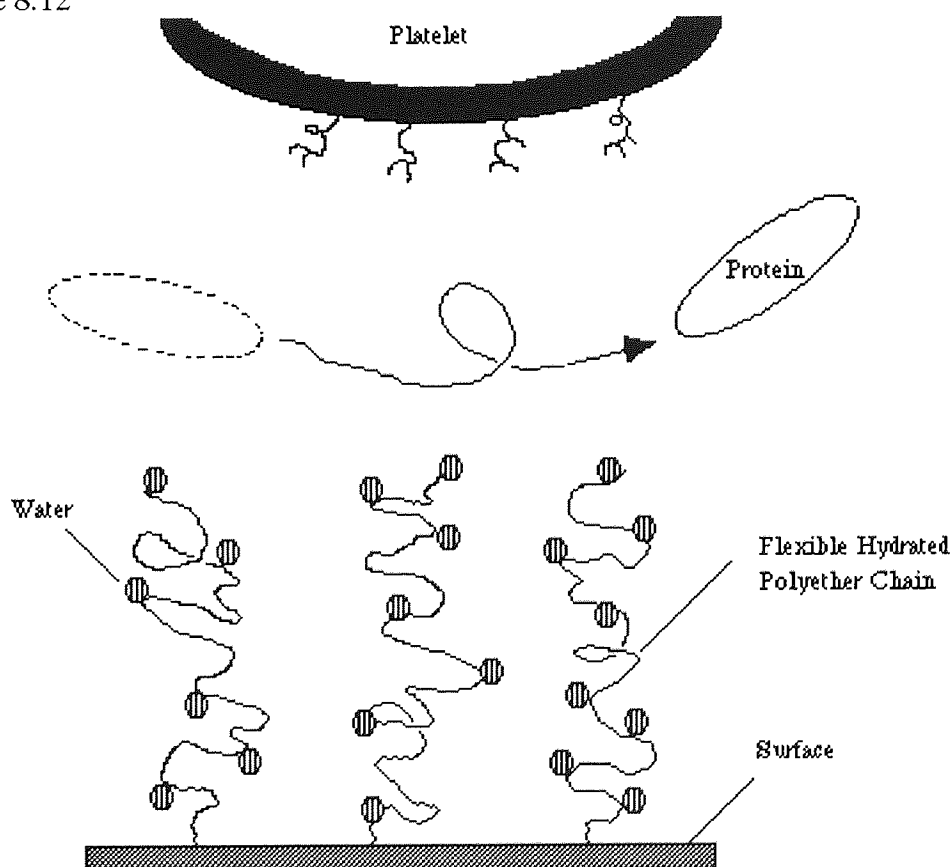


Figure 8.12 Diagrammatic representation of hydrated polyether chains at a polymer surface

8.6 Spoilation Characteristics of HEMA Membranes Modified with Poly(ethylene oxide)

8.6.1 Introduction

The use of polyethers in reducing protein absorption on to hydrogel surfaces is well known. The membranes prepared in this work incorporated methoxy and hydroxy terminated derivatives of polyethers and the aim of this work was to study the spoilation characteristics of these modified materials.

8.6.2 Protein Spoilations

The poly(HEMA) hydrogels modified with the series of methoxy and hydroxy terminated polyethers were cut in to disks of 1 cm in diameter. Their absorption by ultraviolet absorption spectroscopy between 200 and 400 nm and the readings at 280 nm were recorded as blanks. The disks were spoiled in 3 ml solutions of 0.5 mg/ml lysozyme and lactoferrin with frequent shaking at room temperature for 72 hours. The samples were removed from the protein solutions and rinsed once with distilled water to remove any loose surface protein. The U.V. absorbances at 280 nm were then measured using the method described in Chapter 2. The amount of protein absorbed on to the hydrogel was then obtained from a calibration graph obtained for a standard series of protein solutions.

8.6.3 Results

The results of the UV protein absorption are presented in Figures 8.13 and 8.14. Figure 8.13 illustrates the results for the adsorption of lysozyme to HEMA membranes modified with hydroxy and methoxy terminated polyethers. It can be seen that the amount of adsorption decreases with methoxy terminated polyether incorporation and that the quantity of adsorption is further decreased with increasing chain length and increasing amount of the methoxy terminated polyether. However, the amount of lysozyme adsorption is seen to increase with the incorporation of hydroxy terminated polyethers and further increases with increasing chain length and amount of these polyethers.

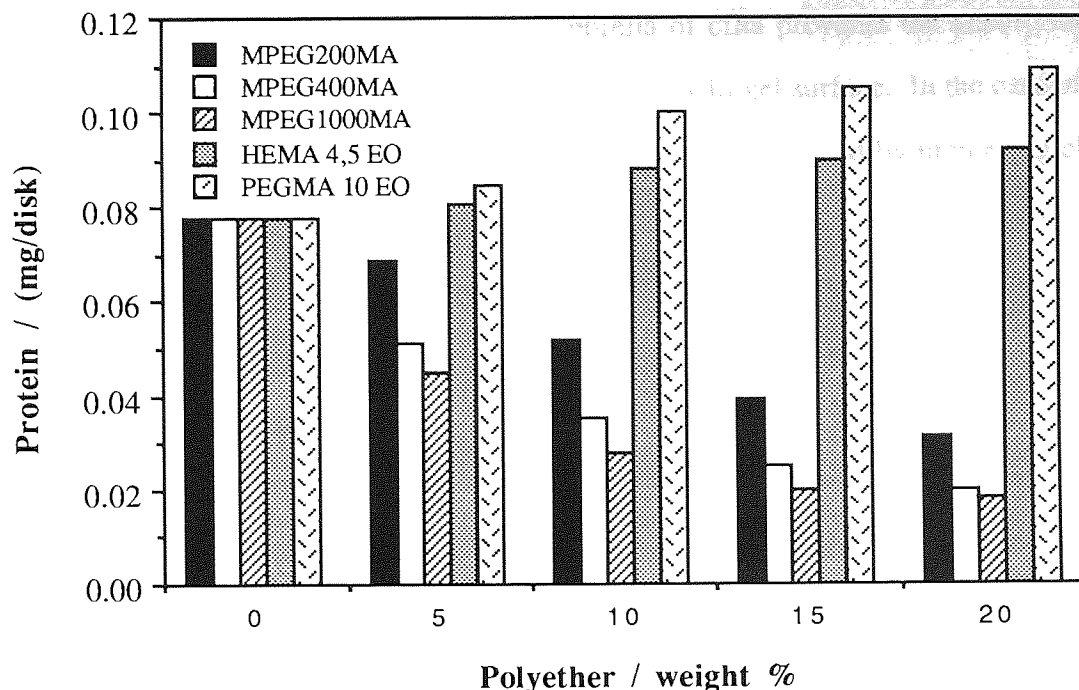


Figure 8.13 Adsorption of lysozyme to HEMA membranes modified with increasing amounts of polyethers

Figure 8.14 shows the adsorption of lactoferrin to HEMA membranes modified with hydroxy and methoxy terminated polyethers. For the incorporation of methoxy terminated polyethers it can be seen that the quantity of lactoferrin adsorbed is decreased. Increasing the chain length and amount of methoxy terminated polyether results in a further decrease in the amount of protein adsorbed. In the case of the hydroxy terminated polyethers it can be seen that the amount of protein adsorbed is increased with their incorporation and that the levels of adsorption are enhanced with increasing chain length and proportion of the hydroxy terminated polyether. Comparison of Figures 8.13 and 8.14 indicate that the levels of lactoferrin adsorbed are less than the amounts of lysozyme adsorbed.

The results of lysozyme and lactoferrin adsorption to the modified HEMA membranes are consistent with the models proposed for polyether modified hydrogels. The model suggests that incorporation of polyether chains expressed at the hydrogels surface produce

a highly mobile, protective umbrella (as shown in Figure 8.12) which mimic the glycocalyx of natural cell surfaces. This umbrella of cilia prevents the adsorption of proteins by excluding them from a volume above the hydrogel surface. In the case of the methoxy terminated polyethers this protective umbrella is enhanced by increasing chain length, because the methoxy terminus does not complex with the polyether chain and therefore the polyether chains maintain their extended conformation. However, in the case of the hydroxy terminated polyethers the effectiveness of these molecular cilia is greatly reduced because of internal complexation of the terminal hydroxyl group with the polyether chain. This complexation is more likely with increased polyether chain length and therefore protein adsorption is enhanced. The higher levels of lysozyme adsorption compared to lactoferrin would be expected because of its smaller size and higher charge.

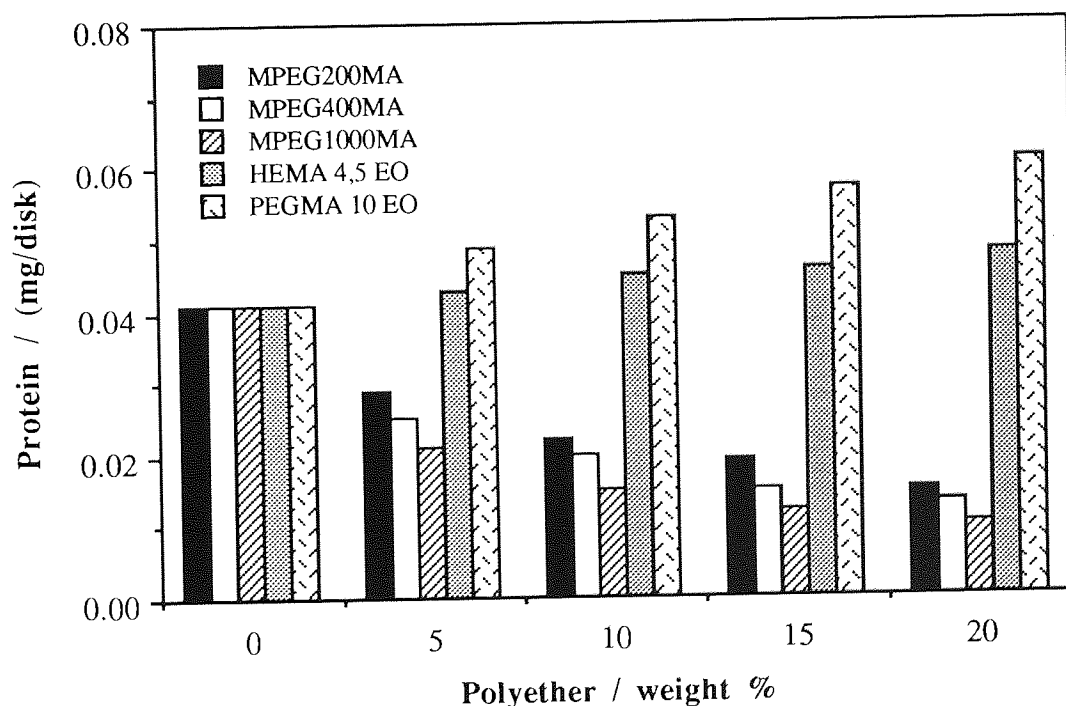


Figure 8.14 Adsorption of lactoferrin to HEMA membranes modified with increasing amounts of polyethers

8.6.4 Conclusion

In conclusion it was observed that protein adsorption was decreased with the incorporation of methoxy terminated polyethers and increased with hydroxy terminated polyethers.

8.7 Examination of the Surfaces of HEMA Hydrogels Modified with Polyethers

8.7.1 SEM Examination of Surfaces of Hydrogels Modified with Linear Polyethers

Scanning electron microscopy (SEM), was initially carried out to look at the surfaces of hydrogel materials. The HEMA hydrogel samples modified with polyethers were dehydrated and vacuum dried to remove all traces of water. The samples were gold-palladium coated and examined using a scanning electron microscope, Stereoscan model from Cambridge Instruments, with an accelerating voltage of 10-25 kV. The SEM micrographs obtained are presented in Figures 8.15 - 8.17.



Figure 8.15 SEM micrograph of the surface of a HEMA hydrogel modified with 20 weight% of PEG1000MA

8.7.2 Results

Figure 8.15 shows the micrograph obtained for a HEMA hydrogel modified with a polyether chain of 1000 molecular weight. Immediately apparent are the clusters on the hydrogel surface. However for lower molecular weight polyethers, for example MPEG400MA, and MPEG200MA these surface characteristics are not observed, as seen in Figures 8.16 and 8.17.



Figure 8.16 SEM micrograph of the surface of a HEMA hydrogel modified with 20 weight% of PEG400MA



Figure 8.17 SEM micrograph of the surface of a HEMA hydrogel modified with 20 weight% of PEG200MA

Previous elevations in the glass transition temperature results of polyether modified HEMA copolymers, suggested the possibility of crystalline regions produced by the longer chain polyethers. The chain length corresponded to a polyether chain length of 1000 molecular weight. The T_g results provided further evidence of the formation of crystalline regions at the surface of the modified hydrogel membranes. However, for short or moderate chain polyethers this elevation in T_g was not observed.

8.7.3 XRD Examination of Hydrogels Modified with Linear Polyethers

To provide further evidence to support the observation of crystalline domains in polyether modified hydrogels, x-ray diffraction (XRD) was used to determine any degree of crystallinity in the samples. Measurements were obtained using a Philips PW1120 x-ray diffractometer.

8.7.4 Conclusions

SEM examination of hydrogel surfaces modified with linear polyethers revealed that the incorporation of polyether chains upto and including a molecular weight of 400 showed no signs of crystallite formation. However, polyethers of molecular weight 1000 incorporated into hydrogel polymers revealed white clusters at the hydrogel surface. These clusters could be attributed to crystallite formation.

XRD measurement of hydrogel surfaces modified with linear polyethers revealed that the incorporation of polyether chains upto and including a molecular weight of 400 gave no XRD signal due to polyether crystallinity within the hydrogel sample. However, polyethers of molecular weight 1000 incorporated into hydrogel polymers gave a signal corresponding to a proportion of crystallinity of 6%. These clusters were attributed to crystallite formation due to the polyether.

8.8 Summary

The sequence simulations of polyether modified HEMA copolymers indicated that as the molecular weight of the polyether increased, the reactivity of the polyether was decreased and therefore the sequence length of the polyether segments was increased.

The results presented in this work also showed that as the amount and molecular weight of the polyether was increased, the EWC increased because of the hydrophilicity of the polyether. The effect of an increase in the EWC was to reduce the mechanical properties of the polyether modified HEMA copolymers, because of the plasticising effect of the imbibed water.

The investigation of the surface properties of the polyether modified HEMA copolymers by dynamic contact angle measurement revealed an increase in contact angle hysteresis. The hysteresis increased with increasing amount and molecular weight of the polyether. This result was consistent with the previous hypothesis of polyether chains expressed at the

hydrogel copolymer surface. The spoolation results provided further evidence of the expression of polyether chains at the hydrogel surface, because the amount of protein deposited at the surface decreased with an increase in the amount and chain length of the polyether.

Further examinations of the modified HEMA copolymers by SEM and XRD revealed the formation of clusters, which were attributed to the crystallisation of the polyether. This effect was observed with the PEG1000MA and not PEG200MA and PEG400MA. The tendency towards crystallisation of the polyether was attributed to the molecular weight and the reactivity of the polyether.

These results highlight the importance of the reactivity of the monomer, as well as the molecular weight and hydrophilicity of a monomer and its effect on the physical characteristics of the final copolymer. The results in this work indicate that the use of polyethers in the modification of HEMA copolymers must be optimised if adverse effects, such as crystallite formation are to be avoided.

CHAPTER 9
CONCLUSIONS AND SUGGESTIONS
FOR FURTHER WORK

9.1 Conclusions

A range of hydrogel copolymers were synthesised which were based on 2-hydroxyethyl methacrylate, (HEMA) copolymerised with acryloylmorpholine, (AMO), N-vinyl pyrrolidone, (NVP) and N,N-dimethyl acrylamide, (NNDMA).

HEMA-NVP copolymers are known to produce copolymers possessing domains of one monomer type^{41, 114}, namely NVP and HEMA-NNDMA copolymers produce mechanically imperfect networks due to chain transfer reactions. Because of these factors, particular emphasis was placed on the sequence distributions, mechanical properties and surface properties of HEMA-AMO copolymers. A study of the physical characteristics of HEMA-AMO copolymers has been completed.

The properties of crosslinked AMO copolymers have not previously been studied, although the properties of linear AMO polymers have been previously mentioned¹²⁸. The reactivity of AMO has previously been determined and the Q-e values for this monomer have been quoted¹²⁸. The quoted Q-e values of AMO were used to produce a sequence simulation of HEMA-AMO copolymers by using the copolymer program and a comparison was made with the equivalent HEMA-NVP and HEMA-NNDMA copolymers.

The results of the sequence simulations indicated that a narrower distribution of sequence lengths was obtained for HEMA-AMO copolymers than HEMA-NVP copolymers. The results also showed that the reactivity behavior of AMO was similar to the structurally related NNDMA. Because of these factors it was essential to extend the investigation of AMO to the physical characteristics of hydrogel membranes incorporating this monomer.

The characterisation of the equilibrium water contents, (EWC's) of HEMA-AMO, HEMA-NVP and HEMA-NNDMA copolymers showed that the hydrophilicity of the nitrogen containing monomers decreased in the order NNDMA>NVP>AMO. However, although

AMO was shown to be the least hydrophilic of these three monomers it was shown that a greater proportion of AMO was incorporated into its copolymers compared to the equivalent NVP copolymers. The more efficient conversion of initial feed ratio to copolymer composition of the AMO copolymers, resulted in EWC's of the AMO copolymers which were comparable to the equivalent NVP copolymers. Overall, it was concluded that AMO was sufficiently hydrophilic to produce hydrogel membranes with high water contents.

The water binding results of HEMA-AMO copolymers were interesting because they showed the greatest proportion of non-freezing water was obtained using AMO in preference to NVP or NNDMA. As water structuring has previously been shown to affect the amount and conformation of adsorbed proteins¹⁹⁰, it was concluded that the combination of the strong water structuring characteristics of AMO and the greater reactivity of AMO to vinyl polymerisations than the commercially used NVP, highlighted the potential of AMO as a hydrophilic monomer for use in hydrogel copolymers where a combination of high equilibrium water content and low amounts of protein adsorption would be required.

Further characterisation of the potential of AMO was undertaken by an investigation of the surface properties of its copolymers with HEMA. The surface properties were studied on both a macroscopic and a molecular scale. The macroscopic properties were examined using contact angle measurements. The results of the contact angle determinations and the subsequent surface energy results illustrated that the polar component of the surface free energy and the total surface free energy was greatest for HEMA-AMO copolymers than either HEMA-NVP or HEMA-NNDMA copolymers. This was attributed to the ring oxygen atom in the AMO ring structure.

The surface properties were investigated on a molecular level using *in vitro* spoolation studies. The systematic study of the effects of the copolymer composition on the amount

of protein and lipid adsorption, illustrated that the amount of adsorption decreased with increasing proportion of AMO. The results also provided evidence that the amounts of proteins and lipids adsorbed to HEMA-AMO copolymers was less than the amounts detected on the surface of HEMA-NVP and HEMA-NNDMA copolymers. The lower levels of adsorption could not be attributed to any one characteristic of the HEMA-AMO copolymers. Therefore it may be concluded that the observed lower levels of adsorption were due to the combination of the sequence distribution, water binding capability and surface properties of the HEMA-AMO copolymers.

Although the preliminary results of the study of AMO were encouraging, the behavior of the hydroxy monomer, HEMA was not ideal with respect to the sequence distributions of the AMO copolymers. The sequence simulation of a HEMA-AMO copolymer indicated that there was the formation of a terminal block of one monomer type, albeit of shorter sequence length than the equivalent NVP copolymer. The structural characteristics of the hydroxy monomer were therefore investigated, so as to attempt to produce a narrower distribution of sequence lengths in a copolymer with AMO. The hydroxy monomers used for the study were 2-hydroxyethyl methacrylate, (HEMA), 2-hydroxypropyl methacrylate, (HPMA) and 2-hydroxypropyl acrylate, (HPA).

The sequence distributions of hydroxy monomer-acryloylmorpholine copolymers were effectively optimised to produce a copolymer composed of narrow distributions of sequence lengths with alternating monomer units resulting in a copolymer free from chemical domains of one molecular type. The tendency of the hydroxy monomers to alternate with AMO decreased in the order HPA > HPMA > HEMA. Of the three hydroxy monomers the HEMA was too unreactive towards AMO and resulted in a terminal block of AMO. In the case of HPA the alternation was to the opposing extreme such that a terminal block of HPA was produced. Whereas the HPMA-AMO system resulted in an alternating copolymer structure undominated by one monomer type.

Copolymer membranes with high water contents (>55%) were obtained by copolymerising a hydroxy monomer with AMO. It was found that the greatest proportions of non-freezing water were obtained in HEMA-AMO copolymers. The values of the equilibrium water contents dominated the mechanical properties of the HEMA-AMO, HPMA-AMO and HPA-AMO copolymers. The HPA-AMO copolymers were mechanically the weakest of the three copolymer systems because they possessed the largest proportions of freezing water which plasticised the copolymer network.

The surface properties of the dehydrated copolymers were consistent with the formation of a molecular complex which orientates the polar groups towards the bulk of the polymer and away from the air interface. The surface properties of the hydrated copolymers indicated that the HEMA-AMO copolymers were more polar than the HPMA-AMO and HPA-AMO copolymers.

The requirements for decreased adsorption of biological species requires a narrow distribution of sequence lengths, a higher proportion of non-freezing water and a polar copolymer. No one of the three hydroxy monomers satisfied all the criteria. The indication was that the structural characteristics of the hydroxy monomers indicated that a hydroxy monomer with a longer side chain length, such as a propyl group would produce the desired reactivity with AMO. However, the results of the physical characteristics of the hydroxy monomer-AMO copolymers indicated that the increased side chain length would also require the addition of another polar group to maintain the water binding, mechanical and surface properties. A monomer such as 1,2-dihydroxypropyl methacrylate would have the structure to potentially meet these requirements.

1,2-dihydroxypropyl methacrylate would be expected to have a reactivity more similar to HPMA than HEMA because of the increased length of the side chain which would produce a narrower distribution of sequence lengths. However, 1,2-dihydroxypropyl methacrylate would be expected to have a higher proportion of non-freezing water than

HPA or HPMA because of the presence of an extra hydroxyl group. Therefore 1,2-dihydroxypropyl methacrylate would be expected to exhibit the best compromise of the characteristics of sequence distribution, water binding, mechanical and surface properties exhibited by the hydroxy monomers presented in this work. This monomer could be the subject of future work with AMO containing copolymers.

One problem common to hydrogel copolymers is the relatively poor mechanical strength associated with polymer networks which imbibe water. Studies were made firstly on the effect of sequence distribution on the mechanical properties of hydrogel copolymers and secondly on the effect of the amount and chain length of the crosslinking monomer.

Two series of copolymer membranes composed of firstly NVP, then AMO hydrophilic monomers copolymerised with a series of hydrophobic monomers, produced sets of copolymers which had comparable equilibrium water contents. However, a dramatic difference was observed in the values obtained for the mechanical properties. It was found that for a hydrophobic and a hydrophilic monomer of widely differing radical reactivity ratios, such as HEMA-NVP, the resulting copolymer exhibited greater elastic modulus, (E_m) and tensile strength, (T_s) than an equivalent copolymer system which possessed radical reactivity ratios that were of similar value to one another, in this case HEMA-AMO.

Observation of the copolymer sequences showed that the NVP copolymers had less tendency to produce an alternating copolymer structure. This resulted in the production of hydrophobic domains which were impenetrable by water and as a result reinforced the hydrogel structure. The reinforcement increased the tensile strength of the copolymers compared to systems with equivalent equilibrium water contents.

It was possible to detect the hydrophobic domains by observation of their glass transition temperatures using differential scanning calorimetry, (DSC). The hydrophobic domains

appeared not to be formed once the proportion of hydrophobic monomer was less than 15 weight% of the total composition of the copolymer. Otherwise the level of hydration along the copolymer chain was then thermodynamically unfavourable for hydrophobic-hydrophobic interactions to occur and therefore produce hydrophobic domains.

A study of the effect of the amount and chain length of the crosslinking monomer has been carried out. The crosslinking monomers used in Chapter 7 were selected because their chemical types had been shown to enhance the compatibility of copolymer networks with biological components by decreasing the amount of adsorbed species at hydrogel surfaces. The study was undertaken to determine if the mechanical properties of a hydrogel could be increased while at the same time maintaining its equilibrium water content, nor increasing the interaction with biological components.

The results obtained indicated that an increase in the polyether chain length of EGDMA to a minimum number of ethylene oxide units resulted in an increase in the mechanical properties of a hydrogel while at the same time increasing the value of its equilibrium water content. This effect was observed for a minimum chain length of 20 ethylene oxide repeat units, which corresponded to the PEG1000DMA crosslinking monomer.

Because poly(ethylene oxides) are known to sequester metal cations, any interaction between the polyethers and a metal cation could potentially lead to biointolerance of the polyether modified materials. The results of ion permeability studies suggested that for the cross-linker chain lengths up to and including PEG1000DMA interaction of a metal cation with the polyether did not occur.

The initial deposition studies of the HEMA membranes modified with polyether cross-linkers indicated that the quantities of proteins and lipids deposited decreased with increasing polyether chain length. This effect was attributed to the increased polarity of the crosslinker associated with increasing polyether chain length. It was also evident that

for the HEMA-PEG1000DMA copolymers that the amount of deposition did not increase with increasing amount of the cross-linking monomer.

The results suggested that the mechanical properties of a hydrogel membrane could be increased while at the same time increasing the hydrogel equilibrium water content. This was achieved by the use of polyether cross-linkers of a minimum chain length, nominally 20 ethylene oxide repeat units. Permeability measurements and protein and lipid interaction studies illustrated that the PEG1000DMA, used to achieve the increase in strength and water content, did not adversely interact with biological species.

The literature survey illustrated that the incorporation of low levels of ionic charge were effective in enhancing the thrombogenicity of polymers for blood contacting applications. In the work presented within this thesis a range of vinyl copolymers were prepared which incorporated monomers with a pendant charge. It was observed that the water binding properties, mechanical properties and surface properties of poly(HEMA) hydrogel membranes were modified with small quantities (<5weight%) of a charged monomer. The effect of incorporating charge within a poly(HEMA) hydrogel increased the equilibrium water content because of the increased polar nature of the resulting copolymer and decreased the mechanical properties due to the plasticising effect of the imbibed water. Although very low levels of 1-2 weight% of charged monomer were shown to enhance the mechanical characteristics of the material by reducing the proportion of elastically ineffective chains within the copolymer network.

To evaluate the significance of charged groups on the surface properties of hydrogels both the surface properties were characterised on macroscopic and molecular level. On a macroscopic level the surface properties of the dehydrated and hydrated copolymers possessing charged monomer units were investigated by the contact angle techniques. The dehydrated surface properties were typical of the behaviour of hydroxyalkyl methacrylates, exhibiting polar group orientation towards the bulk of the polymer and

hydrophobic group expression at the copolymer/air interface. However, this behavior was modified by the inclusion of a monomer with pendant groups on each side of the backbone. Therefore polymer reorientation by backbone rotation still resulted in a polar group being expressed at the interface.

The hydrated surface properties were typical of polar group expression at the surface. It would be expected that expression of the charged monomer at the surface of the hydrogel would govern the interaction of the material with charged biological species such as proteins. It was found that the incorporation of negative charge into HEMA copolymers caused positively charged proteins such as lysozyme to be adsorbed to a greater degree, while the incorporation of positively charged monomers enhanced the adsorption of negatively charged proteins to the surface of the copolymer. The amount of protein adsorbed was also dependant on the equilibrium water content, (EWC) of the hydrogels studied because the mobility of the protein would be greater at higher values of the EWC. This behavior exhibited by hydrogel copolymers modified with charged groups would enable hydrogel copolymers to be designed which preferentially adsorbed or repelled proteins of a particular charge.

The literature survey showed that polyethers had been investigated extensively in their use for the enhancement of the biocompatibility of polymers for blood contacting applications. Previous work at Aston had shown the potential of HEMA copolymers modified with polyethers, but no consideration of the sequence distribution of polyethers had been considered.

The sequence simulations of the HEMA copolymers modified with linear polyethers indicated that blocks of polyether could potentially form, when using a polyether with molecular weight of 1000 or greater. As polyethers are known to crystallise, this could lead to biointolerance of the modified material.

SEM examination of hydrogel surfaces modified with linear polyethers revealed that the incorporation of polyether chains upto and including a molecular weight of 400 showed no signs of crystallite formation. However, examination of hydrogels modified with polyethers of molecular weight 1000, revealed white clusters at the hydrogel surface. These clusters could be attributed to crystallite formation of the polyether.

XRD measurement of hydrogel surfaces modified with linear polyethers, revealed that the incorporation of polyether chains upto and including a molecular weight of 400 gave no signal intensity which could be due to crystallinity within the sample. However, polyethers of molecular weight 1000 incorporated into hydrogel polymers, gave a signal which corresponded to a proportion of crystallinity of 6%. The signal could be attributed to crystallite formation of the polyether.

The results of the investigation highlighted the potential of polyethers for their use in enhancing the compatibility of hydrogels with a biological environment and also showed that careful choice must be made of the polyether chain length.

9.2 Suggestions for Future Work

In general acryloylmorpholine produces vinyl based hydrogels which have a high EWC and surface properties which enhance the compatibility of the hydrogel with biological species. In this work acryloylmorpholine has been copolymerised with 2-hydroxyethyl methacrylate only. Therefore the work could be extended to investigate the properties of acryloylmorpholine with other vinyl based monomers. Of particular interest would be copolymers of acryloylmorpholine with vinyl monomers containing a pendant group with strong hydrogen bonding capability, for example acrylic acid or acrylamide. This would be of interest because of the position of the oxygen atom in the pendant ring of the acryloylmorpholine which may impart unique donor-acceptor properties within hydrogel copolymers of this type.

The sequence distribution has been shown to play a role in its effect on the mechanical and surface properties of hydrogel copolymers. It could therefore be possible to quantify the significance of the sequence distribution by studying a single functional group of varying sequence lengths and observing the effect on the cell or protein adhesiveness. Information derived from such a study could be compared against control materials such as poly(HEMA) or poly(Styrene) materials, which are known to be non-adhesive towards cells.

The effect of charged groups at hydrogel surfaces has been studied and the results have shown that both the charge of the surface and the charge within the biological environment affect the adsorption of biological species to those surfaces. It would be interesting to study the effect of negative and positive charged groups, either separately or combined with each other, over the full range of pH to investigate their adsorption characteristics. It may also be useful to study the permeability of ions through hydrogel membranes modified with charged groups to study any permselectivity characteristics that such materials might possess.

Finally, the significance of polyethers in the role in the design of biomedical materials has been highlighted. The effect of mucin balling on hydrogel surfaces has been mentioned and it is believed that frictional and mechanical interaction of the hydrogel surface with the biological environment lead to the development of this characteristic. It would be of potential use if the frictional characteristics of hydrogels modified with polyethers were studied systematically, to characterise this situation. Frictional investigations could also be extended to charged monomer groups at the surface of hydrogels and also correlated with the water structuring effects of monomers.

REFERENCES

1. Wichterle, O. and Lim, D., Hydrophilic gels for biological use, Nature (London) 1960, 185, 117-118
2. Andrade, J.D., Hydrogels for Medical and Related Applications, ACS Symposium Series 1976, 31, ACS
3. Noguchi, T., Yamamuro, T., Oka, M., Kumar, P., Kotoura, Y., Hyon, S. and Ikada, Y., Poly(vinyl alcohol) hydrogel as a artificial articular cartilage; evaluation of compatibility, J. Appl. Biomats. 1991, 2, 101-107
4. Roorda, W.E., Boddle, H., de Boer, A.G. and Junginger, H.E., Synthetic hydrogels as drug delivery systems, Pharm. Wk. Bul. (Sci) 1988, 12, 165-189
5. Pedley, D.G., Skelly, P.J. and Tighe B.J., Hydrogels in Biomedical Applications, Bri. Polym. J. 1980, 12, 99-110
6. Park, G.B., Burn wound coverings - A review, Biomat. Med. Dev. and Art. Org. 1978, 6, 29-37
7. Sperling, L. H., Interpenetrating Polymer Networks and Related Materials, Plenum Press, New York 1981.
8. Jeronimidis, G., Natural Composite Materials, Advances in Materials Science and Engineering, Ed. Cahn, R. W., Pergamon Press 1989
9. Andrade, J. D., Ed., Hydrogels for Medical and Related Applications, ACS Symposium Series 1976, 31, ACS
10. Wichterle, O., Hydrogels, in Encyclopedia of Polymer Science and Technology, Mark, H. and Gaylord, N., Eds., Interscience, New York, 1971, 15, 273.
11. Ratner, B. D., Biomedical applications of hydrogels, a review and critical appraisal, in Biocompatibility of Clinical Implant Materials, Vol. 2, Williams, D. F., Ed., CRC Press, Boca Raton, FL, 1981, 145
12. Tighe, B. J., Hydrogel materials: the patents and the products (Parts I and II), Optician 1989, 17, 197 (5202), and 17, 197 (5207)
13. Pedley, D. G., Skelly, P. J., and Tighe, B. J., Hydrogels in Biomedical applications, Br. Polym. J. 1980, 12, 99-110

14. Corkhill, P.H., Jolly, A.M., Ng, C.O. and Tighe, B.J., Synthetic hydrogels I: Hydroxyalkyl acrylate and methacrylate copolymers - water binding studies, *Polymer* 1987, 28, 1758-1766
15. Lee, H.B., Jhon, M.S. and Andrade, J.D., Nature of water in synthetic hydrogels I. Dilatometry, specific conductivity and differential scanning calorimetry of polyhydroxyethyl methacrylate, *J. Colloid Interface Sci.* 1975, 51, 225-231
16. Jhon, M.S. and Andrade, J.D., Water and hydrogels, *J. Biomed. Mater. Res.* 1973, 7, 509-522
17. Hatakeyama, T., Yamauchi, A. and Hatakeyama, H., Studies on bound water in poly(vinyl alcohol) hydrogel by DSC and FT-NMR, *Eur. Polym. J.* 1984, 20, 61-64
18. Tanguchi, Y. and Horigome, S., The states of water in cellulose acetate membranes, *J. Appl. Polym. Sci.* 1975, 19, 2743-2748
19. Roorda, W.e., de Bleyser, J., Junginger, H.E. and Leyte, J.C., Nuclear magnetic resonance relaxation of water in hydrogels, *Biomaterials* 1990, 11, 17-23
20. Nagura, M. and Ishikawa, H., State of water in highly elastic poly(vinyl alcohol) hydrogels prepared by repeated freezing and melting, *Polymer Comms.* 1984, 25, 313-314
21. Sung, Y.K., Pulse NMR and thermal analysis of water swelling polymers for biomedical applications, *Polymer* 1986, 10, 576-583
22. Yamada-Nosaka, A., Ishikiriya, K., Todoki, M. and Tanzawa, H., H-NMR studies on water in methacrylate hydrogels I., *J. App. Polym. Sci* 1990, 39, 2443-2452
23. Quinn, F.X., Kampff, E., Smyth, G. and McBrierty, V.J., Water in hydrogels 1. a study of water in poly(N-vinyl-2-pyrrolidone/methyl methacrylate) copolymers, *Macromolecules* 1988, 21, 3191-3198
24. Sung, Y.K., Gregonis, D.E., Jhon, M.S. and Andrade, J.D., Thermal and pulse NMR analysis of water in poly(2-hydroxyethyl methacrylate), *J. App. Polym. Sci.* 1981, 26, 3179-3728

25. Nagashima, N. and Suzuki, E.I., Studies of hydration by broad-line pulsed NMR, *App. Spec. Rev.* 1984, 20, 1-53
26. Carles, J.E. and Scallan, A.M., The determination of the amount of bound water within cellulosic gels by NMR spectroscopy, *J. App. Polym. Sci.* 1973, 17, 1855-1865
27. Kim, E.H., Jeon, S.I., Yoon, S.C. and Jhon, M.S., The nature of water in tactic poly(2-hydroxyethyl methacrylate) hydrogels, *Bull. Korean Chem. Soc.* 1981, 2, 60-66
28. Jhon, M.S., Hattori, S., Ma, S.M., Gregonis, D. and Andrade, J.D., The role of water in the osmotic and viscoelastic behavior of gel networks, *Polymer Preprints* 1975, 16, 281-285
29. Aizawa, M. and Suzuki, S., Properties of water in macromolecular gels III. Dilatometric studies of the properties of water in macromolecular gels, *Bull. Chem. Soc. Jpn* 1971, 44, 2967-2971
30. Pathmanathan, K. and Johari, P., Dielectric and conductivity relaxations in poly(hema) and of water in its hydrogels, *J. Polym. Sci: Part B: Polymer Phys.* 1990, 28, 675-689
31. Kim, E.H., Moon, B.Y., Jeon, S. and Jhon, M.S., The nature of water copolymer hydrogels, *Bull. Korean Chem. Soc.* 1983, 4, 251-256
32. Roorda, W.E., Bouwstra, J.A., de Vries, M.A. and Junginger, H.E., Thermal behavior of poly hydroxyethyl methacrylate (pHEMA) hydrogels, *Pharm. Res.* 1988, 5, 722-725
33. Roorda, W.E., Bouwstra, J.A., de Vries, M.A. and Junginger, H.E., The thermal analysis of water in p(HEMA) hydrogels, *Biomaterials* 1988, 9, 494-499
34. Nakamura, K., Hatakeyama, T. and Hatakeyama, H., Studies on bound water of cellulose by differential scanning calorimetry, *Textile Res. J.* 1981, 51, 607-613
35. Corkhill, P.H., Jolly, A.M., Ng, C.O. and Tighe, B.J., Synthetic hydrogels I. Hydroxyalkyl acrylate and methacrylate copolymers-water binding studies, *Polymer* 1987, 28, 1758-1766

36. Pedley, D.G. and Tighe, B.J., Water binding properties of hydrogel polymers for reverse osmosis and related applications, *Br. Polym. J.* 1979, 11, 130-136
37. Bouwstra, J.A., van Miltenburg, J.C., Roorda, W.E. and Junginger, H.E., Polymer-water interactions in crosslinked gels determined by calorimetric measurements, *Polym. Bull.* 1987, 18, 337-341
38. Frommer, M.A. and Lancet, D., Freezing and non-freezing water in cellulose acetate membranes, *J. App. Polym. Sci.* 1972, 16, 1295-1303
39. Takizawa, A. Kinoshita, T., Nomura, O., Tsujita, Y., Characteristics of water in copoly(methyl methacrylate-N-vinyl pyrrolidone) membranes. *Polym. J.* 1985, 17, 747-752
40. Hamilton, C.J., Transport phenomena in hydrogel membranes, Ph.D. Thesis, Aston University 1988
41. Corkhill, P.H., Novel Hydrogel Polymers, Ph.D. Thesis, Aston University 1988
42. Pathmanathan, K. and Johari, G.P., Dielectric and conductivity relaxations in poly(HEMA) and of water in its hydrogel, *J. Polym. Sci.-Part B Polym. Phys.* 1990, 28, 675-689
43. Hofer, K. and Johari, G.P., Dielectric studies of hydrogen bonding of aqueous ethylene glycol in a hydrogel, *Jou. of Chem. Soc.- Faraday Trans.* 1992, 88, 3047-3051
44. Kim, E.H., Jeon, S.I., Yoon, S.C. and Jhon, M.S., The nature of water in tactic poly(2-hydroxyethyl methacrylate) hydrogels, *Bull. Korean Chem. Soc.* 1981, 2, 60-66
45. Aizawa, M. and Suzuki, S., Properties of water in macromolecular gels III. Dilatometric studies of the properties of water in macromolecular gels, *Bull. Chem. Soc. Jpn.* 1971, 44, 2967-2971
46. Andrade, J.D., Hydrogels for Medical and Related Applications, ACS Symposium Series 1976, 31, ACS
47. Young, T., On the cohesion of fluids, *Phil. Trans. Roy. Soc. (London)* 1805, 95, 65-87

48. Dupre, A., *Theorie mechanique de la chaleur*, Gauthier Villars, Paris 1869, p369
49. Owens, D.K. and Wendt, R.C., Estimation of the surface free energy of polymers, *J. Appl. Polym. Sci.* 1969, 13, 1741-1747
50. Panzer, J., Components of solid surface free energy from wetting measurements, *J. Colloid and Interface Sci.* 1973, 44, 142-161
51. Hamilton, W.C., A technique for the characterisation of hydrophilic solid surfaces, *J. Colloid Interface Sci.* 1972, 40, 219-222
52. Hamilton, W.C., Measurement of the polar force contribution to adhesive bonding, *J. Colloid Interface Sci.* 1974, 47, 672-675
53. Fowkes, F.M., Additivity of intermolecular forces at interfaces I. Determination of the contribution to surface and interfacial tensions of dispersion forces in various liquids, *J. Phys. Chem.* 1963, 67, 2538-2541
54. Tamai, Y., Makuuchi, K. and Suzuki, M., Experimental analysis of interfacial forces at the plane surface of solids, *J. Phys. Chem.* 1967, 71, 4176-4179
55. Adamson, A.W., *Physical Chemistry of Surfaces*, 3rd Edn., Wiley-Interscience, New York, N.Y. 1976
56. Andrade, J.D., King, R.N., Gregonis, D.E. and Coleman, D.L., Surface characterisation of poly(hydroxyethyl methacrylate) and related polymers I. Contact angle methods in water, *J. Appl. Polym. Sci., Polym. Symp.* 1979, 66, 313-336
57. Kolarik, J. and Migliaresi, C., Mechanical properties of hydrophilic copolymers of 2-hydroxyethyl methacrylate with ethyl acrylate, n-butyl acrylate and dodecyl methacrylate, *J. Biomed. Mater. Res.* 1983, 17, 757-767
58. Migliaresi, C., Nicodemo, L., Nicolais, L., Passerini, P., Stol, M., Hrouz, J. and Cefelin, P., Water sorption and mechanical properties of 2-hydroxyethyl methacrylate and methyl methacrylate, *J. Biomed. Mater. Res.* 1984, 18, 137-146
59. Minnema, L. and Staverman, A.J., The validity of the theory of gelation in vinyl-divinyl copolymerisation, *J. Polym. Sci.* 1958, 29, 281-306

60. Turner, D.T., Schwartz, A., Graper, J., Sugg, H. and Williams, J.L., Highly water swollen hydrogels: vinyl pyrrolidone copolymers, *Polymer* 1986, 27, 1619-1625
61. Peppas, N.A. and Merrill, E.W., Development of semicrystalline poly(vinyl alcohol) hydrogels for biomedical applications, *J. Biomed. Mater. Res.* 1977, 11, 423-434
62. Corkhill, P.H. and Tighe, B.J., Synthetic hydrogels VII: high EWC semi-interpenetrating polymer networks based on cellulose esters and N-containing hydrophilic monomers, *Polymer* 1990, 31, 1526-1537
63. Nagaoka, S., Mechanical properties of composite hydrogels, *Polymer J.* 1989, 21, 847-850
64. Lopour, P., Vondracek, P., Janatova, V., Sulc, J. and Vacik, J., Silicone rubber hydrogel composites as polymeric biomaterials II. Hydrophilicity and permeability to water soluble low molecular weight compounds, *Biomaterials* 1990, 11, 397-402
65. Lee, J.W., Kim, E.H. and Jhon, M.S., The swelling and mechanical properties of tactic poly(HEMA), *Bull. Korean Chem. Soc.* 1983, 4, 162-169
66. Barnes, A., Corkhill, P.H. and Tighe, B.J., Synthetic Hydrogels: 3. Hydroxyalkyl acrylate and methacrylate copolymers: surface and mechanical properties, *Polymer* 1988, 29, 2191-2207
67. Huglin, M.B. and Zakaria, M.B., Thermodynamic interactions in copolymeric hydrogels, *Macromolecules* 1986, 19, 2986-2991
68. Davis, T.P., Huglin, M.B. and Yip, D.C.F., Properties of poly(NVP) hydrogels crosslinked with ethylene glycol dimethacrylate, *Polymer* 1988, 29, 701-705
69. Davis, T.P. and Huglin, M.B., Some mechanical properties of poly(HEMA) gels swollen in water/1,4 dioxane mixtures, *Makromol. Chemie Rap. Comms.* 1988, 9, 39-43
70. Davis, T.P. and Huglin, M.B., Studies on copolymeric hydrogels of NVP with HEMA, *Macromolecules* 1989, 22, 2824-2829

71. Janacek, J., Mechanical behaviour of hydroxyalkyl methacrylate polymers and copolymers, *J. Macromol. Sci.-Revs. Macromol. Chem.* 1973, C9, 1-47
72. Migliaresi, C., Nicolais, L. and Vinciguerra, R., Viscoelastic behaviour of water swollen HEMA/MMA networks, in *Biomaterials and Biomechanics 1983*, 403-404
73. Raab, M. and Janacek, J., Effect of chemical crosslinking on ultimate tensile properties of water swollen poly(HEMA) gels, *Intern. J. Polymeric Mater.* 1972, 1, 147-158
74. Peppas, N.A., Tear propagation resistance of semicrystalline polymeric networks, *Polymer* 1977, 18, 403-407
75. Jackson, A.P., Measurement of the fracture toughness of some contact lens hydrogels, *Biomaterials* 1990, 11, 403-407
76. Baker, D. and Tighe, B.J., Polymers in contact lens applications (VIII). The problem of biocompatibility, *Contact Lens J.* 1981, 10 (3), 3-14
77. Horbett, T.A., Protein adsorption on biomaterials, in *Biomaterials: Interfacial Phenomena and Applications*, Eds. Cooper, S.L. and Peppas, N.A., A.C.S. Symposium Series No. 199, A.C.S., Washington, D.C. 1982, 233-244
78. Horbett, T.A., Protein adsorption to hydrogels, in *Hydrogels in Medicine and Pharmacy Vol. I. Fundamentals*, Ed. Peppas, N.A., C.R.C. Press, Boca Raton, Florida 1986, 127-171
79. Ratner, B.D., Hoffman, A.S., Hanson, S.R., Harker, S.R. and Whiffen, J.D., Blood compatibility-water content relationships for radiation grafted hydrogels, *J. Polym. Sci. Polym. Symp.* 1979, 66, 363-375
80. Andrade, J.D., Interfacial phenomena and biomaterials, *Medical Instrumentation* 1973, 7, 110-120
81. Coleman, D.L., Gregonis, D.E. and Andrade, J.D., Blood-materials interactions: The minimum interfacial free energy and the optimum polar/apolar ratio hypothesis, *J. Biomed. Mater. Res.* 1982, 16, 381-393
82. Weathersby, P.K., Horbett, T.A. and Hoffman, A.S., Fibrinogen adsorption to surfaces of varying hydrophilicity, *J. Bioeng.* 1977, 1, 395-402

83. Castillo, E.J., Koenig, J.L., Anderson, J.M. and Lo, J., Characterisation of protein adsorption on soft contact lenses I. Conformational changes of adsorbed human serum albumin, *Biomaterials* 1984, 5, 319-325
84. Hosaka, S., Ozawa, H., Tanzawa, H., Ishida, H., Yoshimura, K., Momose, T., Magatani, H. and Nakajima, A., Analysis of deposits on high water content contact lenses, *J. Biomed. Mater. Res.* 1983, 17, 261-274
85. Horbett, T.A. and Hoffman, A.S., Bovine plasma protein adsorption on radiation-grafted hydrogels based on hydroxyethyl methacrylate and N-vinyl pyrrolidone, in *Applied Chemistry at Protein Interfaces, Advances in Chemistry Series, Vol. 145*, Baier, R.E., Ed., A.C.S., Washington D.C. 1975, 230
86. Norde, W., *Adv. Colloid Interface Sci.* 1986, 25, 341-385
87. Baier, R.E., Dutton, R.C. and Gott, V.L., Surface chemical features of blood vessels walls and of synthetic materials exhibiting thromboresistance, in *Advances in Experimental Medicine, Vol. 7, Surface chemistry of biological surfaces*, Plenum Press, New York, N.Y. 1970, 235-260
88. Hiatt, C.W., Shelokov, A., Rosenthal, E.J. and Galimore, J.M., Treatment of controlled pore glass with poly(ethylene oxide) to prevent the adsorption of rabies virus, *J. Chromatogr.* 1971, 56, 362-364
89. Nagaoka, S., *Polymers as Biomaterials*, Eds S.W. Shalaby *et al* , Plenum Press, New York, USA, 1984, 361-374.
90. Mori, Y., and Nagaoka, S., A new antithrombogenic material with long polyethylene oxide chains, *Trans. Am. Soc. Artif. Intern. Organs* 1982, 28, 459-463
91. Nagaoka, S., Hydrated dynamic surface, *Trans. Am. Soc. Intern. Organs* 1988, 10, 76-78.
92. Nakao, A., Mori, Y. and Nagaoka, S., Hemocompatibility of hydrogels with polyethylene oxide chains, *J. Biomat. Appl.* 1987, 2, 219-234.

93. Gombotz, W.R., Guanghui, W., Horbett, T.A. and Hoffman, A.S., Protein adsorption to poly(ethylene oxide) surfaces, *J. Biomed. Mater. Res.* 1991, 25, 1547-1562
94. Bailey, F.E., Jr. and Koleske, J.V., *Poly(ethylene oxide)*, Academic Press, New York, 1976.
95. Kellander, R. and Florin, E., Water structure and changes in thermal stability of the system poly(ethylene oxide) - water, *J. Chem. Soc. Faraday Trans.* 1981, 77, 2053-2060
96. Graham, N.B., *Biopolymers : Polymers for Biological Applications*, Piskin, E., Ed., Martinus Nijkoff 1986.
97. Nagaoka, S. and Nakao, A., Clinical application of antithrombogenic hydrogel with long poly(ethylene oxide) chains, *Biomaterials* 1990, 11, 119-123
98. Merrill, E.W. and Salzman, E.W., Polyethylene oxide as a biomaterial, *ASA/O J.* 1983, 6, 60-64
99. Andrade, J.D., Nagaoka, S., Cooper, S., Okano, T. and Kim, S.W., Surfaces and blood compatibility : Current hypotheses, *ASA/O J.* 1987, 10, 75-84
100. Lee, J.H., Kopecek, J. and Andrade, J.D., Protein-resistant surfaces prepared by PEO-containing block copolymer surfactants, *J. Biomed Mater. Res.* 1989, 23, 351-368
101. Nagaoka, S., Mori, Y., Takiundi, H., Yokota, K., Tanzawa, H. and Nishium, S., Interaction between blood components and hydrogels with poly(oxoethylene) chains, *Polymers as Biomaterials*, Eds., Shalaby, S.W., Hoffman, A.S., Ratner, B.D. and Herbett, T.A., Plenum Press , New York, 1984, 361-374
102. Grainger, D.W., Nojiri, C., Okano, T. and Kim, S.W., *In vitro* and *ex vivo* platelet interactions with hydrophilic-hydrophobic poly(ethylene oxide)-polystyrene multiblock copolymers, *J. Biomed. Mater. Res.* 1989, 23, 979
103. Lee, J.H., Kopecova, P., Kopecek, J. and Andrade, J. D., Surface properties of copolymers of alkyl methacrylates and their application as protein-resistant coatings, *Biomaterials* 1990, 11, 455-464

104. Okkema, A.Z., Grasel, T.G., Zarahala, R.J., Solomon, D.D. and Cooper, S.L., Bulk, surface and blood contacting properties of polyetherurethanes modified with PEO, *J. Biomat. Sci., Polymer Ed.* 1989, 1 (1), 43-62
105. Lee, J.H., Kopeckova, P., Kopecek, J. and Andrade, J.D., Surface properties of copolymers of alkyl methacrylates and their application as protein-resistant coatings, *Biomaterials* 1990, 11, 455-464
106. Andrade, J.D., Nagaoka, S., Cooper, T., Okano, T. and Kim, Am. Soc. Artif. Intern. Organs J. 1987, 10, 75-82
107. Sawyer, P.N. and Srinivasan, S., *Bull. N.Y. Acad. Med.* 1972, 48, 235
108. Lelah, M.D., Pierce, J.A., Lambrecht, L.K. and Cooper, S.L., Polyetherurethane ionomers: surface property/*ex-vivo* blood compatibility relationships, *J. Colloid Interf. Sci.* 1985, 104, 422-439
109. Walker, F.J. and Esmon, C.T., *Biochem. Biophys. Res. Commun.* 1978, 83, 1339-1341
110. Grasel, T.G., and Cooper, S.L., Properties and biological interactions of polyurethane anionomers : Effect of sulphonate incorporation, *J. Biomed. Mater. Res.* 1989, 23, 311-338
111. Salamone, J. C., Volksen, W., Israel, S.C., Olson, A.P. and Raia, D.C., *Polymer*, 1977, 18, 1058-1062
112. Okkema, A.Z., and Cooper, S.L., Effect of carboxylate and/or sulphonate ion incorporation on the physical and blood - containing properties of a polyetherurethane, *Biomaterials*, 1991, 12, 668-676
113. Jozefowicz, M. and Jozefonvicz, J., New approaches to anticoagulation heparin-like biomaterials, *ASA/O* 1985, 8, 218-222
114. Ashraf, N., Sequence distributions in free radical polymers, Ph.D. Thesis, Aston University 1993
115. O'Neill, C., Jordan, P., Riddle, P. and Ireland, G., Narrow linear strips of adhesive substratum are powerful inducers of both growth and total focal contact area, *J. Cell Sci.* 1990, 95, 577-586

116. Muramatsu, N., Yoshida, Y., Kataoka, Y., Ohshima, Y. and Kondo, T., Adsorption of negatively charged microcapsules to a poly(2-hydroxyethyl methacrylate) / polyamine graft copolymer surface, *J. Biomed. Mater. Res.* 1991, 2 (2), 139-146
117. Minoura, N., Aiba, S., Fujiwara, Y. and Koshisaki, N., Interactions of cultures of cells with membranes composed of random and block copolypeptides, *J. Biomed. Mater. Res.* 1989, 23, 267-279
118. Lai, Q., Protein and cell adhesion to block copolymer micro domains, Conference Proceedings, Fourth World Biomaterials Congress, Berlin, 1992, 450
119. Ostromyslensky, I.I., *J. Soc. Phys-chem. russe.* 1915, 47, 1928
120. Staudinger, H. *Ber. dtsh. chem. Ges.* 1920, 53, 1073
121. Alfrey, T. and Goldfinger, G., The mechanism of copolymerisation, *J. Chem. Phys.* 1944, 12, 205-209
122. Mayo, F.R. and Lewis, F.M., Copolymerisation I. A basis for comparing the behavior of monomers in copolymerisation; the copolymerisation of styrene and methyl methacrylate, *J. Am. Chem. Soc.* 1944, 66, 1594-1601
123. Hill, D.J.T., O'Donnell, J.H. and O'Sullivan, P.W., Analysis of the mechanism of copolymerisation, *Macromolecules* 1982, 15, 960-966
124. Bartlett, P.D. and Nozaki, K., The polymerisation of allyl compounds III. The peroxide induced copolymerisation of allyl acetate with maleic anhydride, *J. Am. Chem. Soc.* 1946, 68, 1495-1504
125. Whitmore, F.C., *Indust. Eng. Chem. (industr.)* 1934, 26, 94
126. Alfrey, T. and Price, C.C., Relative reactivities in vinyl copolymerisation, *J. Polym. Sci.* 1947, 2, 101-106
127. Varma, I.K. and Patnaik, S., Copolymerisation of 2-hydroxyethyl methacrylate with alkyl acrylates, *Eur. Polym. J.* 1976, 12, 259-261
128. Chiantore, O., *Makromol. Chem. Rapid Commun.* 1982, 3, 303-309
129. Vogel, A. I., *Elementary Practical Organic Chemistry*, Longmans, London 1966
130. Macleod, S.K., *Karl Fischer Titrations, Analytical Chemistry* 1991, 63, A 557

131. Trevett, A.S., The mechanical properties of hydrogel copolymers, Ph.D. Thesis, Aston University 1991
132. Alfrey, T. and Goldfinger, G., The mechanism of copolymerisation, *J. Chem. Phys.* 1944, 12, 205-209
133. Corkhill, P.H., Hamilton, C.J. and Tighe, B.J., The design of hydrogels for medical applications, *Critical Reviews in Biocompatibility* 1990, 5, 363-436
134. Okano, T., Nishiyama, S., Shinohara, I., Akaike, T. and Sakurai, Y., Interaction between plasma protein and microphase separated structure of copolymers, *Polymer J. (Tokyo)* 1978, 10, 223-228
135. O'Neill, C., Jordan, P., Riddle, P. and Ireland, G., Narrow linear strips of adhesive substratum are powerful inducers of both growth and total focal contact area, *J. Cell Sci.* 1990, 95, 577-586
136. Muramatsu, N., Yoshida, Y., Kataoka, Y., Ohshima, Y. and Kondo, T., Adsorption of negatively charged microcapsules to a poly(2-hydroxyethyl methacrylate) / polyamine graft copolymer surface, *J. Biomed. Mater. Res.* 1991, 2 (2), 139-146
137. Minoura, N., Aiba, S., Fujiwara, Y. and Koshisaki, N., Interactions of cultures of cells with membranes composed of random and block copolypeptides, *J. Biomed. Mater. Res.* 1989, 23, 267-279
138. Lai, Q., Protein and cell adhesion to block copolymer micro domains, Conference proceedings, Fourth World Biomaterials Congress, Berlin, 1992, 450
139. Reddy, B.S.R., Arshady, R. and George, M.H., Copolymerisation of N-vinyl-2-pyrrolidone with 2,4,5-trichlorophenyl acrylate and with 2-hydroxyethyl methacrylate; Reactivity Ratios and Molecular Weights, *Eur. Polym. J.* 1985, 21, 511-515
140. Al-Issa, M.A., Davis, T.P., Huglin, M.B. and Yip, D.C.F., Copolymerisations involving N-vinyl-2-pyrrolidone, *Polymer* 1985, 26, 1869-1874
141. North, A.M. and Scallan, A.M., The Free Radical Polymerization of N,N-dimethyl acrylamide, *Polymer* 1964, 5, 447-455

142. Alfrey, T. and Price, C.C., *Journal of Polym. Sci.* 1947, 2, 101-105
143. Evans, M.G., Gergeley, J. and Seaman, E.C., *J. Polym. Sci.* 1948, 3, 866-872
144. Pedley, D.G. and Tighe, B.J., Water binding properties of hydrogel polymers for reverse osmosis and related applications, *Br. Polym. J.* 1979, 11, 130-136
145. Coleman, D.L., Gregonis, D.E. and Andrade, J.D., Blood-materials interactions: The minimum interfacial free energy and the optimum polar / apolar ratio hypothesis, *J. Biomed. Mater. Res.* 1982, 16, 381-391
146. Andrade, J.D., Interfacial phenomena and biomaterials, *Medical Instrumentation* 1973, 7, 110-120
147. Holly, F.J. and Refojo, M.F., Wettability of hydrogels. I. Poly(2-hydroxyethyl methacrylate), *J. Biomed. Mater. Res.* 1975, 9, 315-322
148. Thomas, K.D., Biological interactions with synthetic polymers, Ph.D. Thesis, Aston University 1988
149. Franklin, V.J., Lipoidal species in ocular spoilage processes, Ph.D. Thesis, Aston University 1990
150. Mayo, F.R. and Walling, C., *Chem. Rev.* 1950, 46, 191-198
151. Evans, M.G., Gergeley, J. and Seaman, E.C., *J. Polym. Sci.* 1948, 3, 866-872
152. Barnes, A., Corkhill, P.H. and Tighe, B.J., Synthetic hydrogels 3. Hydroxyalkyl acrylate and methacrylate copolymers: surface and mechanical properties, *Polymer* 1988, 29, 2191-2202
153. Brandrup, J. and Immergut, E.H., *Polymer Handbook* 3rd Ed., Wiley Interscience 1989
154. Oxley, H.R., Hydrogels containing linear and cyclic polyethers, Ph.D. Thesis, Aston University 1991
155. Corkhill, P.H. and Tighe, B.J., Synthetic Hydrogels: 7. High EWC semi-interpenetrating polymer networks based on cellulose esters and N-containing hydrophilic monomers, *Polymer* 1990, 31, 1526-1537
156. Al-Issa, M.A., Davis, T.P., Huglin, M.B. and Yip, D.C.F., Copolymerisations involving N-vinyl-2-pyrrolidone, *Polymer* 1985, 26, 1869-1874.

157. Huglin, M.B. and Mahmoud, M.A.-M. Rehab., Mechanical and thermodynamic properties of butyl acrylate-N-vinyl pyrrolidone hydrogels, *Polymer* 1987, 28, 2200-2206
158. Fougnot, C., Jozefonvicz, J., Samama, M. and Bara, L., New heparin like insoluble materials: Part I, *Ann. Biomed. Eng.* 1979, 7, 429-439
159. Fougnot, C., Jozefonvicz, J., Samama, M. and Bara, L., New heparin like insoluble materials: Part II, *Ann. Biomed. Eng.* 1979, 7, 441-450
160. Santerre, J.P., VanderKamp, N.H. and Brash, J.L., Effect of sulphonation of segmented polyurethanes on the transient adsorption of fibrinogen from plasma: possible correlation with anticoagulant behavior, *Trans. Soc. Biomat.* 1989, 12, 113-119
161. Treloar, L.R.G., *The Physics of Rubber Elasticity* 1975, Oxford University Press
162. Hasa, J., Ilvasky, M. and Dusek, K., Deformational, Swelling and Potentiometric Behaviour of Ionized Poly(methacrylic acid) Gels. I Theory, *J. Polym. Sci.-Phys.* 1975, 13, 253-262
163. Oppermann, W., Rose, S. and Rehage, G., The Elastic Behaviour of Hydrogels, *British Polym. J.* 1985, 17, 175-180
164. Norde, W., *Adv. Colloid Interface Sci.* 1986, 25, 341-385
165. Sariri, R., Tear Protein Interactions with Hydrogel Contact lenses, Ph.D. Thesis, Aston University, 1995
166. Okano, T., Nishiyama, S., Shinohara, I., Akaike, T., Sakuri, Y., Kataoka, K. and Tsuruta, T., Effect of hydrophilic and hydrophobic microdomains on mode interaction between block polymer and blood platelets, *J. Biomed. Mater. Res.* 1985, 15, 393-402
167. Tian, Y., Zhu, S., Hamielec, A.E., Fulton, D.B. and Eaton, D.R., Conformation, environment and reactivity of radicals in copolymerisation of methyl methacrylate / ethylene glycol dimethacrylate, *Polymer* 1992, 33, 384-390

168. Suzuki, T. and Tomono, T., Syntheses of monomethoxy polyethyleneglycol vinyl ether macromonomers and their radical copolymerisation with maleic anhydride, *J. Polym. Sci. Chem.* 1984, 22, 2829-2839
169. Gnanou, Y. and Lutz, P., The ability of macromonomers to copolymerise: A critical review with new developments, *Makromol. Chem.* 1989, 190, 577-588
170. Gramain, P. and Frere, Y., Preparation of monomethoxy-(polyethylene oxide) acrylate and methacrylate and its polymerisation: self gelling polymers, *Polymer Commun.* 1986, 27, 16-18
171. Capek, I. and Akashi, M., On the kinetics of free radical polymerisation of macromonomers, *J. Macromol. Sci.-Rev. Macromol. Chem. Phys.* 1993, C33, 369-436
172. Madruga, E.L. and Romain, J.S., Kinetic study of the radical copolymerisation of polystyrene macromonomer with butyl acrylate, *Makromol. Chem., Rapid Commun.* 1991, 12, 319-323
173. Chen, G.F. and Jones F.N., Synthesis of acrylic macromonomers by free radical initiated polymerisation. Conversion to comblike polymers, *Macromolecules* 1991, 24, 2151-2155
174. Ito, K., Tanaka, K., Tanaka, H., Imai, G., Kawaguchi, S. and Itsuno, S., Poly(ethylene oxide) macromonomers 7. Micellar polymerisation in water, *Macromolecules* 1991, 24, 2348-2354
175. Ishihara, K., Tsuji, T., Sakai, Y. and Nakabayashi, N., Synthesis of graft copolymers having phospholipid polar group by macromonomer method and their properties in water, *Jou. Polym. Sci. Part A: Polym. Chem.* 1994, 32, 859-867
176. Hazer, B., Erdem, B. and Lenz, R.W., Styrene polymerisation with some new macro or macromonomeric azoinitiators having PEG units, *Jou. Polym. Sci. Part A: Polym. Chem.* 1994, 32, 1739-1746
177. Tsutsumi, K., Okamoto, Y. and Tsukahara, Y., Radical polymerisation behaviour of macromonomers 3: Effect of macromonomer concentration, *Polymer* 1994, 35, 2205-2209

178. Raab, M. and Janacek, J., Effect of chemical crosslinks on the ultimate tensile properties of water swollen poly(2-hydroxyethyl methacrylate), *Int. J. Polymeric Mater.* 1972, 1, 147-156
179. Bowers, R.W.J. and Tighe B.J., Studies of the ocular compatibility of hydrogels. White spot deposits - incidence of occurrence, location and gross morphology, *Biomaterials* 1987, 8, 89-93
180. Abbott, J.M., Bowers, R.W.J., Franklin, V.J. and Tighe B.J., Studies in the ocular compatibility of hydrogels (IV) Observations on the role of calcium in deposit formation, *J. Br. Contact Lens Assoc.* 1991, 14, 21-28
181. Hamilton, C.J., Murphy, S.M., Atherton, N.D. and Tighe, B.J., Synthetic hydrogels: 4. The permeability of poly(2-hydroxyethyl methacrylate) to cations-an overview of solute-water interactions and transport processes, *Polymer* 1988, 29, 1879-1886
182. Murphy, S.M., Hamilton, C.J. and Tighe, B.J., Synthetic hydrogels: 5. Transport processes in 2-hydroxyethyl methacrylate copolymers, *Polymer* 1988, 29, 1887-1893
183. Horbett, T.A., Protein adsorption to hydrogels, in *Hydrogels in Medicine and Pharmacy Volume 1 Fundamentals*, Peppas, N.A.
184. Okano, T., Aoyagi, T., Kataoka, K., Abe, M., Sakurai, Y., Shimada, M. and Shinohara, I., Hydrophilic-hydrophobic microdomain surfaces having an ability to suppress platelet aggregation and their *in vivo* antithrombogenicity, *J. Biomed. Mater. Res.* 1986, 20, 919-927
185. Okano, T., Uruno, M., Sugiyama, N., Shimada, M., Shinohara, I., Kataoka, K. and Sakurai, Y., Suppression of platelet activity on microdomain surfaces of 2-HEMA-polyether block copolymers, *J. Biomed. Mater. Res.* 1986, 20, 1035-1047
186. Ito, K., Tanaka, K., Tanaka, H., Imai, G., Kawaguchi, S. and Itsuno, S., *Macromolecules* 1990, 22, 1982-1992

187. Suzuki, T. and Tomono, T., Syntheses of monomethoxy polyethyleneglycol vinyl ether macromonomers and their radical copolymerisation with maleic anhydride, *J. Polym. Sci. Chem.* 1984, 22, 2829-2839
188. Ranby, B.G., Chan, K.S. and Brumberger, J. *Polym. Sci.* 1962, 58, 545
189. Iobst, S.A. and Manson, J.A., *ACS Polymer Preprints* 1970, 11, 765
190. Thomas, K.D., *Biological interactions with synthetic polymers*, Ph.D. Thesis, Aston University 1988

APPENDIX I

Copolymer Program Listing

COPOL 1

```

10  REM COPOLYMER-by the Monte Carlo Method
20  REM S.J.MOSS modified by P.H.Corkhill
30  REM Chemical Engineering and Applied Chemistry
40  REM Aston University, Birmingham, B4 7ET, ENGLAND
100 REM *** MAIN PROGRAM ***
110 GOSUB 500
120 GOSUB 1000
130 GOSUB 1500
140 GOSUB 1800
150 GOSUB 2000
160 GOSUB 3000
170 GOTO 4000
200 STOP
500 REM *** INITIALISE ***
510 INCA=0:INCB=0
530 TA=0:TB=0:SUM=0
540 NA=0:NB=0
550 SA=0:SB=0:AMAX=0:BMAX=0
560 CLS:PRINT"PLEASE WAIT INITIALISING ARRAYS"
570 FOR I=1 TO 200
580 NA(I)=0:NB(I)=0:NEXT I
590 PRON=0: COMP=0
600 RETURN
1000 REM *** ENTER DATA ***
1010 CLS:PRINT :PRINT"Input name of monomer 1";
1020 INPUT M1$
1030 PRINT :PRINT"Input name of monomer 2";
1040 INPUT M2$
1050 PRINT :PRINT"Enter the reactivity ratios"
1060 PRINT :PRINT"r1";
1070 INPUT R1$:R1= VAL(R1$)
1080 PRINT :PRINT"r2";
1090 INPUT R2$:R2=VAL(R2$)
1100 PRINT :PRINT"Enter theoretical mole percentage of";M1$;" in the polymer";
1110 INPUT PA$:PA=VAL(PA$)
1120 IF PA>=0 AND PA<=100 THEN 1141

```

```

1130 1100 PRINT :PRINT "MOLE PERCENTAGE MUST BE BETWEEN 0 AND 100:
      PLEASE RE-ENTER ";
1140 GOTO 1110
1141 COMP=0:PRINT :PRINT "Polymerise to 100% conversion ?"
1142 A$=INKEY$
1143 IF A$= "N" OR A$= "n" THEN 1150
1144 IF A$= "Y" OR A$= "y" THEN 1146
1146 COMP = 1
1150 CLS:PRINT :PRINT M1$: PRINT "REACTIVITY ratio =";R1:PRINT
      PA;"Mole %"
1160 PRINT :PRINT M2$: PRINT "REACTIVITY ratio =";R2:PRINT
      (100-PA);"Mole %"
1162IF COMP=0 THEN 1170
1165 PRINT :PRINT "Polymerise to 100% conversion"
1170 PRINT :PRINT "Is this correct ?"
1180 A$=INKEY$: IF A$="Y" OR A$="y" THEN 1210
1190 IF A$="N" OR A$="n" THEN 1200
1195 GOTO 1180
1200 PRINT :PRINT "PLEASE RE-ENTER DATA":FOR I = 1 TO 500:
      NEXT I: GOTO 1000
1210 RETURN
1500 REM *** CALCULATE FEED RATIO ***
1510 INCA=INT(20*PA):INCB=2000 - INCA
1515 IF INCA=0 OR INCB=0 THEN RETURN
1530 COUNT = 0
1540 MR= INCA / INCB
1560 P1= R1*MR : P2=R2/MR
1570 RETURN
1800 REM *** OUTPUT DATA TO PRINTER ? ***
1810 CLS:PRINT :PRINT "Would you like a hard copy ?"
1820 A$=INKEY$: IF A$="Y" OR A$="y" THEN 1850
1830 IF A$="N" OR A$="n" THEN RETURN
1840 GOTO 1820
1850 PRON = 1
1860 LPRINT :PRINT M1$:LPRINT "Reactivity ratio =" ;R1LPRINT PA;"Mole %"
1870 LPRINT :PRINT M2$:LPRINT "Reactivity ratio =" ;R2LPRINT (100-PA);"Mole
      %"
1872 IF COMP = 0 THEN 1880
1875 LPRINT :LPRINT "POLYMERISED TO 100% CONVERSION"

```

```

1880 LPRINT:RETURN
2000 REM *** CALCULATION AND PRINTOUT ***
2020 IF PRON <> 1 THEN 2040
2030 LPRINT:LPRrNT "In the simulated copolymer ";M1$;" is represented by O and
";M2$;" is represented by X" : LPRINT : PRINT : GOTO 2050
2040 CLS : PRINT:PRINT "In the simulated copolymer ";M1$;" is represented by O
and";M2$;" is represented by X" :PRINT:PRINT
2050 WSUM = 1 + MR: W1 = MR/WSUM :W2 = 1/WSUM
2060 X = WSUM * RND (7)
2070 RAD$ = "X" THEN 2280
2110 IF INCA<=0 AND COMP = 1 THEN 2220
2120 REM *** REACTIONS OF MONOMER 1 ***
2130 X1=(1+P1) * RND (TIMER)
2135 IF INCB<=0 AND COMP=1 THEN 2150
2140 IF X1<1 THEN 2220
2150 NA=NA+1:SA=SA+1:INCA=INCA-1:COUNT = COUNT + 1
2160 IF PRON<>1 THEN 2180
2170 LPRINT".,":GOTO 2190
2180 PRINT ". ";
2190 IF COUNT = 100 AND COMP=1 THEN GOSUB 1515
2200 NEXT I
2210 GOTO 2340
2215 REM *** CHANGE MONOMER 1 TO MONOMER 2 ***
2220 RAD$="X":NB=NB+1:SB=SB+1: NA(SA)=NA(SA)+1:SA=0:INCB=INCB-
1: COUNT = COUNT+1
2230 IF PRON<>1 THEN 2250
2240 LPRINT "X,":GOTO 2260
2250 PRINT "X"
2260 IF COUNT = 100 AND COMP=1 THEN GOSUB 1515
2270 GOTO 2200
2275 REM *** REACTIONS OF MONOMER 2 ***
2280 IF INCB<=0 AND COMP=1 THEN 2320
2290 X2=(1+P2) * RND(TIMER)
2295 IF INCA<=0 AND COMP = 1 THEN 2310
2300 IF X2<1 THEN 2320
2310 NE=NB+1:SB=SB+1:INCB=INCB-1: COUNT=COUNT+1:GOTO 2230
2320 REM *** CHANGE FROM MONOMER 2 TO MONOMER 1 ***
2330 RAD$=",:NA=NA+1:SA=SA+1:NB(SB)=NB(SB)+1:SB=0:INCA=INCA-1:
COUNT = COUNT+1:GOTO 2160

```

```

2340 REM *** COUNT LAST SEQUENCE ***
2350 IF SA=0 THEN 2370
2360 NA(SA)=NA(SA)+1:GOTO 2380
2370 NB(SB)=NB(SB)+1
2380 TA=TA+NA:TB=TB+NB:SUM=TA+TB
2390 IF PRON=1 THEN 2410
2400 PRINT :PRINT "The simulated copolymer contains";TA;M1$;"units and";TB;M2$;"
      units" : PRINT INT((TA/2000)*1000)/10;"Mole %";M1$ :GOTO 2420
2410 LPRINT :LPRINT "The simulated copolymer contains";TA;M1$;"units
      and";TB;M2$;" units":LPRINT INT((TA/2000)*1000)/10;" Mole %";M1$
      :GOTO 2420
2420 RETURN
3000 REM *** SEQUENCE ANALYSIS ***
3010 PRINT :PRINT "PRESS ANY KEY FOR SEQUENCE ANALYSIS"
3020 A$= INKEY $: IF A$ = "" THEN 3020
3030 CLS:PRINT :PRINT "ANALYSING THE SEQUENCES"
3040 FOR I=1 TO 2000
3050 IF NA(I)>0 THEN AMAX=I
3060 IF NB(I)>0 THEN BMAX=I
3070 NEXT I
3080 LI=BMAX:IF AMAX>BMAX THEN LI=AMAX
3090 IF PRON<>1 THEN 3150
3100 LPRINT :LPRINT "Sequence Distributions"
3110 LPRINT :FOR J=1 TO 79:LPRINT "-"; :NEXT J
3120 LPRINT :LPRINT "Length",,M1$,,M2$
3130 LPRINT :FOR J=1 TO 79:LPRINT "-";:NEXT J
3140 LPRINT: GOTO 3200
3150 CLS:PRINT :PRINT "Sequence Distributions"
3160 PRINT :FOR J=1 TO 79:PRINT "-";: NEXT J
3170 PRINT :PRINT "Length",,M1$,, M2$
3180 PRINT :FOR J=1 TO 79:PRINT "-";:NEXT J
3190 PRINT
3200 FOR I=1 TO LI
3210 IF NA(I)=0 AND NB(I)=0 THEN 3250
3220 IF PRON<>1 THEN 3240
3230 LPRINT I,,NA(I),,NB(I): GOTO 3250
3240 PRINT I,,NAI),,NB(I)
3250 NEXT I
3260 RETURN

```

```
4000 PRINT :PRINT "ANOTHER RUN ?"  
4010 A$=INKEY$:IF A$="" THEN 4010  
4020 IF A$="Y" OR A$="y" THEN RUN  
4030 IF A$="N" OR A$="n" THEN END  
4040 GOTO 4010
```

APPENDIX II

Hydrogel Copolymer Composition	Dispersive Component of Surface Free Energy (mN/m)	Polar Component of Surface Free Energy (mN/m)	Total Surface Free Energy (mN/m)
HEMA-AMO 100:0	29.0	21.5	50.5
HEMA-AMO 90:10	33.6	21.7	55.3
HEMA-AMO 80:20	34.2	19.5	53.7
HEMA-AMO 70:30	34.6	18.0	52.6
HEMA-AMO 60:40	35.0	17.8	52.8
HEMA-AMO 50:50	35.9	16.2	52.1
HEMA-NVP 90:10	37.0	7.3	44.3
HEMA-NVP 80:20	38.8	5.5	44.3
HEMA-NVP 70:30	40.0	4.8	44.8
HEMA-NVP 60:40	40.5	4.7	45.2
HEMA-NVP 50:50	41.7	3.8	45.3
HEMA-NNDMA 90:10	31.7	13.9	45.6
HEMA-NNDMA 80:20	32.7	12.3	45.0
HEMA-NNDMA 70:30	33.9	10.2	44.1
HEMA-NNDMA 60:40	35.0	8.8	43.8
HEMA-NNDMA 50:50	35.5	7.7	43.2

APPENDIX III

Hydrogel Copolymer Composition	Dispersive Component of Surface Free Energy (mN/m)	Polar Component of Surface Free Energy (mN/m)	Total Surface Free Energy (mN/m)
HEMA-MAA 100:0	23.1	42.2	65.3
HEMA-MAA 99:1	22.8	43.1	65.9
HEMA-MAA 98:2	22.4	44.0	66.4
HEMA-MAA 97:3	21.5	44.8	66.3
HEMA-MAA 96:4	21.6	45.2	66.8
HEMA-MAA 95:5	21.7	45.6	67.3
HEMA-ITC 99:1	22.8	43.1	65.9
HEMA-ITC 98:2	22.4	44.0	66.4
HEMA-ITC 97:3	21.5	44.8	66.3
HEMA-ITC 96:4	21.6	45.2	66.8
HEMA-ITC 95:5	21.7	45.6	66.3
HEMA-NVI 99:1	22.2	43.1	65.3
HEMA-NVI 98:2	21.3	44.0	65.3
HEMA-NVI 97:3	21.8	44.0	65.8
HEMA-NVI 96:4	21.0	44.8	65.8
HEMA-NVI 95:5	21.5	44.8	66.3
HEMA-SPE 99:1	22.2	43.1	65.3
HEMA-SPE 98:2	21.8	44.0	65.8
HEMA-SPE 97:3	21.3	44.4	65.7
HEMA-SPE 96:4	21.5	44.8	66.3
HEMA-SPE 95:5	21.5	44.8	66.3